A STUDY OF COLORATION AND BLEACHING PHENOMENA IN ALKALI HALIDES AND SODALITE

by
M.J. REDMAN

A Dissertation Submitted to The University of Warwick for Admission to the Degree of Doctor of Philosophy

1971

CONTENTS

Abstract

Experiments are described in this thesis on the optical bleaching at room temperature of F centres in freshly cleaved single crystal KBr, coloured by fast electron ($\sim$ 50 KV) irradiation and illuminated with light from a focused helium-neon laser. Using a specially constructed microspectrophotometer bleaching apparatus, which is described in Chapter Two, data was obtained on optical bleaching at illuminating power densities up to 10 KW.cm.$^{-2}$ in KBr having initial F centres concentrations of 10^{18} - 10^{19} centres cm.$^{-3}$. The bleaching light intensity is some 10^{6} times greater than that used in previous experiments, and the initial defect concentrations produced by electron irradiation are considerably higher than those found in the additively coloured specimens used in earlier experiments. Essentially, there have been no previous studies made on the optical bleaching of electron irradiated alkali halide, and very little work has been done on the laser bleaching of this material coloured by any of the other methods possible.

It is found that KBr which has been coloured by electron irradiation at room temperature bleaches by the random aggregation of F centres, a process which also occurs in additively coloured material. Prolonged bleaching, to absorbed doses of $> 4 \times 10^{8}$ J.cm^{-3}, does not result in a complete disappearance of absorption in the F band region, but leads to the formation of a residual coloration which is due to excited states of the M and R centres. A technique of optical modulation spectroscopy, described in Chapter Five, showed that R^{+} centres are formed during illumination, which points to the importance of the $F + \alpha \longrightarrow M^{+}$ and $M + \alpha \longrightarrow R^{+}$ reactions in the aggregation process.

In marked contrast, a vacancy interstitial recombination mechanism occurs in KBr which has been coloured by electron irradiation at 90°K and warmed in the dark to room temperature for bleaching. There is a direct proportionality between the height of the V band and the total number of vacancies present in F, M and R centres throughout the

optical bleaching of KBr coloured at low temperature. Prolonged bleaching leads to the complete disappearance of the F,M, R and V bands, and the optical absorption spectrum of the crystal is similar to that seen prior to coloration.

The atomic mechanisms responsible for bleaching under illumination at room temperature in KBr coloured additively, and by fast electron irradiation at room and liquid nitrogen temperatures, are discussed at length in Chapters Four and Five.

Chapter Six describes investigations into the coloration and bleaching properties of the sodalites, using a dark trace cathode ray tube with an aluminised chlorosodalite powder screen. Coloration curves are given which show the increase in F centre concentration with electron dose during the reversible photochromic stage of coloration. Optical bleaching measurements are described for a number of bleaching sources , ranging from a low intensity microscope illuminator to a 1000 joule xenon flash tube. The fatigue observed in the sodalites is discussed, and its connection with changes in the cathodoluminescence spectrum noted.

The final chapter summarises optical bleaching phenomena in both electron irradiated KBr and sodalite, and makes comparisons, where appropriate, between the two materials. Some suggestions are also made for further experiments. In conclusion, a number of important technological applications of colour centre phenomena are described and discussed.

Acknowledgements

The studies described in this thesis were carried out in the School of Physics of the University of Warwick. I am therefore grateful to Professor A.J. Forty of this department for the generous provision of research facilities and for his encouragement and advice.

The assistance of the technical staff of the School of Physics is gratefully acknowledged.

My thanks go to my colleagues in the School of Physics for many helpful discussions and critiscisms.

I would like to thank Mrs. C. Allsopp for her assistance with the drawings, and Mrs. A.J. Heal for typing the manuscript so efficiently.

It is a pleasure to acknowledge my supervisor Dr. M.R. Tubbs, to whom I am exceedingly indebted for his friendship, guidance and constructive critiscism throughout the duration of this research.

I am grateful to Dr. P.A. Forrester, of the Royal Radar Establishment, for several helpful discussions, and for providing the iodosodalite crystals.

I would like to thank the Science Research Council and Ferranti Ltd. for their financial support (in the form of a C.A.P.S. Studentship) throughout this work. Ferranti Ltd. must also be thanked for providing some of the equipment, and laboratory facilities for much of the experimental work described in Chapter 6.

Lastly, but by no means least, I would like to thank my wife Penny, for her encouragement and for her great patience during the completion of this work.

CHAPTER ONE

INTRODUCTION

1.1 General Properties of the Alkali Halides

The alkali halides have long been of interest to physicists, and may be regarded as one of the first groups of materials to be studied by the methods of solid state physics. For a considerable time they were one of the few groups of materials that were readily available as large single crystals of relatively high purity; although now, of course, there are many materials available to the physicist in single crystal form, and the purity of some specimens, notably the elemental semiconductors germanium and silicon, far surpasses that of the very best alkali halide crystals.

Synthetic single crystals of the alkali halides are usually grown from the melt, the Bridgman-Stockbarger and Kryopoulos[1,2] methods being two of the techniques most commonly employed. Naturally occurring single crystal deposits of the alkali halides, rock salt in particular, are the result of the very slow evaporation of a saturated aqueous solution of the salt, and this process can also be used in the laboratory with some success. However, the commercial preparation of single crystal is carried out almost exclusively by the Bridgman-Stockbarger method. Most of the alkali halides crystallise in the NaCl structure, which is illustrated diagrammatically in Fig.1.1(a). This arrangement may be thought of as two interpenetrating face centred cubic lattices of alkali metal and halogen ions respectively, such that each Cl^- ion is octahedrally co-ordinated by six nearest neighbour Na^+ ions, and similarly each Na^+ by six Cl^- ions. One or two of the alkali halides, CsCl for example, crystallise slightly differently, in the manner shown in Fig.1.1(b). This structure may, like that of NaCl, be looked upon as being composed of two separate, but interpenetrating lattices, although in this case the unit cells are simple cubic, so that each Cs^+ ion is co-ordinated by eight nearest neighbour Cl^- ions, and vice versa.

FIG. 1.1(a)

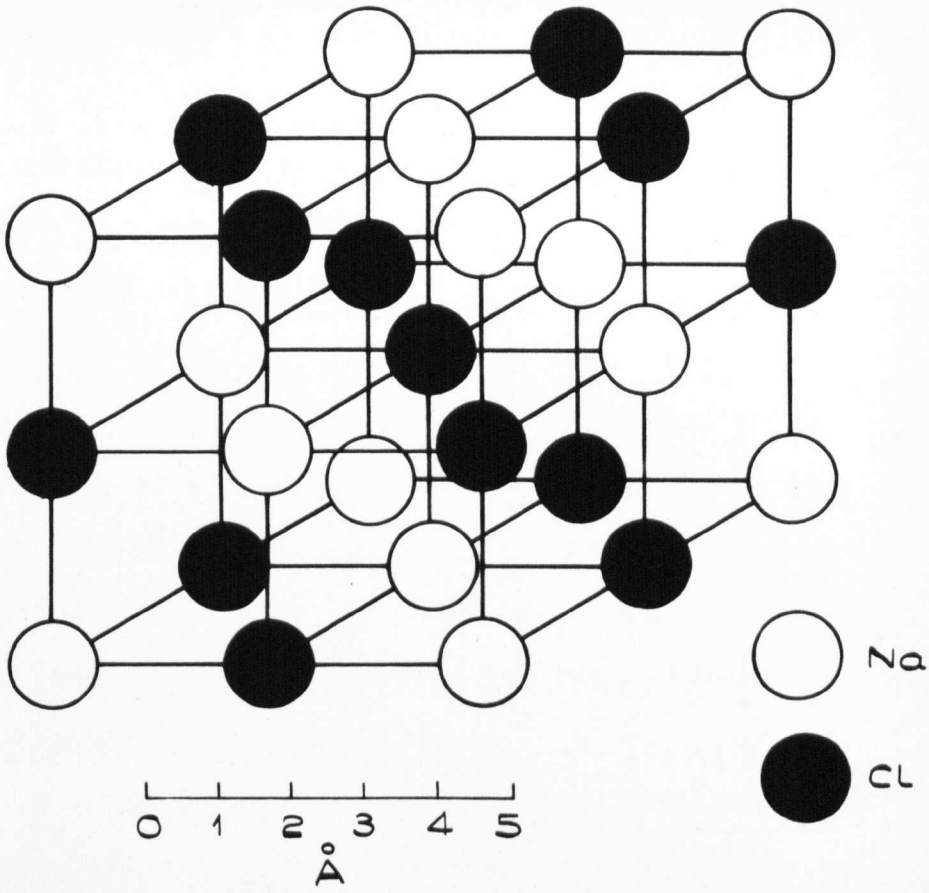

THE STRUCTURE OF THE NaCl TYPE ALKALI HALIDES.

FIG. 1.1(b)

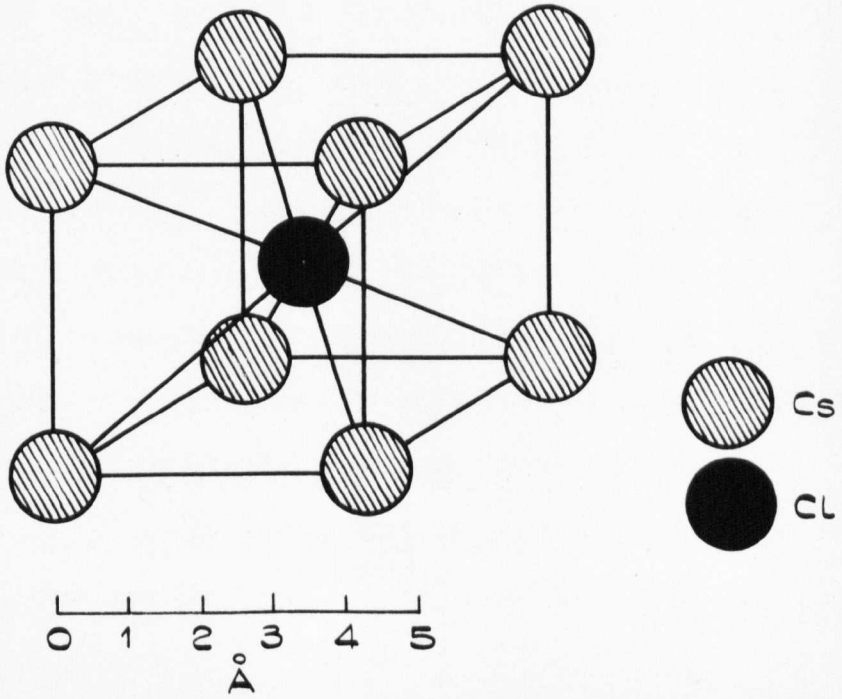

THE STRUCTURE OF THE CsCl TYPE ALKALI HALIDES.

At low temperature the alkali halides are highly insulating solids, but upon heating they exhibit ionic conductivity. That this conductivity is in fact ionic, and not electronic in nature is demonstrated by the fact that electrolysis occurs, which can be shown to obey Faraday's laws. Thus, on a simple band theory model the electron distribution can be represented by a system of completely filled and completely empty energy bands, separated by a characteristic energy gap, which is very much greater than kT. If one considers the crystal as a collection of interacting ions, the upper filled band may be associated with the occupied p^6 levels of the halide ions, and the empty conduction band with unoccupied s and d levels of the alkali metal ions. It is likely that in real crystals the conduction band corresponds to an ionisation continuum of overlapping unoccupied levels.

However, it is the unusual optical properties of the alkali halides that have really stimulated the large research effort devoted to them over the last 40 years. They are completely transparent over the spectral region extending from about 200 nm. in the ultra violet through the visible and well into the far infra red, to beyond 100 μm. in some cases. (Typical absorption spectra are illustrated in Fig.1.2. [3,4].) This range of transparency is unequalled by any other group of materials. On a simple energy band model the absorption in the ultra-violet, below 200 nm., is associated with electronic transitions between the filled valence band and the conduction band, and, as might be expected, at sufficiently high incident photon energies photoconductivity is observed. The absorption maximum seen in the far infra red part of the spectrum is known as the Restrstrahl region, and is caused by the coupling of the incident electromagnetic radiation to the characteristic transverse modes of vibration of the charged ions. From a practical standpoint the optical study of the alkali halides has been facilitated by the ease with which good quality specimens can be obtained; as was

FIG. 1.2.

ULTRAVIOLET[3] AND INFRARED[4] ABSORPTION SPECTRA OF NaCl.

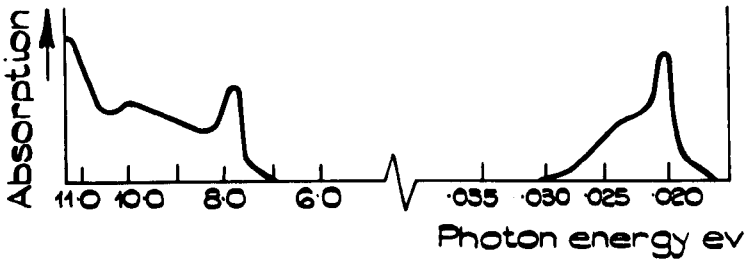

mentioned earlier large single crystals can be grown with little difficulty, and these may be directly cleaved into samples with good quality surfaces which usually require no further treatment (such as etching or polishing) before use.

A close examination of the u-v absorption in the alkali halides reveals that there is a strong absorption peak at a lower photon energy than that necessary to cause photoconductivity. This introduces the first complication into the elementary energy band model, the low energy optical absorption maximum is explained in terms of electronic transitions between the upper filled band and bound states, known as exciton states, lying just below the conduction band. It is reasoned that light of longer wavelengths is not sufficiently energetic to completely separate the electron from its complementary hole in the upper filled band, and that the two remain bound to each other by Coulomb attraction. The electron hole pair is known as an exciton, and can be likened to a particle which has no net electric charge but which is free to migrate through the crystal, transferring excitation energy from ion to ion. It is similar to the notion of the excited states of a free atom, except that now the excitation energy is coupled to the lattice of the solid, and so may propagate through the crystal. When the electron-hole interparticle distance is large in comparison with an atomic radius, the exciton is said to be weakly bound, and gives rise to a series of Rydberg type energy levels thus:

$$E_n = -\frac{M_n e^4}{2\epsilon^2 \hbar^2} \cdot \frac{1}{n^2}$$

where n is the principle quantum number, M_n the reduced mass of the electron hole combination and ϵ the dielectric constant of the lattice medium, e and $\hbar$ have their usual meanings. Weakly bound, or Mott-Wannier excitons are observed in the alkali halides; the ultraviolet absorption spectra of thin films of these materials show considerable structure, of

which the first non-photoconductive absorption peaks are due to excitons. In physical terms an exciton in an alkali halide may be considered to be the result of the excitation of a halide ion, or the transfer of an electron from a halide ion to a nearest neighbour alkali metal ion. The alternative to the Mott-Wannier exciton model is the tight-binding or Frenkel model. Frenkel excitons are observed in molecular crystals, where the binding within a molecule is strong in comparison with the binding between molecules. In this type of solid the exciton energies are more closely related to the spectroscopic properties of the isolated molecule, rather than to the hydrogenic Mott-Wannier model.

The incorporation of impurities, even in concentrations of a few parts per million, leads to further complications in the simple band scheme for the alkali halides given here, by introducing localised energy levels lying in the "forbidden gap" between the valence and conduction bands. Electronic transitions may then occur which give rise to optical absorption in a spectral region where the material is normally transparent. As an example of this, Cu^+ ions in NaCl cause the appearance of a pronounced absorption peak at 255[5] nm. A schematic diagram of the energy level configurations discussed so far appears in Fig.1.3.

1.2 Defects and Colour Centres in Alkali Halide Crystals

Up to this point only crystals having absolutely regular arrays of ions have been discussed, even though real crystals are known not to exhibit such a high degree of regularity. Imperfections occur in all crystalline solids, and these usually have a marked influence on the overall physical properties of the material. This is particularly true of the alkali halides, in which microscopic crystal defects give rise to a whole host of interesting optical phenomena. Absorption bands appear in the broad spectral region in which the crystal is normally transparent, and frequently this absorption occurs at wavelengths in the visible spectrum, making the crystal appear coloured. It is for this

FIG. 1.3.

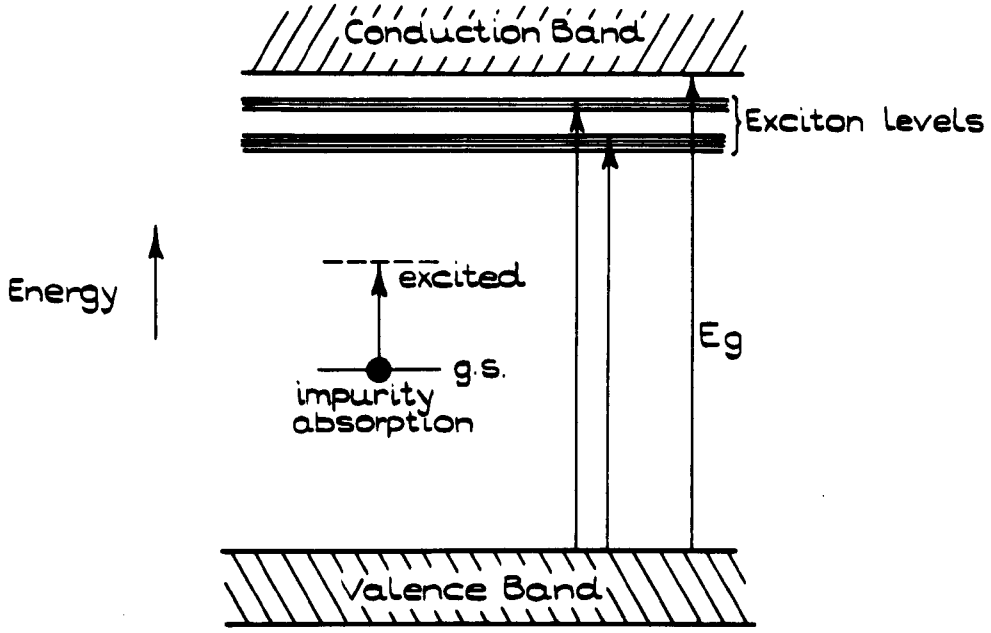

SCHEMATIC BAND PICTURE OF AN ALKALI HALIDE, SHOWING ENERGY LEVELS AND OPTICAL ABSORPTIONS DUE TO EXCITONS AND IMPURITIES.

reason that the defects responsible have been named colour centres.

There are a number of different types of defect which can occur in real crystals, but for the purposes of a brief introduction to colour centres only three need be mentioned. They are:

(i) interstitial ions (interstitials)

(ii) vacant lattice sites (vacancies)

(iii) impurity ions, incorporated into the lattice substitutionally or interstitially

On purely thermodynamic reasoning cation and anion vacancies are expected to occur in equal numbers in real ionic crystals, either singly (Schottky defects) or paired with complementary interstitial ions (Frenkel defects). Both configurations are illustrated in Fig.1.4. A crystal that contains only interstitial ions, without any vacancies, is theoretically possible, but has never been found in practice, and will therefore not be discussed further. Since the ionic radii of anions are frequently greater than those of cations, one might expect the energy required to move a cation to an interstitial site to be lower than that for the corresponding anionic displacement. On this reasoning cationic Frenkel defects will have a lower energy of formation than anionic ones, and will therefore be created more readily in real crystals. Moreover, a difference between the formation energies of Frenkel and Schottky defects might also be expected, and estimates of these energies have shown that in the alkali halides the latter are more likely to occur. It ought to be pointed out at this juncture that these deductions have been based on the existence of thermal equilibrium in the crystals. This is not necessarily the case during some processes which generate defects, and the possibility cannot be ruled out of other than Schottky defects being formed in the alkali halides.

The addition of impurity ions to an alkali halide crystal can also bring about the formation of vacancies. In a typical case divalent

FIG. 1.4.

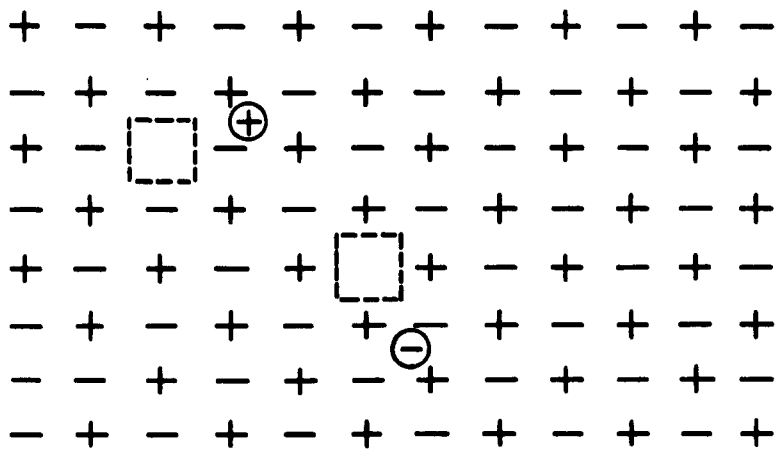

FRENKEL DEFECTS (INTERSTITIAL CATIONS AND ANIONS WITH CORRESPONDING VACANCIES).

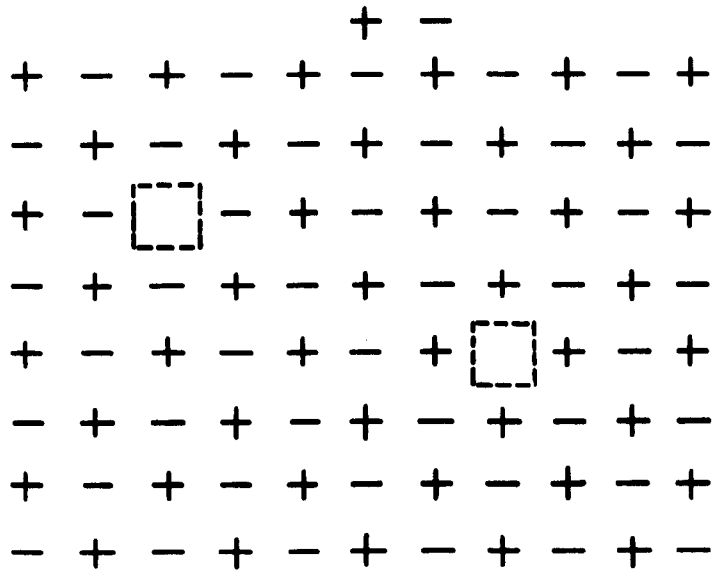

SCHOTTKY DEFECT (CATION AND ANION VACANCIES).

positive ions are substitutionally incorporated into the lattice at cation sites. In order to preserve the electrical neutrality of the crystal as a whole, either extra negative ions must be incorporated interstitially or alkali metal ion vacancies must be formed. Since the formation of Schottky type defects is favoured in the alkali halides, one might expect that doping such a crystal with a divalent metal, e.g. Ca, would bring about an increase in the number of alkali ion vacancies (Fig.1.5). By using sensitive density measuring techniques this hypothesis has been verified experimentally[6].

Schottky defects play an important role in the processes of diffusion and electrolytic conduction in the alkali halides. A vacant lattice site may be propagated through the crystal by an adjacent ion, of the appropriate sign, jumping into the vacancy, provided sufficient activation energy is available. This leaves both the vacancy and the ion in new positions in the lattice, and when repeated a large number of times by a large number of vacancies it results in the observation of ionic diffusion. Interstitial ions, if any are present, can obviously migrate by a similar jumping mechanism and contribute to the observed diffusion. Clearly, in a perfect crystal, in which all of the lattice sites are occupied by the correct ions, diffusion is impossible, since a given ion has nowhere to go.

Mapother et al[7] measured the diffusion of radioactive sodium in NaCl by depositing a thin layer of salt containing the radioisotope Na^{24} onto one face of a cubic crystal of NaCl, and then holding the crystal at a constant temperature for a certain length of time. The distribution of Na^{24} was then determined by a sectioning technique. Repeating this measurement over a range of temperature enabled the variation of the diffusion coefficient (D) with temperature (T) to be plotted. The results of Mapother et al. (Fig.1.6) show that D follows an exponential variation with temperature, of the form $D = D_0 e^{-\epsilon/kT}$, with

FIG. 1.5.

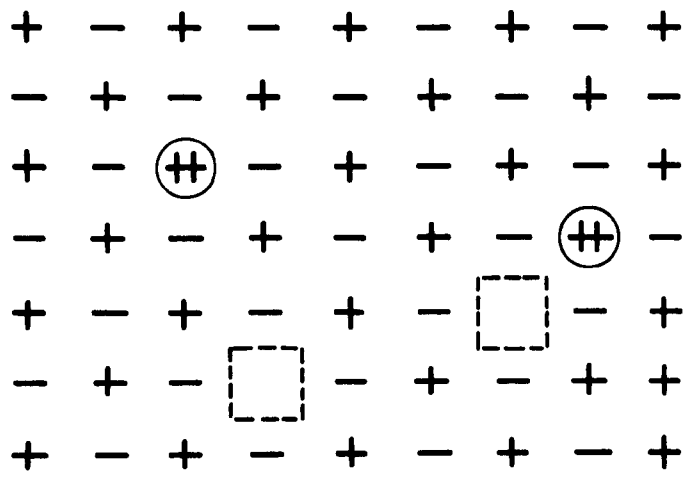

DIVALENT CATION IMPURITIES IN AN ALKALI HALIDE LATTICE.

FIG. 1.6.

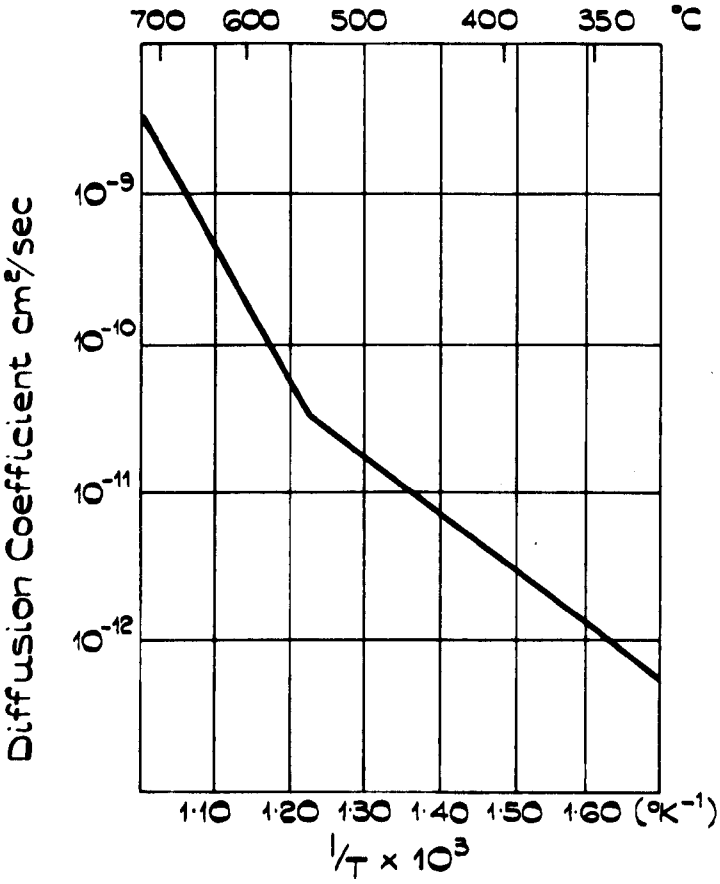

VARIATION OF THE DIFFUSION COEFFICIENT OF Na IN NaCl WITH TEMPERATURE (7).

different values for the activation energy ϵ at low and high temperature. The smaller slope at the low temperature region of Fig.1.6 is thought to be due to the presence of divalent positive ion impurities. Divalent impurities will, in the manner discussed earlier, lead to the formation of a fixed number of positive ion vacancies. At lower temperatures this will mean that the crystal contains a greater than thermal equilibrium number of positive ion vacancies, which will make D higher than it would be if only Schottky vacancies were present.

Applying an electric field to an alkali halide crystal effectively lowers, in the direction of the field, the potential barrier which has to be overcome before an ion can jump into an adjacent vacancy. Jumps in the field direction are therefore favoured, and there is a net diffusion of positive ions towards the cathode and negative ions towards the anode. The conductivity observed in the alkali halides is thus due to the diffusion of ions in the applied field; the currents are certainly too large to be explained in terms of electronic motion, since the number of conduction band electrons at any temperature will be far too small. The ionic nature of the conductivity of the alkali halides is demonstrated by the fact that decomposition occurs at the electrodes when a current is passed through such a crystal. The addition of divalent metal impurities has a significant effect on the conductivity of an alkali halide, particularly at lower temperatures, where the conductivity is dominated by impurity induced positive ion vacancies[8] (Fig.1.7).

The processes of electrical conductivity and diffusion in the alkali halides are therefore totally dependent on the presence of crystalline defects, and in particular vacant lattice sites. This is also true for a lot of the interesting optical properties. The principle optical phenomenon associated with the presence of microcrystalline defects in the alkali halides is the F absorption band, the term being

Fig. 1.7.

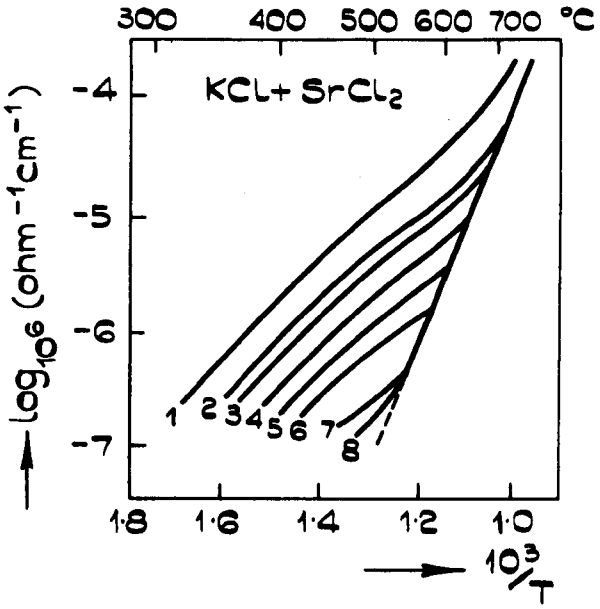

Impurity content in mole fractions $\times 10^{-5}$

1 : 19
2 : 8·7
3 : 6·1
4 : 3·5
5 : 1·9
6 : 1·2
7,8 : 0

THE IONIC CONDUCTIVITY OF KCl CRYSTALS CONTAINING VARIOUS AMOUNTS OF $SrCl_2$ [8].

derived from "farbe", the German word for colour. It is observed when the crystals are exposed to ionising radiation or heated in alkali metal vapour, and gives them a coloration that is characteristic of the particular alkali halide. For example, potassium chloride assumes a deep magenta colour, potassium bromide becomes blue and sodium chloride yellowish brown. It was found by Ivey[9] that the wavelength of the maximum (λmax Å) of the bell shaped F absorption band in the alkali halides is given empirically by the relationship

$$\lambda \text{ max} = 703d^{1.84} \qquad \text{(i)}$$

where d is the lattice constant in Angstrom units. This relationship is valid over the complete range of alkali halides, from LiF with a lattice constant of 4.1Å and F-band peak at 250nm. to RbI with d = 7.33Å and λmax = 756nm. The shape of the F band in a typical alkali halide crystal (KBr) at various temperatures is illustrated in Fig.1.8. It is evident that as the temperature is lowered the absorption band narrows and shifts to shorter wavelengths.

De Boer[11], in 1937, proposed that the F absorption band was caused by an electron trapped at a halogen ion vacancy (Fig.1.9). It is easy to see that if a negative ion is removed from the lattice, leaving a vacancy, the coulomb field of the six nearest neighbour positive ions can trap a free electron that diffuses into the vicinity of the vacant site, the result being the entity known as the F centre. The electron will, in general, be a primary or secondary photoelectron, released by illuminating the crystal with ionising radiation. A crystal containing F- centres will thus have further bound states lying inside the forbidden gap on the simple energy level scheme of the alkali halides (Fig.1.10), such that the optical excitation of the F centre electron from its ground state to the excited state lying just below the conduction band requires the absorption of visible photons, of typical photon energy $\sim$ 2eV. Since it was first proposed, there have been numerous experiments devised to check that de Boer's model of the F centre is

Fig. 1.8.

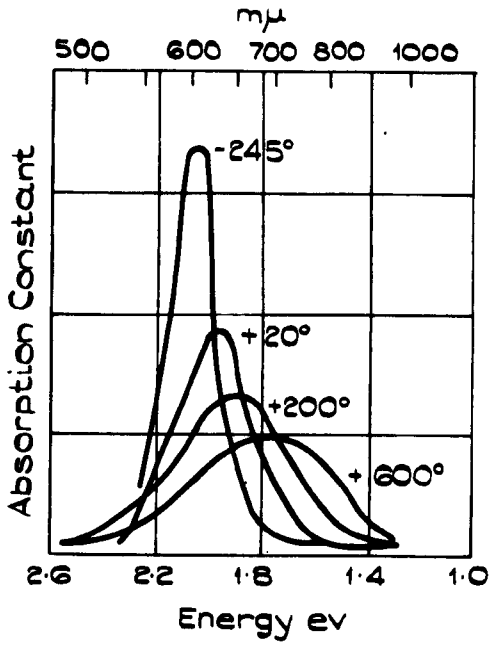

TEMPERATURE DEPENDENCE OF THE F BAND IN KBr[10].

FIG. 1.9.

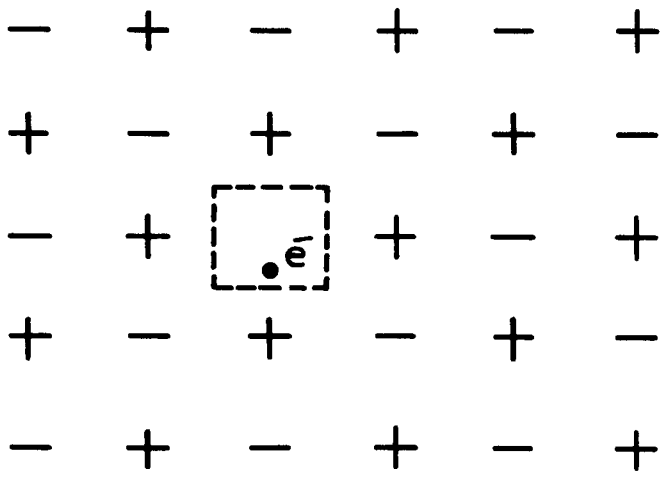

SCHEMATIC DIAGRAM OF AN F CENTRE (ELECTRON TRAPPED AT AN ANION VACANCY).

FIG. 1.10.

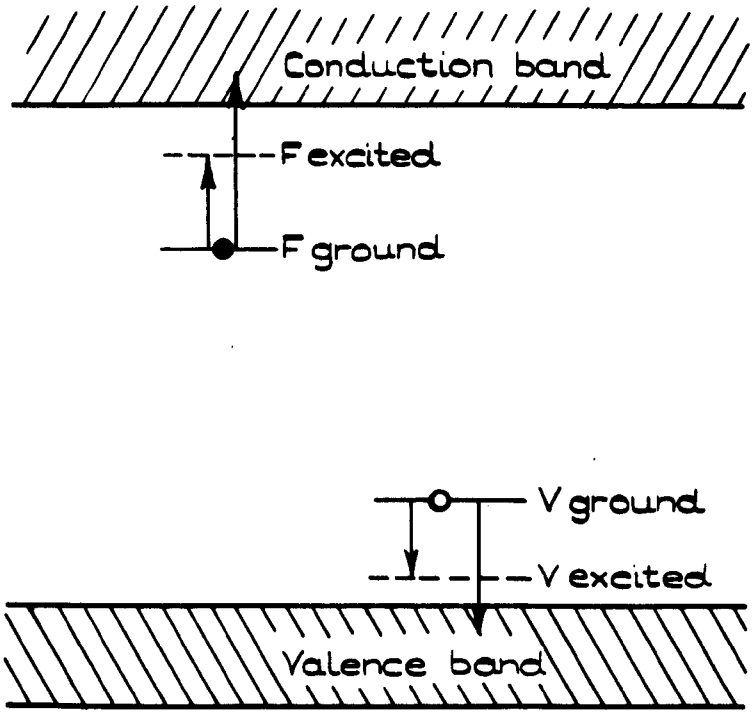

SCHEMATIC BAND DIAGRAM OF THE ENERGY LEVELS IN AN ALKALI HALIDE ASSOCIATED WITH AN F CENTRE (TRAPPED ELECTRON) AND A V CENTRE (TRAPPED HOLE).

correct, but paramagnetic resonance techniques have produced the most conclusive proof of its validity. The shape and position of the resonance line obtained from these measurements has been quantitatively interpreted in terms of the model and the width of the resonance suggests that the F centre electron not only interacts with the six metal ions surrounding the vacancy, but also with the twelve next nearest neighbour halogen ions [12]. The improved resolution of the electron spin double resonance technique has shown the latter hypothesis to be correct [13]. It is therefore generally accepted that the F absorption band can be attributed to optical transitions of the type 1s→2p of electrons trapped at halogen ion vacancies.

The equation due to Smakula [14] is of considerable importance in the quantitative study of colour centre phenomena. This relates the observed half width and amplitude of the F band to the number of F centres present in the crystal.

The equation is expressed as follows:

$$Nf = \frac{9mc}{2e^2} \cdot \frac{n}{(n^2+2)^2} \alpha_{max} W$$

$$= 1.29 \times 10^{17} \cdot \frac{n}{(n^2+2)^2} \alpha_{max} W \qquad \text{(ii)}$$

where N = the F centre density (centres cm.$^{-3}$)

f = the oscillator strength of the F centre

n = the refractive index of the crystal at the wavelength of the F absorption peak

α_{max} = the absorption coefficient at the peak of the F band (cm.$^{-1}$)

W = the half width of the absorption band (eV)

m = the mass of the electron

e = the charge on the electron

c = the velocity of light

If a transparent optical specimen is illuminated with light of a particular wavelength, it follows that

$$A + T + R = 1$$

where A is the fraction of the incident light absorbed, T the fraction transmitted and R the fraction reflected. Also, if I_o is the light intensity at a particular position in the specimen and I is the intensity after it has travelled a further path length x from that position,

$$I = I_o e^{-\alpha x}$$

where α is the absorption coefficient. If one then considers the reflections at the front and interior surfaces of a specimen, and the absorption in terms of the absorption coefficient α and path length x , the fraction of the incident intensity transmitted by the specimen is given by the relationship:

$$T = (1 - R)^2 e^{-\alpha x}$$

If R = 0 a simple expression for α may be derived, thus:

$$\alpha = \frac{2.303 \log_{10} (1/T)}{x} = \frac{2.303\ D}{x} \qquad \text{(iii)}$$

where D is known as the optical density of the specimen. This simplified expression for α may usually be used in the spectroscopy of colour centres by introducing an uncoloured specimen into the reference beam of the spectrometer, to cancel out the reflection losses. Therefore, by using Smakula's equation, the F centre concentration in a specimen may be estimated from directly measurable quantities.

Smakula derived equation (iii) from classical dispersion theory, treating the F centres as damped oscillators. A later treatment by Dexter [15] took into account the fact that the width of the absorption band arises from interactions of the centre with lattice vibrations, and that observed F bands have an approximately Gaussian shape rather than the Lorentzian form assumed in the classical treatment. This produced an equation similar to (ii), except that the numerical constant is 0.87×10^{17} rather than 1.29×10^{17}. Which constant is used in practice

is unimportant, provided one uses the relevant f value. Care is obviously needed when comparing published f's, since some workers use Smakula's equation and others Dexter's version. Dexter's form of Smakula's equation has been used throughout this thesis.

The irradiation of an alkali halide crystal at room temperature with virtually any type of ionising radiation generates a strong F absorption band, and the production of F centre densities (calculated using Smakula's equation) in excess of 10^{18} cm^{-3} is possible, even when illuminating with ultra violet light [16]. This appears to indicate that the ionising radiation somehow creates vacancies, since estimates of the concentration of Schottky defects in the crystal before irradiation are very much lower than this (typical) F centre density. Estermann et al. were in fact able to show that the density of KCl crystals decreases during X irradiation [17]. For a while the explanation of this phenomenon posed a problem, since in most cases the obvious vacancy formation mechanism (direct ionic displacement by elastic collision) can be ruled out, on the grounds that the irradiating photons or electrons will not have sufficient momentum.

A number of mechanisms [18] have been proposed to resolve this difficulty, none of which are satisfactory in every respect. However, the most likely explanation is based upon the radiationless recombination of an electron and a hole [19]. One way in which this might occur is when an electron combines with a V_K centre. A V_K centre is formed by the loss of an electron from a halogen ion and the subsequent moving together of the resulting atom and an adjacent negative ion; it is thus a self trapped hole (Fig.1.11). An electron combining with such a centre can lead to an exciton like state, which may decay without the emission of a photon, imparting some 3-5ev of kinetic energy to the two halogen ions. It is then reasoned that if this kinetic energy is unequally shared between the two anions, due to interactions with the lattice, it

FIG. 1.11.

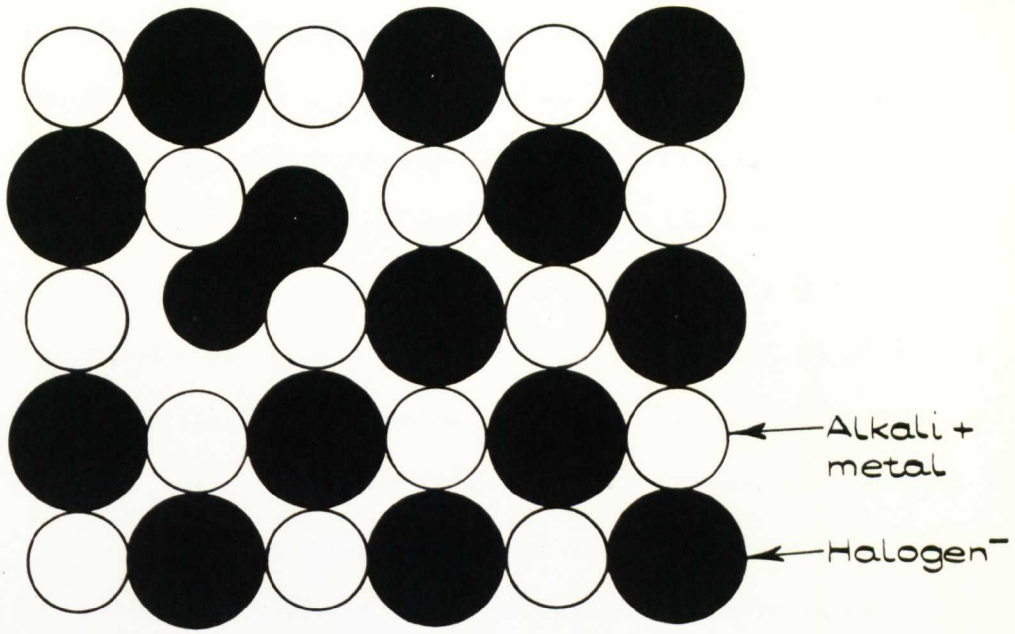

MODEL OF A V_K CENTRE.

may bring about the formation of a negative ion vacancy and a halogen interstitial, by a focused collision sequence in the close packed direction. This mechanism can therefore lead to an F centre density greater than the thermal equilibrium concentration of Schottky defects present in the crystal prior to irradiation. It must be pointed out that some calculations [20] suggest that an energy of 20-25ev is necessary for an ion replacement sequence; this is clearly too high to be derived from the mechanism just described. However, the energy obtained from such calculations depends sensitively on the interionic potential chosen, the form of which has not been generally agreed.

It is evident from coloration curves (plots of F band coloration versus the accumulated radiation dose) that there are two distinct stages in the coloration of an alkali halide crystal by exposure, at room temperature, to ionising radiation. (Fig.1.12) There is an early stage, in which the crystal coloration builds up rapidly and saturates after a relatively short exposure, and a later stage during which the coloration continues to build up, but much more slowly, and shows signs of saturation only after very large exposures. The early stage is found to vary from specimen to specimen, whereas the late stage is not markedly dependent on the specimen's origin or previous history. It was assumed at first that the early stage coloration is simply the result of anion vacancies already present in the crystal trapping photoelectrons [22], and that the wide variation observed among different specimens in this region is associated with the varying concentrations of vacancies "frozen" into the crystals. However, no early stage is observed in crystals irradiated at 77°K and below [21], regardless of their origin, and certain impurities, notably H^-, OH^- and divalent alkaline earths, considerably enhance stage 1 coloration [23]. These, and other experiments suggest that the simple explanation for the first stage coloration may be incorrect, at least in certain specific

FIG. 1.12.

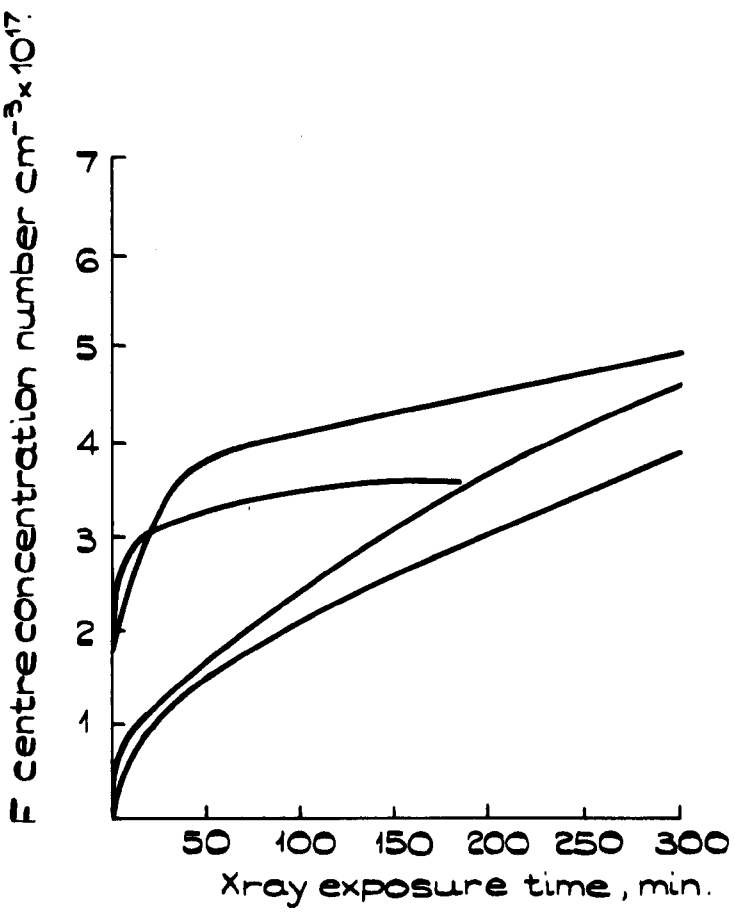

GROWTH OF THE F BAND IN VARIOUS NOMINALLY PURE NaCl CRYSTALS AT ROOM TEMPERATURE[21]

cases. It is now generally thought that the first, easy coloration stage may be the result of impurities in the crystals, and that the later, harder to colour stage is, in fact, the intrinsic region of the coloration curve. The production of F centres during this later stage of coloration has already been discussed; all of the specimens used for the experiments described in this thesis were irradiated long enough to be well into this region. (The second stage coloration saturates at F centre concentrations of a few $x10^{19}$ centres cm^{-3})

Another method commonly used to generate a strong F absorption band in the alkali halides is that known as additive coloration. The crystal is sealed into a container and heated in an atmosphere of alkali metal vapour, so as to produce a stoichiometric excess of metal ions. The excess cations are incorporated substitutionally into the lattice with the simultaneous formation of negative ion vacancies, which act as traps for the electrons which must accompany the added metal ions, in order to preserve the electrical neutrality of the bulk crystal. In general, therefore, an F centre will be created for each atom of stoichiometric excess alkali metal incorporated in the crystal. The practical aspects of additive coloration will be discussed in more detail in the next chapter of this thesis.

It might be conjectured from the preceding paragraphs that the formation of an F absorption band is the only change observed in the optical spectrum of an alkali halide crystal when it is exposed to ionising radiation. This is, in fact, a gross oversimplification, for although the F absorption is quite often the most predominant feature in the spectrum, other bands, attributable to different sorts of defect centre are also formed. Even if F centres are the only type of trapped electron centre present, their generation by ionising radiation is accompanied by the formation of complementary trapped hole centres, generically referred to as V centres, with one important exception, the

H centre. H centres are formed, together with F centres, when an alkali halide is irradiated at very low temperatures ($\sim 5^{\circ}K$), and is the initial product of any ionisation displacement event. It consists of a $(halide)_2^-$ molecule ion occupying a single halide ion site, with the unpaired electron interacting weakly with the two nearest neighbour halide ions, so that it effectively involves 4 halogen nuclei occupying 3 halide sites lying along the <110> direction (Fig.1.13). H centres are readily converted to other types of trapped hole centre if the crystal is warmed above $20^{\circ}K$. In general it is found that a number of different trapped electron and trapped hole absorption centres are formed, depending on the temperature of irradiation, the type of ionising radiation and the temperature at which the absorption spectrum is measured. The absorption bands are classified according to their properties and designated F, F', M, R, V_1, V_2, V_3 .... etc; obviously the labelling of bands does not vary from one alkali halide to another, for although the absorption maxima are located at different wavelengths in different materials the configurations and properties of the absorbing centres remain the same. Whilst a large number of different absorption bands have been observed and tabulated in the alkali halides, the precise nature of the defect centres responsible for many of them are still unknown, or the models are somewhat speculative. Particularly lacking are reliable models for many of the trapped hole (V) centres that are stable at room temperature.

Two examples of the variety of spectra that may be observed in the same alkali halide under different coloration conditions are illustrated in Fig.1.14; curve (a) shows the spectrum at $90^{\circ}K$ of KBr that has been X irradiated at that temperature, and curve (b) the spectrum at $293^{\circ}K$ of the same material coloured at room temperature by 50KeV electrons. The absorption peak designated "M" to the long wavelength side of the F band in curve (b) is attributed to the simplest of the F aggregate colour

FIG. 1.13.

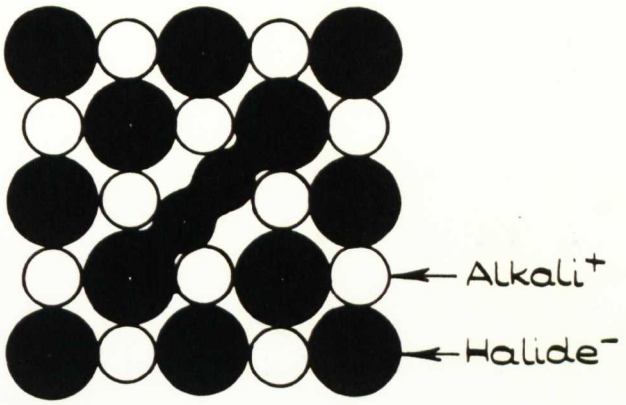

THE H CENTRE (42)

Fig. 1.14

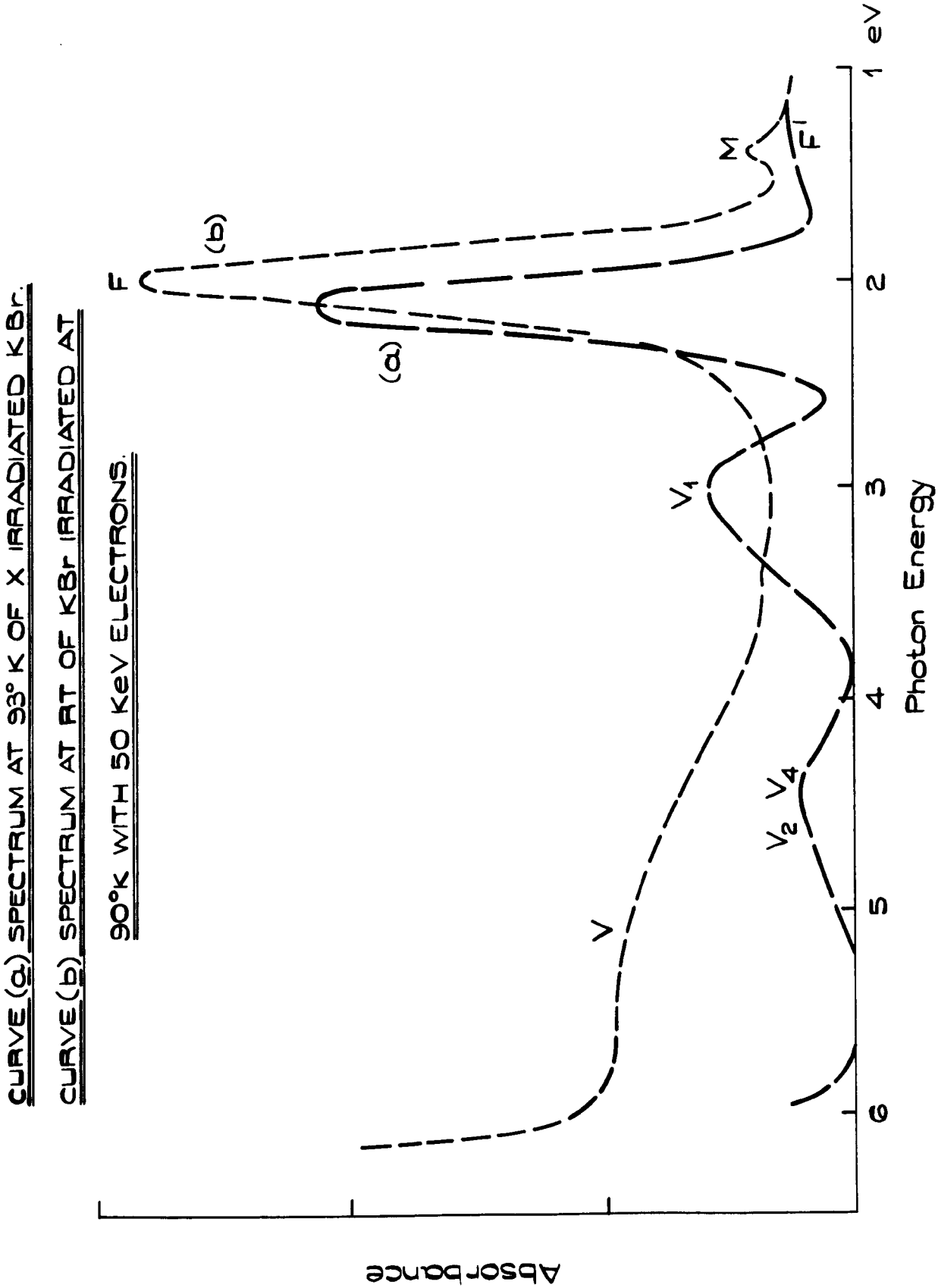
CURVE (a) SPECTRUM AT 93° K OF X IRRADIATED KBr.
CURVE (b) SPECTRUM AT RT OF KBr IRRADIATED AT 90°K WITH 50 KeV ELECTRONS.
Absorbance
Photon Energy
1 eV
2
3
4
5
6
F
(b)
(a)
M
F'
V
V1
V2
V4

centres. These consist of a number of adjacent halide ion vacancies sharing a number of electrons. Thus the M centre may be depicted (Fig.1.15) as two electrons trapped at a pair of adjacent anion vacancies. The next member of the series, known as the R centre, obviously consists of 3 nearest neighbour F centres, and this, and the higher order aggregates, can exist in a number of different configurations, which may lead to anisotropic absorption or a number of separate absorption bands, or both. Charged forms of F aggregate centres (e.g. M^+, two adjacent anion vacancies sharing one electron) can also exist, and these may give rise to further absorption bands.

The broad absorption band labelled F' in curve (a) of Fig.1.14 is attributed to a centre that consists of two electrons trapped at an anion vacancy. The F' centre is not stable at room temperature, but is readily formed in additively coloured crystals by illuminating them at about $-100^{\circ}C$ with F light. Models for the V centres whose absorption bands appear in Fig.1.14 are, in common with most other V centres, still very speculative, apart from the V_1 band, which is due to a defect that consists of an H centre adjacent to an impurity alkali ion.

The addition of impurity ions to an alkali halide crystal can cause colour centre phenomena not found in the pure material. For example, new colour centre absorption bands may be observed, due to the trapping of electrons or holes by impurity ions or impurity ion-vacancy complexes, or absorption bands normally found in the host lattice may be broadened and shifted in wavelength. Some impurities may also increase or decrease the colorability of the crystal. The hydride impurity is probably one of the best understood additives to an alkali halide crystal. Hydride doped crystals may be produced by growth from a melt that contains some alkali metal hydride, or by heating an additively coloured crystal in a hydrogen atmosphere. The hydride ion replaces a halide ion substitutionally in the lattice, and gives rise to an absorption band in the ultraviolet, which is known as the U band. (Fig.1.16) The height of the U absorption band is proportional to the amount of hydride impurity in the crystal.

FIG. 1.15

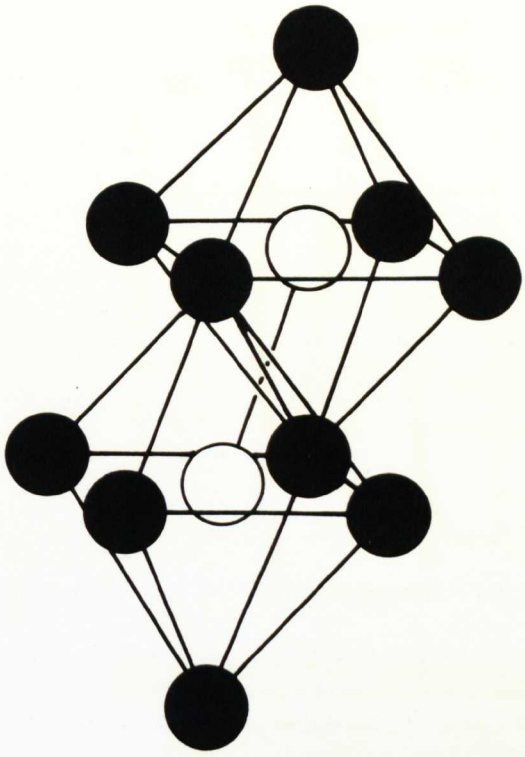

THE MODEL OF THE M CENTRE: TWO NEIGHBOURING HALOGEN ION VACANCIES WITH TWO ELECTRONS.

FIG. 1.16

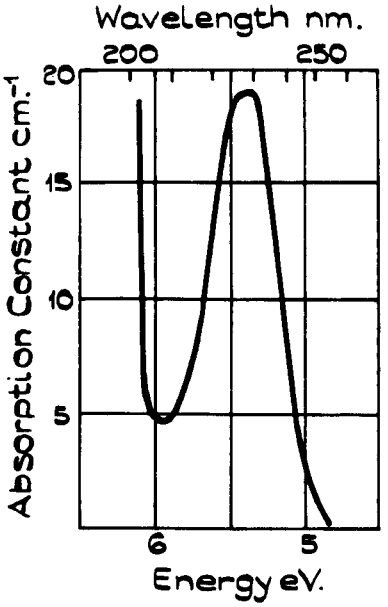

ABSORPTION SPECTRUM OF U CENTRES IN KBr[24].

When a crystal that contains U centres is illuminated with U band light, at temperatures below -100°C, the U band decreases and the F band is generated, without any external photocurrent being measured. (25) Raising the temperature to above 600°C converts the F centres back into U centres. The mechanism of the U→F conversion appears to be as follows: The excited state of the U centre, produced by light absorption, corresponds to a hydrogen atom and an electron shared by the nearest neighbour alkali metal ions. If the temperature is sufficiently high, the H atom diffuses away, into an interstitial position, to leave an F centre. Raising the temperature still further increases the mobility of the hydrogen atom, and hence the probability of the U→F conversion occuring. At temperatures below -100°C U band illumination appears to convert the U centres into vacancies and interstitial hydride ions, since the U band is observed to decrease and the α band grow. (The α band is a perturbation of the ultraviolet absorption edge caused by single negative ion vacancies). Illumination into the α band regenerates the U band, so presumably the interstitial hydride ions remain close to their complementary vacancies. (26)

The addition of impurities such as Tl^{+}, Ag^{+} and Pb^{++} have been found to be useful in the study of V centres, since they act as efficient electron traps and decrease the rate of electron-hole recombination. This effectively enhances the rate of V centre production.

Many other impurity bands in the alkali halides have been recorded, and it may be that some of the properties of the nominally "pure" alkali halides are due to impurities also. (The connection between the first stage of coloration and impurities has already been mentioned.) In particular the presence of hydroxyl ions (OH^{-}) is thought to be common in even the purest of synthetic crystals. (27,28)

For later reference a tabulation of some of the colour centres observed in KBr is given in Fig.1.17. As a conclusion to this very brief

FIG. 1.17.

COLOUR CENTRES IN KBr

Designation	Wavelength of Abs^{n} Peak nm	Temp. of Observation °K	Model
F	625	300	ELECTRON TRAPPED AT HALIDE ION VACANCY.
F^{1}	700	170	2 ELECTRONS TRAPPED AT A HALIDE ION VACANCY.
R_1 R_2	735 790	300 300	3 ELECTRONS TRAPPED AT 3 ANION VACANCIES.
M	918	300	2 ELECTRONS TRAPPED AT 2 ANION VACANCIES.
α	201	~90	PERTURBATION OF U-V ABSORPTION EDGE BY SINGLE VACANCIES.
β	192	~90	PERTURBATION OF U-V ABSORPTION EDGE BY F CENTRES.
H	380	4	$(HALIDE)_2^-$ MOLECULE-ION, SITUATED AT A SINGLE HALIDE ION SITE, ALONG WITH 2 ADJACENT HALIDE IONS, ALL LINED UP ALONG <110> DIRECTIONS.
$V_{[K]}$	385	77	HALOGEN MOLECULE ION X_2^- ORIENTED ALONG <110> CRYSTAL DIRECTIONS.
V_1	410	77	H CENTRE WITH ADJACENT IMPURITY ALKALI ION.
V_2 V_3 V_4	265 231 275	300 300 90	CONFIGURATIONS NOT CERTAIN, BUT LIKELY TO BE VARIOUS CLUSTERS OF H CENTRES.

background of colour centre phenomena in the alkali halides it is worth noting that the defect centres discussed in these paragraphs are true absorbing centres which do not exhibit light scattering. It is, however, very easy to produce small colloidal metal particles in such crystals, either by prolonged irradiation and aggregation of vacancy centres or slow cooling after additive coloration. These colloids do exhibit Tyndall scattering, and their obsorption bands may easily be distinguished from those due to colour centres by the fact that their spectral position and band width are temperature independent.

1.3 Colour Centres in Other Materials

Colour centre phenomena are not unique to the alkali halides, they may be observed in quite a large number of other materials. For example CaF_2, both natural and synthetic, exhibits strong absorption bands at visible wavelengths when it is exposed to ionising radiation or heated in Ca vapour. The coloration in CaF_2 is found to be particularly dependent on impurities, and on the method of coloration. The alkaline earth oxides BaO and MgO are also of interest, since they are structurally analogous to the FCC alkali halides. Additively colouring BaO by heating to 1000°C in an atmosphere of barium vapour produces blue crystals, whereas when grown from a melt containing Ba metal they are red. The centres responsible for the coloration in BaO, MgO and CaF_2 are still somewhat speculative although recently F, M, H and V_K centres were identified in CaF_2. The many varieties of natural quartz, fused silica and other glasses all exhibit colour centre phenomena in varying degrees, along with germanium and silicon. The coloration of Ge and Si is entirely in the infrared, and has marked effects on their electrical properties. Many natural minerals, besides those already mentioned, can be coloured by ionising radiation and a group of particular interest is the sodalites. The sodalites have the basic chemical composition $6Na\ Al\ SiO_4.2NaCl$, and have a crystal structure that consists of open aluminosilicate cages with Na^+ and Cl^- ions lying within the cages, such that the lattice has

overall cubic symmetry. The absorption band produced when a sodalite is exposed to ionising radiation is due to true F centres, i.e. electrons trapped at vacant Cl^- sites within the aluminosilicate cages (although in this case there are only 4 nearest neighbour Na^+ ions), and there does not appear to be any evidence to suggest that vacancy centres any more complex than this are formed. A more detailed account of the structure and general properties of the sodalite family is given in the introduction to Chapter 6 of this thesis.

1.4 Bleaching of Colour Centres in the Alkali Halides

When an alkali halide crystal containing F centres is illuminated at an appropriate temperature with F band light, the amplitude of the F absorption band decreases, a process which is not surprisingly referred to as bleaching. This decrease in amplitude of the F band is usually accompanied by changes in absorbance in other regions of the crystal spectrum, and it is found, moreover, that the products of bleaching are very much dependent on the method and temperature of coloration, and on the temperature at which bleaching is carried out. In particular, when crystals coloured by a stoichiometric excess of alkali metal are optically bleached at room temperature, pronounced absorption bands due to F aggregate centres appear, indicating that in some way vacancies have become mobile during bleaching. [29] The mechanism of colour centre bleaching in the alkali halides is thus fairly complex, but bleaching phenomena have received less attention and are not understood as well as the colour centre formation processes.

The earliest studies of the bleaching and aggregation of F centres were made in the 1920's by Przibram [30] and Ottmar [31], the latter making the first observations of the M band. It was Molnar [32], however, who first made a general survey of the absorption bands that appear when additively coloured crystals are illuminated with F light. Independently Pettroff [33] carried out investigations very similar to Molnar's, which

were not published until 1950. A general feature of bleaching observed by these and other workers was that F band bleaching occurs rapidly at first and then becomes increasingly difficult. Oberly [34] investigated the changes in photoconductivity that occur when the F band in X irradiated KBr is optically bleached. He came to the surprising conclusiom that there were two types of colour centre responsible for the F band absorption, "soft" centres that bleached and were photoconductive and "hard" centres that were neither bleachable nor photoconductive. This idea was refuted soon after by Markham [35], who was able to explain most of Oberly's results in terms of only one type of F centre, although these and other workers were severly hindered in their explanations by the lack of correct models for the M,R and N centres formed during bleaching.

During the ten years following Oberly's work there seems to have been little interest shown in the detailed investigation of the bleaching of colour centres, possibly because of the lack of satisfactory models for most of the defect centres observed, and the fact that the coloration process itself was not all that well understood. Over the past ten years, after Pick [36] and van Doorn [43] proposed plausible models for the F aggregate centres, there have been a number of systematic examinations of the bleaching processes that occur in the alkali halides. These experiments have been conducted on crystals that were coloured either additively or by X irradiation, to F centre densities of approximately $10^{16} cm^{-3}$. Moreover, relatively weak sources of F band light were used, necessitating long exposures in order to achieve a significant reduction in F band optical density [37,38].

The development of the laser over the last decade has made available compact, high intensity, monochromatic light sources, which are ideally suited to studying the kinetics of F centre bleaching, with the obvious proviso that the laser wavelength must coincide with, or at least lie fairly close to the wavelength of the peak of the F absorption band in the

material being studied. In particular the helium neon gas laser, with its output at 632.8nm., is eminently suitable for bleaching coloured KBr, which has an F band centred about 625nm. at room temperature. Furthermore, whilst the other types of laser (argon ion, krypton, He-Cd etc.) have emission lines which closely match the wavelengths of the F band peaks in a number of alkali halides, the reliability, stability and relative cheapness of the He-Ne laser further encourages its use in bleaching studies.

An alkali halide (KCl) coloured by fast electron irradiation was the basis of a rader display device, known as the skiatron, invented nearly 30 years ago [39], and it is likely that future optical data storage and display devices based on the alkali halides and other materials will also utilise fast electron irradiation as the means of coloration[40,41]. The radar information stored in the skiatron could be erased by illuminating the warmed KCl screen, and any new devices will probably also rely on optical bleaching for erasing the information display. However, there has been relatively little investigation into the kinetics of bleaching of electron irradiated material; as was previously stated most of the detailed studies of the subject have been carried out with crystals coloured additively or by X irradiation. The obvious difference between room temperature electron and X irradiated material is their F centre densities; X rays produce fairly uniform coloration throughout the crystal, with defect concentrations typically around 10^{16} F centres cm^{-3}, whereas electrons, having only a short range in the material, produce a surface coloration that ranges from 0.5 to 400 μm. for electron energies of 5 to 400 KeV respectively with F centre densities from 10^{18} to more than 10^{19} cm^{-3}. Also the rate of energy deposition is much higher for electrons than for X rays. The successful use of an alkali halide crystal as the storage medium in a memory device depends to some extent on the efficiency of bleaching, and on the products of bleaching, since the aggregation of

F centres to more complex entities can lead to fatigue and ultimately, to the failure of the memory due to the formation of metal colloids which cannot be removed by illumination. There is, therefore, a need for detailed investigation into the kinetics of optical bleaching of fast electron coloured alkali halide crystals, and the experiments to be described in this thesis do, to some extent, satisfy that need.

The investigations cover the optical bleaching, at room temperature, of KBr single crystals which have been coloured at room temperature or below by irradiation with electrons having energies within the range 40 to 50 KeV. A helium neon laser was used as the light source for bleaching; this particular combination of alkali halide and laser was chosen for the reasons given earlier. The output of the laser could be focused onto the specimen to give power densities of up to 10 $KWcm.^{-2}$, some 10^6 times larger than those used in previous experiments. It was thus possible to study optical bleaching phenomena under high intensity illumination and after large absorbed doses of F light, in crystals initially having colour centre concentrations of 10^{18}-10^{19} cm^{-3}. Information was thus gained on interactions between defects at high defect concentrations and on a new mode of bleaching that does not occur in additively coloured crystals.

Some experimental data was also obtained on the coloration and bleaching properties of sodalites, which were briefly mentioned in section 1.3. Most of these measurements were made using a specially manufactured dark trace cathode ray tube, with an aluminised sodalite powder screen. The bleaching sensitivity of the sodalite was much higher than that of KBr, consequently it was possible to use a conventional tungsten light source for bleaching, instead of a laser. These experiments are described in Chapter 6, which also contains further background details on the sodalites.

References

(1) von Hippel, A.R., Molecular Science and Engineering, John Wiley, New York. (1959) Chapter XII by A. Smakula.

(2) Lawson, W.D. and Nielsen, S., Preparation of Single Crystals. Butterworth's Scientific Publications, London. (1958)

(3) Eby, J.E., Teegarden, K.J. and Dutton, D.B., Phys. Rev 116 1099 (1959)

(4) Price, W.C. and Wilkinson, G.R., Infrared Physics, Oxford University Press, (1966)

(5) MacMahon, A.M., Zeits. f. Physik, 52, 336 (1928)

(6) Pick, H. and Weber, H., Zeits. f. Physik 128, 409 (1950)

(7) Mapother, D., Crooks, H.N. and Maurer, J., J. Chem. Phys., 18 1231 (1950)

(8) Kelting, H. and Witt, H., Z. Physik, 126, 697 (1949)

(9) Ivey, H., Phys. Rev. 72, 341 (1947)

(10) Russell, G.A. and Klick, C.C., Phys. Rev. 101, 1473 (1956)

(11) de Boer, J.H., Rec. Trav. Chim. Pays-Bas, 56, 301 (1937)

(12) Kip, A.F., Kittel, C., Levy, R.A. and Portis, A.M., Phys. Rev. 91, 1066 (1953)

(13) Feher, G., Phys. Rev. 105, 1122 (1957)

(14) Smakula, A., Zeits. f.Physik 59, 603 (1930)

(15) Dexter, D.L., Phys. Rev. 101, 48 (1956)

(16) Pooley, D. and Runciman, W.A., Solid State Commun. 4, 351 (1966)

(17) Estermann, I., Leivo, W.J. and Stern, O., Phys. Rev. 75, 627 (1949)

(18) Crawford, J.H., Advances in Phys. 17, 93 (1968)

(19) Pooley, D., Solid State Commun. 3, 241 (1965)

(20) Torrens, McC. and Chadderton, L.T., Phys. Rev. 159, 671 (1967)

(21) Rabin, H. and Klick, C.C., Phys. Rev. 117, 1005 (1960)

(22) Nowick, A.S., Phys., Rev., 111, 16 (1958)

(23) Sibley, W.A. and Russell, J.R., J. Appl. Phys., 36, 810 (1965)

(24) Schulman, J.H. and Compton, W.D. Colour Centres in Solids 164, Pergamon Press (1963)

(25) Martienssen, W. Zeits. f. Physik 131, 488 (1952)

(26) Thomas, H., Ann. Physik, 38, 601 (1940)

(27) Rolfe, J., Phys. Rev. Letters 1, 56 (1958)

(28) Etzel, H.W., and Patterson, D., Phys. Rev. 112, 1112 (1958)

(29) Compton, W.D. and Rabin, H., Solid State Phys. 16 121 (1964)

(30) Przibram, K., Sitzber. Akad. Wiss. Wien. 135, 202 (1926)
& Z. Physik 130, 269 (1951)

(31) Ottmar, R, Z. Physik 46, 798 (1928)

(32) Molnar, J.P., Thesis (unpublished) M.I.T. (1940)

(33) Petroff, St. Zeits. f. Physik 127, 443 (1950)

(34) Oberly, J.J., Phys. Rev. 84, 1257 (1951)

(35) Markham, J.J., Phys. Rev. 86, 433 (1952)

(36) Pick, H., Zeits. f. Physik 159, 69 (1960)

(37) Bron, W.E., Phys. Rev. 119, 1853 (1960)

(38) Bron, W.E. and Heller, W.R., Phys. Rev. 119, 1864 (1960)

(39) King, P.G.R. and Gittins, J.F., I.E.E. Journal 93,822 (1946)

(40) Tubbs, M.R. and Wright, D.K., to be published.

(41) Taylor, M.J. Phys. Bull. 21, 485 (1970)

(42) Känzig, W. and Woodruff, T.O., J. Phys. Chem. Solids, 9, 70 (1958)

(43) van Doorn, C.Z. and Haven, Y., Philips Res. Repts. 11, 479 (1956)

(44) van Doorn, C.Z., Philips Res. Repts. 12, 309 (1957)

CHAPTER TWO

EXPERIMENTAL TECHNIQUES

2.1 The Design of the microspectrophotometer

An apparatus for studying colour centre bleaching with high intensity light in samples coloured to high F centre concentrations would, ideally, allow one to both measure the absorption spectrum of a coloured crystal and simultaneously bleach the coloration with a high intensity F band light source. It should, moreover, provide for precise measurement of the energy absorbed by the crystal during bleaching. It is also important that the intensity of the measuring source should be as low as possible (consistent with a reasonable signal to noise ratio) so that the measuring light would cause no significant bleaching. An apparatus having these general design features was successfully constructed, and will now be described in more detail.

(i) The Bleaching Source

For a particular matched laser/absorption band combination, a laser bleaching source offers the distinct advantages of a high optical power density in a parallel monochromatic beam, making it relatively easy to obtain measurements, in suitable materials, over as wide a range of absorbed energies as possible, going, if required, up to 10^6 or 10^7 J.cm^{-2} in a reasonable period of time.

Our experiments were designed for bleaching using a helium-neon gas laser to study the bleaching of F centres in potassium bromide single crystals. A low and a medium power laser were available; both were manufactured by Scientifica and Cook Electronics and gave output powers, at 632.8 nm., of $\frac{1}{2}$ - 2 mW. and 15 - 25 mW. The 25 mW. device lased in a single mode pattern and gave a less divergent, more stable output than the low power laser, which had to be operated in a multi-mode fashion to obtain maximum power. The beam diameter, of both lasers, was of the order of 2 - 3 mm. To obtain the power densities necessary for measurements to be made, in a reasonable time, to absorbed energies up to 10^7 J. cm.$^{-2}$ it was necessary to reduce the beam diameter

to less than 10^{-2} cm., without appreciable power loss. A Vickers Microplan 10X objective, with a nominal N.A. of 0.25, was chosen for this purpose. It would focus the laser beam down to a spot about 2×10^{-3} cm. in diameter, to give a maximum power at the specimen of about 3.5×10^{3} W.cm^{-2} (this figure includes various reflection losses at other optical components used in the system). Measurement of the spot size was carried out with an auxiliary microscope and stage micrometer. The diameter of the focused laser spot is much larger than one would expect, since the diameter of the first dark ring of the Airy disc is only $\sim 2.5 \mu$m. for red light brought to a focus by an objective of numerical operture 0.25. However, the effective N.A. of the 10X objective is reduced to a value of $\sim$ 0.07, because the laser beam fills only the central part of the lens aperture and is parallel rather than divergent. This increases the estimated diameter $\left(\sim \frac{\lambda}{\text{N.A.}}\right)$ of the first dark ring of the Airy disc to approximately 10 μm , which is of the same order of magnitude as that of the measured spot. By changing the 10X objective for one of greater magnification, higher power densities could have been obtained, but difficulties would then have been experienced in timing the short exposures needed at the start of the experiments, and with the depth of focus and working distance.

The penetration depth of the coloration in the crystal can also impose a limit on the numerical aperture of the objective lens. If a lens of very short focal length (i.e. high N.A.) were chosen, the laser beam would diverge appreciably whilst passing through the coloured region of the crystal (Fig. 2.1). This would make it difficult to assess absorbed energy and transmittance. Using the expression [1]

$$d = 0.035 \, (V)^{1.7} \; \mu \text{ m.}$$

to calculate the penetration depth, where V is the acceleration voltage of the electron beam in KV., one finds that at 50 KV. d is $\sim$ 27 μm. in KBr. In normal use the depth of focus of the chosen 10X (0.25 N.A.)

FIG. 2.1.

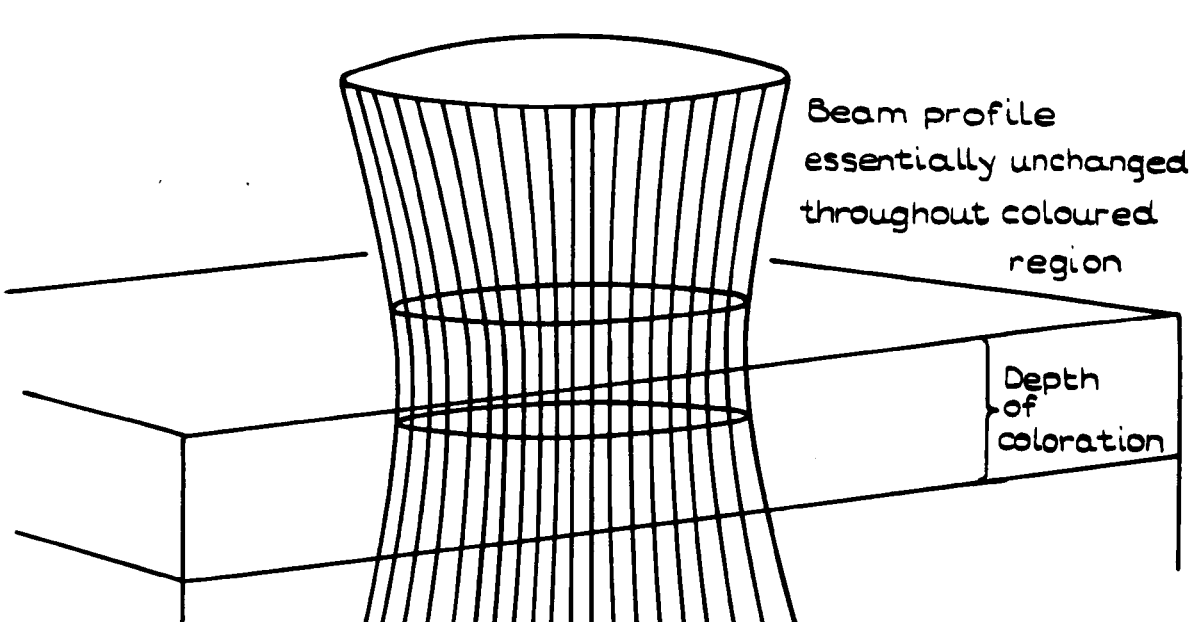

MODERATE BEAM DIVERGENCE.

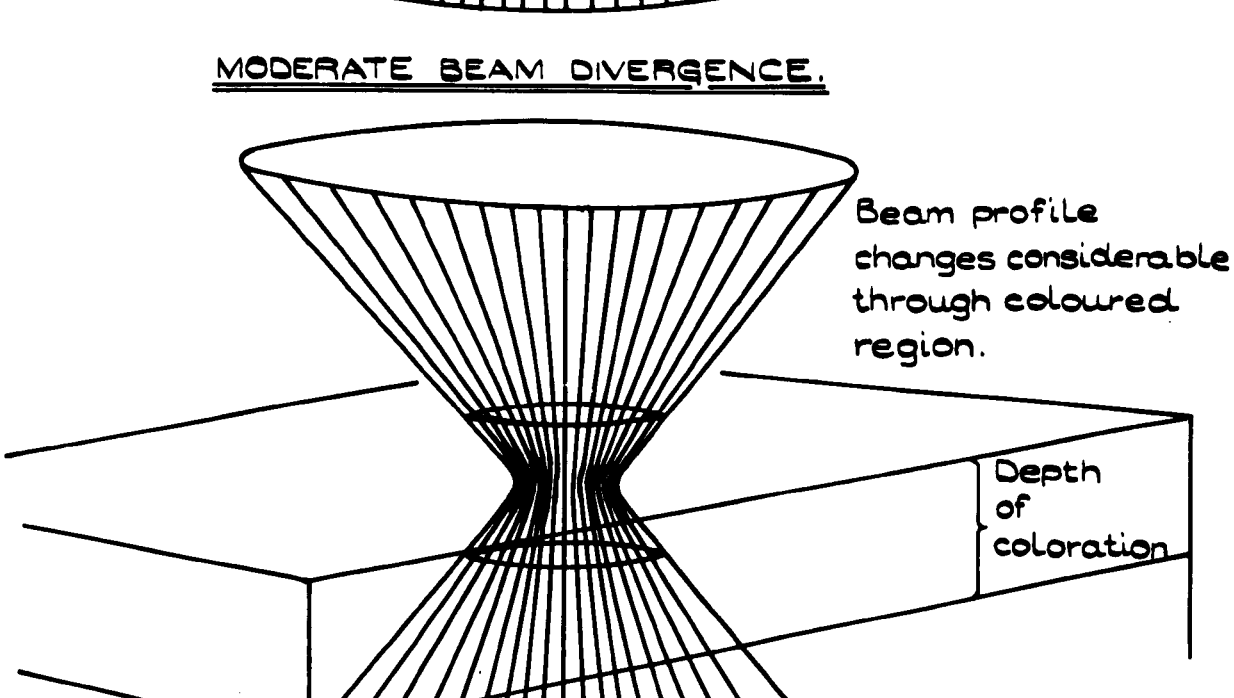

APPRECIABLE BEAM DIVERGENCE USING A LENS OF HIGH MAGNIFICATION.

objective is 12 μm. (from the Rayleigh criterion for the depth of focus $\sim \lambda/(\text{N.A.})^2$), but due to the reduction in N.A. caused by the laser beam not filling this lens completely, it is increased to $\sim$130 μm. There will, therefore, be no significant change in the diameter of the laser beam as it travels through the coloured region of a crystal irradiated by 50 KeV electrons. As a simple check on the validity of this assumption, a crystal was coloured by 25 KeV electron irradiation and bleached by the focused laser beam. Despite the fact that the depth of coloration was now only 7 μ m., the characteristics of the bleached areas (i.e. diameter and coloration profile across the diameter) in this case were no different to those of similarly bleached areas in the normal 50 KeV irradiated specimens. One would clearly not expect to find such a close correspondence if the laser beam diverged by a significant amount in the 27 μ m. coloration depth of the 50 KeV irradiated specimens.

A Compur shutter assembly was used to govern the time of exposure of the crystal to laser light; this could be varied from $\frac{1}{500}$ second up to an hour or more using the "time" setting. The higher speed settings of the shutter were calibrated using a photocell and C.R.O. The power output of the laser could be measured with a Scientifica and Cook Electronic's power meter; it's output, directly calibrated in milliwatts at 632.8 nm., could be fed into a chart recorder to give a continuous record of laser power.

(ii) The Spectrophotometer

Having made the decision to use a focused He/Ne laser for bleaching, it was necessary to design a spectrophotometer system for measuring the absorption spectra of the specimens, bearing in mind the restrictions imposed on this system by the bleaching arrangement. The most severe limitation was, quite obviously, that the spectrophotometer should only measure the transmittance of that part of the coloured crystal through which the laser beam had passed. Hence the beam diameter

at the specimen needed to be less than 2×10^{-3} cm., and its position readily adjustable. Clearly the best way to ensure that this was so was to make the laser and photometer beams coaxial by using a beam splitter, and then focus them onto the specimen through the same optical system.

The spectroscopic examination of a small, well defined area of a specimen is known as microabsorption spectroscopy. This technique has been used for some time in the study of biological materials, but only recently has it been applied to thin single crystals [2]. Basically there are two different ways in which a microspectrophotometer can be designed for the study of the laser bleaching of electron irradiated KBr. These are as follows:

(a) With the monochromator placed in the photometer beam before it passes through the specimen, so that the selected area is under monochromatic illumination.

(b) With the monochromator placed after the specimen, with a photomultiplier tube coupled directly to the exit slit. In this case the specimen receives white light illumination.

The first case is desirable from the point of view of minimising the amount of light reaching the crystal from sources other than the bleaching laser. It does, however, make the layout of the apparatus somewhat complicated, since the monochromator has to be positioned so that the laser beam does not pass through it, i.e. before the laser and spectrophotometer beams are made coaxial. It also makes it more difficult to block the high intensity laser beam from the photomultiplier tube.

The second case, with the monochrometer situated after the specimen, was finally chosen. It yielded a system that was simple in design and reasonably easy to use; the fact that more of the measuring light reached the specimen with this arrangement did not appear to adversely affect the accuracy of the results. This is because the intensity of the measuring light was very much less than that of the

bleaching light, and the F centre bleaching efficiency at wavelengths away from the F band is never appreciably larger than its value at the F band peak.

As pointed out by Tubbs [2], whichever arrangement is used, two conditions need to be met if quantitative results are to be obtained:

(i) The photometric photomultiplier tube must receive all of the light passing through the chosen region of the specimen and no light from any other area.

(ii) All rays passing through the selected area of the specimen should have the same optical path length in the specimen.

Having chosen to use the second experimental configuration, with the monochromator placed after the specimen, it is apparent that the first condition can be partly met by ensuring that all of the light leaving the specimen is collected by the lens that focuses it onto the monochromator slit. In addition to this, the aperture in front of the light source must be faithfully imaged onto the coloured crystal surface by the first (10X) objective, and again by the second lens onto the monochromator slit. It is also necessary to ensure that the intensity and coloration distributions across this primary aperture are even. Condition (ii) can be satisfied either by using small condenser lens apertures or specimens with high refractive indices. KBr has only a moderate refractive index (1.55), so condition (ii) is best satisfied by using an objective with a fairly low numerical aperture to focus the spectrophotometer beam onto the specimen. (Using a 0.25 N.A. objective there is<1% difference between the path lengths of axial and marginal rays in KBr). It is apparent, therefore, that both of the conditions for quantatitive microabsorption spectroscopy in KBr can be met without resorting to the use of specially manufactured optical components.

The choice of whether to make the spectrophotometer a single or double beam instrument also had to be made; schematic diagrams of both types are illustrated in Fig. 2.2.

FIG. 2.2.

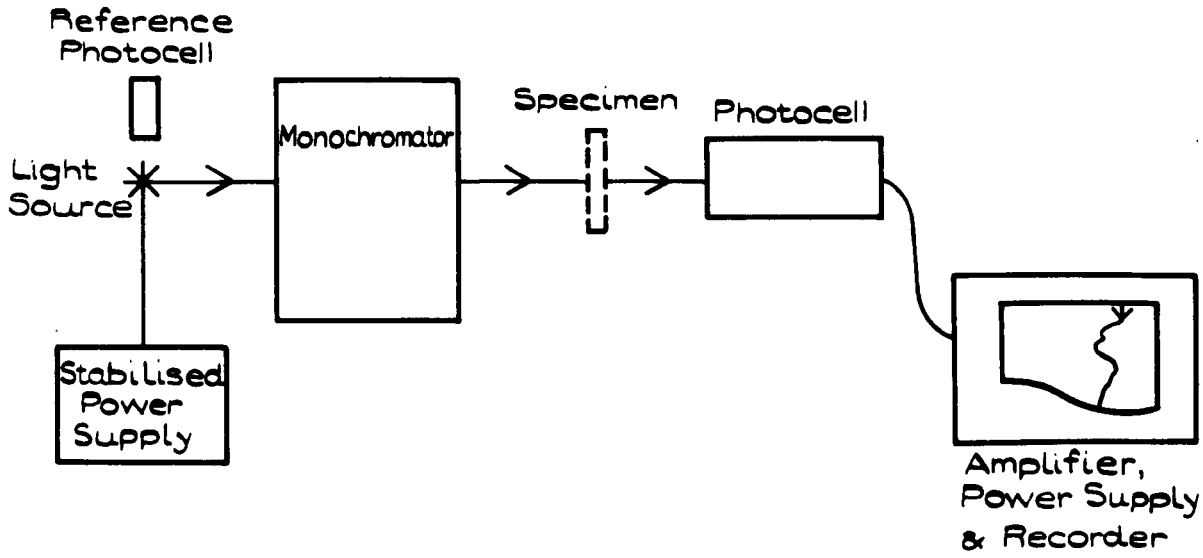

SCHEMATIC DIAGRAM OF A SINGLE BEAM SPECTROPHOTOMETER.

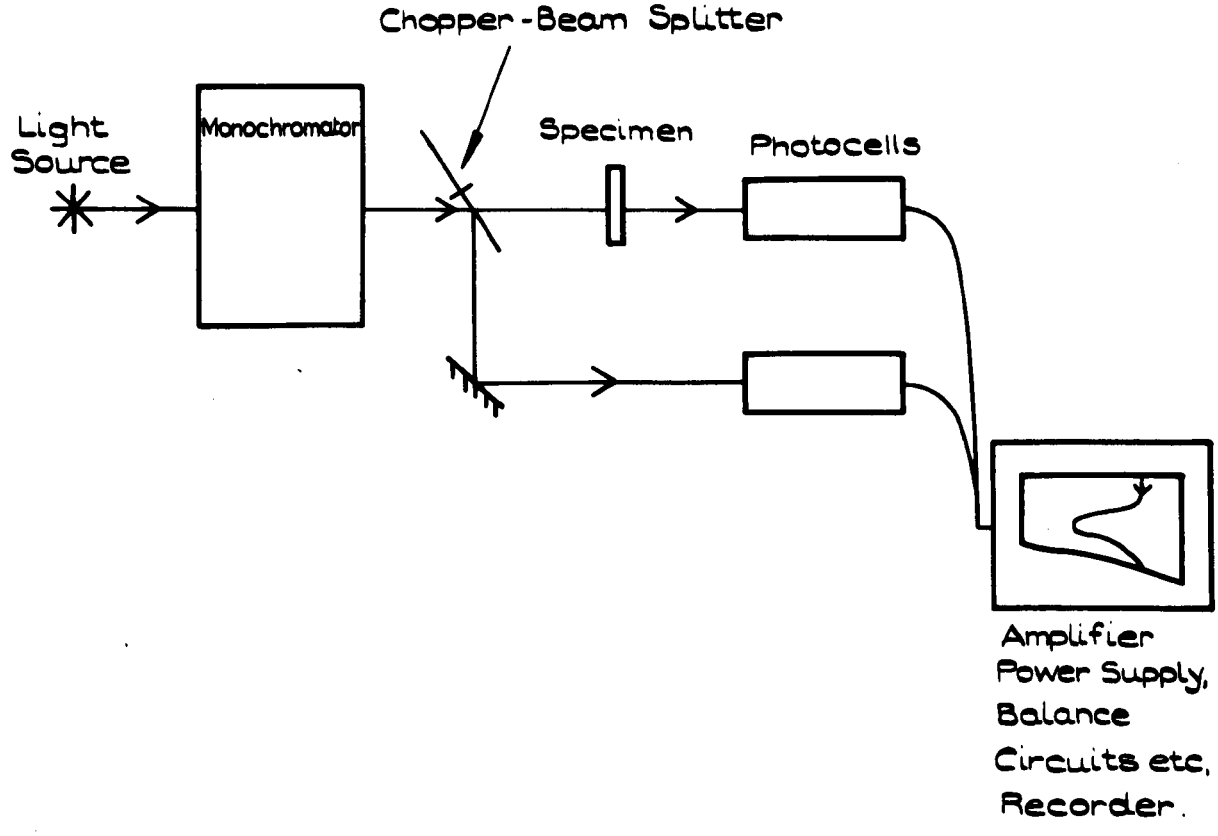

SCHEMATIC DIAGRAM OF A DOUBLE BEAM SPECTROPHOTOMETER.

The double beam spectrophotometer has a separate, 100% transmittance, reference beam, and will thus give, with suitable electronic circuitry, an output that is the percentage transmittance (or the absorbance) spectrum of the specimen, i.e. it is a direct reading device. It does, however, suffer from the disadvantage of being difficult to set up and balance to give the required flat baseline in the absence of a specimen. (i.e. zero absorbance).

On the other hand, the single beam instrument is relatively simple to set up and requires fewer components, and less sophisticated electronic equipment, but is not a direct reading instrument. The absorption spectrum of a specimen has to be calculated point by point from the outputs obtained by scanning through the wavelength range with and without the sample in the beam. Producing a spectrum is therefore a fairly lengthy process, involving numerous simple, if rather tedious, calculations. One also must have greater stability of the light source and photomultiplier assembly, since the 100% transmittance level is not being continuously monitored, and fluctuations automatically corrected for, as they would be in a double beam instrument.

With careful design, however, the overall performance of both types of spectrophotometer should be comparable, and the only real advantages to be gained by a double beam instrument are simplicity and the convenience of a continuous record of absorbance versus wavelength. For these reasons most commercial instruments are of the double beam type.

A simple single beam spectrophotometer was finally decided upon, because the system had to be designed and constructed from first principles, with quite stringent conditions imposed on the optics. Not only were mechanical stability and beam diameter critical, but also the laser bleaching beam had to be introduced into the system without adversely affecting the measurements. Some important design features of the microspectrophotometer system about to be described were:

(i) At the specimen the spectrophotometer beam diameter must be less than the diameter of the laser bleaching beam. i.e. $< 2 \times 10^{-3}$ cm. In the final instrument it was ~ 10 μ m.

(ii) If the beam diameter is to be that required (i), the previously mentioned conditions imposed on microabsorption spectroscopy systems must be satisfied. These were satisfied by careful optical alignment etc., and the use of fairly small condenser lens apertures with specimens of medium refractive index.

(iii) There must be a fine, precise adjustment of the position of either the spectrophotometer beam, or the laser beam, or both, to enable them to be made concentric. This was provided by mounting the primary aperture of the spectrophotometer system in a special holder, with vertical and horizontal positioning screws.

(iv) Some adjustment of the specimen position be provided, in a plane perpendicular to the direction of the laser and spectrophotometer beams. In the final design the specimen crystal was mounted in a carrier which provided the desired movement.

(v) If spectrophotometry is to be carried out simultaneously with bleaching, the laser beam must be excluded from the detector when the monochromator scans through the laser wavelength. Alternatively, if bleaching is not to occur concurrently with spectral measurement, it must be verified that the absorbance of the specimen does not change when the laser beam is interrupted. (It is possible that the intensity of the focused laser beam would be sufficiently high to cause a significant population of F centre excited states, which would lead to the measurement of a reduced F band absorbance.) This condition may be checked by measuring the F band absorbance of a coloured specimen using the spectrophotometer (with the laser off), and comparing it

with that measured by monitoring the transmitted laser power. No difference could be found between the two measured optical density values at the highest laser power available ($\sim$ 10KW cm.$^{-2}$), and so the alternative system, of interrupting the laser beam during spectral measurement, was used.

(vi) The mechanical and electrical stability of the system must be high. This was achieved fairly easily, by careful mechanical design, and the use of stable electrical supplies and amplifiers.

(vii) The intensity of the spectrophotometer beam must be sufficiently low not to cause any bleaching of the specimen on it's own. In the instrument to be described, exposing a coloured crystal to the spectrophotometer beam for 10 minutes produced a change in coloration that was insignificant compared to that produced by a $^{1}/_{500}$ second exposure to the laser.

(viii) The apparatus must be capable of scanning the entire visible region of the spectrum, and if possible part of the near infra red and ultra violet, in a fairly short time. The final instrument could scan from 250 to 1000 nm. in about 3 minutes.

(ix) The specimen be mounted in a holder such that its temperature may he held constant at a predetermined value within the range 80^{o}K to room temperature and above. It is particularly important that the temperature of the illuminated area of the specimen does not change during bleaching. This was accomplished by mounting the specimen in a specially designed annular cryostat.

(x) The levels of scattered light in the spectrophotometer optics, and in the monochromator, must be low. This is to avoid photometric errors, and errors in wavelength measurement. In the final system scattered light was kept to a minimum by the use of baffles etc., and good photometric accuracy achieved.

2.2 The Microspectrophotometer in its Final Form

A schematic diagram of the apparatus used to obtain much of the experimental data presented in this thesis appears in Fig. 2.3.

All of the optical components were mounted on a rigid, cast metal optical bench, resting on a standard laboratory table. The laser was also free standing, on a similar table placed at right angles to the main optical system. After the initial alignment the baseplates of the kinematic slides carrying the monochromator and the specimen holder assembly were screwed to the table top. No vibrational difficulties were encountered with this set up; no special precautions were needed with the tables, they stood directly on the concrete floor. Fig 24 is a photograph showing the general layout of the components making up the apparatus shown diagramatically in Fig. 2.3, these will be described, where necessary, in more detail in the following paragraphs.

The specimens were mounted in a holder that was a simplified version (for use with refracting objectives) of the annular liquid nitrogen cryostat described by Tubbs [2] (Fig. 2.5). This cryostat permitted the 10X microscope objectives to be moved close enough to the specimen to be within their working distances, a more conventional design would not have allowed this. The cryostat rested in a carrier that formed part of the kinematic cross slide assembly, shown in Fig. 2.6, that enabled one to make precise adjustment of the specimen position relative to the laser and spectrophotometer light beams. Height adjustment was provided by a screw which pushed the carrier vertically on two silver steel pillars; these pillars were screwed into a baseplate which formed the moving part of the ball, plane and groove kinematic slide. A micrometer adjustment on the baseplate provided a means of rotating the cryostat about a vertical axis, to ensure that the light beams were perpendicular to the crystal. The adjustment was carried out by reflecting the laser beam from the backplate of the specimen holder, against which the crystal was clamped, and using the micrometer

Fig. 2.3.

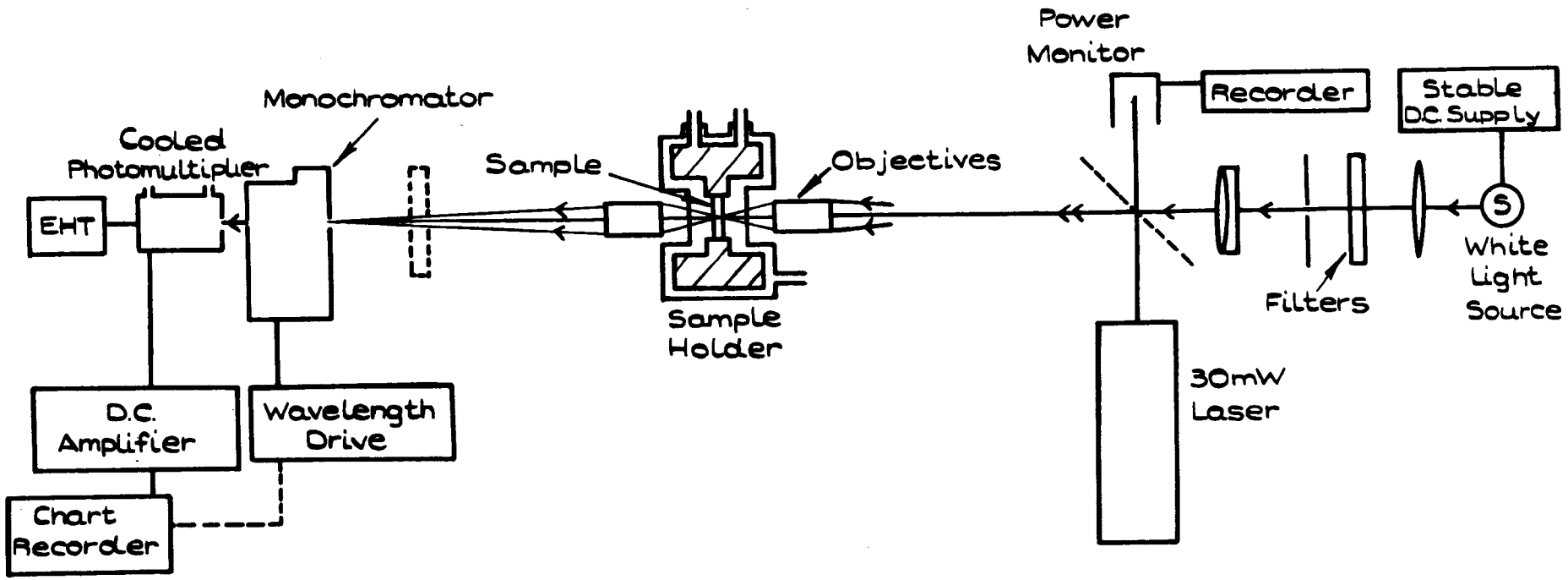

SCHEMATIC DIAGRAM OF THE MICROSPECTROPHOTOMETER.

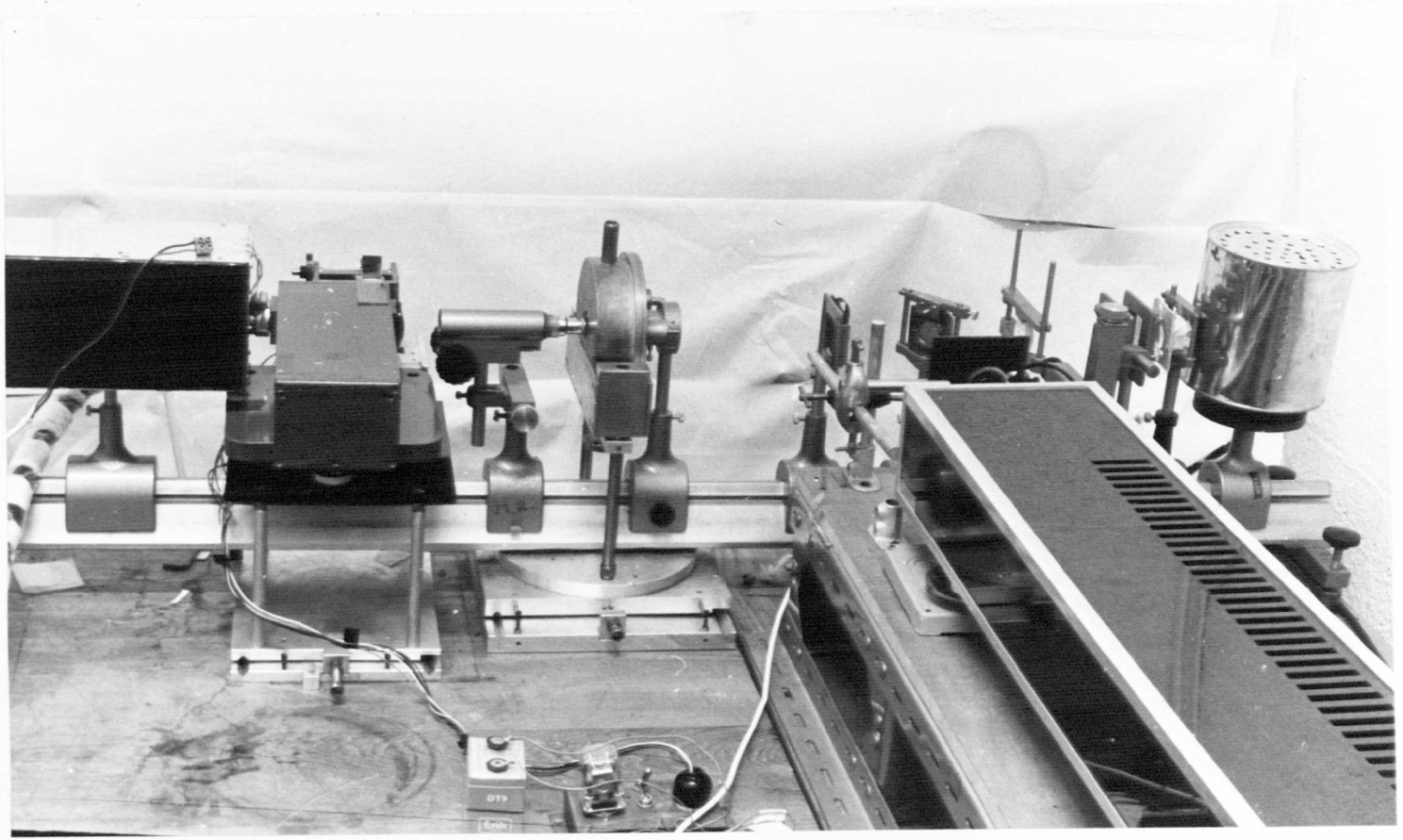

GENERAL VIEW OF THE MICROSPECTROPHOTOMETER.

FIG. 2.5.

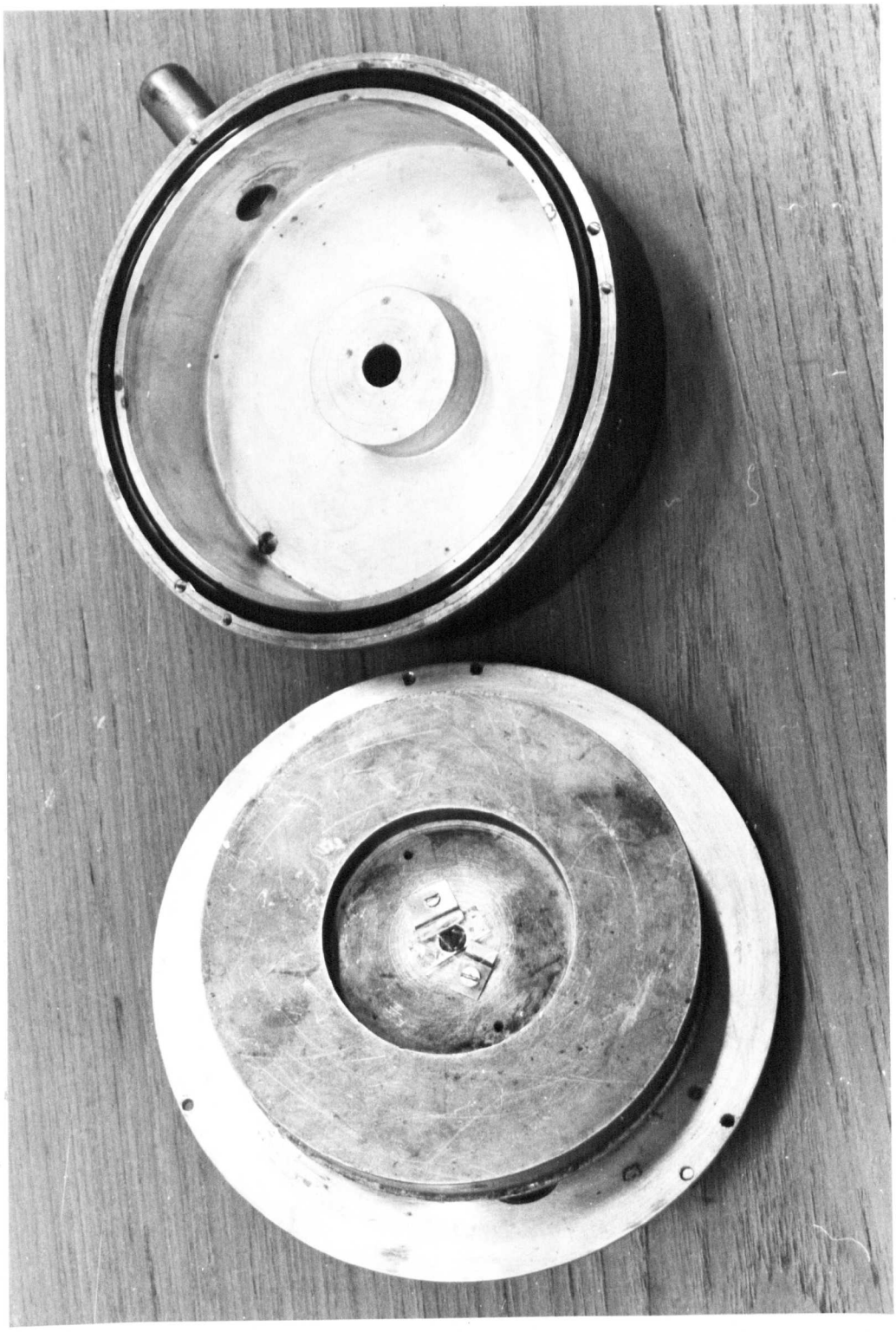

THE ANNULAR CRYOSTAT, USED AS A SPECIMEN HOLDER.

FIG. 2.6.

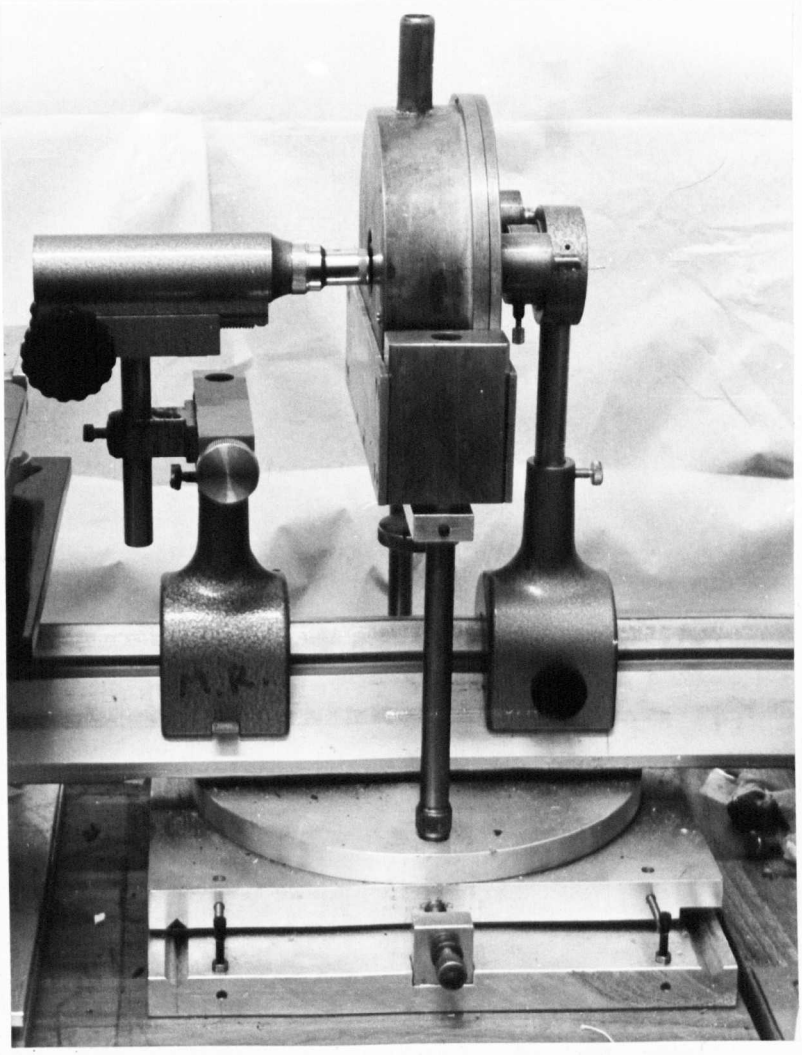

THE CRYOSTAT IN ITS CARRIER, WITH THE 10X OBJECTIVE LENSES IN POSITION.

to make the incident and reflected beams coincident. The specimen holder, mounted in the cross slide, was driven perpendicularly across the optic axis by a small screw, against return springs.

The monochromator was a Hilger and Watts type D292. This is a small, inexpensive grating instrument, covering the wavelength range 200 to 1000 nm. The replica diffraction grating had 576 rulings per millimetre, and the slit width could be adjusted, by a micrometer screw thread, to a maximum of 1 mm. The aperture of the device, about 11, was quite sufficient for this application. The monochromator rested on a kinematic cross slide, of simpler design than that used for the specimen holder. Vertical height adjustment was provided on the instrument itself, and no rotation about the vertical axis was necessary, so that only a basic horizontal motion, in a plane perpendicular to the optic axis was needed. The monochromator grating drive knob was removed, and a small synchronous motor and gearbox assembly fitted in its place (Fig. 2.7), in order to provide a continuous wavelength scan when required. The drive unit also momentarily closed a contact set every 10 nm., to give a wavelength mark on the output chart recorder. The pentaprism mounted over the wavelength scale is simply to enable the latter to be read at a distance, without risk of disturbing or vibrating the apparatus.

The light source for the microspectrophotometer was a Philips prefocus projector bulb, rated at 8 volts 50 Watts. In order to achieve high output stability and long life it was fed from a 5 volts a.c. stabilised power supply (Fig. 2.8). The addition of a bridge rectifier and large reservoir capacitor greatly decreased the long term stability of the light output, due, apparently to rectifier heating. A feed back stabilised d.c. power supply of adequate rating was not available to see whether this would improve the stability and noise level.

The lamp filament was focused onto an electron microscope aperture of $\sim$ 80 μ m. diameter, which acted as the primary aperture

Fig. 2.7.

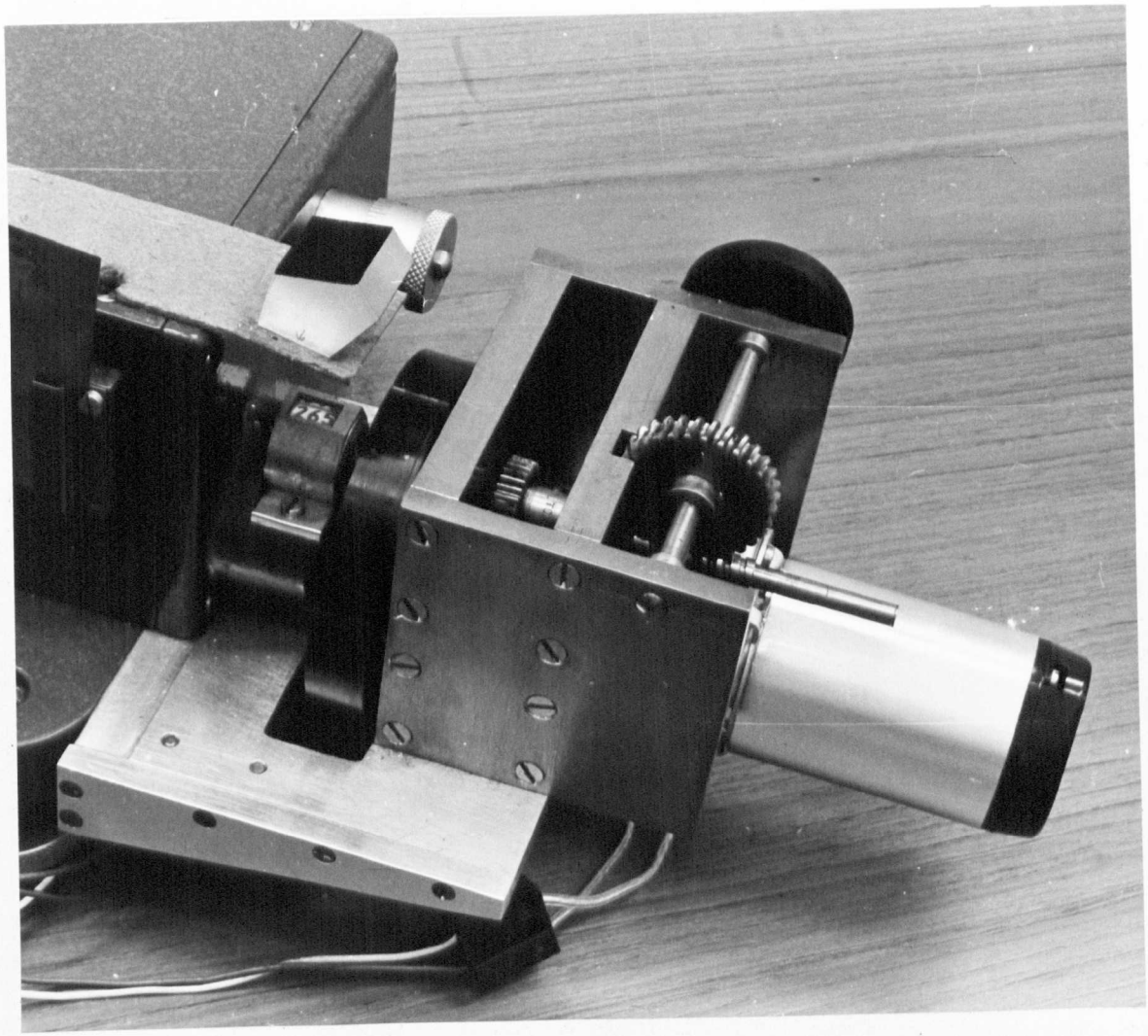

THE MONOCHROMATOR DRIVE UNIT.

FIG. 2.8.

THE POWER SUPPLY FOR THE MICROSPECTROPHOTOMETER LIGHT SOURCE.

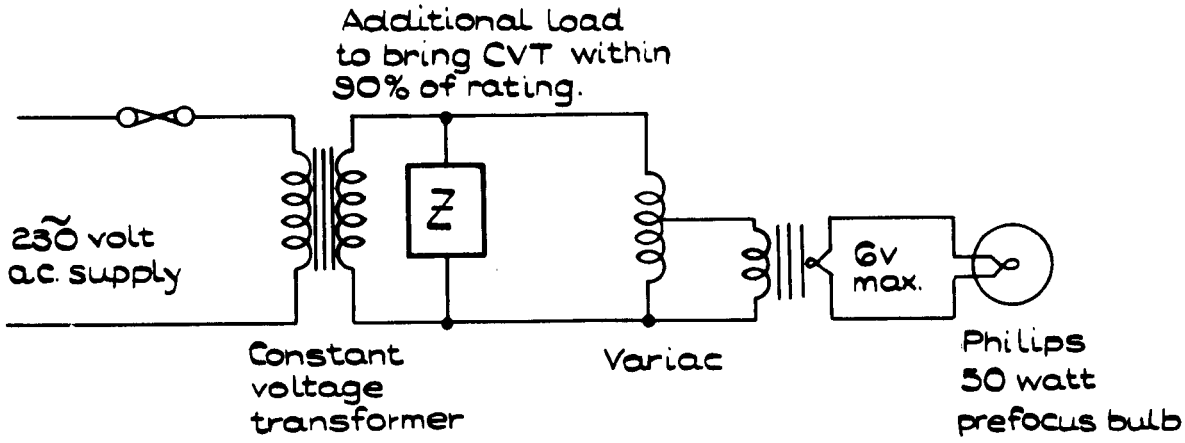

of the microspectrophotometer system. Precise positioning of the aperture was achieved by mounting it in a holder which gave horizontal and vertical motion in a plane perpendicular to the optic axis (Fig. 2.9). The evenly illuminated aperture was focused onto the specimen surface by a 10X microscope objective and an auxiliary achromatic lens. This microscope objective, and the one focusing the spectrophotometer beam onto the monochromator entrance slit, were, Vickers Microplan components, screwed into standard focusing mounts. The first microscope objective was not operating under the conditions for which it was designed (Fig. 2.10), since the light from both the laser and the spectrophotometer was nearly parallel. (The purpose of the auxiliary achromat near the primary aperture of the spectrophotometer was to render the spectrophotometer beam nearly parallel, and to assist in focusing the photometer beam on the specimen after the laser beam had been focused.) However, the spherical aberration of this arrangement was not serious enough to warrant using additional lenses so that the objective operated in the standard configuration.

The laser beam was introduced into the system by a 45° beam splitter between the objective and achromatic lenses; the power monitor was placed behind it to collect the transmitted beam, and thus give a continuous recording of laser output.

Fig. 2.11 illustrates the "front end" of the microspectrophotometer system. The system was focused by removing the monochromator and photomultiplier tube, adding an eyepiece after the second objective lens, and using the microscope thus formed to examine the coloured surface of the crystal. The laser could then be focused onto the specimen, after first putting a very dense optical filter in the beam to avoid eye damage; care had to be taken to ensure that the filter was perpendicular to the beam, otherwise the latter was laterally displaced. With the laser focused one then used the achromatic lens to focus the spectrophotometer beam onto the crystal, and by moving

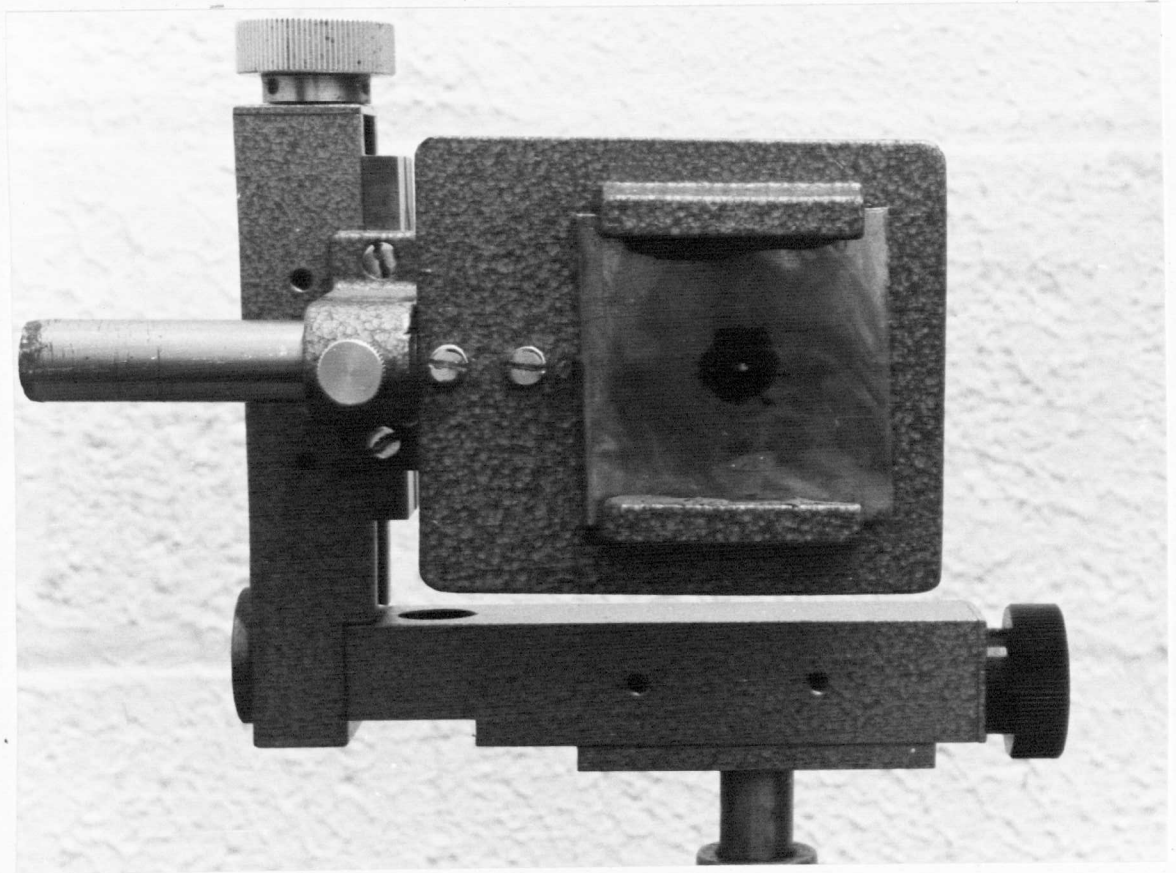

THE ELECTRON MICROSCOPE APERTURE MOUNTED ON ITS ADJUSTABLE HOLDER.

FIG. 2.10.

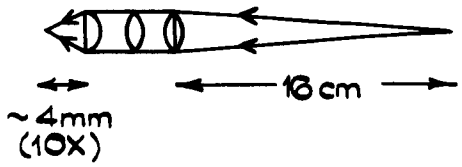

OBJECTIVE LENS OPERATING IN STANDARD CONFIGURATION.

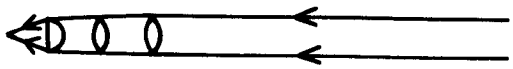

OBJECTIVE LENS OPERATING IN CONFIGURATION USED IN MICROSPECTROPHOTOMETER.

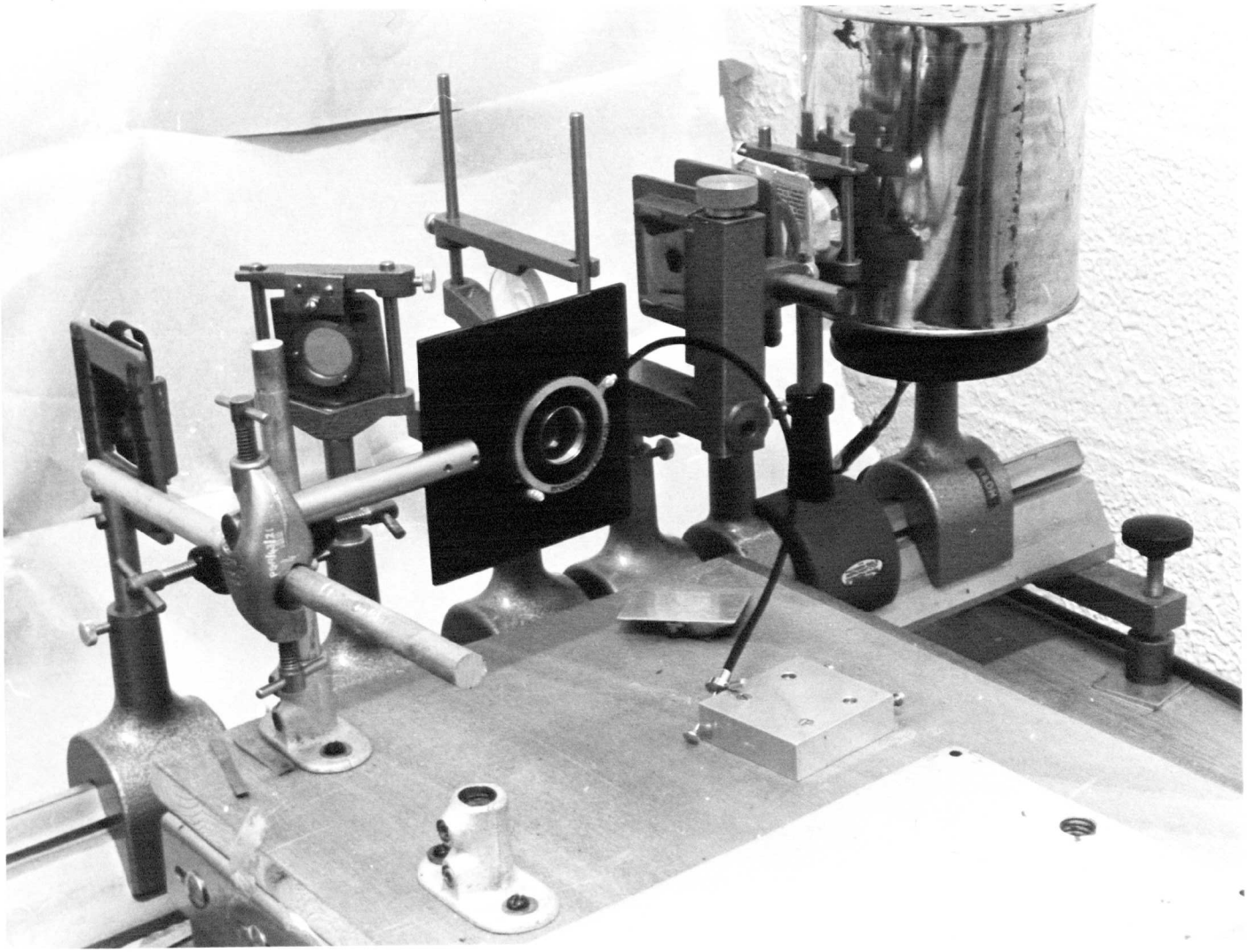

THE LIGHT SOURCE, AND ITS ASSOCIATED OPTICS.
(THE LASER HAS BEEN REMOVED FOR CLARITY.)

Fig. 2.11.

the aperture, position it in the centre of the laser spot. Finally the eyepiece was removed, the photomultiplier and monochromator replaced, and the position of the second objective adjusted to image the illuminated area of the specimen onto the entrance slit.

In order to provide coverage from 350 nm. to 1 μ m., two photomultiplier tubes were needed. The first, an R.C.A. type 6217, with an S-10 response photocathode, was useful from about 350 nm. to 700 nm.; the second, a Mullard type 150 CVP with an S-1 response, was used between 500 nm. and 1 μ m. The spectral response for these two tubes is shown in Fig. 2.12. The 150 CVP, because of its near infra red sensitivity, suffered from a high thermally generated dark current, and in order to achieve a satisfactory signal to noise ratio it had to be cooled to around -40°C. It was enclosed by a jacket, thermally insulated from the surroundings, through which cold nitrogen gas was passed. The nitrogen gas was obtained from a 25 litre dewar of liquid nitrogen, with a 75 watt heater immersed in it to increase the rate of boil off. The front window of the tube housing had to be heated, to eliminate misting, since it was found to be impossible to completely insulate the inner cold jacket from its surroundings. The heater was a 25 watt soldering iron element, running at about $^{2}/_{3}$ the rated voltage.

The housings for both tubes were, of course, light tight, except for an end window through which the light passed onto the photocathode. The housings were coupled to the monochromator by a sleeve, which was a sliding light proof fit over a similar tube around the exit of the latter. The manufacturer's recommendations on the operation of the photomultiplier tubes were followed and they were both fitted with mu-metal magnetic shields, connected to the photocathode to provide electrostatic shielding. High stability, close tolerance resistors were used for the anode loads and dynode voltage divider chains; these were mounted directly onto the base of the 6217 tube, and

FIG. 2.12.

THE SPECTRAL RESPONSE OF THE PHOTOMULTIPLIER TUBES.

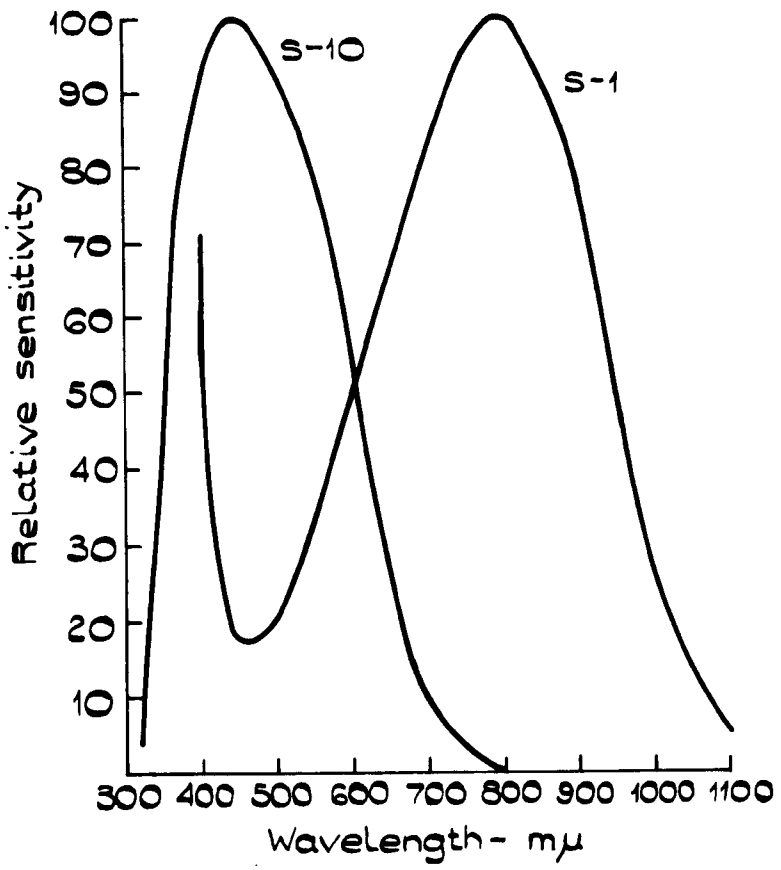

on short leads just outside the cooling jacket of the 150 CVP. Fig. 2.13 shows the monochromator, on its cross slide, connected to the 150 CVP phototube housing.

The stabilised high voltage required by the photomultipliers (1100 volts for the 6217, 1650 volts for the 150 CVP) was provided by a Fluke Model 415B High Voltage Supply; this unit had an output voltage stability of better than 2 parts in 10^5 per hour. The e.h.t. and signal connections to the tubes were made using low noise anti-microphony coaxial cable, terminated by Greenpar H.H.F. connectors.

The signal developed across the photomultiplier anode load was amplified by a Keithley Model 150B Microvolt Ammeter; this instrument had a high input impedance ($> 10^6$ ohms on most ranges), a maximum sensitivity of 3×10^{-6} volts full scale deflection, and excellent long term stability. The lowest signal fed to the Keithley 150B was about 3 orders of magnitude greater than the minimum required by it, hence it operated with a high signal to noise ratio. The output was connected to a Honeywell Brown Electronik potentiometric recorder, which was fitted with an event marker pen operated by the pulses from the monochromator drive unit.

When operating in the wavelength range 500 nm. to 1000 nm., a Kodak Wratten No. 15 filter was introduced into the measuring beam, to greatly attenuate any second order blue light reaching the photomultiplier tube.

Clearly it was also necessary to place a shutter over the monochromator entrance slit when exposing the crystal to the laser, for even when the wavelength drum was not set to 632.8 nm. there was sufficient light internally scattered to the exit slit to give an excessive, and possibly damaging photocurrent.

2.3 Performance and Stability of the Microspectrophotometer

Tests were first of all carried out to see whether the spectrophotometer beam would cause any bleaching of a coloured specimen. A

FIG. 2.13.

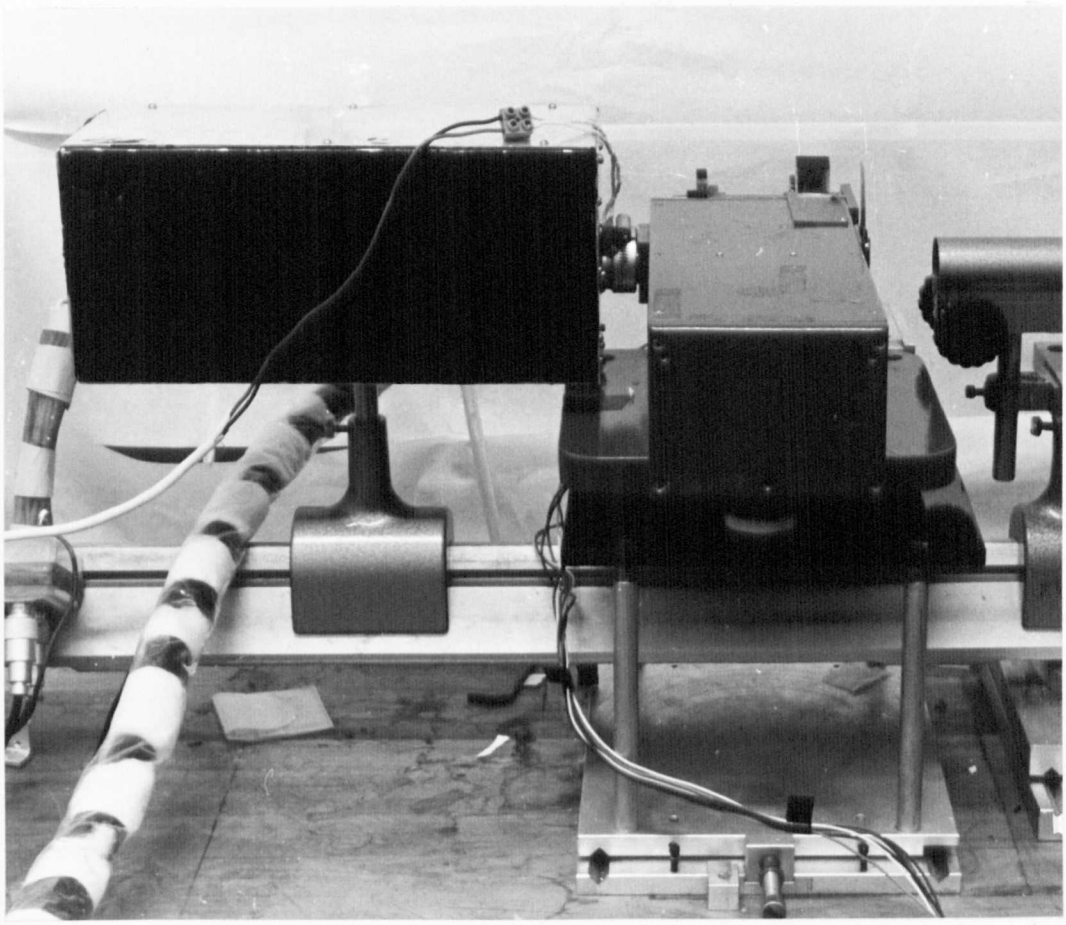

THE MONOCHROMATOR AND 150 CVP PHOTOMULTIPLIER ASSEMBLY.

very small change in transmittance could be observed after about 10 minutes illumination, but in view of the fact that a $^{1}/_{500}$ second exposure to the laser gave a significant decrease in absorbance, it was felt that the error introduced by spectrophotometer bleaching was negligible. This minor fault could probably have been eliminated by putting the monochromator before the specimen, as was discussed in section 2.1. This, however, could have led to further problems, particularly in the final optical alignment.

The main problem with using the apparatus was that of preventing stray light reaching the photomultiplier tube. All of the experiments were carried out in a darkroom, and light baffles used, where necessary, to shield the photomultiplier-monochromator assembly from any extraneous light. This proved to be a perfectly satisfactory solution.

A more elegant remedy, which would have also given a higher signal to noise ratio, would have been to interrupt the white light source at a constant frequency e.g. 800 Hz. One would then have been able to connect the photomultiplier output to a tuned amplifier or phase sensitive detection system. Although a phase locking amplifier system was not readily available during most of the experimental work, it was subsequently found that there was no significant improvement in signal to noise ratio when the Keithley amplifier was changed for an A.S.L. phase sensitive detection system. Fortunately, the signal to noise ratio, long and short term stability, and the accuracy of the apparatus with the d.c. amplifier system were quite good.

The accuracy of the measurements was checked by measuring a number of standardised filters, ranging from N.D. 0.3 to N.D. 2.0; the results were always in agreement to better than $\pm 1\%$. The filters used for evaluating the accuracy of the microspectrophotometer were specially made for the purpose, by the vacuum evaporation of carbon onto a glass slide. In this way an uncoated area of the slide could be used for the 100% transmittance measurement, to avoid divergence and

scatter errors. The filters were standardised using a Perkin Elmer 450 spectrophotometer, with an uncoated slide in the reference beam. (Care obviously had to be taken to ensure that there was no significant variation in transmittance over the area of these filters, because of the size difference between the area of the filter measured by the P.E. 450 and that measured by the microspectrophotometer.)

A graph of the stability of the apparatus is illustrated in Fig. 2.14, it shows the variation in 100% transmittance signal for a period of 8 hours from turning on. It is evident that the stability greatly improves after a running time of about 3 hours, so in order to avoid having to wait this length of time before using the apparatus, it was left running overnight, except for the precaution of switching the photomultiplier power supply to the "stand-by" position. An experiment could then be started after only an hours delay whilst the 150 CVP photomultiplier was cooled. (E.H.T. volts were applied during cooling) No delay at all was encountered when using the 6217 tube, it apparently gave consistent results from turn on of the E.H.T., provided that it had not been subjected to any high level illumination since its last use. Fig. 2.15 shows the output variations for an 8 hour running period with the equipment warmed up at the start. This shows a very satisfactory stability, particularly as some workers report long term fluctuations in photomultiplier signals as high as $\pm$10% over a few hours (at constant illumination intensity).

It is also worth stating that most of the experiments reported in this thesis took less than 2 hours to perform, over this time period the accuracy of the results would be that much higher. Taking any time period of 2 hours length (outside the first hour) the worst error in transmittance shown in Fig. 2.15 is a variation of about $\pm$1.5%, which would yield an error of $\pm$0.01 in optical density.

2.4 The Specimens

The potassium bromide specimens used in the initial experiments

FIG. 2.14.

PHOTOMETER STABILITY, RECORDED FROM THE TIME OF TURNING ON.

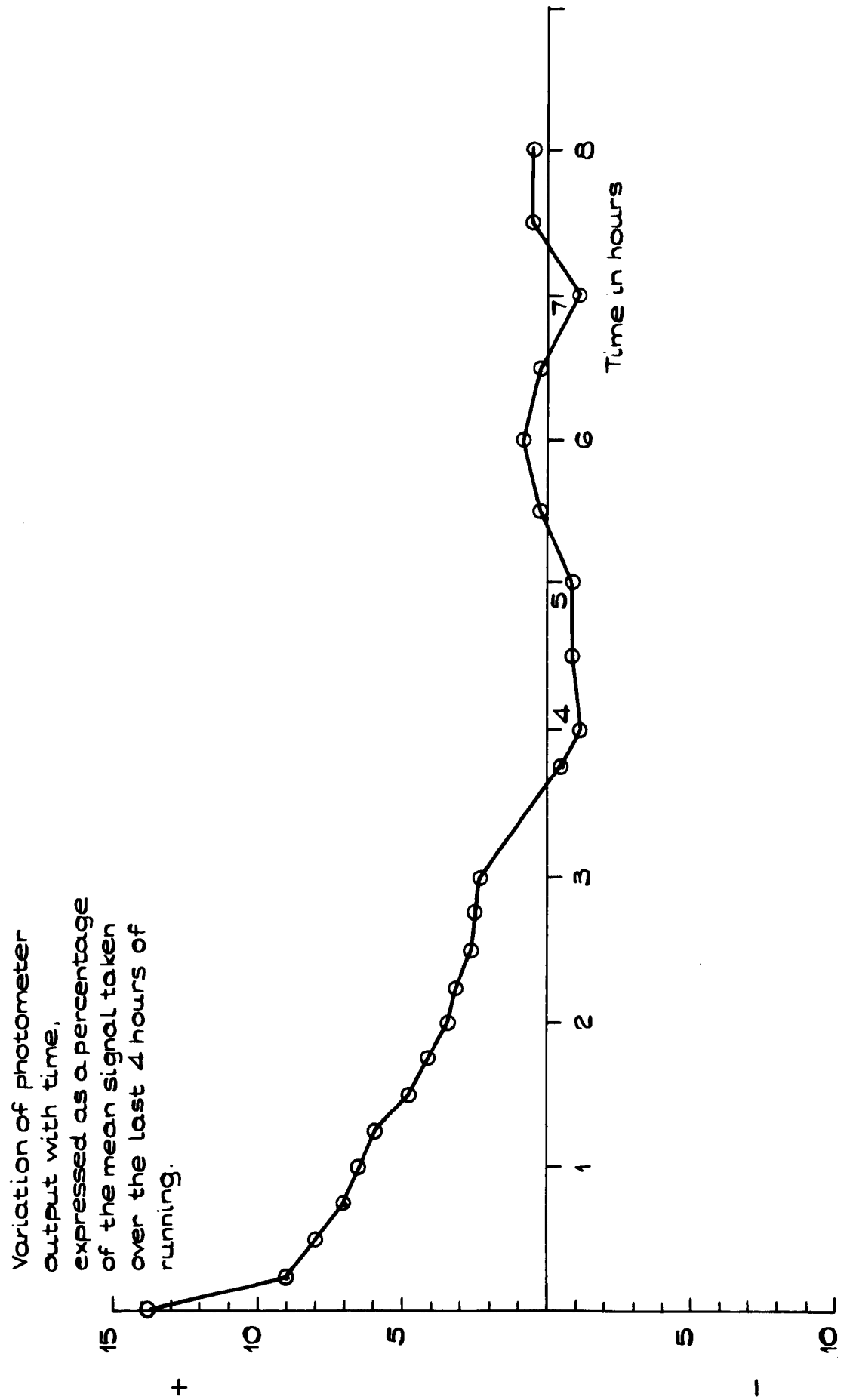

VARIATION OF PHOTOMETER SIGNAL AFTER TURNING ON EHT VOLTS FROM THE 'STANDBY' CONDITION.

Two separate experiments are shown.

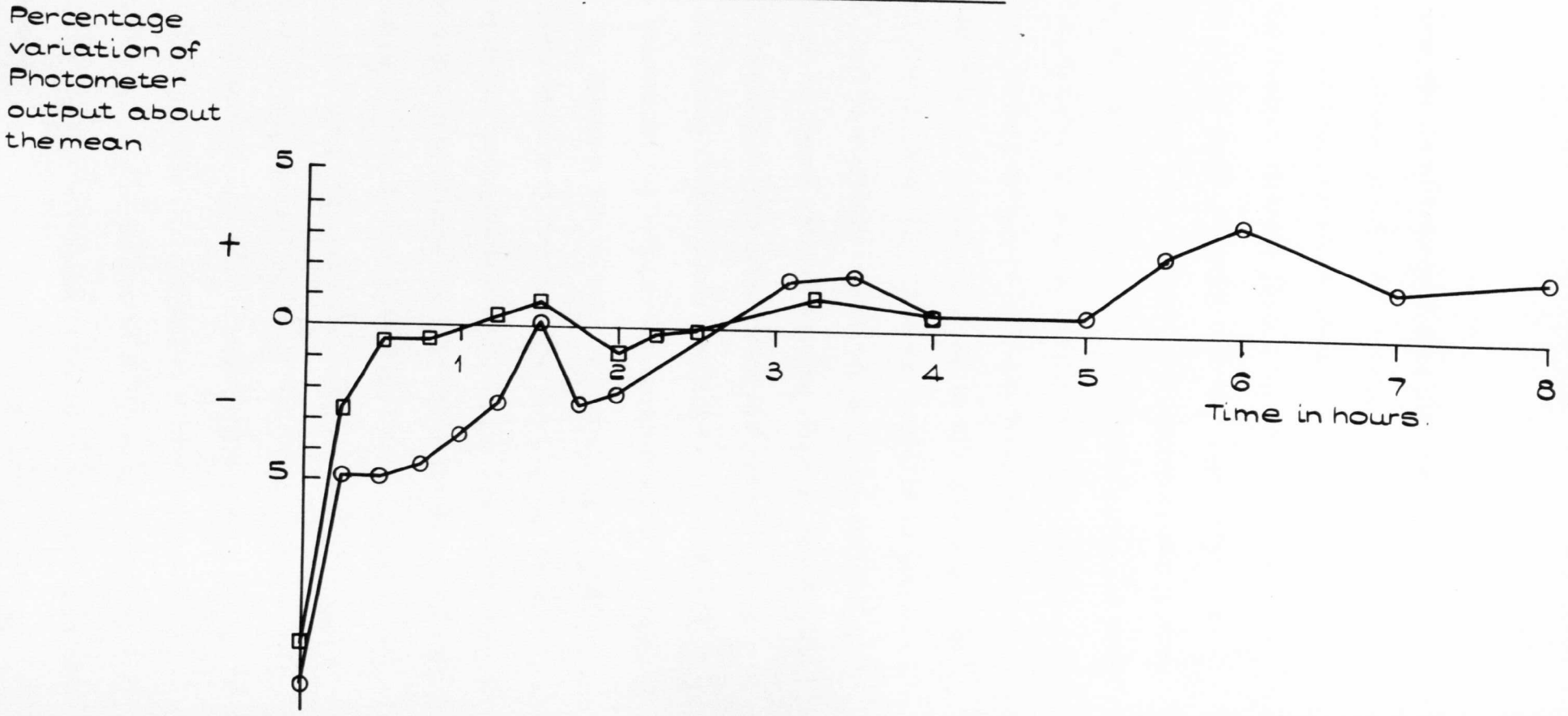

FIG. 2.15.

were obtained from Hilger and Watts Ltd., in the form of single crystal slabs having dimensions 25 mm. x 25 mm. x 6 mm. One could then cleave from them small pieces of rectangular side 25 mm. x 6 mm. and a few mm. thickness, and use the freshly cleaved face for the experiment. KBr is particularly easy to cleave along < 100 > directions, one merely holds a single edge razor blade on the surface of the crystal, with the blade parallel to the desired cleavage plane, and then taps the back of the blade smartly with a small cleavage hammer. Throughout the experimental work the crystals were handled with tweezers, since, like the other alkali halides, KBr is hygroscopic and rather soft, and very rapidly loses its transparent surfaces if handled with the fingers.

After the microspectrophotometer had been constructed and tested most of the experiments were carried out on KBr single crystal obtained from the Harshaw Chemical Co. This was supplied in pieces slightly larger than that from Hilger and Watts, and was, curiously, somewhat more difficult to cleave without leaving steps on the surface of the specimen. To ensure that these specimens did not absorb any moisture from the air during cleaving and mounting in the irradiation cryostat, they were handled in the totally dry environment of a nitrogen flushed glove box. The nitrogen was obtained by immersing a 65 watt heater in a sealed dewar of liquid nitrogen, and passing the boiled off gas through a regulator system before it went into the glove box, in order to maintain a pressure differential of about 100 mm. of water.

The glove box was fitted with a simple dew point indicator, of the type where one cools down a polished metal surface with a suitable refrigerant, such as solid CO_2 and acetone; the dew point is the temperature at which the surface mists over with condensation. After the box had been thoroughly purged, no misting was observed until the metal indicating surface was cooled to around 80°K; it was likely that this condensation was not water vapour, but an organic solvent or mould release agent used during the construction of the glove box. All of

the experimental results described in this thesis were obtained from crystals prepared in this manner, unless otherwise stated, and should be characteristic of clean surfaces cleaved from the bulk of the crystal.

It was felt that dry handling after coloration was not absolutely necessary, since no differences in the spectra or shape of bleaching curves were apparent for crystals that had been similarly treated up to the end of irradiation and then mounted either in the glove box or in air. Consequently it was advantageous to omit the complicated step of mounting the coloured specimens in a dry atmosphere, since it reduced the time between coloration and bleaching. It also made handling a lot less difficult, since after irradiation the crystals had to be kept in the dark, or at least subjected to only very subdued light.

Mention will be made in the next chapter of the absolute impurity content of the specimens, and particularly of the hydroxyl ion concentration.

2.5 Electron Coloration of the Specimens

The vacuum cryostat in which crystals were irradiated is shown in Fig. 2.16; filled with liquid nitrogen it allowed specimen temperatures of around 90°K to be attained. When carrying out room temperature irradiations it was filled with acetone, to provide a better sink for conducting away any heat generated by the electron beam. Besides room temperature and liquid nitrogen temperature, irradiations were also carried out at an intermediate temperature obtained by filling the cryostat with a mixture of crushed solid CO_2 and acetone.

In order to measure the actual temperatures reached with these refrigerants, and the rise, if any, that occured during irradiation, a fine wire copper-constantan thermocouple was inserted into a small hole drilled in a standard 6 mm. x 25 mm. x 3 mm. KBr specimen. The thermocouple junction was inserted from the non irradiated face of the crystal, and positioned so that it was in the centre of the irradiated area as

Fig. 2.16.

THE CRYOSTAT USED FOR ELECTRON IRRADIATION.

close to the front surface as possible. The specimen was mounted in the cryostat, cooled, the temperature measured, and then irradiated for 30 minutes with 50 KV electrons at a beam current of 50 μ A. The final temperature was then recorded. The results of this experiment are tabulated below; it can be seen that the temperature stability in all three cases is very satisfactory.

	Temperature of Specimen	
Liquid in cryostat	Before Irradiation	After Irradiation
acetone	295°K	295°K
crushed solid CO_2 + acetone	203°K	205°K
liquid nitrogen	93°K	98°K

The electron irradiations were carried out on a High Voltage Engineering Company Van de Graaff accelerator, this machine would operate between 25 and 450 KeV with beam currents of up to about 150 μ A. The beam diameter could be varied between $\sim$ 1 mm. and 1.5 cm. at most energies. For the bleaching experiments it was necessary to choose an electron penetration depth less than the depth of focus of the 10X objective lens. To fulfil this requirement all crystals were coloured by 50 KV electrons, with a penetration depth of 27 μ m, and a beam current density of approximately 50 μ A. cm^{-2}. Irradiation times of around 45 minutes were usual, giving an optical density of approximately 0.8. To ensure even coloration, the electron beam was scattered by a thin aluminium foil placed about 10 cm. from the crystal. The foil also performed the important function of shielding the crystals from the white light of the accelerator filament. Crystals were irradiated in their "as cleaved" form. The evaporated metal or graphite conducting films used by some workers, to avoid surface charging effects, did not appear to be necessary; the coloration was usually quite even, although there was sometimes a slight surface crazing.

2.6 The Additive Coloration of Specimens

Some experiments were carried out on crystals that had been

additively coloured, that is to say on non-stoichiometric crystals containing an excess of potassium metal. As was mentioned in Chapter One, excess alkali metal atoms are usually incorporated into the crystal lattice substitutionally, with the simultaneous formation of F centres. (They may, of course, also go in as colloidal metal particles.)

One can additively colour alkali halide crystals simply by heating them in a suitable container while surrounded by an atmosphere of alkali metal vapour. The time of exposure of the crystal to metal vapour, and the vapour pressure of the latter are important parameters in the additive coloration process, which may be carried out in a number of different ways.

The additive coloration of crystals for the experiments described in later chapters was carried out in an improved form of Van Doorn's apparatus, illustrated in Fig. 2.17 [3]. This apparatus allows the pressure of the alkali metal vapour to be regulated independently of the temperature, in order to give some control over the final F centre concentration. A piece of potassium metal is put into the cylindrical stainless steel container, and a KBr crystal clipped into the nickel mesh specimen holder. The container is sealed, and evacuated through the small side tube near the top. Nitrogen is then admitted, through the same tube, to a pressure of a few mm. of Hg. When the container is heated in a vertical tube furnace, the potassium metal vaporises and diffuses upwards into the water cooled section, where it condenses and runs back down the container walls into the hotter region for revaporisation. A continuous diffusion process will thus be established, with a region of pure potassium vapour in the hotter part of the tube separated from nitrogen in the cooler part by a zone of mixed composition. The vapour pressure of the potassium can thus be controlled by varying the nitrogen pressure. After exposing the crystal to potassium vapour at a few mm. pressure for about 10 minutes, with the furnace at $\sim 700^{\circ}C$, nitrogen is admitted to atmospheric pressure, the lid removed

FIG. 2.17

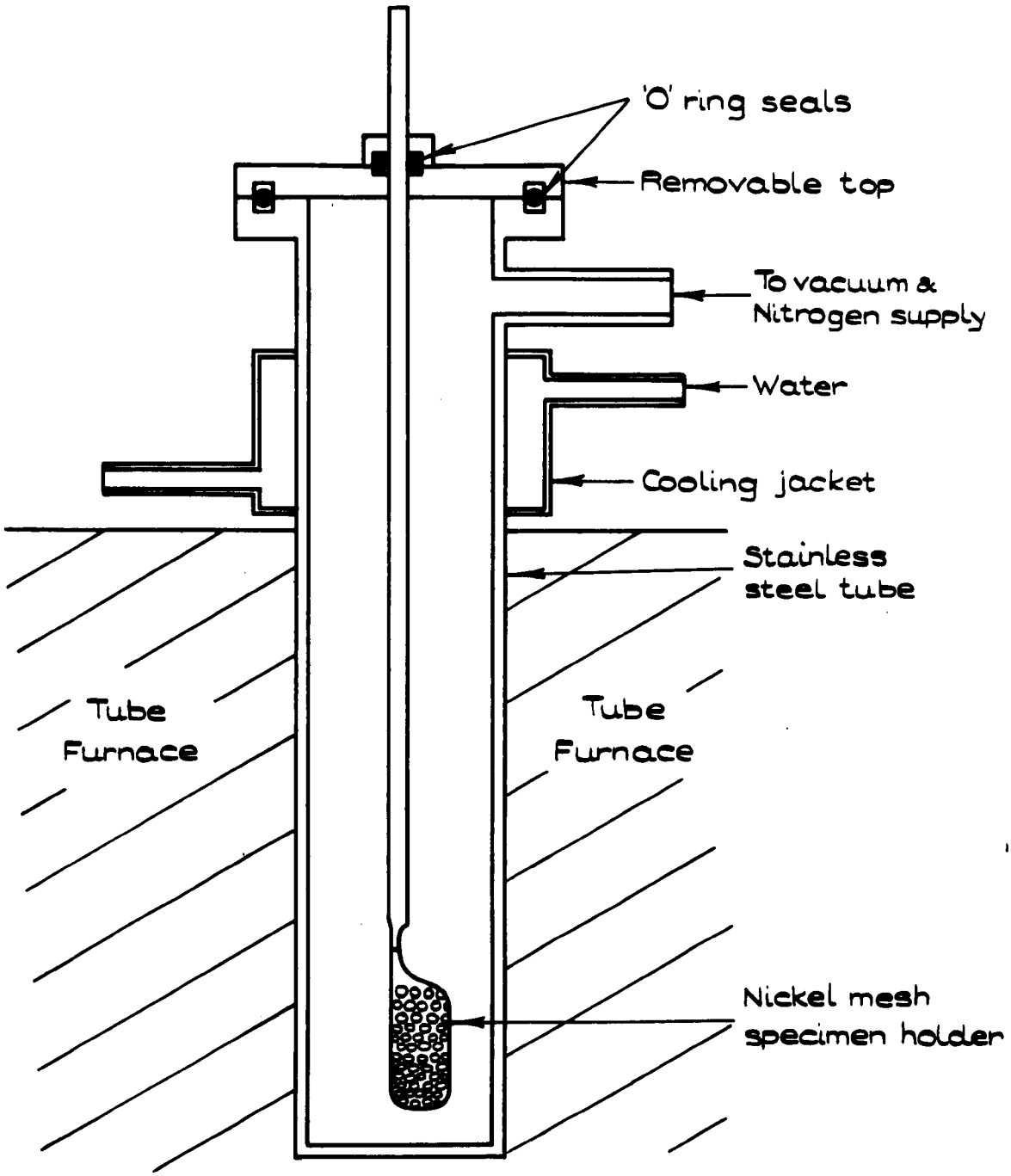

THE ADDITIVE COLORATION APPARATUS[3]

(In Section).

and the specimen quenched in liquid nitrogen. Alternatively the lid may be left on and the container lifted from the furnace and plunged into liquid nitrogen. This cools the crystal more slowly, and so avoids the risk of crazing and fracturing it due to thermal shock. It does, however, lead to a fairly high concentration of F-aggregate centres, but this can be adjusted by subsequently reheating the crystal to around 550°C and then quenching it on a copper block at room temperature. This operation must be carried out in the total absence of light.

The additive coloration of crystals was carried out with the apparatus standing in a large glove box, flushed with dry nitrogen gas, to prevent the potassium metal reacting with atmospheric moisture.

The F-centre coloration obtained by this process extended right into the bulk of the crystal, and in order to obtain specimens for bleaching on the microspectrophotometer, thin sections had to be cleaved off the large crystals in a device made for this purpose. The crystals were attached by suction to a specimen holder and cleaved by a stainless steel razor blade fixed in a guide mechanism. There was a micrometer adjustment of the specimen thickness and with careful setting up and use it was possible to cleave slices as thin as 125 μm. The crystals prepared in this way were rather small and fragile, and needed to be attached to microscope cover glasses, using a spot of cyanoacrylate adhesive, before they could be mounted in the specimen holder of the microspectrophotometer.

2.7 Summary

The apparatus described in this chapter was designed to permit the study of F centre bleaching in potassium bromide single crystals, coloured by fast electron irradiation. Bleaching could be carried out using a focused He-Ne laser, at F band power densities up to 5×10^3 W.cm.$^{-2}$. A microspectrophotometer system allowed the absorbance of the bleached area ($\sim$ 20 μm. diameter) to be measured over the wave-

length range 350 nm. to 1 μm. The spectrophotometer beam was brought to a focus several μm. in diameter at the specimen surface, and could be accurately positioned relative to the laser bleaching beam. The laser and the microspectrophotometer beams thus travelled coaxially through the specimen and most of the optical system. The specimen could be cooled to liquid nitrogen temperature, although this facility was never used in any of the experiments described in this thesis. The accuracy and stability of the microspectrophotometer system was found to be good, the typical error in absorbance measurement being ±0.01 O.D. units, which is perfectly satisfactory for the experiments to be described in the following chapters.

References

(1) Schul'man A.R. and Gel' E.P., Fiz Tuerdoga Tela, 2, 524 (1960)
(translation in Sov. Phys. Sol. State, 2, 489 (1960))

(2) Tubbs, M.R., J. Sci. Inst., 43, 498, (1966)

(3) Van Doorn, C.Z., Rev. Sci. Inst. 32, 755 (1961)
& Philips Res. Rpts. Suppl. 4 (1962)

CHAPTER THREE

MEASUREMENT OF THE BLEACHING KINETICS OF ELECTRON IRRADIATED KBr

3.1 The Use of the Microspectrophotometer to Obtain Bleaching Curves for Electron Coloured KBr

The microspectrophotometer described in Chapter 2 was used to make bleaching measurements at room temperature on single crystals of KBr that had been coloured by electron irradiation at various temperatures. Specimens coloured at low temperature were warmed, in the dark, to room temperature before bleaching. In all of the experiments to be reported the irradiating electron energy was between 40 and 50 KeV at beam current densities of the order of $50\,\mu A.cm^{-2}$. This enabled peak F band optical densities of 0.7 to 1.0 to be obtained with reasonably short exposure times, and without any significant rise in temperature of the specimen. The penetration depth of the coloration at this electron energy is about $27\,\mu m$ [1]. Thus an F band optical density of 1.0 corresponds to an F centre concentration of about 4.9×10^{18} F centres cm^{-3}, which is over an order of magnitude greater than that for the additively coloured or X-irradiated crystals used by previous workers for optical bleaching studies [2,3]. Moreover, this depth of coloration was sufficiently small to allow the satisfactory use of 10X microscope objectives on the microspectrophotometer, and enabled measurements to be taken at illuminating power densities of up to $10\ KW.cm^{-2}$. This is a very much greater intensity (by a factor of 10^6) than was used in previous optical bleaching measurements [2,3].

Freshly cleaved crystals were coloured in the cryostat described in Chapter 2, at room temperature (RT), liquid nitrogen temperature (LNT), or at an intermediate temperature obtained by filling the cryostat with a mixture of crushed solid CO_2 and acetone. The actual temperatures of the specimen under these conditions were $294^{\circ}K$, $93^{\circ}K$ and $203^{\circ}K$ respectively. When irradiating at room temperature the cryostat was filled with acetone, in order to improve the temperature stability.

Specimens coloured at low temperature were allowed to warm slowly in total darkness; they took between one and two hours from the time when the refrigerant was tipped from the cryostat to reach room temperature.

The coloured crystals were removed from the cryostat and transferred to the specimen stage of the microspectrophotometer in very subdued lighting. The specimens were positioned so that a small section of uncoloured crystal could be moved into the spectrophotometer beam, to allow a 100% transmittance value to be measured at the start and finish of the experiment. The laser power monitor was connected to a potentiometric recorder, so that the laser output could be monitored throughout an exposure, for although its stability was good, the output occasionally changed discontinuously by as much as 10%, presumably due to the effects of thermal expansion on the dimensions of the cavity.

At the end of an experiment, the crystal was removed from the specimen holder and examined under a Zeiss optical microscope to locate the bleached area and measure its diameter, for the purpose of calculating the energy absorbed by it during the exposure to laser light. The appearance of a typical crystal after such an experiment is shown in Fig. 3.1; several circular bleached areas are visible on this particular specimen. The crazing of the surface is caused by electron irradiation, it can be avoided by evaporating a thin conducting film of aluminium or carbon onto the crystal before coloration. This extra operation would, however, have made the dry handling of the freshly cleaved specimens considerably more difficult, and for this reason it was not carried out. Moreover, the use of aluminium films seems to alter the coloration kinetics of the alkali halides, and they are not always successful in preventing surface degradation, since they are inclined to peel off of the specimen whilst under irradiation. It was usually possible during the microspectrophotometer alignment to position the laser beam so that it passed through a region without any surface markings; if microscopic examination at the end of the experiment revealed that the bleached spot

Fig. 3.1.

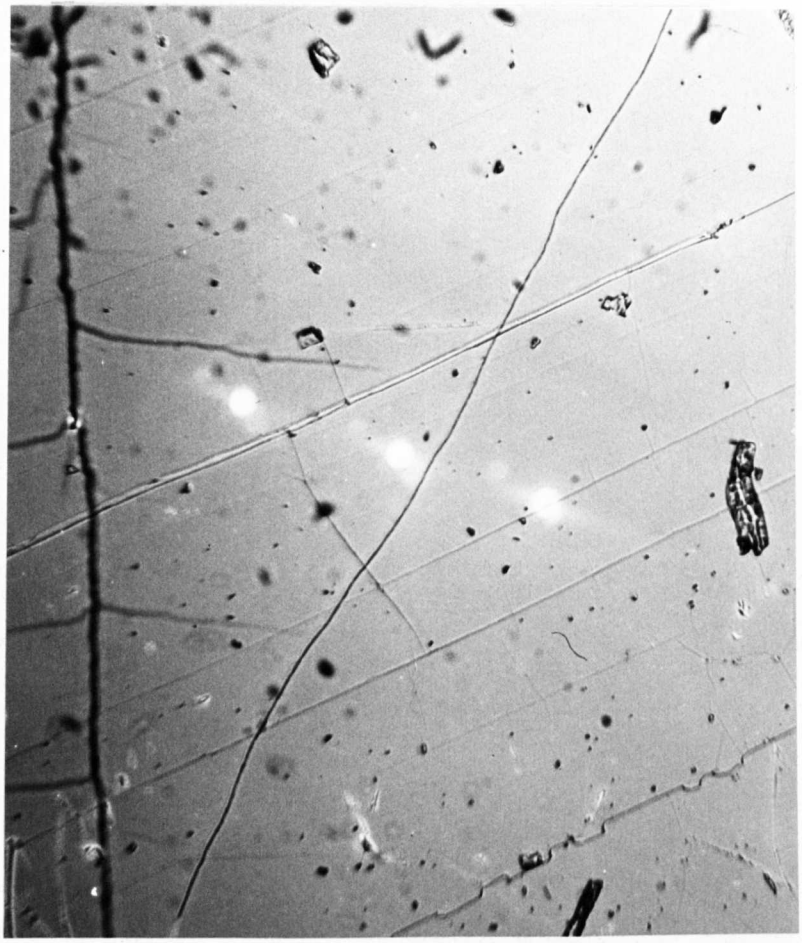

PHOTOMICROGRAPH OF A CRYSTAL AT THE END OF AN EXPERIMENT, SHOWING A NUMBER OF LASER BLEACHED AREAS.

did have a surface crack or cleavage step running through it, the results were discarded. The diameter of the bleached spots was typically between 20 and 30 μm, measured with a Zeiss stage micrometer. The coloration profile through the centre of a bleached area is illustrated in Fig.3.2; this was measured using a Joyce-Loebl Recording Microdensitometer.

With the experimental data thus obtained, a preliminary plot of optical density vs. time could be made. Typical results are illustrated in Fig.3.3, which shows the bleaching at room temperature of specimens coloured at 294°K, 93°K and 203°K. These three specimens were chosen to have starting optical densities of between 0.75 and 0.90, to aid the comparison between samples coloured at different temperatures. Some optical bleaching of the specimen inevitably occurs during the alignment of the microspectrophotometer, the "starting optical density" quoted here is therefore the O.D. at the start of bleaching measurement, and not the O.D. directly after irradiation. More will be said about this in Section 3.3. The most striking and important difference between RT coloured specimens and those coloured at LNT is that the F band in the latter can be completely bleached, to zero O.D., by prolonged F light illumination at RT. A more meaningful way of expressing these results is shown in Fig.3.4, a plot of optical density at 625 nm. against total laser energy absorbed in the F band. Plotting coloration (or F centre concentration) against absorbed energy instead of time eliminates one of the difficulties associated with these bleaching experiments, that of making a direct comparison between results that were obtained with the laser running at different output levels. Fig.3.4 was plotted in the manner illustrated diagramatically in Fig.3.5, from the laser output data (a) (i.e. a plot of laser power vs. time) and a graph of the specimen's percentage absorbance (at 625 nm) vs. time (b). By combining these two graphs a curve showing the variation in the rate of absorption of energy in the F band $\left|\frac{dE}{dt}\right|$ with time can be plotted (c). Curve (c) also incorporates a numerical factor which takes into account the reflection losses at the various optical components in the microspectrophotometer. The area under

FIG. 3.2.

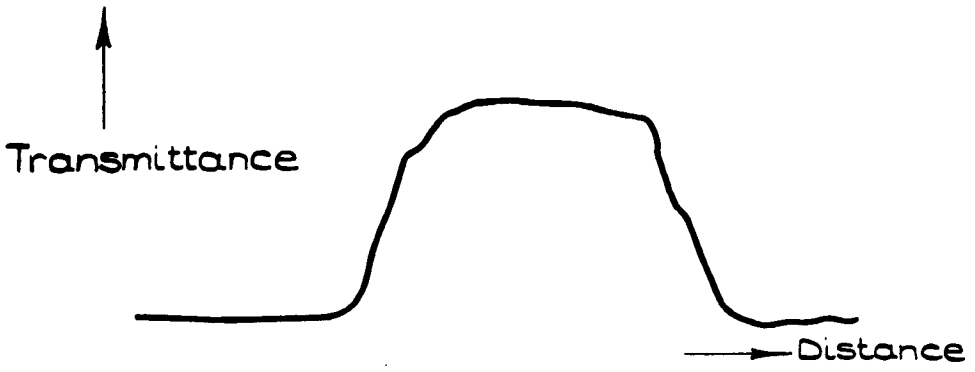

COLORATION PROFILE ACROSS A BLEACHED AREA.

FIG. 3.3

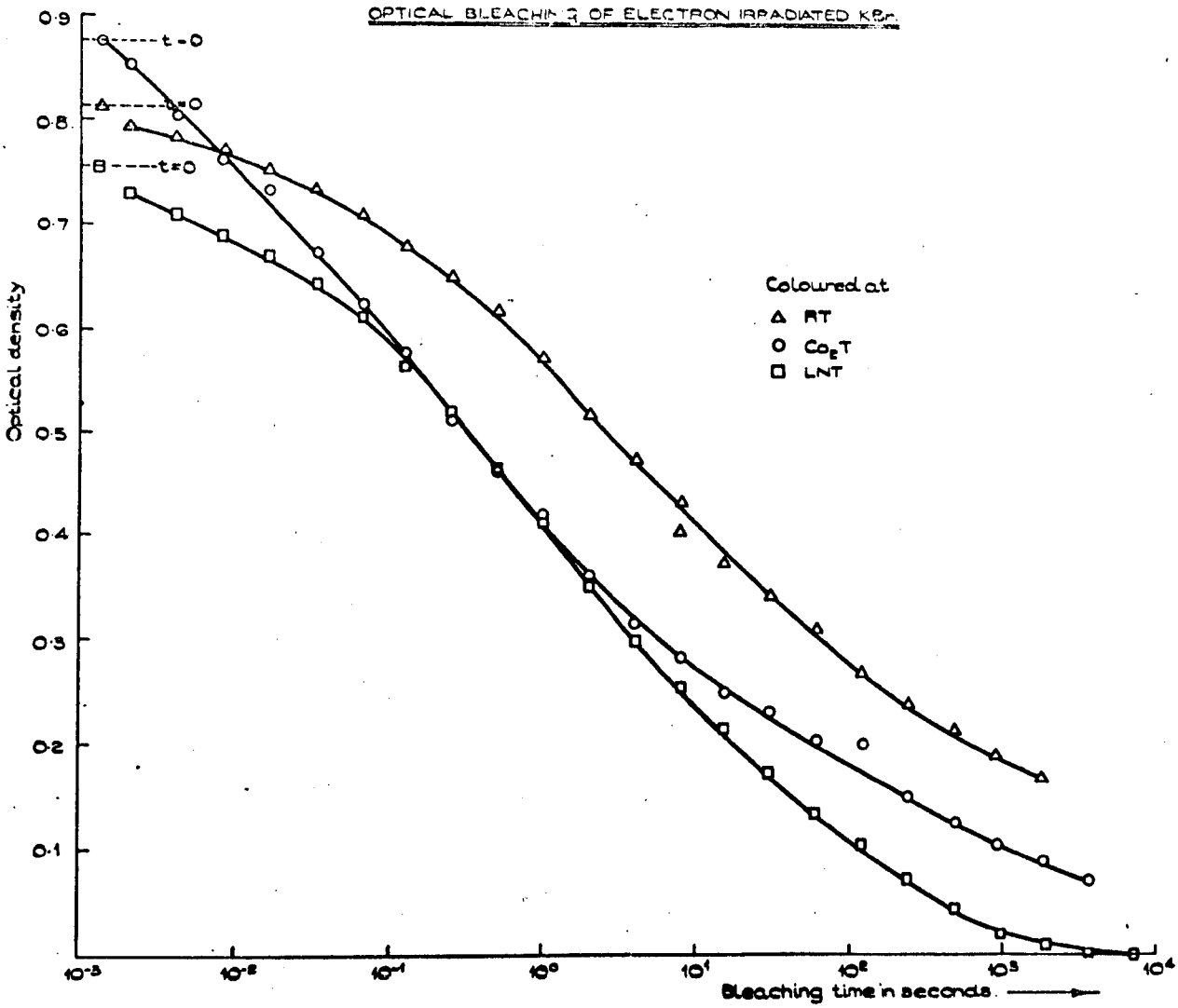
OPTICAL BLEACHING OF ELECTRON IRRADIATED KBr
Optical density
0·9
0·8
0·7
0·6
0·5
0·4
0·3
0·2
0·1
t=0
t=0
t=0
Coloured at
RT
$Co_{\epsilon}T$
LNT
10^{-3}
10^{-2}
10^{-1}
10^{0}
10^{1}
10^{2}
10^{3}
10^{4}
Bleaching time in seconds

FIG. 3.4

BLEACHING OF ELECTRON IRRADIATED KBr

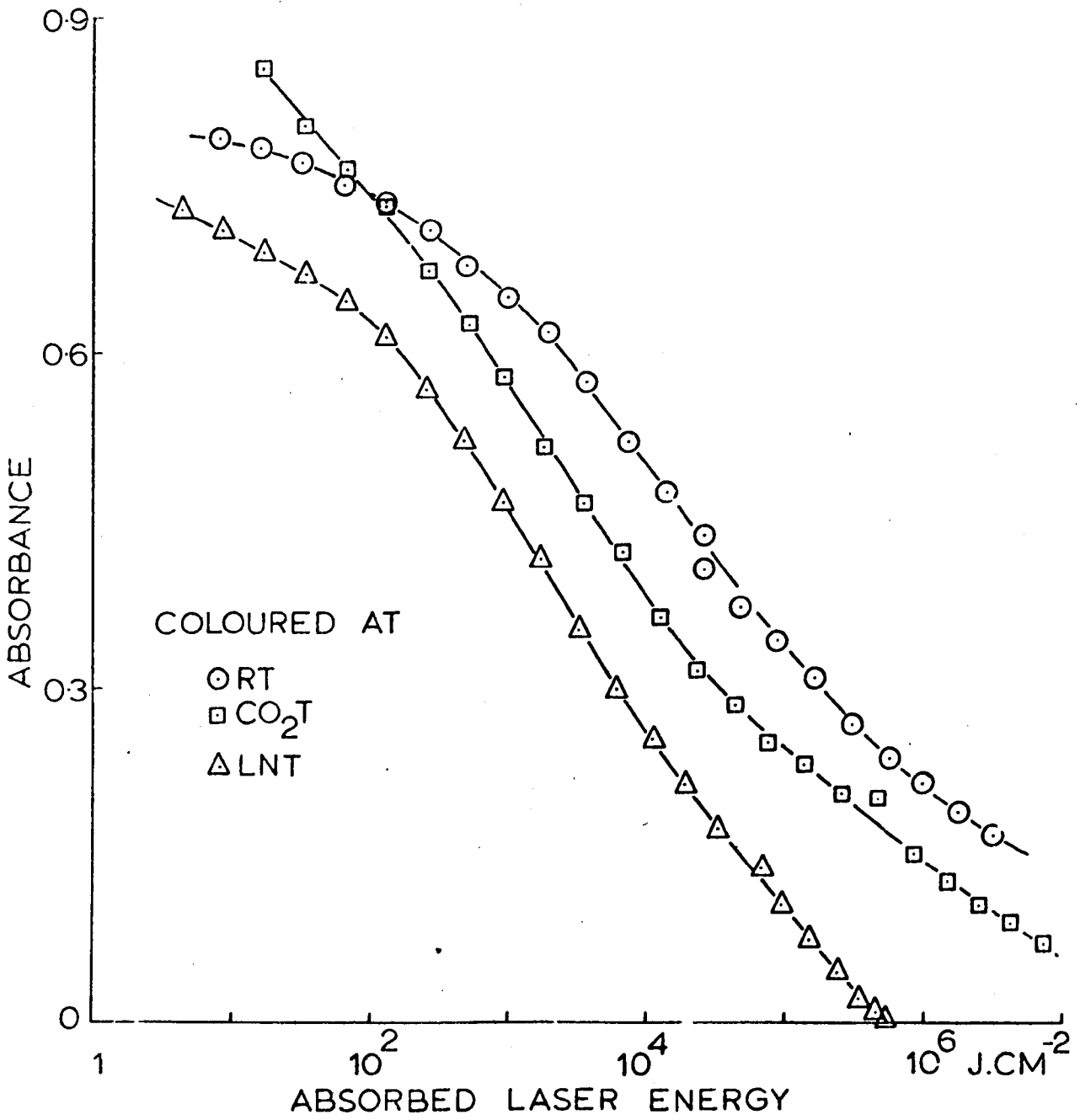

FIG. 3.5.

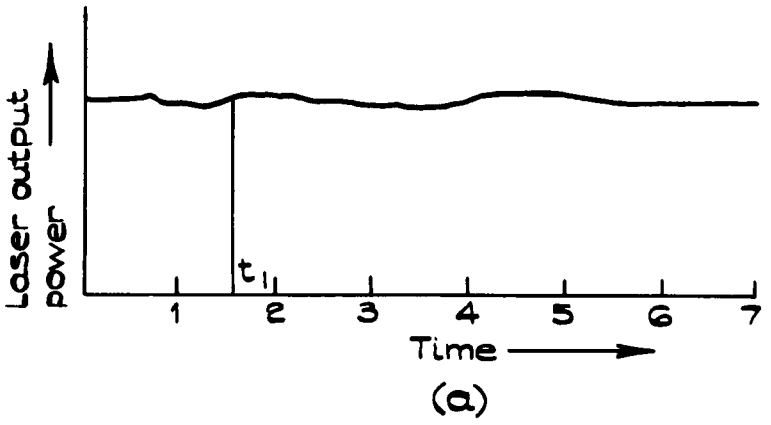
Laser output power
t_1
1
2
3
4
5
6
7
Time

(a)

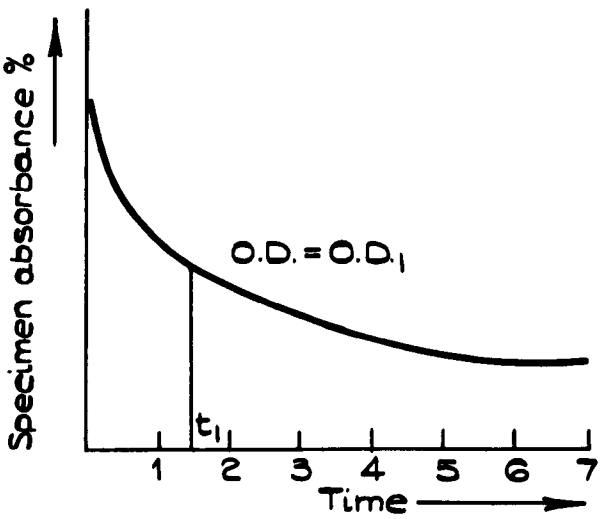
Specimen absorbance %
O.D. = O.D.$_1$
t_1
1
2
3
4
5
6
7
Time

(b)

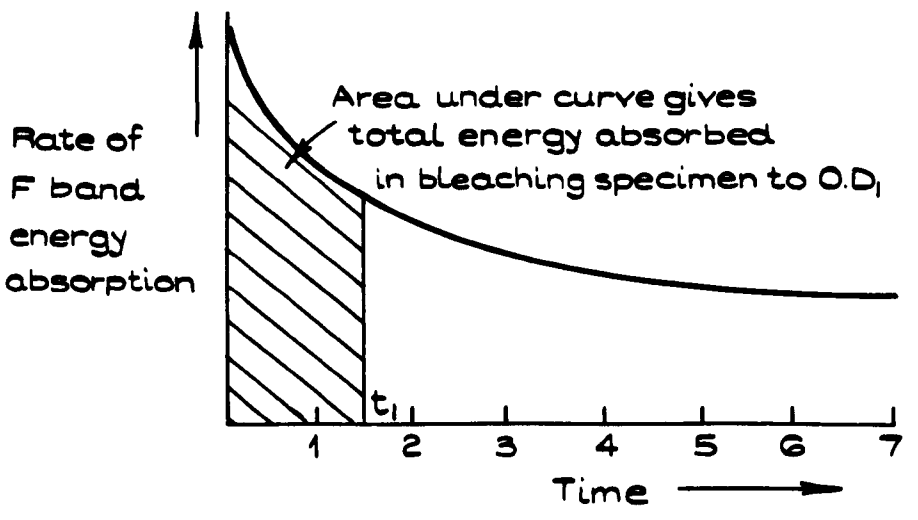
Rate of F band energy absorption
Area under curve gives total energy absorbed in bleaching specimen to O.D$_1$
t_1
1
2
3
4
5
6
7
Time

(c)

this curve is then integrated to find the total energy absorbed by the specimen from the start of bleaching to the time the O.D. has reached a particular value. Strictly speaking the specimen absorbance at the laser wavelength (632.8 nm.) should have been used for these calculations, instead of the value at the F band peak. However, the F centre absorption band in KBr is sufficiently broad to make these two values virtually the same. For example, in a crystal with an optical density of 0.705 at the F band peak, the absorbance at 633 nm. is 0.700. Thus, the errors in absorbed energy introduced by using the 625 nm. transmittance value are very small, particularly when compared to the inherent inaccuracies in measuring areas under the $\left(\frac{dE}{dt}\right)$ curve, and in the measurement of the laser power and beam diameter at the specimen.

Fig.3.4 very clearly illustrates the differences in bleaching behaviour at RT between specimens coloured at RT and those coloured at LNT. It is evident that the RT coloured material is harder to bleach, particularly in the later stages of bleaching. An optical density (at 625 nm) of 0.17 remains in the RT coloured specimen after the absorption of 3×10^6 J.cm^{-2}, whereas the O.D. of the LNT coloured sample (starting from an absorbance only 0.05 units lower) has fallen to less than 0.005 after 5×10^5 J.cm^{-2} of laser light has been absorbed. The behaviour of the KBr coloured at 203°K lies somewhere between these two; an O.D. of 0.05 remains after 1.4×10^6 J.cm^{-2} have been absorbed.

Furthermore, all samples, whatever their temperature of coloration, become progressively harder to bleach as the magnitude of the F band decreases. This is perhaps demonstrated more clearly by Fig. 3.6, which shows curves of the average energy absorbed per F centre bleached (η) vs. the number of F centres bleached, the latter quantity being expressed as a fraction of those present at the start of bleaching. It is apparent that initially there is very little difference in the bleaching efficiencies of specimens coloured at LNT and RT, certainly no more than

FIG 3.6

OPTICAL BLEACHING EFFICIENCY OF ELECTRON IRRADIATED KBr.

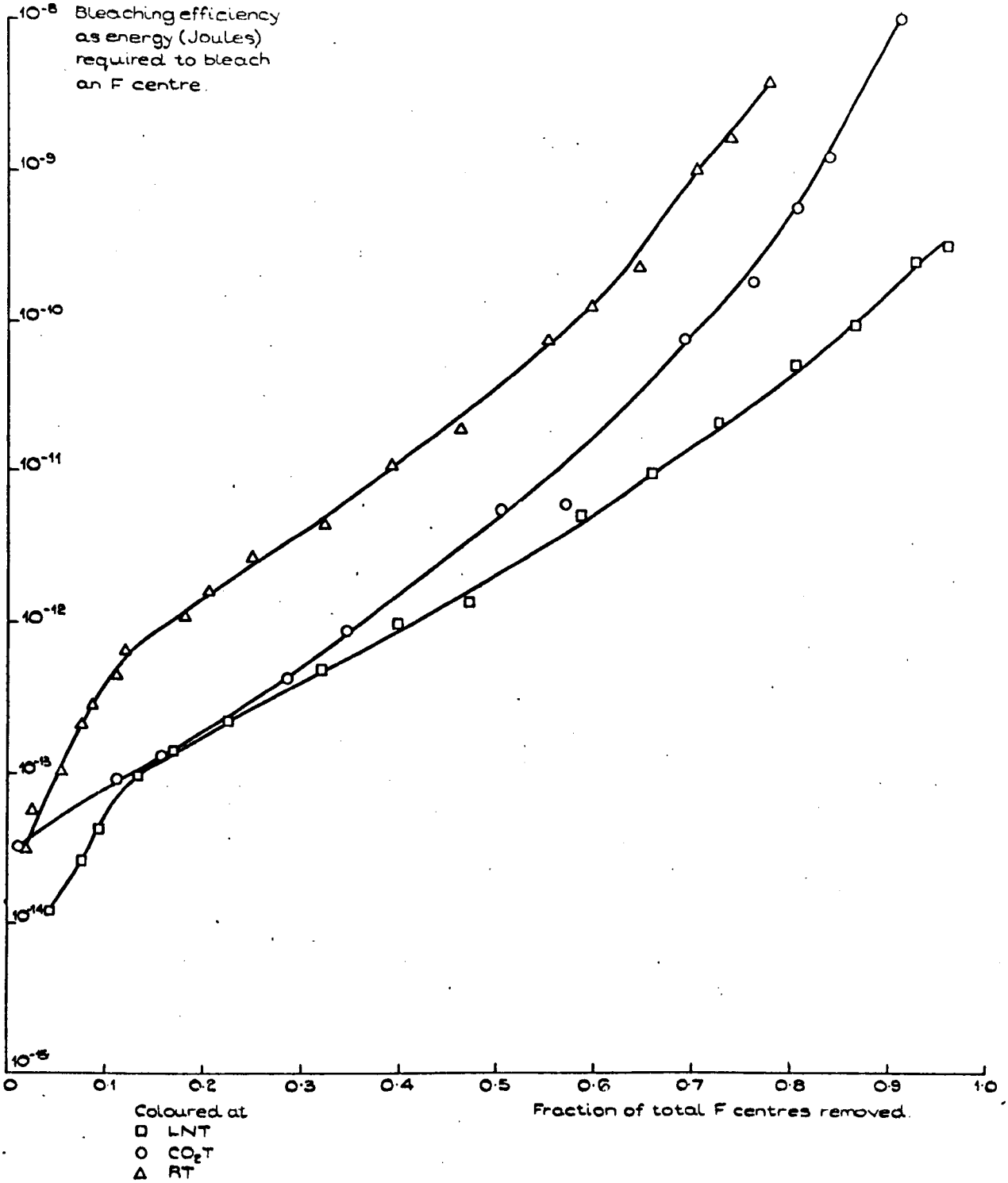

a factor of 3 or 4 when less than 2% of the F centres have been bleached. From 3.6, η at the start of bleaching corresponds, approximately, to the absorption of 3.1×10^4 F band photons per F centre bleached for KBr coloured at LNT, and $\sim 10^5$ photons per F centre for material coloured at RT. However, as bleaching proceeds, the efficiency decreases, rapidly at first, until about 10% of the F band has gone, when there is a fairly marked "knee" in the curves and the slope decreases. The gap between the data for RT and LNT coloured specimens widens as the F band absorbance decreases; for example, with 70% of the F band bleached the LNT coloured specimens required 1.5×10^{-11} J. ($\sim 4.7 \times 10^7$ photons) to bleach an F centre, whereas that irradiated at RT required 10^{-9} J. ($\sim 3.1 \times 10^9$ photons). The temperature of electron irradiation thus has an important influence on the optical bleaching at room temperature of the F band in KBr.

Surprisingly, if the slope $\left|\frac{dD}{dE}\right|$ of each of the curves in Fig.3.4 is plotted as a function of the total energy absorbed, the results all lie on the same approximately straight line on a logarithmic plot, over six decades of absorbed energy (Fig.3.7). The dotted line in Fig.3.7 represents the equation

$$\frac{dD}{dE} = \frac{5 \times 10^{-2}}{E} \qquad \ldots\ldots (1)$$

or $D_o - D = 5 \times 10^{-2} \log_e E$, where D_o is the F band optical density at the start of bleaching, and D its value after the absorption of E $J.cm^{-2}$. The bleaching mechanism occurring in RT and LNT irradiated KBr are clearly not the same, from the evidence already presented in Figs.3.3 and 3.4, and plotting the energy derivative of the F band coloration $\left|\frac{dD}{dE}\right|$ does, of course, remove any differences in optical density existing between specimens at the start of bleaching. Also the curves for the three different specimens in Fig.3.4 are nearly parallel; plotting $\frac{dD}{dE}$ on a logarithmic scale will tend to accentuate this feature, and flatten the curvature in the O.D. vs. E plots at low and high absorbed energy.

FIG. 37

BLEACHING OF ELECTRON IRRADIATED KBr

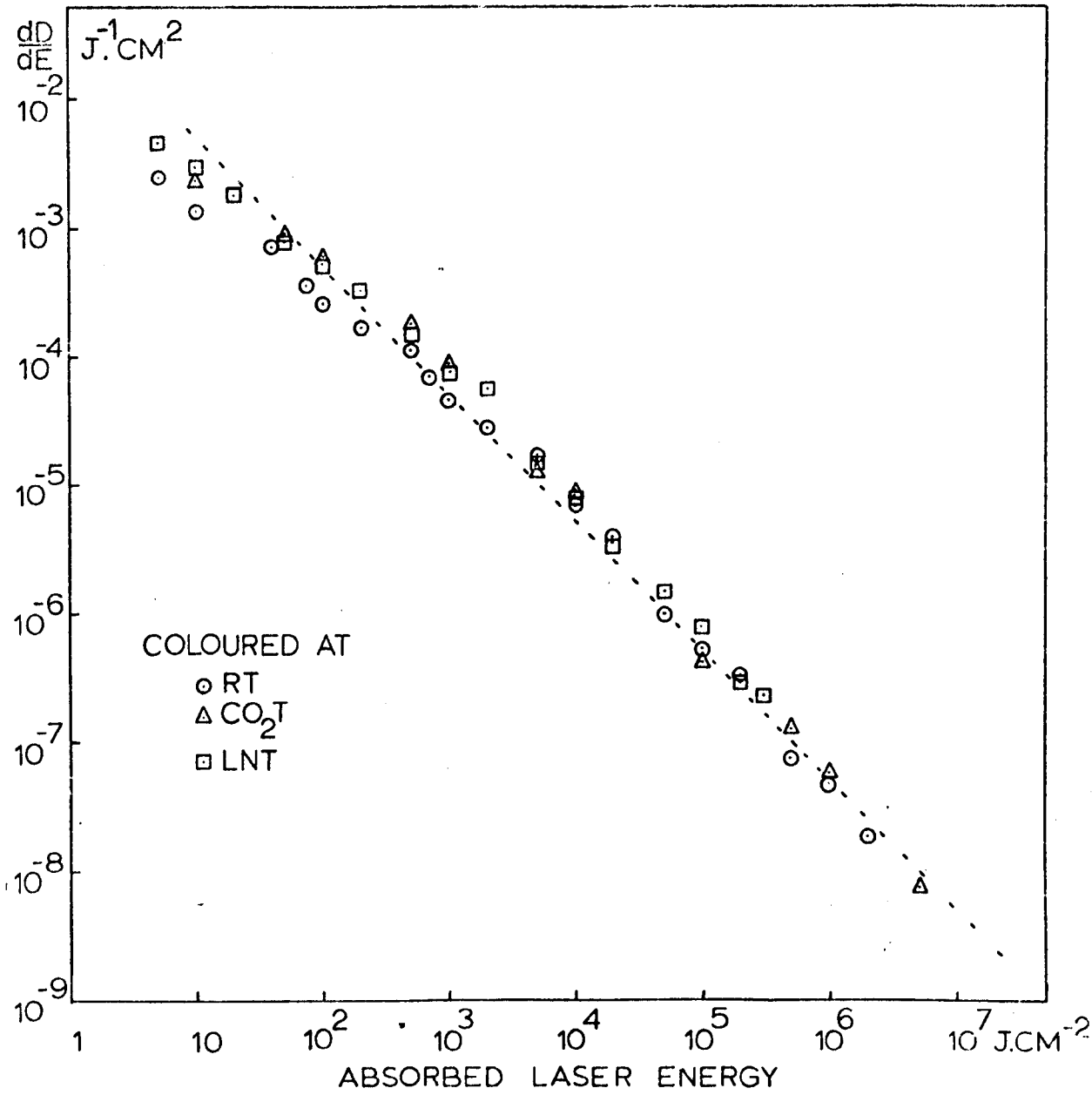

However, Fig. 3.7 does seem to suggest that there is some similarity between the optical bleaching mechanisms occurring in RT irradiated crystals and those coloured at low temperature.

3.2 Intensity Dependence

Other workers have reported that, at low levels of illumination, the rate of optical bleaching $\left|\frac{dn_F}{dt}\right|$ of the F band in X irradiated KCl varied linearly with intensity, and that at higher intensities $\left|\frac{dn_F}{dt}\right|$ tended to reach a saturation value [3]. The range of intensities in these experiments was from approximately 3×10^{-5} W cm^{-2} up to a maximum of 2.4×10^{-4} W cm^{-2}, with $\left|\frac{dn_F}{dt}\right|$ saturating at 1.6×10^{-4} W cm^{-2}. Similar low intensity bleaching curves have been published for additively coloured KBr but the intensity of the light source was not recorded [4].

The intensity dependence of the optical bleaching of R.T. electron coloured KBr was investigated over a wide range of incident power densities, using the microspectrophotometer with Neutral Density filters in the laser beam to attenuate it to the desired intensity. Over the range 1 Watt cm^{-2} to 5×10^3 W cm^{-2} no evidence was found to suggest that the bleaching rate $\left|\frac{dD}{dt}\right|$ was anything other than linearly dependent on the intensity of the F band illumination. Fig.3.8 illustrates the variation of bleaching efficiency η vs. the fraction of F centres bleached for a number of specimens illuminated at different intensities. η does not appear to change significantly with intensity, since the order of the curves is quite random, and bears no relationship to the bleaching intensities.

The results were expressed in this manner to assist comparison between different specimens. It was quite obviously impossible to colour five crystals to precisely the same density; Fig. 3.8 essentially normalises the data by expressing the height of the F band at any time as a fraction of its value at the start of measurement, rather than absolutely. The alternative would have been to carry out 5 consecutive bleaching experiments on the same piece of coloured crystal. It was felt

FIG. 3.8

INTENSITY DEPENDENCE OF BLEACHING
(Specimens coloured at RT)

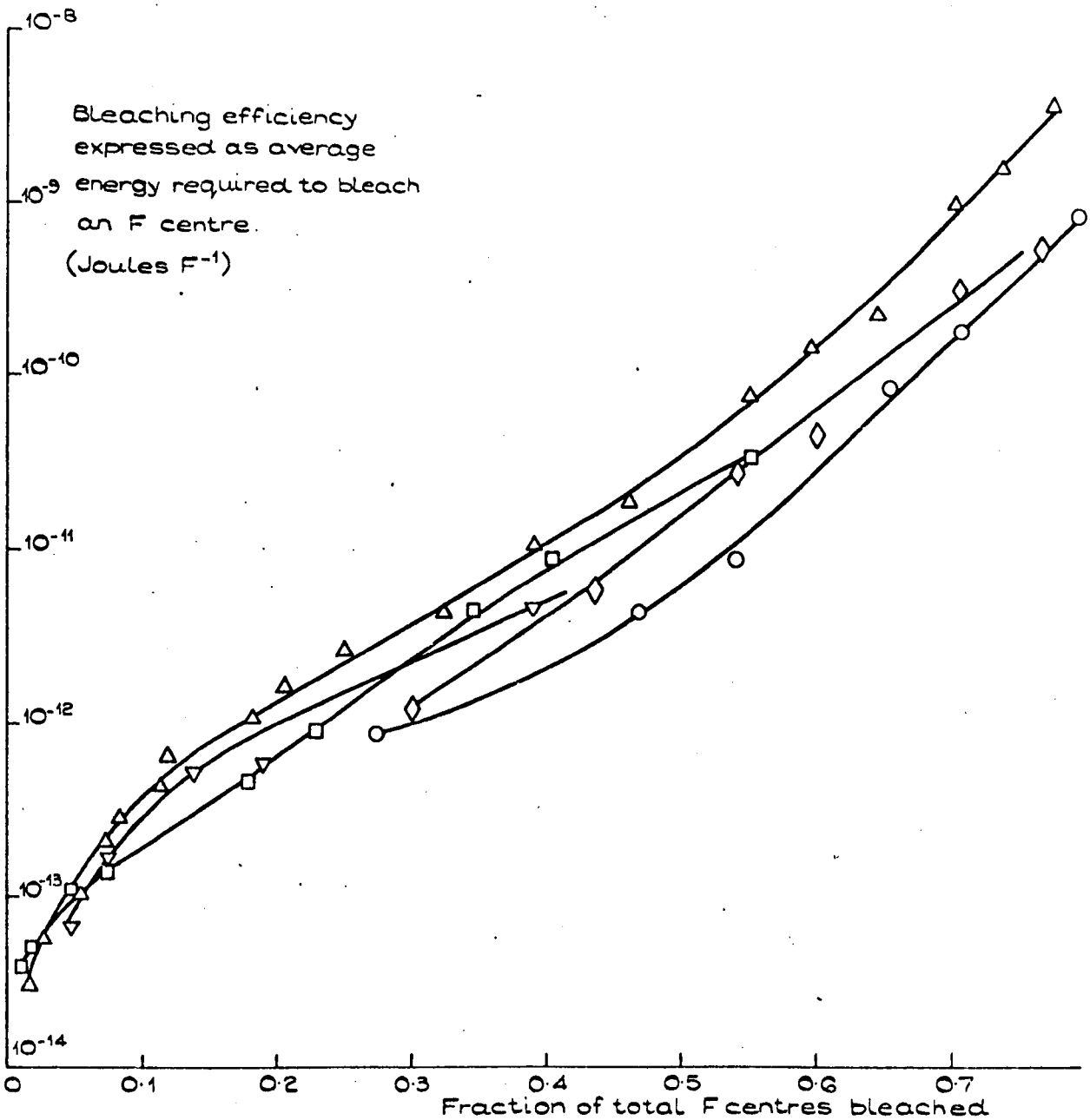

that the results obtained by this method would have been of somewhat more questionable validity than those of Fig.3.8, owing to the significant time interval that there would have been between the starting of the first and last experiments, and the effects of scattered light in the specimen holder.

It was not possible to thoroughly investigate the intensity dependence of bleaching for specimens coloured at low temperature, since it was found that the spread in results obtained with crystals bleached at the same nominal laser power density was sufficiently great to mask anything but a very non linear relationship. Fig.3.9 illustrates a selection of curves for crystals coloured at LNT, and Fig.3.10 shows the corresponding efficiency curves. The variation from specimen to specimen is quite marked, much more than that observed with the RT coloured crystals. It is, however, not unreasonable to say from Fig. 3.10 that the intensity dependence of the bleaching rate $\left|\frac{dD}{dt}\right|$ appears to be linear, at least for incident F band intensities lying between $10\ W\ cm^{-2}$ and $3 \times 10^{3}\ W\ cm^{-2}$. More will be said later concerning the considerable variation from specimen to specimen of the data obtained for low temperature coloured specimens.

3.3 Bleaching Measurements Made on Crystals That Had Not Been Previously Exposed To Light

It is evident from the results of the experiments described in Sections 3.1 and 3.2 that the rate of decrease of the F band in an electron coloured crystal is at its highest at the onset of bleaching. The very nature of the apparatus used for such measurements means that specimens received some exposure to light before measurements were started. A crystal had first to be transferred from the irradiation cryostat to the specimen holder, which was then placed in the microspectrophotometer beam. The microspectrophotometer optics were then aligned and the attenuated laser and photometer beams focused onto the coloured

Fig. 3.9.

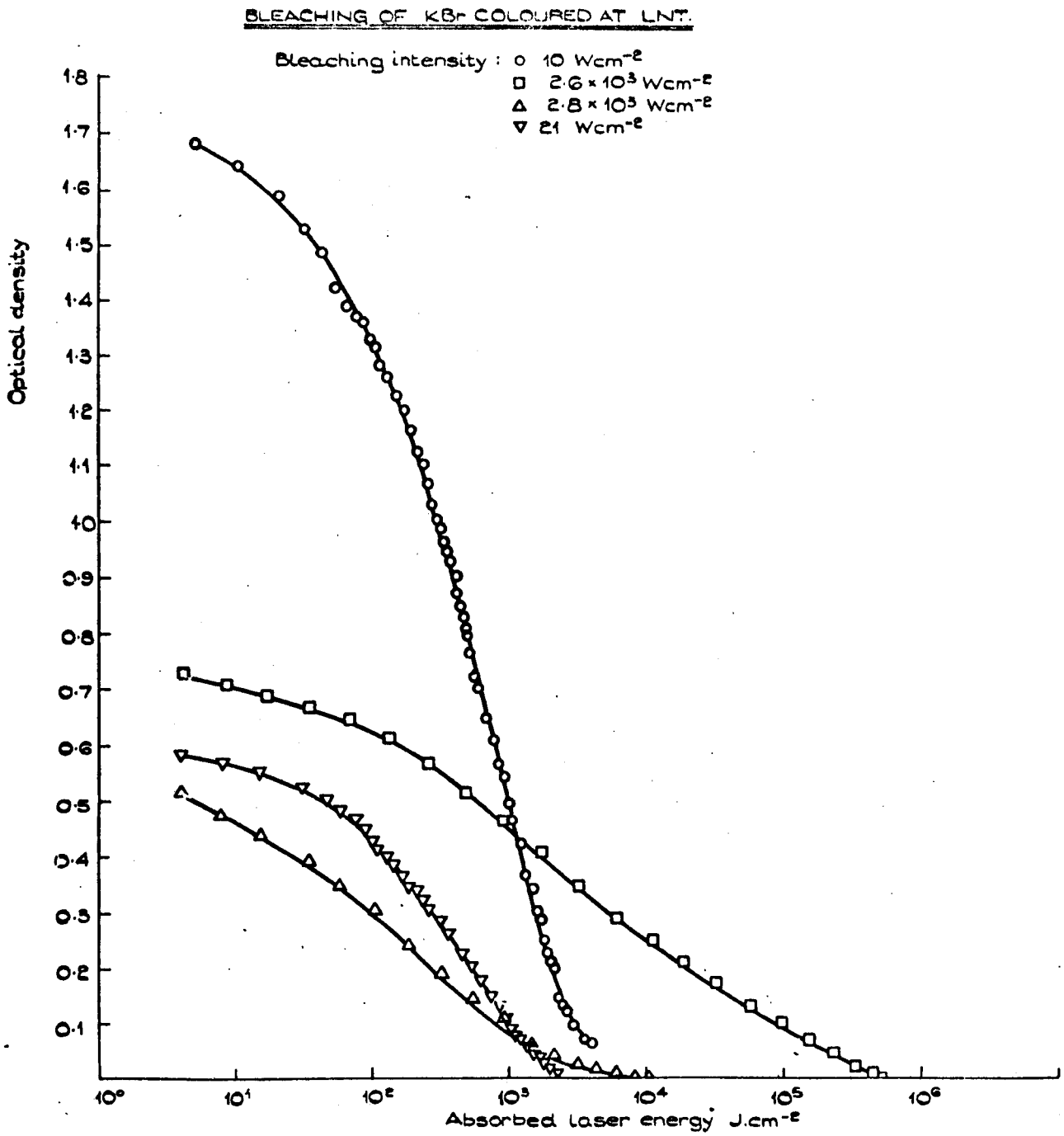
BLEACHING OF KBr COLOURED AT LNT.
Bleaching intensity : o 10 Wcm⁻²
□ 2·6 × 10³ Wcm⁻²
△ 2·8 × 10³ Wcm⁻²
▽ 21 Wcm⁻²
Optical density
1·8
1·7
1·6
1·5
1·4
1·3
1·2
1·1
1·0
0·9
0·8
0·7
0·6
0·5
0·4
0·3
0·2
0·1
10⁰
10¹
10²
10³
10⁴
10⁵
10⁶
Absorbed laser energy J.cm⁻²

FIG. 3.10

BLEACHING OF KBr COLOURED AT L.N.T.

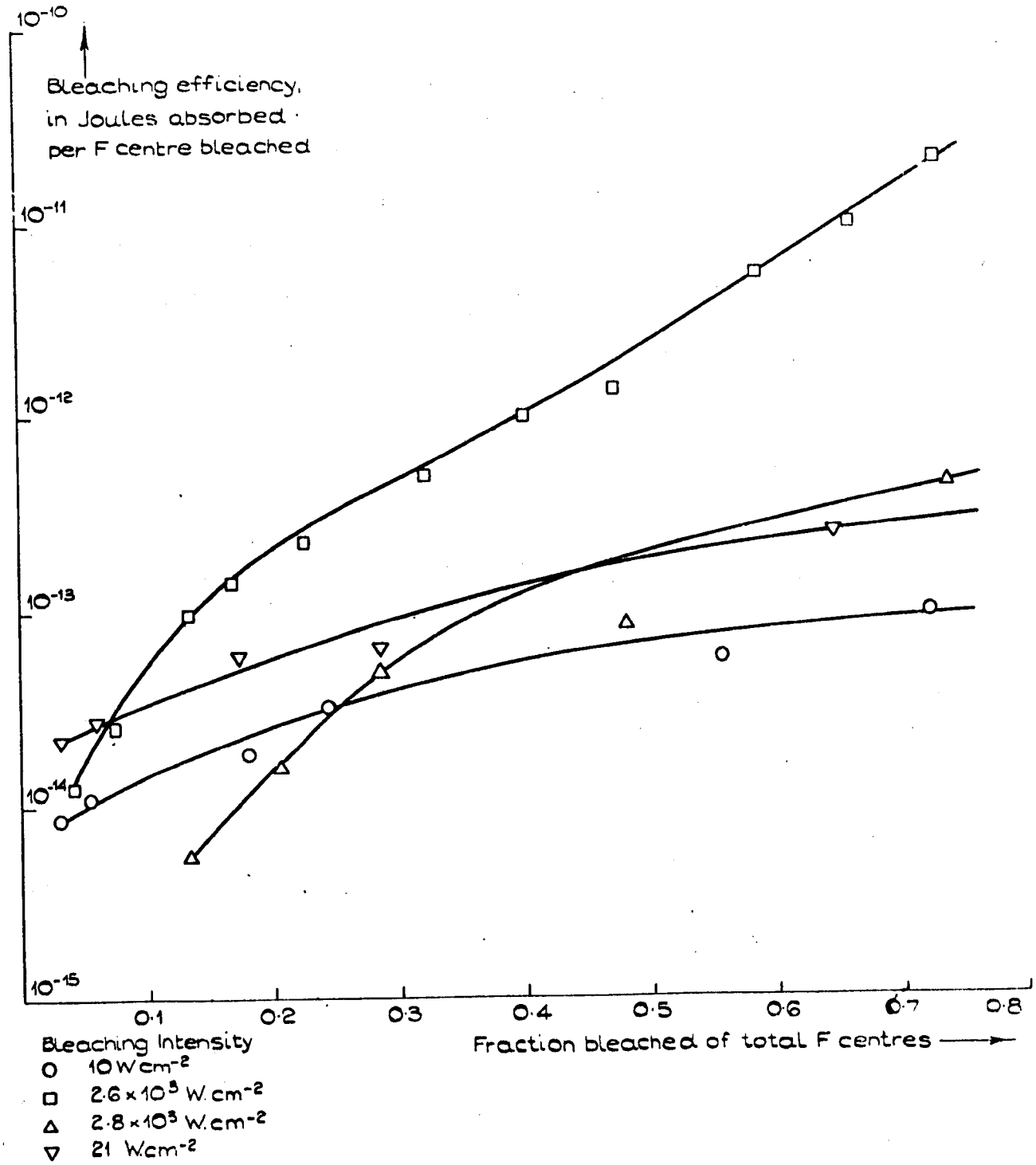

surface region of the crystal. Even if the transfer from the irradiation cryostat to the specimen holder were carried out in the most subdued lighting, and the time of alignment of the spectrophotometer were absolutely minimal, it was not possible to avoid exposing the specimen to a certain amount of F band energy before the experiment started. A reasonable estimate of the energy involved is around 1 Joule cm^{-2}. Coupling this fact with the observation that the rate of bleaching was larger at the start of the experiment, it seemed useful to investigate the early stage of bleaching by making measurements on a crystal that had received no previous illumination.

The apparatus illustrated schematically in Fig.3.11 was constructed for this purpose. It allowed the crystal to be coloured by electron irradiation on the Van de Graaff accelerator, and then be bleached, without removing it from the irradiation cryostat. An unfocused 1mW. He/Ne laser was used for bleaching and monitoring the specimen transmittance.

The specimen was mounted in a cryostat (e), on the end of a liquid nitrogen vessel that could be rotated through 90^{o} whilst under vacuum. In this way one could place the specimen perpendicular to either the electron beam (for coloration) or the laser beam (for bleaching). Between the laser and the irradiation cryostat there was a light proof box (a), containing a beam splitter mirror (b), a shutter (c) and a power monitor detector head (d). This enabled the power incident on the specimen to be measured. The beam splitter was an unsilvered microscope cover slide; the glass by itself had a sufficiently high reflectivity to provide a satisfactory signal for the power monitor. Three centring screws were provided on the collar that attached the laser to the box (a), so that the beam could be positioned prior to starting the experiment. A photomultiplier tube measured the intensity of the laser light transmitted by the specimen; it was attached to the

FIG. 3.11.

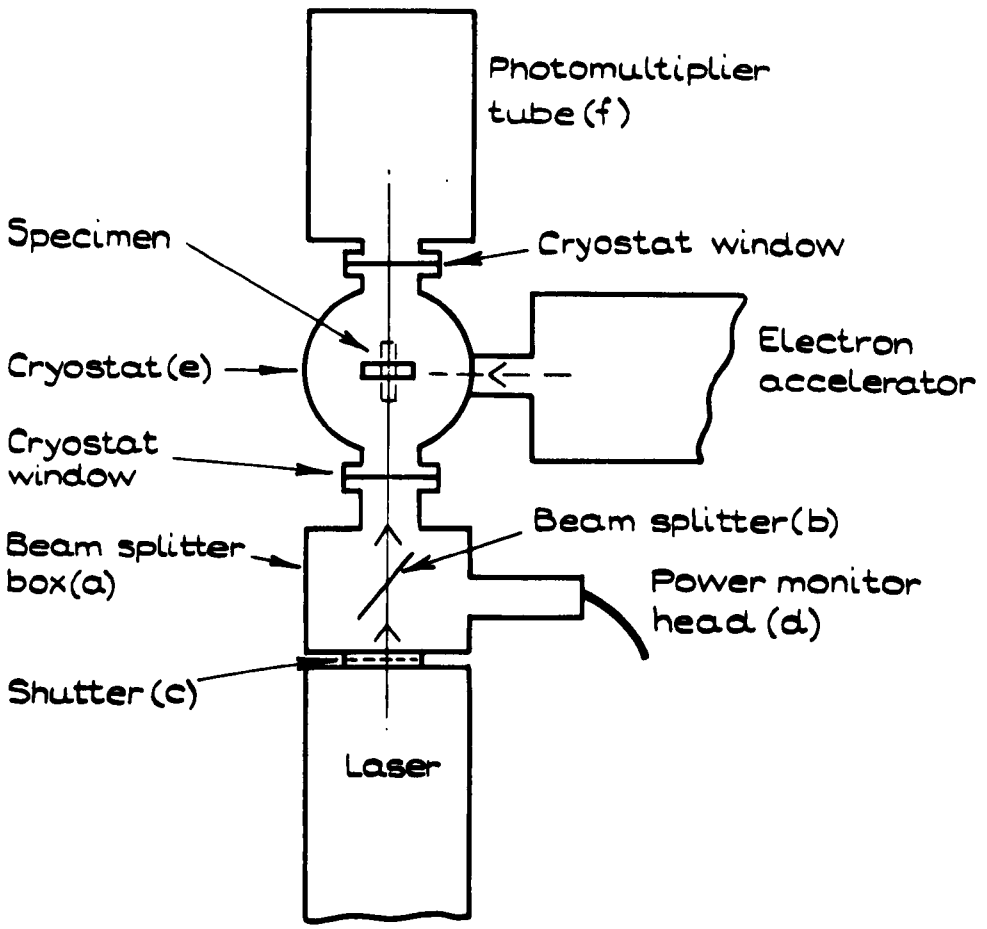

SCHEMATIC DIAGRAM OF THE EARLY STAGE BLEACHING APPARATUS.

cryostat window by a short coupling tube. It was found necessary to attenuate the laser beam by a factor of 10^3 before allowing it to illuminate the cathode of the photomultiplier; this was accomplished using Kodak "Wratten" neutral density filters. Since it was necessary to leave the e.h.t. voltage connected to the p.m.t. during electron irradiation, it was considered advisable to protect it from X rays generated by the electron beam striking parts of the cryostat or flight tube, in order to preserve a low dark current. A screen made from two thicknesses of 1/8" lead sheet was fitted around the photomultiplier housing, with 1/2" of lead glass in front of the photocathode window; no increase in dark current was observed when the accelerator was operating at 50 KV and 50 μ A. The laser, cryostat and photomultiplier tube assembly was made completely light tight, so that there was no possibility of extraneous light reaching the crystal before or during bleaching. The specimen was shielded from light from the accelerator filament by the thin aluminium foil used to scatter the electron beam and give a more even coloration. Nothing, of course, can be done to shield the crystal from its own cathodoluminescence during irradiation.

A photograph of this apparatus appears in Fig. 3.12. The laser is in the foreground and the cryostat in the centre of the picture, with the photomultiplier housing behind. The accelerator beam tube and vacuum isolation valve is attached to the right hand side of the cryostat.

At the start of an experiment, a freshly cleaved piece of KBr was mounted in the cryostat, and rotated until it was perpendicular to the laser beam. The position of the laser was carefully adjusted so that the beam passed through the centre of the crystal. The photomultiplier eht was turned on, and a 100% transmittance measurement made after allowing a reasonable period for dark current stabilisation. Both the output of the laser power monitor and the pmt were connected to recorders, the traces of which could be synchronised by the initial step when the

FIG. 3.12.

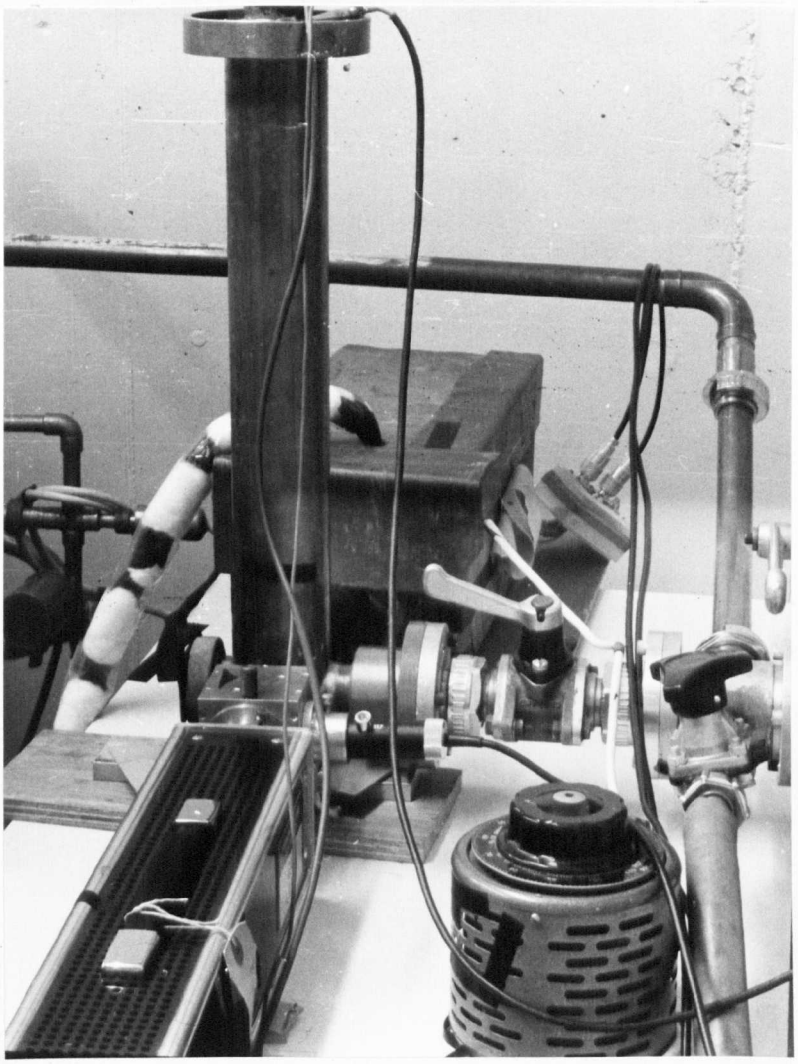

PHOTOGRAPH OF THE EARLY STAGE

BLEACHING APPARATUS.

shutter (c) was lifted, and by event marks which were put on at intervals. In this way, variations in laser output, and hence 100% signal level, could be compensated for when calculating the specimen absorbance. (The stability of the photomultiplier tube assembly had already been shown to be perfectly adequate for this purpose; it was the same system used with the microspectrophotometer.) The inner vessel of the cryostat was then rotated to bring the specimen perpendicular to the electron beam, for irradiation. After irradiation for about half an hour at 50 KV and 40μ A, the specimen holder was rotated back through 90°, to once again make it normal to the laser beam. Then, with both recorders running, the shutter was lifted to start the exposure. This yielded a continuous record of both the laser output and the specimen transmittance, from which curves of optical density vs. time or absorbed energy could be computed, similar to those of section 3.1. The optical density was obviously the value at the laser wavelength (632.8 nm.), and a correction ought to have been applied to increase this value to that which would have been measured at the peak of the F band (625 nm.) This correction would, however, have been very small ($\sim$ x 1.005), and the error introduced by not making use of it is negligible.

These experiments were performed on crystals coloured at 294° K (with acetone in the cryostat as a temperature stabiliser) or at 93° K using liquid nitrogen as a refrigerant. The LNT coloured specimens were warmed to room temperature, in the dark, before bleaching. Prior to irradiation the KBr specimens, which were supplied by the Harshaw Chemical Co., were cleaved and mounted in the nitrogen flushed glove box, in precisely the same manner as those used in the earlier experiments. To further assist in the comparison between these results and those obtained using the microspectrophotometer, the starting optical densities were arranged to lie between 0.7 and 0.9.

The unfocused laser beam gave a power density at the surface of the specimen of about 5 mW cm^{-2}, which enabled very satisfactory plots

of the early, fast part of the optical bleaching curves to be obtained, for absorbed energies between 10^{-2} J.cm^{-2} and 10 J.cm^{-2}. Typical results of such experiments are illustrated as curves of the variation of optical density with time of illumination in Fig. 3.13. The corresponding absorbed energy plots are shown in Fig. 3.14. The striking thing about these two curves, when compared against those obtained using the microspectrophotometer (Fig. 3.4) is the slope. For example, on examining the results for the RT coloured specimen of Fig. 3.4, one finds that in reducing the optical density from 0.8 to 0.4, approximately 3 x 10^{4} J.cm^{-2} were absorbed. In Fig. 3.14 only about 10 J.cm^{-2} were required to give the same absolute reduction in coloration, a very considerable decrease in the energy absorbed. This apparently greater efficiency of bleaching is reflected in Fig. 3.15, which is a graph of the average energy absorbed per F centre bleached against the fraction of F centres destroyed. These curves are directly comparable with the microspectrophotometer results of Fig. 3.6. A further point arises out of Fig. 3.15, that the average energy absorbed for the bleaching of an F centre remains approximately constant (at around 10^{-16} J.F^{-1} for RT coloured specimens) until about 20% of the F band has been removed, after which it starts to steadily increase. The constancy of this parameter is clearly never seen in Fig. 3.6, it increases steadily throughout the measurements. It may be that a significant number of easier to bleach F centres are destroyed by luminescence whilst the specimen is still under irradiation. This means that the bleaching efficiency measured at the onset of bleaching (i.e. the <u>average</u> energy absorbed per F centre bleached) will be reduced from what it would be if there were no bleaching due to cathodoluminescence. This could produce the constant efficiency region in Fig. 3.15. It is difficult to make accurate estimates of the optical energy absorbed in the F band whilst the specimen is under irradiation, but it is likely to be between 10^{-5} and 5 x 10^{-3} J.cm^{-2}. This estimate

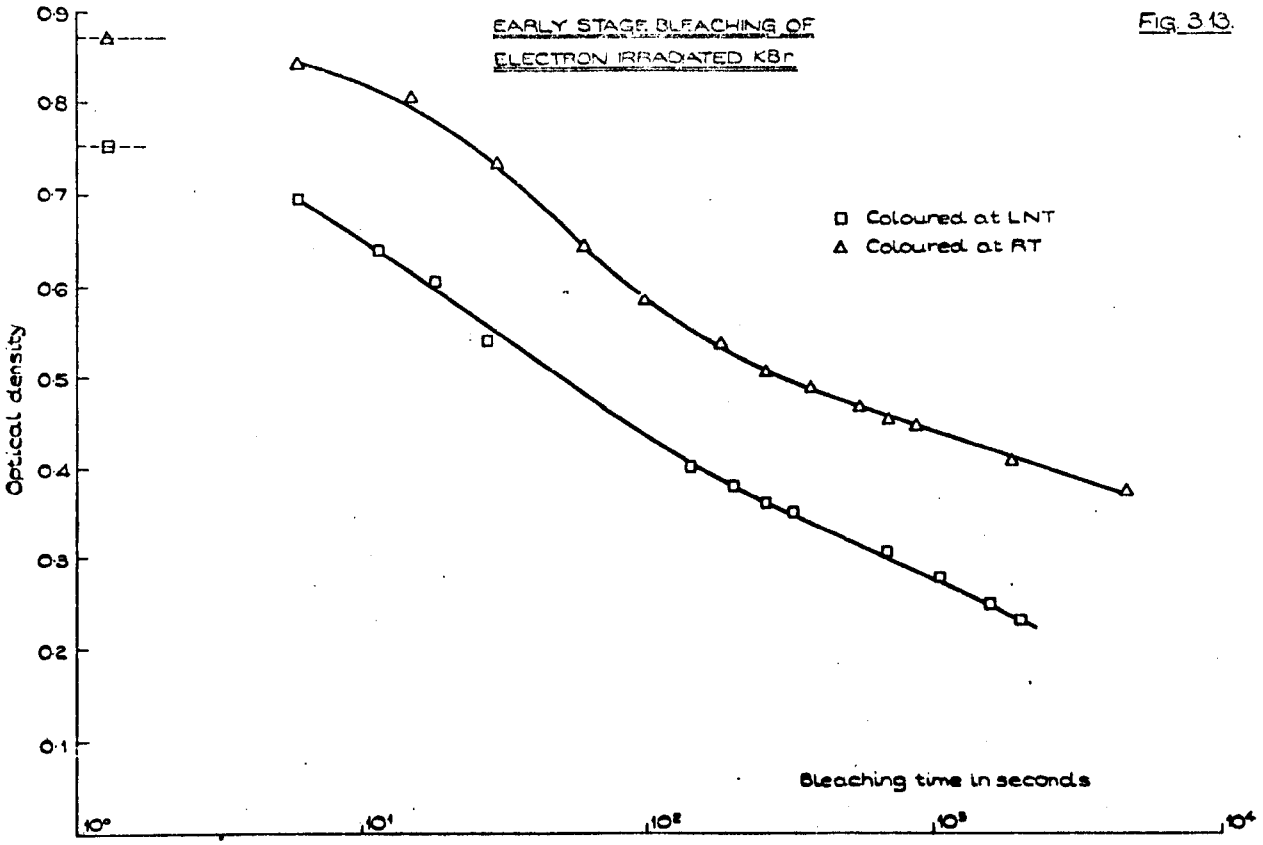
EARLY STAGE BLEACHING OF
ELECTRON IRRADIATED KBr
FIG. 3.13.
Coloured at LNT
Coloured at RT
Optical density
0·9
0·8
0·7
0·6
0·5
0·4
0·3
0·2
0·1
A
B
Bleaching time in seconds
10⁰
10¹
10²
10³
10⁴

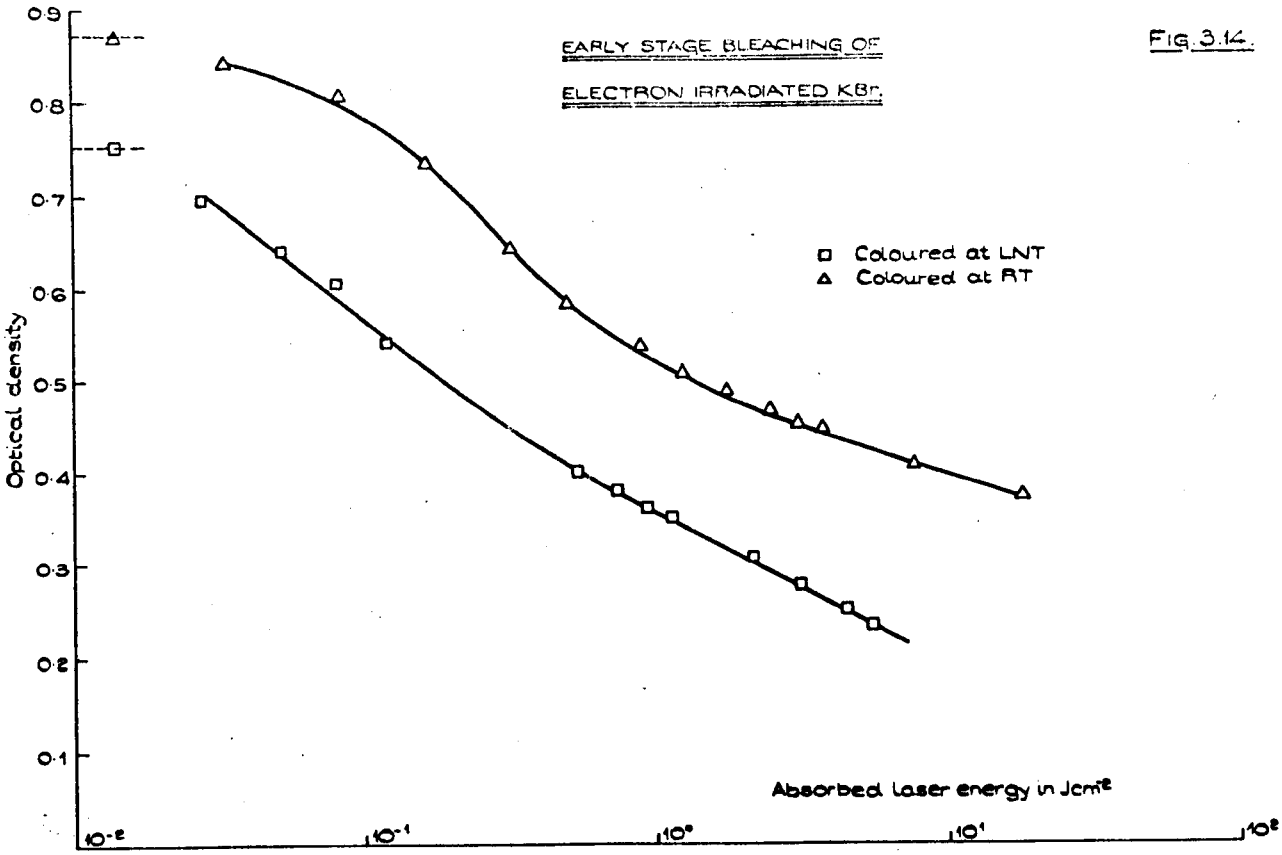
EARLY STAGE BLEACHING OF
ELECTRON IRRADIATED KBr.
Coloured at LNT
Coloured at RT
Optical density
0·9
0·8
0·7
0·6
0·5
0·4
0·3
0·2
0·1
Absorbed laser energy in Jcm⁻²
10⁻²
10⁻¹
10⁰
10¹
10²

FIG. 3.14.

Fig. 3.15.

EARLY STAGE BLEACHING EFFICIENCIES.

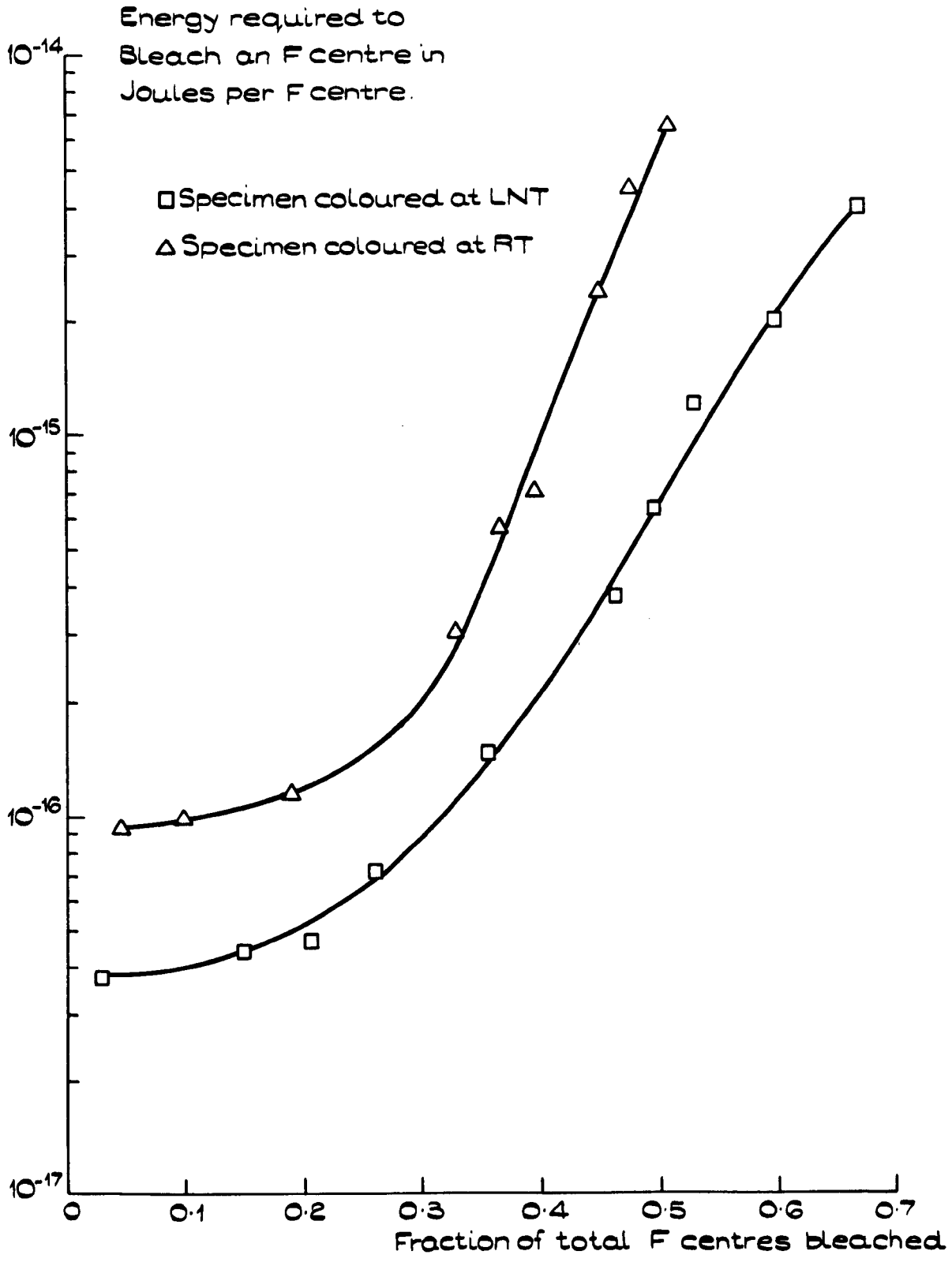

is based on observations of the brightness of the cathodoluminescence made with the CCTV system used to monitor the interior of the Van de Graaff enclosure during irradiation. Clearly if the actual optical energy absorbed in the F band from cathodoluminescence is near the upper limit of the estimate, then it is reasonable to expect some effect to be seen in the bleaching curves.

There is, however, a good correspondence between the initial stage bleaching data and that obtained using the microspectrophotometer when it is expressed as a curve of the rate of bleaching $\left|\frac{dD}{dE}\right|$ vs energy absorbed (E). Fig. 3.16 shows this rate curve for the data of Fig. 3.14; it is to be compared with Fig. 3.7. The dotted line in Fig. 3.16 represents the line $\frac{dD}{dE} = \frac{9 \times 10^{-2}}{E}$, which is very close to the value for $\frac{dD}{dE}$ of $\frac{5 \times 10^{-2}}{E}$ found using the microspectrophotometer. (The departure from the straight line at $E < 10^{-1}$ J.cm^{-2} obviously corresponds to the nearly horizontal region of the curves in Fig. 3.15).

Taken as a whole, the evidence of the initial stage bleaching experiments strongly suggests that the optical density of the specimens used in the microspectophotometer experiments was between 1.5 and 2.0 (directly after irradiation), and that it had fallen to the observed value of between 0.7 and 0.9 by the time they had absorbed some 1 J.cm^{-2} during the optical alignment. Taking this into account, the apparent differences between the two sets of data are resolved, since the starting F centre concentrations are not the same in the two cases. Further substantiation is afforded by the continuity of the slope of the two sets of "rate" curves (Fig. 3.16 and 3.7); this, coupled with the previously found linear intensity dependence over the range 1 to 10^3 J.cm^{-2} (sect. 3.2), tends to rule out the alternative possibility of there being a non linear dependence of bleaching on energy when going to relatively low intensities, of the order of mW. cm^{-2}.

It is worth noting that the spread in results over a number of different specimens for the initial stage experiments was appreciably less than that found when using the microspectrophotometer, particularly

FIG. 3.16.

EARLY STAGE BLEACHING OF ELECTRON IRRADIATED KBr

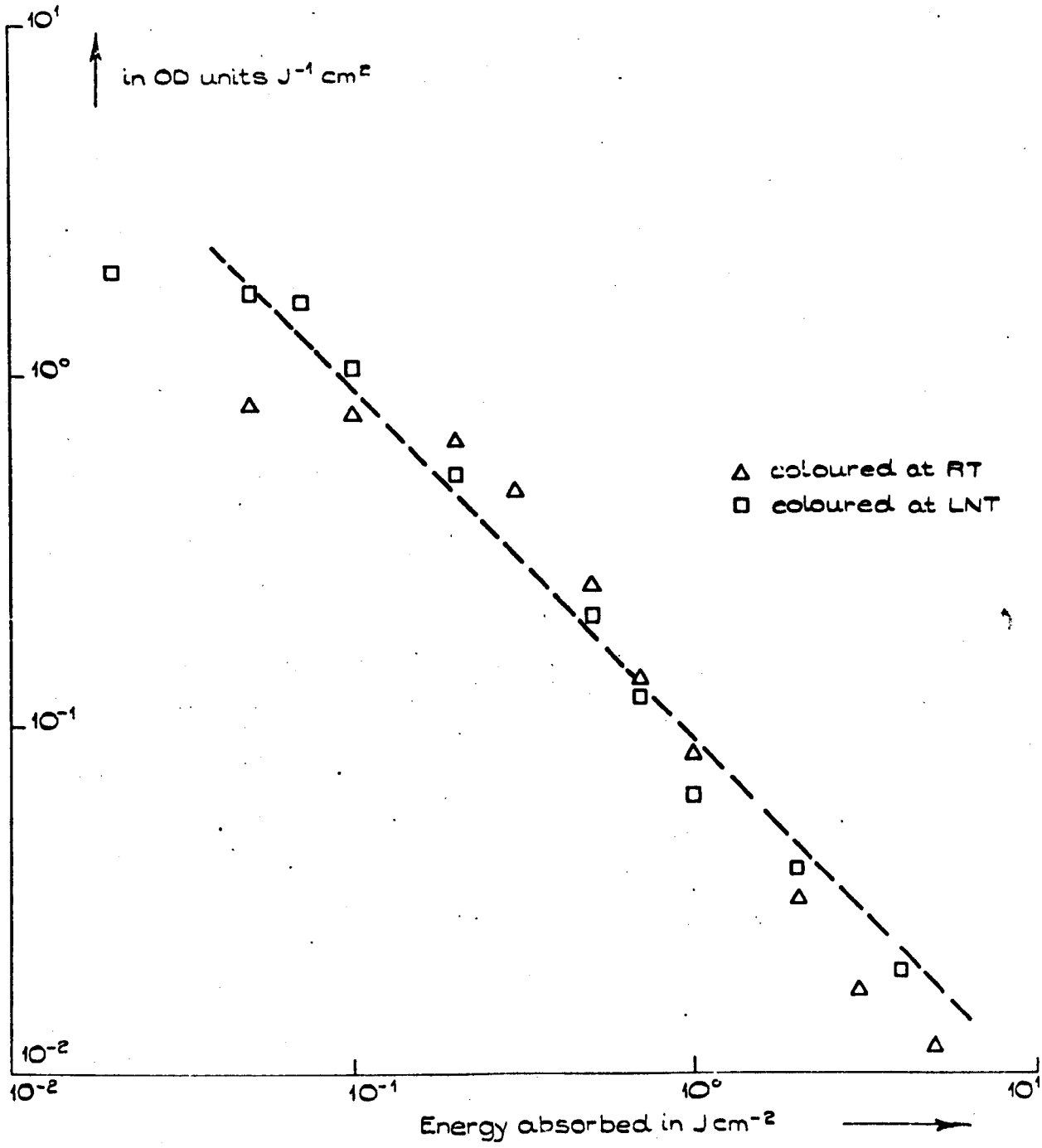

in those specimens coloured at LNT. This is no doubt due to the fact that in the latter measurements there was no guarantee that two crystals whose optical densities were the same at the start of the experiments were identical just after irradiation i.e. that both were truly comparable results. Small variations in the energy absorbed during alignment were inevitable, and, at this stage of bleaching, as has been shown, small exposures to light produce quite significant changes in F band optical density.

3.4 Impurities in the specimens, and their influence on bleaching kinetics

The experiments described in the first 3 sections of this chapter were carried out on specimens that had been cleaved from single crystal slabs of KBr, grown from the melt by the Harshaw Chemical Company. These crystals were at all times stored in a vacuum dessicator, to prevent the absorption of atmospheric moisture. However, KBr does not appear to be as hygroscopic as some of the alkali halides (notably Na Br), the surface did not noticeably deteriorate on crystals that were deliberately exposed to the atmosphere for many weeks.

Some preliminary measurements were made, whilst the apparatus was being developed and evaluated, on single crystal KBr supplied by Hilger and Watts Ltd. This was thought to be of lower purity than the Harshaw material, but in fact it yielded bleaching curves that were very similar to those of section 3.1. The differences between the two sets of data were no greater than the variation found between different Harshaw specimens.

A number of workers have found an ultraviolet absorption band in uncoloured alkali halides which has been attributed to the presence of OH^- ions. The association of this band with hydroxyl ions has been verified by correlating its intensity with the absorption in the infra-red known to be due to the OH^- band resonance; it occurs at about 215nm. in KBr. A strong vibrational absorption between 7 and 8 μm is also seen. During the growth process, the high temperature of the melt apparently

favours the incorporation of water from the surrounding atmosphere into the crystal; this can clearly be prevented by growing the crystals from water free material in a vacuum or inert gas. Natural crystals of NaCl which have grown by slow evaporation from solution show the lowest OH^- absorptions [5,6]. Since the OH^- impurity is reported to affect the coloration properties [7] (at least for u-v irradiation) and to influence the formation of colloidal centres, it was decided to investigate whether or not it was present in the Harshaw crystals, and if it was, to make measurements for comparison on crystals that were grown specifically to have a low water content.

The transmission spectrum of a sample of Harshaw KBr was therefore measured over the range 200 to 240 nm., using a Perkin Elmer model 450 spectrophotometer. It exhibited, as the earlier workers had found in Harshaw KBr a reasonably well defined absorption band at 215 nm., signifying the presence of an undefined concentration of OH^- ions in all of the specimens used in the optical bleaching experiments. It was not possible to see the corresponding i.r. absorption, since a crystal having the necessary thickness ($\sim$2 cm) was not available. There was certainly no evidence of any absorption bands between 1 and 25 microns in a specimen of 6 mm thickness.

A boule of KBr was obtained from British Drug Houses which had been grown (by the Bridgman-Stockbarger method) in a completely water free, inert, atmosphere, from 'Optran' spectroscopic grade raw material. This crystal arrived from BDH in a sealed, dessicated bottle, and at all times was handled in the dry nitrogen flushed glove box. It ought, therefore, to have yielded specimens of very high intrinsic purity, uncontaminated by atmospheric moisture. This boule of KBr proved to be very difficult to cleave, as it contained a number of low angle grain boundaries which made it difficult to determine the precise orientation of the cleavage planes. However, a small number of specimens were

finally produced, and whilst their optical quality left a lot to be desired, bleaching measurements were made on them. The results were virtually indistinguishable from those obtained previously, using the Harshaw material. The two most reliable sets of data (one specimen coloured at RT and one at LNT) are illustrated in Fig. 3.17; the similarity, particularly for the RT coloured specimen, between it and Fig. 3.4 is obvious. It is concluded, therefore, that the optical bleaching performance of electron coloured KBr is not greatly affected by the purity of the specimens, relatively low purity crystal (Hilger and Watts) yielding results that are directly comparable with those obtained from high purity (BDH) material. The variation between specimens from different samples was no greater than the variation found between specimens cleaved from the same sample.

In order to gain some quantitative information on the purity of the specimens, samples of the Harshaw and BDH crystals were sent to Johnson Matthey Chemicals Ltd. for analysis. They were asked specifically to look for foreign metal ions, and to carry out a determination of the water content. Their report is reproduced as Fig. 3.18. The cation impurity content is what might be expected, particularly in regard to the presence of the alkali metals rubidium and sodium. In both cases, however, the water content is surprisingly high, and more than a little unlikely, considering the strength of the UV OH^- absorption in the specimens, and the fact that no optical absorption (in the ir.)due to the hydroxyl ion bond resonance could be detected. Great care was taken to avoid contamination of these samples, they were despatched to Johnson-Matthey in small glass containers that had been packed and sealed in a dry nitrogen flushed glove box. Furthermore, the specimens were cleaved from the centre of the boules in the glove box, such that none of the surfaces had been previously exposed to the atmosphere.

The OH^- absorption at 215 nm is shown in Fig. 3.19 for a number

FIG. 3.17

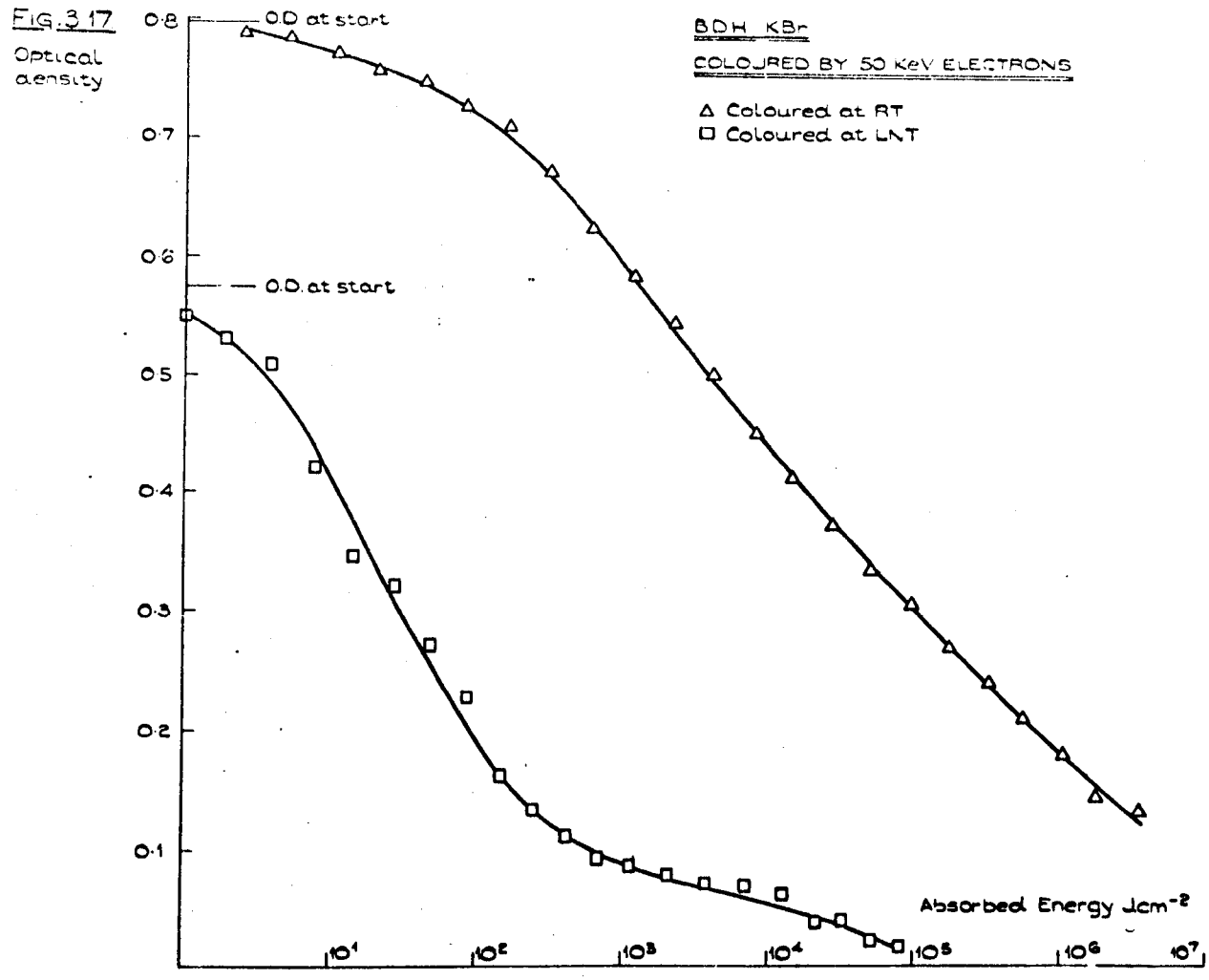
Optical density
0·8
0·7
0·6
0·5
0·4
0·3
0·2
0·1
O.D at start
O.D. at start
B.D.H. KBr
COLOURED BY 50 KeV ELECTRONS
△ Coloured at RT
□ Coloured at LNT
Absorbed Energy Jcm⁻²
10¹
10²
10³
10⁴
10⁵
10⁶
10⁷

Reference No. R/A 2139

Fig. 3.18.

Johnson Matthey Chemicals Limited

Analytical Laboratories

Orchard Road Royston Herts

Telephone: 0763 2021

23rd January 1970

Certificate of Analysis

To The University of Warwick, Attn. Mr. Redman

Dear Sir(s),

We have examined the one sample marked B.D.H. and one marked Harshaw received from you ~~on the~~ recently and submit the following report:

Element	Estimated Quantity Present Results as parts per million	
	BDH	Harshaw
Aluminium	ND	< 1
Calcium	1	< 1
Magnesium	< 1	< 1
Rubidium	10	10
Sodium	3	2

The following elements were specifically sought but not detected:-
Ag, As, Au, Ba, Be, Bi, Cd, Co, Cr, Cs, Cu, Fe, Ga, Ge, Hf, Hg, In, Ir, Li, Mn, Mo, Nb, Ni, Os, P, Pb, Pd, Pt, Rb, Re, Rh, Sb, Se, Si, Sn, Sr, Ta, Te, Ti, Tl, V, W, Zn, Zr.

	BDH	Harshaw
Water Content	2.35%	3.29%

for Johnson Matthey Chemicals Ltd.,

P.W. GERRARD
Superintendent, Analytical Laboratory

M. 550

FIG. 3.19

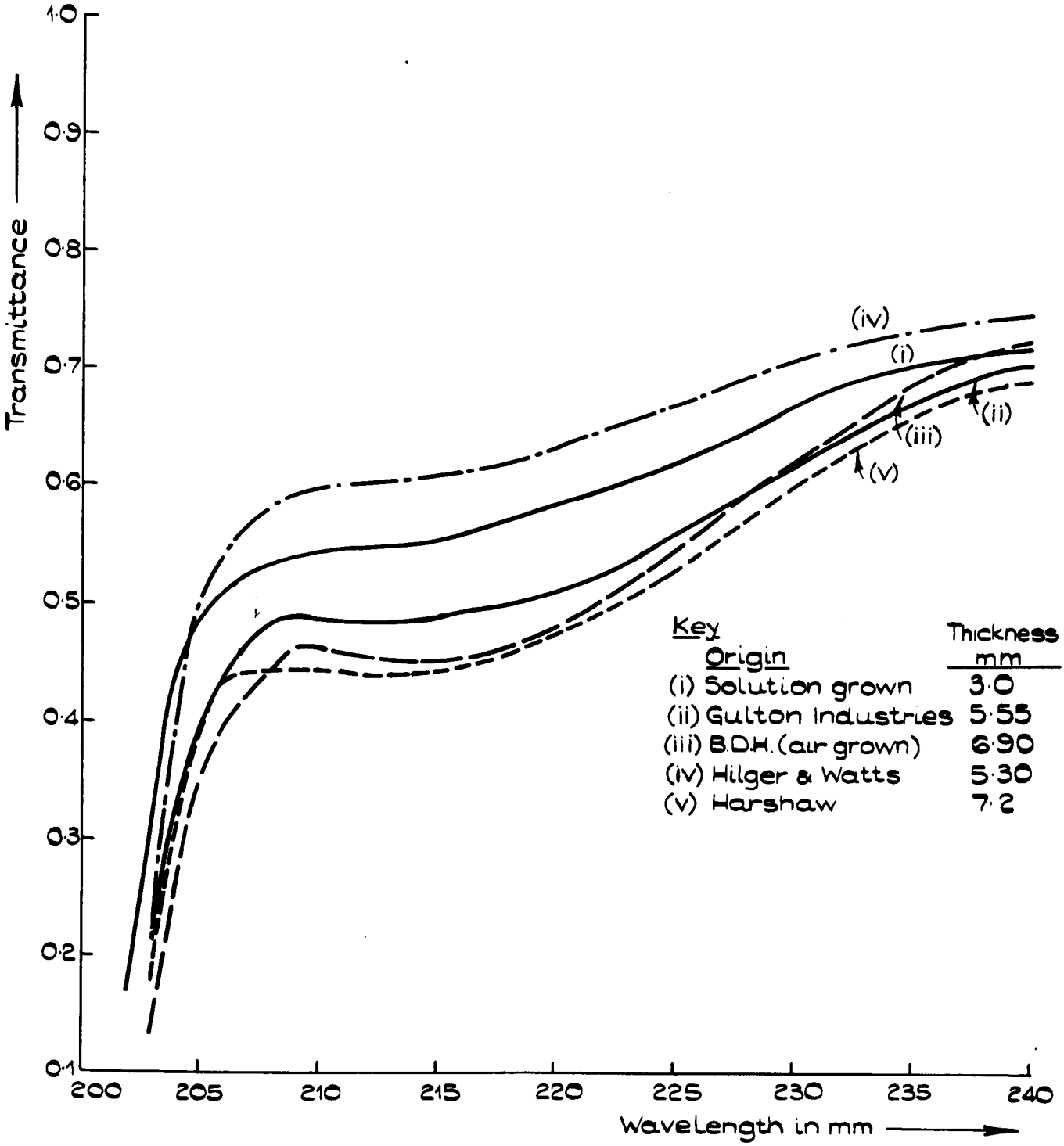

THE OH^- ABSORPTION BAND IN VARIOUS SAMPLES OF KBr.

of specimens from different sources. Considering the thickness of the specimens, this absorption band is not very pronounced in any of the samples. The solution grown crystal was simply the result of dissolving "Analar" KBr powder in distilled water, and allowing the solution to stand undisturbed for a period of several weeks, until all of the water had evaporated. If one can reasonably compare solution grown crystals produced in the laboratory and those that occur naturally, it might be expected that the solution grown material has a low water content, which, from Fig. 3.19, implies that all of the specimens examined, including Harshaw, have a low hydroxyl ion concentration. The major objection to making comparisons between natural and synthetically produced solution grown alkali halide is the great age ($>10^6$ years) of the former. During this time the crystals could have been subjected to treatment (e.g. a high temperature anneal) which may have driven off their water content. From Fig. 3.19, using the results of Klein et al [10], it is deduced that the hydroxyl ion concentration in all of the specimens is no more than a few p.p.m.

A further point of interest is that the Johnson-Matthey water content figures are about an order of magnitude greater than those given by B.D.H. for their 'Analar' grade KBr powder; it is rather unlikely that the growth process would yield crystals with a water content so much higher than that of the starting material.

Since the water content figure of the analysis was obviously doubtful, attempts were made to make another measurement, using both of the methods used by Johnson-Matthey in their determination. Initially a weight loss on heating method was tried, on a crystal weighing 3 grammes, with a high surface area to volume ratio. It was appreciated that heating a KBr crystal might result in its slow evaporation, so in order to check that only moisture was evolved the heating was carried out under vacuum with a mass spectrograph (G.E.C. MS10) continuously sampling

any pumped off gases. The specimen was carefully weighed, and then placed on a heating stage in an all glass vacuum system; the apparatus had been thoroughly outgassed beforehand. The heating stage was simply two copper slabs, with a 60 watt soldering ion element sandwiched between them in a recess. The crystal was separated from the copper by a platinum foil, and a thermocouple was provided for temperature measurement.

After establishing a vacuum in the system, a spectrum was recorded before the heater was turned on (Fig. 3.20 (a)); the lines are all attributable to residual CO, N_2 and O_2, with a very characteristic series of lines due to the hydrocarbon vacuum pump oil (despite a double cold trap). The specimen was than heated to around 200°C, and left for 5 days at this temperature. Periodically the mass spectrograph was used to check for the evolution of any gases. Fig.3.20 (b) shows such a spectrum; quite clearly it does not differ very much from Fig.3.20 (a) or indeed from the spectrum obtained without the specimen present. Throughout the heating there was neither any increase in the background spectrum to indicate that H_2O, in any of its ionised forms, was being liberated from the crystal, nor was there any suggestion that the specimen itself was evaporating. Reweighing the specimen (to an accuracy of 0.0001 gm) at the end of the heat treatment showed that it had not lost any weight, which can be either interpreted as demonstrating that the H_2O concentration in the crystal was very low, or that the specimen had not been heated to sufficiently high a temperature to drive the moisture off. It is likely that heating to a higher temperature would have initiated specimen evaporation, and so a further attempt was made at a determination of the moisture content by a wet chemical method, using the Karl Fischer reagent.

The Karl Fischer technique for moisture determination is a well established method that is used for the routine examination of a very wide range of substances [8] e.g. foodstuffs, paints, soaps and detergents,

MASS SPECTRUM PRIOR TO HEATING.

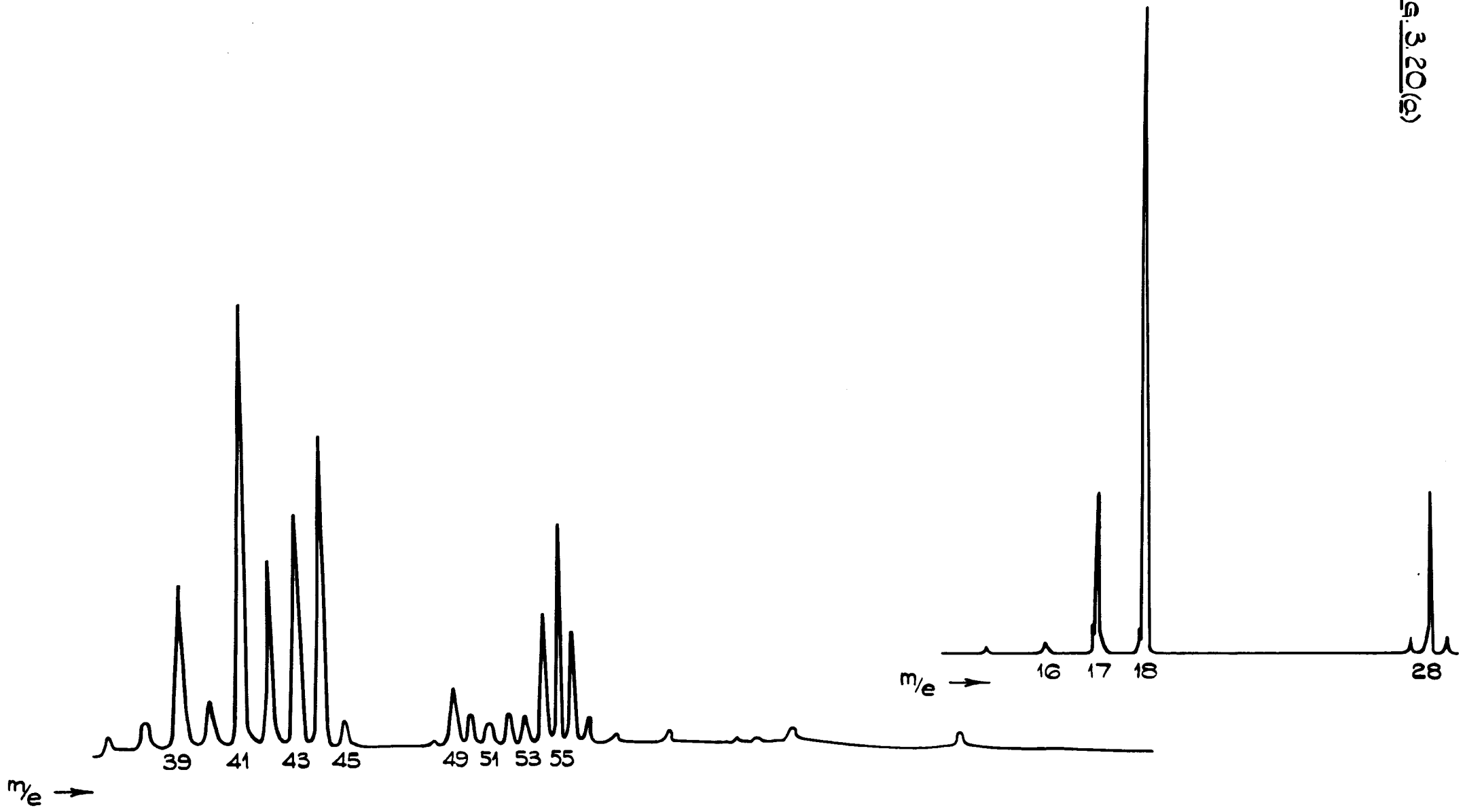

Fig. 3.20(a)

MASS SPECTRUM DURING HEATING.

(specimen temp. ~200°C)

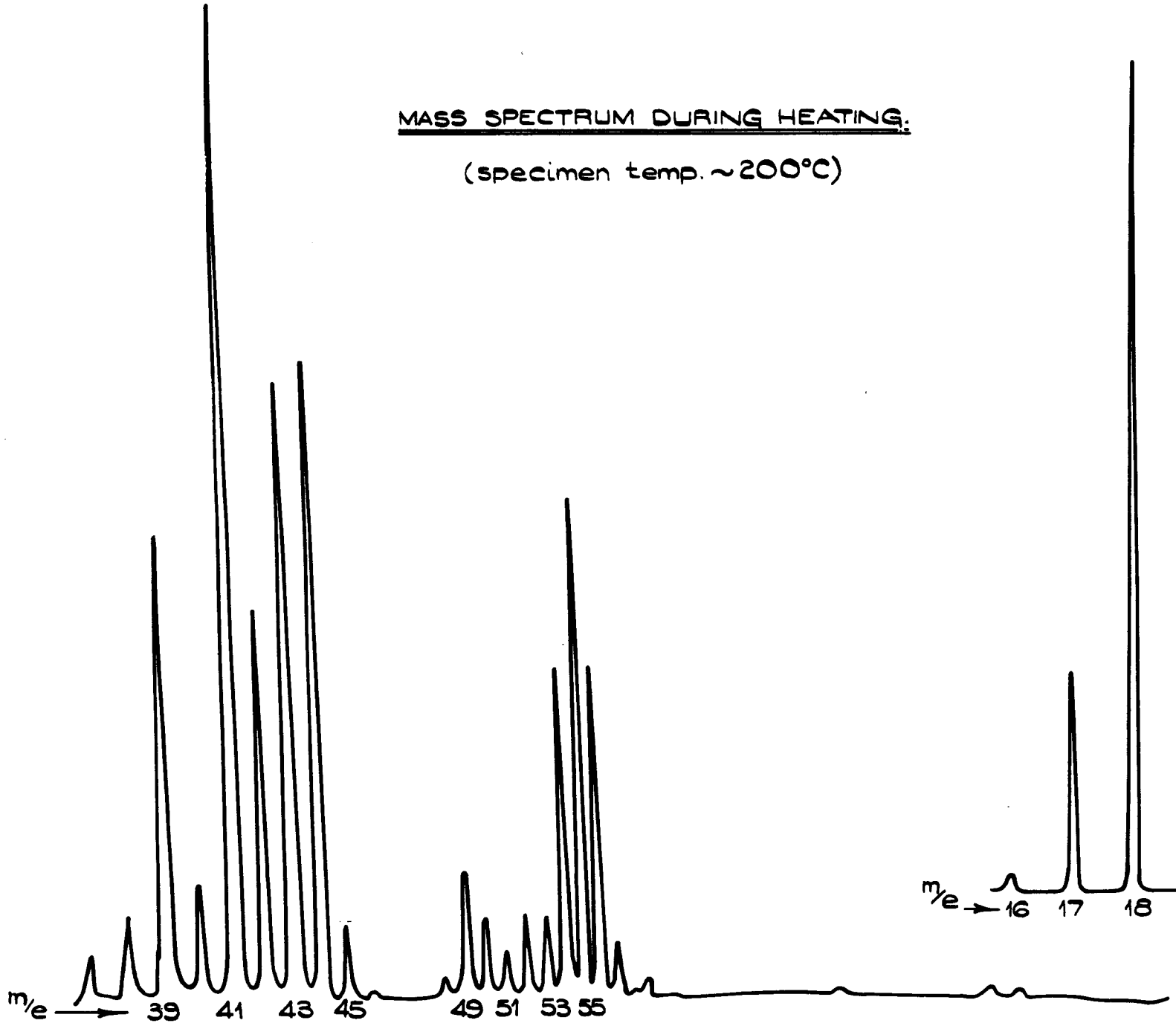

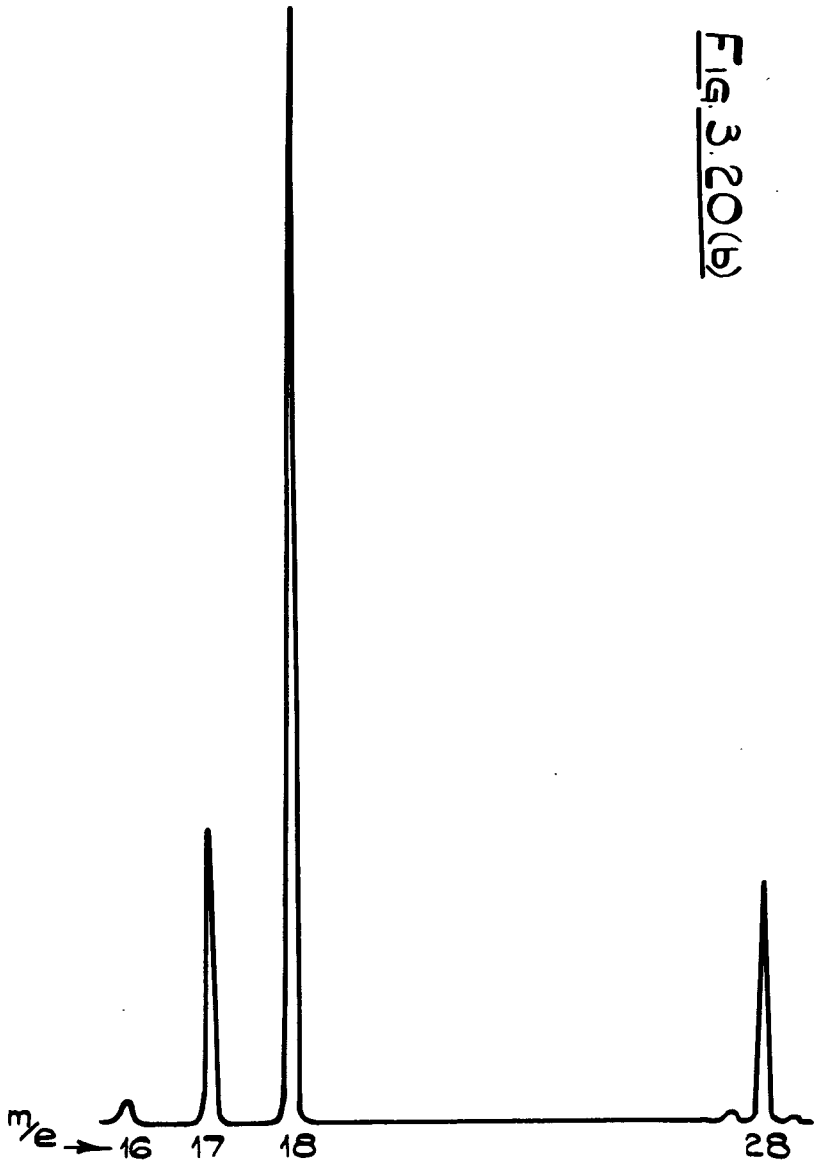

FIG. 3.20(b)

plastics, explosives. The basic reaction, on which the method depends, may be represented by

$$I_2 + SO_2 + 2H_2O \rightleftharpoons 2HI + H_2SO_4$$

Fischer used anhydrous methanol to dissolve the iodine and sulphur dioxide, and added pyridine to the mixture to remove the acidic products of the reaction. In fact both the methanol and pyridine take part in the reaction, which has been shown to be more accurately represented by (9)

(i) $SO_2 + I_2 + H_2O + 3C_5H_5N \rightarrow 2C_5H_5N.HI + C_5H_5N\langle^{SO_2}_{O}$

(ii) $C_5H_5N\langle^{SO_2}_{O} + CH_3OH \rightarrow C_5H_5N\langle^{SO_4CH_3}_{H}$

In principle the method involves dissolving the specimen in a moisture free solvent, such as anhydrous methanol, and titrating it against a standardised Fischer solution, to an end point that can be determined either visually or electrically (free iodine alters the conductivity of the solution, and gives it a reddish brown tinge when an excess of reagent is added).

The necessary Fischer reagent, and dry methanol solvent were obtained from British Drug Houses, and their recommendations followed on the construction and use of the apparatus. The visual end point method was chosen, in view of the simplicity of the equipment required (Fig.3.21); its sensitivity would have been quite sufficient for detecting moisture contents of the order of one or two percent in specimens of a few grammes weight. A certain amount of difficulty was experienced in dissolving the specimens in dried methanol, they were found to be comparatively insoluble in this solvent. However, since a more suitable water free solvent could not be found, methanol had to be used; the crystals were left to dissolve for about 24 hours in a

FIG. 3.21

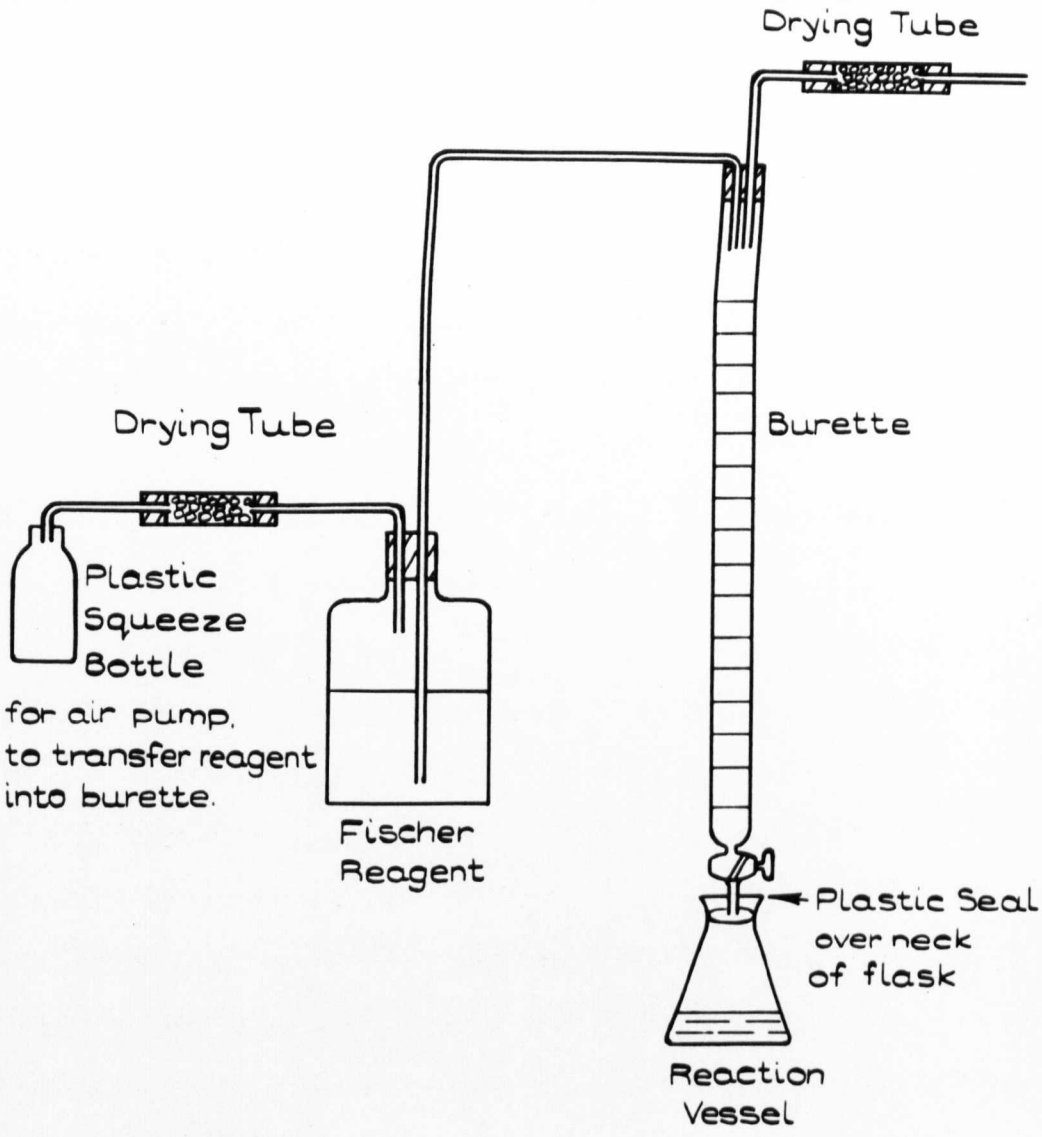

KARL FISCHER APPARATUS FOR MOISTURE DETERMINATION.

sealed flask, to prevent the ingress of atmospheric moisture. The end point was not particularly easy to determine, but after a number of trial standardisation runs, using a solution of 5 mg. H_2O per ml. of CH_3OH, the final colour change could be detected with reasonable certainty. However, when the reagent was titrated with the KBr - anhydrous methanol solution, the end point was extremely difficult to determine, the solution in the reaction flask started to assume a brownish tinge more or less directly the titration was commenced, unlike the standardisation solution (H_2O in CH_3OH) which gave a fairly distinct point at which the coloration appeared.

The conclusion to be drawn from the results of the two moisture determination experiments is that the concentration of H_2O was below the level of detection, and appreciably lower than the 2 or 3% quoted on the Johnson-Matthey analysis certificate. This conclusion is substantiated by the rather weak OH^- absorption in the ultraviolet (which suggests that the hydroxyl ion concentration is no more than a few p.p.m.), and the absence of any absorption in the infrared.

The KBr specimens used to obtain all of the experimental results in this chapter, and in the following ones, were thus of high purity, with the total concentration of foreign alkali metal ions <15 ppm, divalent metal ions <5 ppm, and other metal ions individually below their levels of detection. The specimens also contained a very small, indeterminate quantity of water.

3.5 Summary of Chapter 3

A series of optical bleaching experiments were carried out on high purity KBr single crystals, which had been coloured by irradiation with 50 KeV electrons. The bleaching source was a He/Ne laser which was focussed, using a microscope objective, to give an optical power density (at 632.8 nm) at the surface of the specimen of up to 10 KW cm^{-2}. It was found that there is a marked difference between the bleaching of

crystals coloured at room temperature and ones coloured at 90° K and warmed, in the dark, to room temperature. The F centre coloration of the low temperature irradiated specimens, with an initial O.D. between 0.7 and 0.9, can be completely removed by the absorption of less than 10^{6} J.cm^{-2}, whereas those coloured at RT are much harder to bleach, and it was found that a residual O.D. at 625 nm. of between 0.1 and 0.2 remains after the absorption of nearly 10^{7} J.cm.$^{-2}$ of F band light. It was also found for both types of specimen that the bleaching efficiency is highest at the onset of illumination, and that it decreases as the F centre concentration falls. Directly after coloration, when the specimen has received no illumination other than its own cathodoluminescence, the bleaching efficiency (at RT) of specimens coloured at LNT is $\sim$ 125 photons per F centre removed, and $\sim$ 310 photons per F centre for specimens coloured at RT (from Fig. 3.15). Some bleaching must occur prior to this fast stage, whilst the crystal is under electron irradiation, due to cathodoluminescence. Although the cathodoluminescence absorbed by the specimen during coloration was not measured, it was probably of the same order as the threshold energy in the fast stage bleaching measurements, i.e. $\sim 10^{-2}$ J.cm^{-2}. (With a CCTV camera close to the end window of the irradiation cryostat, and the accelerator enclosure in total darkness, it was possible to observe a faint glow, due to cathodoluminescence, on the screen of the television monitor. The glow faded as irradiation proceeded.) The bleaching efficiency of both types of specimen remains approximately constant during the fast bleaching stage until about 20% of the F band has been bleached, after the absorption of approximately 10^{-1} J.cm^{-2} of F light. After this the efficiency of bleaching of both RT and LNT coloured specimens decreases steadily, such that it requires the absorption of some 10^{-10} J. ($\sim 3.1 \times 10^{8}$ photons) to remove each of the remaining 10% of the F centres in a crystal coloured at LNT, and 4×10^{-9} J. per F centre ($\sim 1.25 \times 10^{10}$ photons

per F centre) in the residual coloration region of RT coloured KBr.

A logarithmic plot of the energy derivative of the F band optical density $\left|\frac{dD}{dE}\right|$ against absorbed energy E is, strangely, an approximately straight line for both RT and LNT coloured specimens, over more than 6 decades of absorbed energy. A relationship of the form $\frac{dD}{dE} = \frac{5 \times 10^{-2}}{E}$ was followed. No evidence was found to suggest that the bleaching rate $\left|\frac{dD}{dt}\right|$ varied in any way other than linearly with the intensity of the bleaching source, over the range 1W. cm^{-2} to 5×10^{3} $W.cm^{-2}$.

References

(1) Schul'man, A.R. and Gel', E.P, Fiz. Tuerdoga Tela 2; 524 Translation in Soviet Physics Sol. St. 2, 489 (1960)

(2) Bron, W.E., Phys. Rev. 119, 1853 (1960)

(3) Bron, W.E. and Heller, W.R., Phys. Rev. 119, 1864 (1960)

(4) Jain, S.C. and Jain, V.K., J. Phys. C. (Proc. Phys. Soc.) 1, 895 (1968)

(5) Otterson, D.J. Chem. Phys. 33, 227 (1960)

(6) Rolfe, J,. Phys. Rev. Lett. 1, 56 (1958)

(7) Etzel, H.W. and Allard, J.G., Phys. Rev. Lett. 2, 452 (1959)

(8) Moisture Determination by the Karl Fischer Reagent. B.D.H. Chemicals Ltd. (1966)

(9) Smith, D.M. and Bryant, W.M.D., J. Amer, Chem. Soc. 57, 841 (1935)

(10) Klein, M.V., Kennedy, S.O., Gie, T.I., Wedding, B., Mat. Res. Bull. 3, 677 (1968)

CHAPTER FOUR

OPTICAL BLEACHING MECHANISMS IN ELECTRON IRRADIATED KBr

4.1 Possible mechanisms for the optical bleaching of F centres in the alkali halides

The strength of the F band absorption in a coloured alkali halide crystal may be reduced (bleached) in a number of different ways. Basically, the crystal may either be heated to a suitable temperature (thermal bleaching) or illuminated with F band light (optical bleaching) or subjected to a combination of both heat and F light. In the dark at room temperature thermal bleaching occurs very slowly, time periods of several tens of hours are necessary before significant changes in absorption spectra are observed.(1) In general crystals need to be heated well above room temperature before thermal bleaching becomes significant. (Appreciable thermal bleaching may, however, occur during the warming to RT of crystals coloured by irradiation at a lower temperature.) If a crystal is illuminated at RT with F band light, the F band absorbance decreases quite rapidly, in the manner described in Chapter 3; this phenomenon of optical bleaching will now be discussed in more detail.

The first step in permanent F centre bleaching involves the removal of electrons trapped at negative ion vacancies. Illuminating a crystal with F light excites a number of F centre electrons into the excited state F*, from where, at a suitable elevated temperature, they may be thermally excited into the conduction band. Having thus freed the electrons by F light excitation, there are a number of events which can occur to prevent them being retrapped by anion vacancies and regenerating F centres. These events may be broadly grouped into two different classes, those which are purely electronic in nature, and those which also involve ionic motion.

The $F \rightarrow F'$ conversion is an example of a purely electronic bleaching process. If additively coloured KBr is illuminated with F light at a temperature of $\sim 123^{\circ}K$ a decrease in F centre concentration

results, and a broad absorption band appears on the long wavelength side of the F band (Fig. 4.1) Electrons freed from F centres by light are trapped at other F centres, forming the entities known as F' centres, which consist of pairs of electrons trapped at single halide ion vacancies. This particular electronic bleaching process is completely reversible; optical excitation in the F' band regenerates the F band, by the loss of one of the F' centre electrons and its subsequent recapture by an anion vacancy. The $F \rightarrow F'$ reaction only occurs at low temperatures owing to the weak binding of the second electron to the F centre. There are, however, a number of other ways in which electrons, liberated from F centres, may be trapped so as to prevent their recapture by anion vacancies. They may, for instance, be captured by impurities or other crystal defects, and the deliberate addition of impurities such as Tl^{+} and Pb^{2+} to act as electron traps has facilitated the study of certain V centres, by preventing electron-hole recombination. However, the impurity levels in the specimens used for the experiments described in this thesis are clearly not high enough for such an impurity process to be important.

The electrons liberated from F centres by optical excitation will also be prevented from recombining with anion vacancies if they are annihilated by self trapped holes (e.g. V_K centres) or holes associated with interstitial ions (V centres). The coloration of an alkali halide crystal by ionising radiation generates quite strong V absorption bands, some of which are stable at room temperature. Whilst the configurations of the centres responsible for these bands are uncertain, they are, presumably, holes trapped at clusters of halide interstitials, or multiple H centres, and so could act as electron annihilation sites.

A decrease in F band absorbance due to wholly electronic processes can also be observed when additively coloured crystals are illuminated with very high intensity (>10 MW.) light pulses from a

FIG. 4.1.

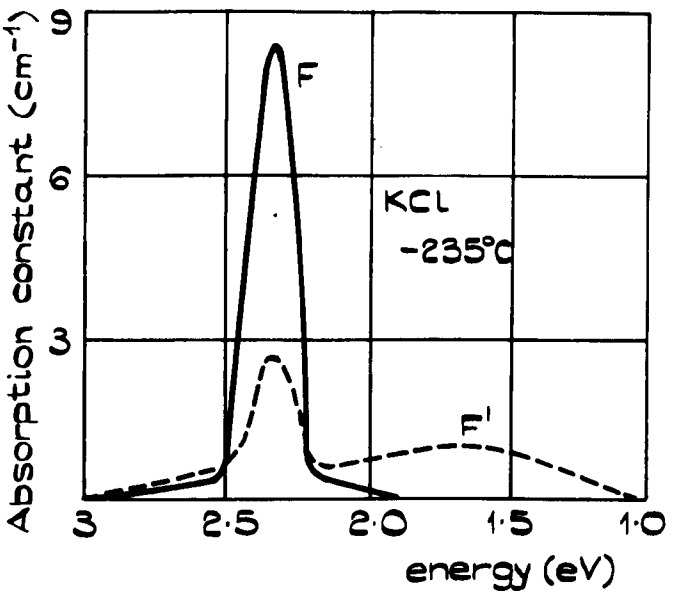

FORMATION OF THE F' BAND IN KCl.

Q switched ruby laser.[2] There is a transitory shift of absorbance out of the F band region, due to depopulation of the F centre ground state, which results in an increase in the absorption bands due to the relaxed excited state (F^* or β^* bands) of the F centre. After the excitation is removed, the F centre absorption rapidly returns to nearly its original value (some F centres will be bleached by alternative processes).

The second type of event which can cause the destruction of F centres involves ionic motion. For example, vacancies and interstitials may recombine, thus removing electron trapping sites. Alternatively, single anion vacancies can aggregate into complexes, which, although they can still retrap electrons, will produce absorption bands on the low energy side of the F bands.

KBr which has been coloured by electron irradiation at LNT certainly does not bleach at room temperature by a wholly electronic process, since the disappearance of the α band may be seen in such specimens. The α band is a perturbation of the fundamental lattice absorption of an alkali halide crystal by negative ion vacancies,[3] and its presence can therefore be taken as indicating the existence of a number of isolated anion vacancies in the specimen. This band is superimposed on the steep slope of the fundamental absorption edge of the crystal (at 201 nm. in KBr), and it is necessary to cool the crystal to LNT to observe it. Fig. 4.2, curve (a) shows the u-v spectrum (at 90°K) of a KBr specimen before irradiation. No absorption band is seen at 201 nm., since the as grown vacancy concentration was insufficient to cause significant perturbation of the u-v band edge. Curve (b) is the u-v spectrum (at 90°K) after the specimen had been irradiated with 50 KeV electrons, maintaining the temperature at 90°K. There is now a well resolved α band, indicating the presence of a large number of vacancies, and one can also see the steep tail of the β band, which is attributed to a perturbation similar to the α band,

FIG. 4.2.

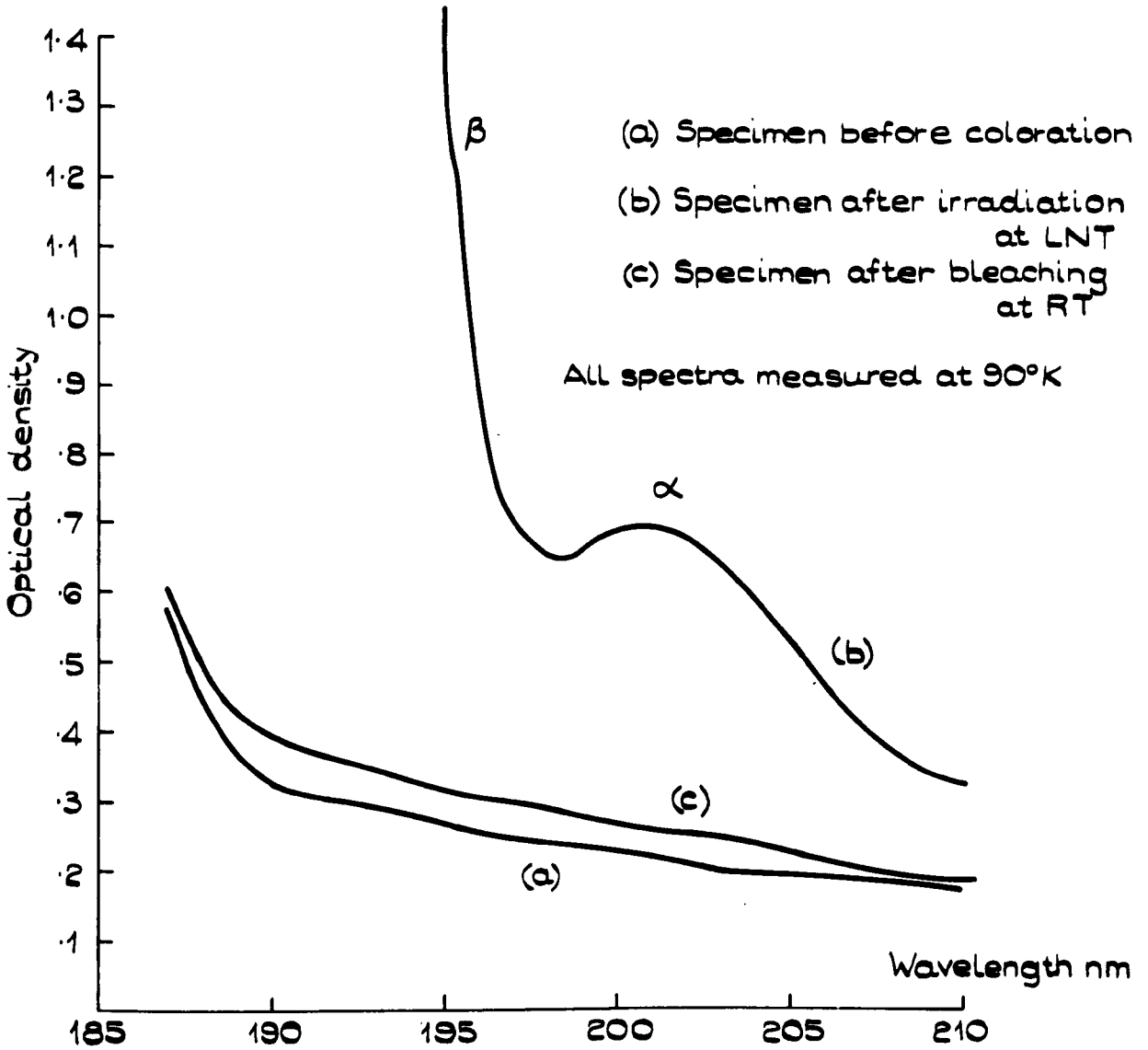

THE DISAPPEARANCE OF THE α BAND IN KBr SPECIMEN COLOURED AT LNT AND BLEACHED AT RT.

but caused by F centres [3]. The specimen showed the intense blue coloration of the F band. The crystal was warmed in the dark to room temperature, and then given a prolonged exposure to F light, until all of the blue coloration had disappeared. On recooling to LNT, the spectrum labelled (c) in Fig. 4.2 was obtained, showing the complete disappearance of the α and β bands, which clearly indicates that ionic motion had taken place. It ought to be pointed out that the α band largely disappears after warming alone, since at room temperature vacancy diffusion and vacancy pair formation is possible. For this reason the α band is not seen in crystals irradiated at RT, although the β band, associated with F centres, may be observed if the crystal is cooled to low temperature.

Previous workers, studying the low intensity optical bleaching (at RT) of Xray or additively coloured materials have also shown that ionic motion takes place during bleaching. They found that vacancy aggregation mechanisms, leading to the formation of M, R, N etc. centres predominate, and consequently much more is known about this class of reaction, and the centres involved. In particular, the formation of M centres from pairs of F centres has been studied in some detail, although it is not yet fully understood.

4.2 The Optical Formation of M centres

The rate of formation of M centres with time $\left|\frac{dn_m}{dt}\right|$ from the pairs of F centres is found to vary with temperature (T) as $e^{-E/kT}$ over the small range of temperatures that it can be measured. The activation energy E is very small, being about 0.4 eV in KBr [4], and is considerably less than the activation energies measured for anion vacancy diffusion (> 0.87 ev [5,6] in KBr). This is at first sight a little strange, since it is apparent that the conversion of two F centres to an M centre must involve the diffusion of anion vacancies in one form or another. It is, however, far from clear that the measured activation energy can be directly compared to a diffusion

energy.

Two processes have been proposed to account for the formation of M centres when a crystal containing F centres is illuminated, at room temperature, with F band light. Illumination into the F band excites a number of F centre electrons into the excited state F^*, from where, at RT, they may be thermally excited into the conduction band. The net result of illumination is therefore to ionise some of the F centres, which results in a crystal that contains anion vacancies (α-centres), F centres, free electrons and metastable F' centres formed by the temporary trapping of some of the photoelectrons at F centres. The first M centre formation process involves the coulomb attraction between α- centres and F' centres, and their direct combination to yield M centres [7,8]. The alternative suggestion is that an α centre is attracted by an F centre (by dipolar, covalent forces) to form a positively ionised M centre (the M^+ centre) which subsequently captures a further electron to become a neutral M centre [9,10]. The production of one M centre from two F centres, by either mechanism, requires the absorption of many photons.

These mechanisms can be represented schematically as follows:

(i) the direct process

$$F + h\nu \rightarrow \alpha + e^-$$

$$F + e^- \rightleftharpoons F'_{\text{Metastable}}$$

$$F'_{\text{Metastable}} + \alpha \rightarrow M$$

(ii) the indirect process, via the formation of the M^+ centre

$$F + h\nu \rightarrow \alpha + e^-$$

$$F + \alpha \rightarrow M^+$$

$$M^+ + e^- \rightarrow M$$

In a careful study of the activation energy E in KCl, Asai and Okuda [11] concluded that the M^+ indirect process is most likely to occur, and proposed that the small activation energy arises because it is, in fact, the activation energy for α centre diffusion minus half

the thermal ionisation energy of the F' centre. The latter quantity is involved because of its effect on the $\propto$ centre concentration. Experiments on LiF have also shown that M^+ centres are a likely intermediate in the M centre formation process [12-14], and it has been proposed that the F centre electron forms a covalent bond between an F centre vacancy and an $\propto$ centre when they are separated by several interionic distances [10]. The formation of this covalent bond would then tend to lower the energy for the motion of a free $\propto$ centre towards the observed value of the F to M activation energy. Despite the support given by many workers to the indirect F to M conversion mechanism, there is, however, no real evidence against the direct $F' + \propto \rightarrow M$ process. It may be, therefore, that both mechanisms can occur.

Clearly, mechanisms for the formation of higher order F aggregate centres may be proposed along similar lines to those for M centres. There are a number of ways by which, for example, an R centre may be formed from an M centre and the ionisation products of F centres.

e.g. $M + \propto \rightarrow R^+$

$R^+ + e^- \rightarrow R$

or $M + e^- \rightarrow M^-$

$M^- + \propto \rightarrow R$

or $F + \propto \rightarrow M^+$

$M^+ + F' \rightarrow R$ (Metastable)

Prolonged illumination with F light may thus lead to the formation of higher order F aggregate centres, and ultimately could result in the observation of coloration due to colloidal alkali metal centres.

4.3 The optical bleaching spectra of single crystal KBr electron irradiated at room temperature.

Measurements of the absorption spectra of freshly cleaved KBr crystals before, during and after bleaching were made using a Perkin Elmer model 450 double beam spectrophotometer, which had been set up and calibrated according to the manufacturers instructions before any

quantitative measurements were made. The specimens remained under vacuum in the irradiation cryostat during the measurements, with a duplicate pair of 'Spectrosil' windows in the spectrophotometer reference beam to assist in compensating the instrument to give a flat zero absorbance baseline. The KBr specimens received precisely the same treatment as those used in the measurements of Chapter 3, i.e. they were cleaved in a totally dry environment from single crystal Harshaw material and coloured by irradiation with 50 KeV electrons on the Van de Graaff accelerator. Bleaching was effected with the 30 mW. He-Ne laser, using a lens to diverge the beam slightly so that its diameter was slightly larger than the dimensions of the specimens.

Fig. 4.3 curve (a) shows the optical absorption spectrum of a freshly cleaved Harshaw KBr single crystal for comparison with the spectrum after electron coloration at RT (curve b). Curve (b) shows that irradiation has led to the formation of a strong F band at 625 nm., a small M band at 920 nm. and a broad absorption band in the ultraviolet region between 200 and 300 nm. which is probably associated with interstitial halogen complexes (V_2 and V_3 centres). Exposing the crystal to approximately 250 J. $cm.^{-2}$ of F light results in the F band decreasing to less than one half of its initial intensity, the M band doubling in height, and the appearance of strong R (790 nm.) and N (1.1μm.) bands (curve (c) of Fig. 4.3). The appearance of the ultraviolet band is unchanged. This evidence strongly suggests that the optical bleaching of samples coloured at room temperature involves only the aggregation of F centres to M, R, N.... centres, without any significant vacancy interstitial recombination. This would not, of course, follow if there were interstitial centres that did not have absorption bands in the spectral region covered by the Perkin Elmer 450 spectrophotometer, or if colloids were formed that gave a very broad, weak absorption band, or one that lay under the F, M, R or N absorption bands.

FIG. 4.3.

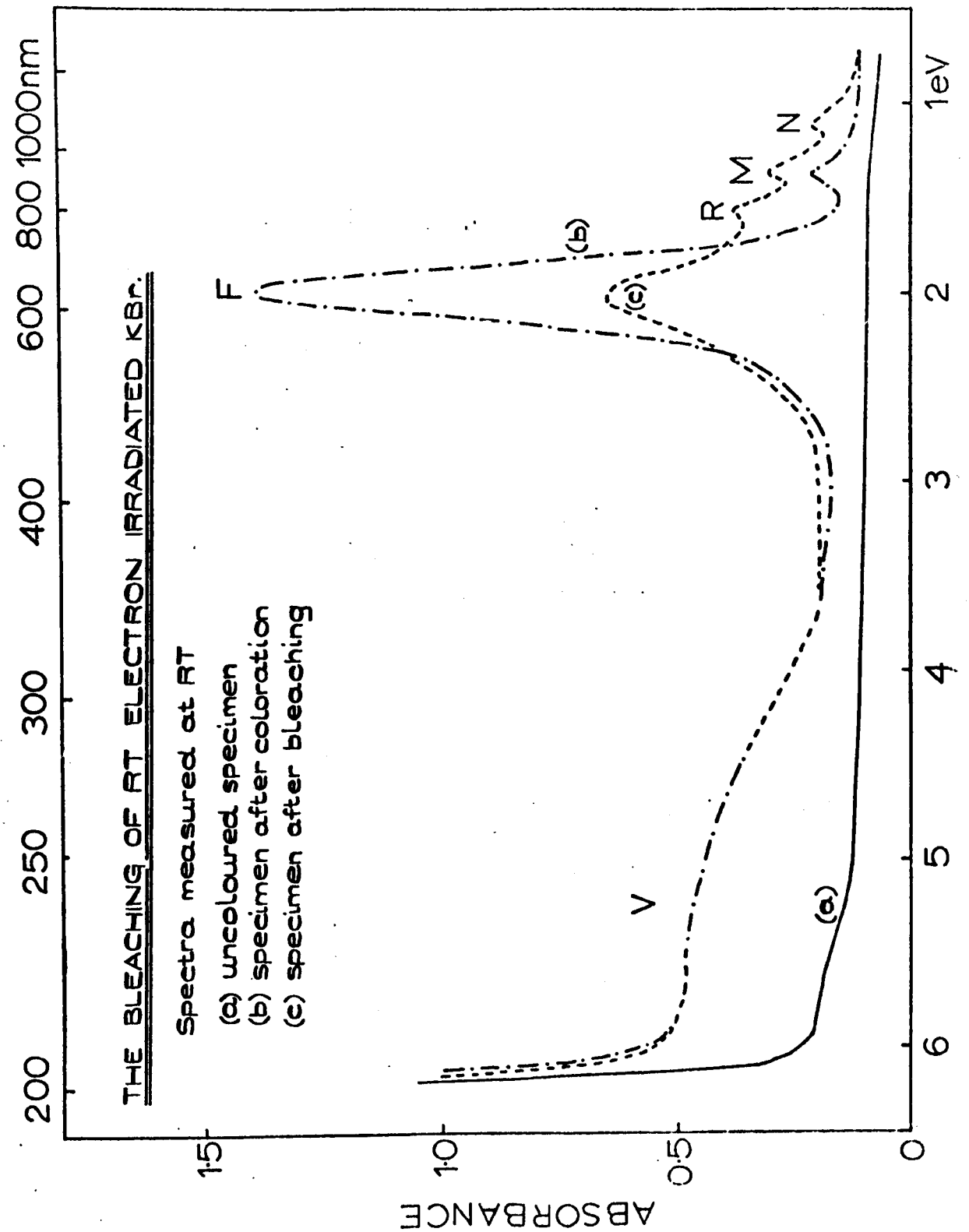
THE BLEACHING OF RT ELECTRON IRRADIATED KBr.
Spectra measured at RT
(a) uncoloured specimen
(b) specimen after coloration
(c) specimen after bleaching
200
250
300
400
600
800
1000nm
1eV
2
3
4
5
6
0
0.5
1.0
1.5
ABSORBANCE
F
V
R
M
N
(a)
(b)
(c)

In order to check the aggregation hypothesis, an extended bleaching experiment was performed in which absorption spectra were recorded at intervals during the bleaching. Using this data, a graph (Fig. 4.4) was plotted of the estimated total number of vacancies present in aggregates against the number of F centres removed. The oscillator strengths for the various absorption bands needed to calculate the absolute vacancy concentration from the optical density values were those published for additively coloured KBr[1]. There is a clear indication that most of the bleached F centres have aggregated to form M, R, N .... centres, rather than recombined with interstitials. Any interstitials taking part would obviously not be those responsible for the ultra violet absorption band, since its intensity does not change during bleaching. Some higher order aggregate centres, and possibly small colloids may be formed in the later stages of bleaching; this would tend to make the curve bend over after large doses of F light had been absorbed. The data of Fig. 4.4 apparently suggests that the number of vacancies present in aggregates exceeds the number of F centres removed. This is not due to there being large numbers of isolated vacancies in the crystal, since the α band is not observed in crystals coloured at RT. The discrepancy almost certainly arises from the use of oscillator strength values that are too low, and will be discussed further in connection with the statistical theory of vacancy aggregation to be presented in the next section of this Chapter.

In Chapter 3 it was stated that crystals coloured at room temperature still showed a residual optical density at 625 nm. even after 10^7 J. cm^{-2} of F light had been absorbed. The explanation of this phenomenon lies in the equilibrium concentrations of the various aggregate centres that are established after an extended bleach. There are allowed optical transitions of M and R centres (giving rise to the M_F and R_F bands) which fall close to the peak of the F band but on the short wavelength side of it. It is these bands which are responsible

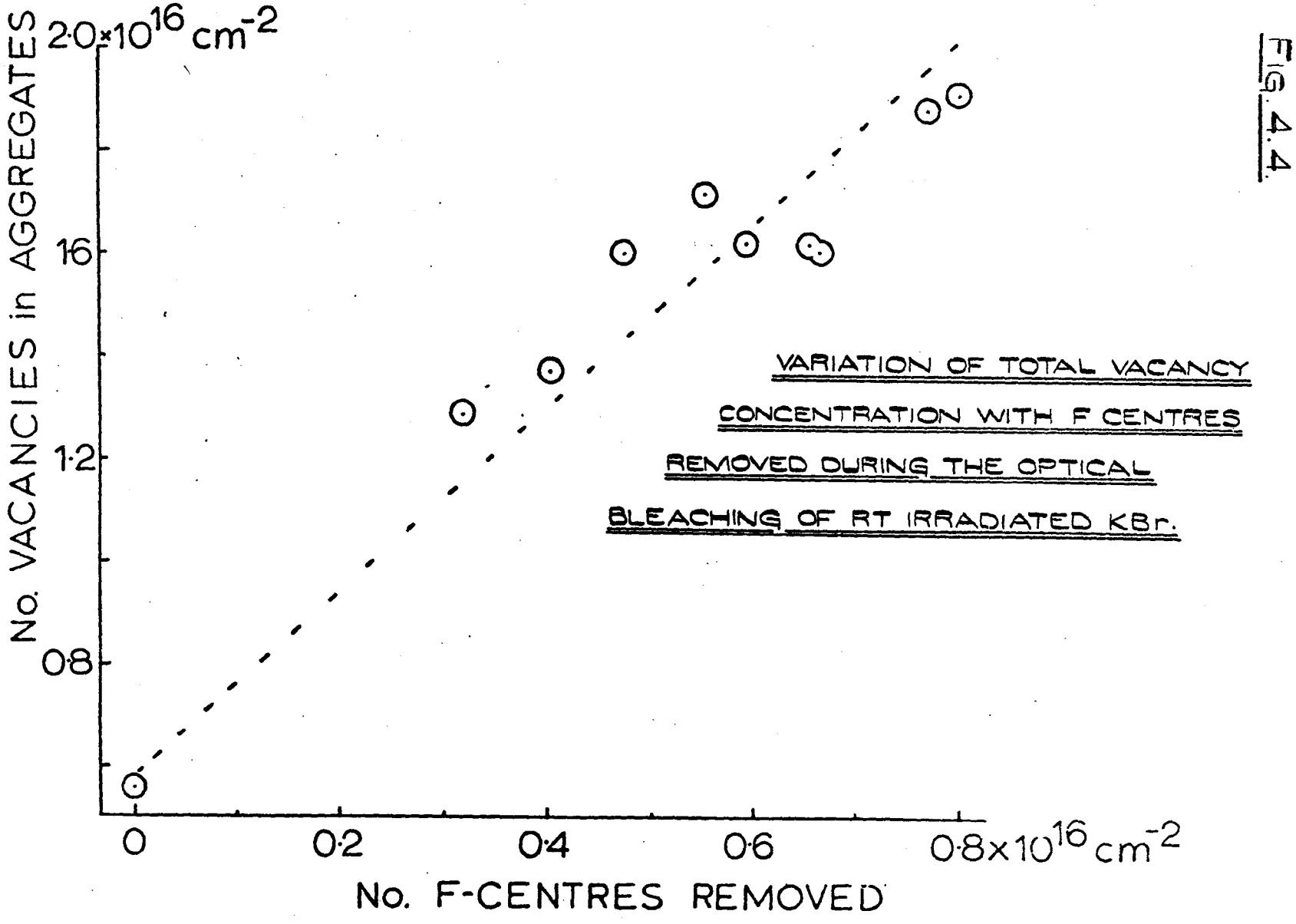

FIG. 4.4.

VARIATION OF TOTAL VACANCY CONCENTRATION WITH F CENTRES REMOVED DURING THE OPTICAL BLEACHING OF RT IRRADIATED KBr.

for the slight shift of the F band peak to shorter wavelengths evident in curve (c) of Fig. 4.3. It is thus proposed that the residual coloration at 625 nm. in crystals given an extended high intensity bleach is due mainly to these M_F and R_F bands, with only a small contribution from unaggregated F centres. In the spectra of Fig. 4.3, if all of the F centres were removed by bleaching, there would still be an optical density of between 0.15 and 0.25 in the region of the R and M bands. The height of the M_F band is 80% of the M band [15], so that together with a contribution from the R_F band a residual optical density of around 0.2 in the F band might be expected after the prolonged bleaching of a specimen having an initial O.D. of about 1.4. This compares quite favourably with the value of 0.17 that remained in the RT coloured specimen of Fig. 3.4.

4.4 A statistical theory of vacancy aggregation [16]

The low energy electron irradiation of an alkali halide crystal produces an approximately random distribution of F centres, provided one ignores the long range variation in F centre density caused by the non-uniform penetration depth of the bombarding electrons in the crystal. It has been shown that optical bleaching is independent of F light intensity, and leads to the formation of M, R, N ..... centres. It is therefore reasonable to assume that bleaching occurs through the aggregation of relatively close pairs of F centres. The early stages of bleaching involve the aggregation of close pairs of F centres, whilst the later stages are governed by pairwise aggregation during a condensation of F centres, in which the peak of the F centre distribution shifts to smaller separations between centres. The actual mechanism of the F centre condensation will be one of the two discussed in section 4.2, namely either the coulombic $F' - \alpha$ [8] or the dipolar $F - \alpha$ [10] interactions. However, if it is assumed that only single vacancy interactions are important at relatively long range, it is possible to describe the accumulation of F aggregate centres as a

random process similar to the generation of F and M centres during irradiation [17]. The aggregation of F centres during bleaching can thus be described by a Poisson distribution of n aggregation events per cm.^{3}, over v^{-1} aggregation volumes in unit volume of the crystal. The implicit assumption is that prolonged bleaching causes a"condensation" of the F centres in each volume, which leads to the formation of an aggregate centre; the relatively small number of aggregate centres that are already present in the crystal directly after coloration are not given any special status as nuclei for further aggregation. The number of centres of each type present in the crystal after n aggregation events will be given by the following equations:

$$\eta_{F_2} = \eta_M = ne^{-nv}$$

$$\eta_{F_3} = \frac{n^2 ve^{-nv}}{2}$$

$$\eta_{F_4} = \frac{n^3 ve^{-nv}}{6} \qquad \text{etc.} \qquad \ldots\ldots (1)$$

where it has been assumed that $\overset{a}{\phi}$n F_3 centre (e.g. $\overset{a}{\phi}$n R centre) will be formed if two aggregation events follow the condensation in one volume v. The predictions of this model may be compared with experimental data on the growth of the aggregate bands as a function of the number of aggregation events. There are, however, two problems involved in doing this. Firstly, there has been no agreement as to the precise nature of the centre responsible for the N band absorption in KBr; the band has variously been identified with an aggregate of four F centres [18], a configuration of three F centres different from that responsible for the R band [19], and even with the R^+ centre [20]. It seems likely that a substantial part of the N band is caused by groups of three F centres so, since this band is normally smaller than the M or R bands, the sum of the optical densities of the N and R absorptions are used as a measure of the number of F_3 centres. The second difficulty is that the values of the oscillator strengths of the R and, particularly, the N bands may not be entirely reliable. This was overcome by using

optical densities $(O.D.)_M$ and $(O.D.)_{R+N}$ in place of the actual numbers of centres (n_{F_2} and n_{F_3}) in equations(1), n, the number of aggregation events per cm^3, was estimated from the number of F centres removed and the number of M centres present (using the oscillator strengths of Jain & Jain [1]. Fig. 4.5 shows the variations of $(O.D.)_M$ and $(O.D.)_{R+N}$ with the number of aggregation events per cm^3 (n), for a sample of KBr coloured and bleached at room temperature. This data was obtained in a similar manner to that described in section 4.3, using the Perkin Elmer 450 spectrophotometer and the 30 mW. He/Ne laser for bleaching. Care was taken in the early stages of this experiment to ensure that a sufficient number of measurements were obtained to allow the increase in the M band to be plotted, as it was found in practice that only a brief exposure to the laser was required to take the M centre concentration past its peak value. The optical density in the M band directly after irradiation was only 0.06, and this was treated as aggregation induced by cathodoluminescence during irradiation. The dotted lines in Fig. 4.5 illustrate the behaviour predicted by equations(1), with $v^{-1} = 1.9 \times 10^{18}\ cm^{-3}$. The vertical scale of the theoretical curves was chosen so that the peak optical densities were equal to the measured values. The experimental points for $(O.D.)_M$ lie close to the theoretical curve and even the $(O.D.)_{R+N}$ data (which are affected by uncertainties about the oscillator strength and configuration of the N band) lie fairly close to the predicted values. The peak value of $(O.D.)_M$ occurs at $n = v^{-1}$ and the peak value of $(O.D.)_{R+N}$ should then occur at $n = 2v^{-1}$. The experimental data show that this condition is approximately fulfilled. n_M, the M centre concentration, would be expected to attain a maximum value of $(ev)^{-1}$, and n_{F_3} (R and N bands) a maximum of $2v^{-1}e^{-2}$. The peak in n_{R+N} should thus lie below that in n_M. The maximum value of $(O.D.)_{R+N}$ is nearly twice that of $(O.D.)_M$ in Fig. 4.5 but, using the half widths and oscillator strengths of Jain and Jain [1], the peak value of n_{R+N} does lie below that of

FIG. 4.5.

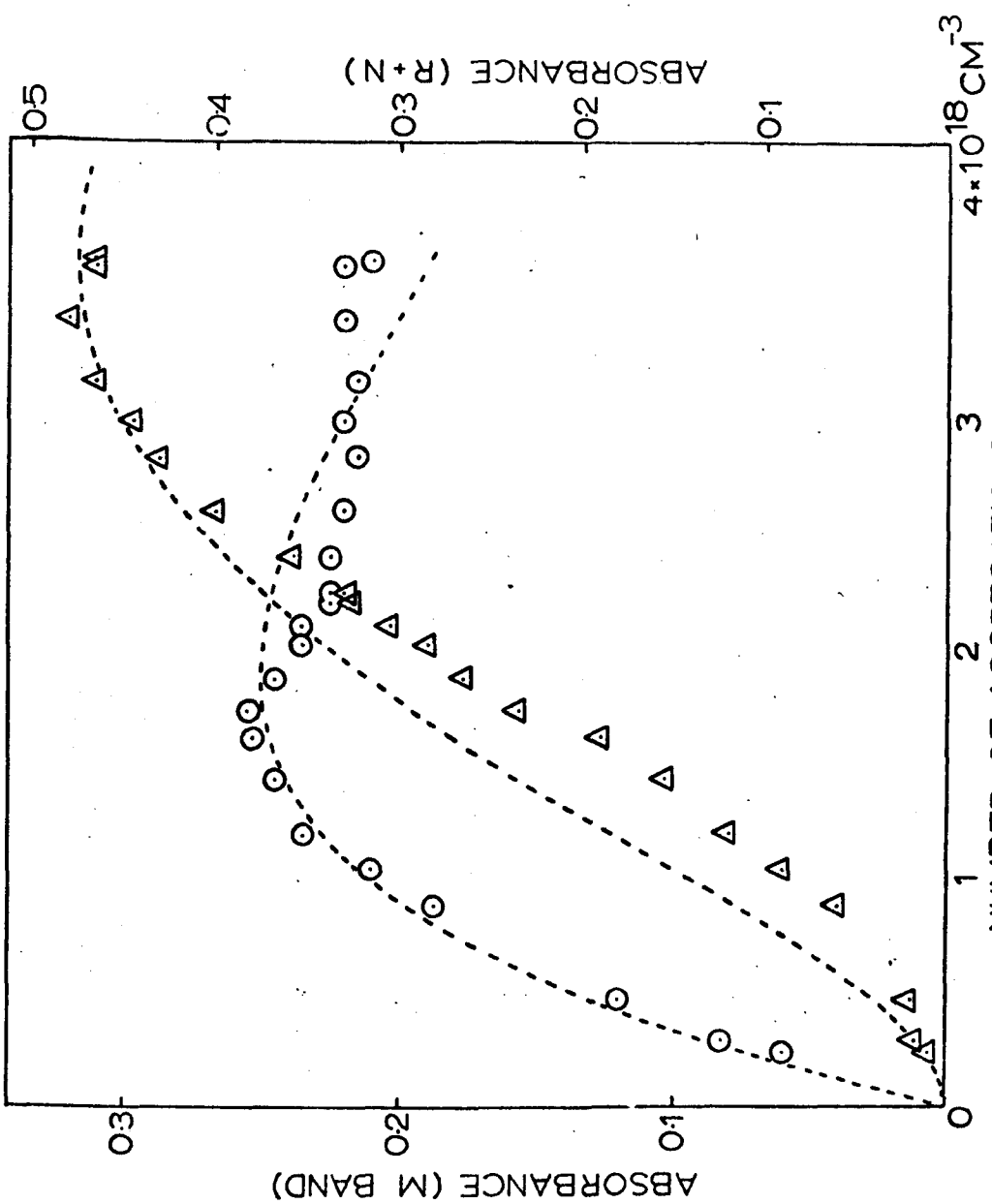

VARIATION IN THE M, R & N BANDS DURING THE OPTICAL BLEACHING OF RT IRRADIATED KBr.

η_M as expected. However, the peak value of η_M is between 3 and 4 times larger than $(ev)^{-1}$. The two quantities would only be equal if the M centre oscillator strength were some three times larger than the value of 0.11 given by Jain and Jain. An increased value of the oscillator strength of the M centre would also be needed to remove the apparent discrepancy of Fig. 4.4, by making the number of vacancies aggregated during bleaching equal to the number of F centres removed. Neither discrepancy can be ascribed to interstitial-vacancy recombination, since this would reduce the number of aggregate centres formed.

Determination of the oscillator strengths of F aggregate centres in the alkali halides is by no means easy, since it is usually impossible to obtain one particular type of aggregate centre in a specimen without the presence of one or more of the others. This eliminates the direct chemical method that has been used to determine the number of F centres present in an additively coloured specimen [21], and makes counting them by other means difficult. Taking the electron spin resonance technique as an example [22-24], the resonance, if one is observed at all, has to be separated from those due to other aggregate centres, and must be positively identified as being caused by the centre whose oscillator strength is being determined. Consequently there have been very few determinations of the oscillator strengths of F aggregate centres in the alkali halides, the work of Jain and Jain probably being the most detailed [1] for KBr.

The method used by these researchers was based on the assumption that if the number of excess alkali metal atoms (i.e. vacancies) in an additively coloured crystal remains constant, changes in the concentrations of F and F aggregate centres during optical or thermal interconversion of the centres can be described by [15]:

$$\Delta n_F + 2\Delta n_M + 3\Delta n_R + \ldots\ldots = 0 \qquad (2)$$

where Δn denotes the change in concentration of the colour centres during bleaching. Equation (2) can be rewritten as

$$\frac{W_F}{f_F}\Delta\alpha_F + \frac{2W_M}{f_M}\Delta\alpha_M + \frac{3W_R}{f_R}\Delta\alpha_R + \ldots = 0 \qquad (3)$$

where W_j denotes the half width of the absorption band, f_j the oscillator strength and $\Delta\alpha_j$ the change in absorption coefficient associated with the change in colour centres concentration Δn . Equation (3) is simplified by assuming that the variation in refractive index of the crystal over the range of wavelengths of the F, M, R & N bands is small enough to be neglected. Therefore, by making three different measurements of $\Delta\alpha_F$, $\Delta\alpha_M$, $\Delta\alpha_R$ and $\Delta\alpha_N$ on the same additively coloured specimen, and using the established value of f_F [15] and some previously obtained half width measurements, three simultaneous equations can be obtained which are solvable for the unknown oscillator strengths. Jain and Jain further simplified the calculations by arranging in some of the experiments for two of the four $\Delta\alpha$'s to be zero. The main drawback with this method is that for equations (2) and (3) to be valid all of the aggregate bands must be included, to ensure that a constant number of vacancies is always observed. This presupposes that the configurations of the centres responsible for the absorption bands are known; the N band will obviously present some difficulty in this respect, as will colloidal centres. (Jain and Jain took the N centre to be a 4 vacancy entity). Failure to take all of the aggregate bands into account in equation 3 will result in low values of the oscillator strengths calculated from such measurements.

It is worth noting that the oscillator strength of the M centre in KCl is 0.23, and an early X ray measurement indicates a value of 0.19 in KBr [15], so further doubt is cast upon Jain and Jain's figure of 0.11 for KBr. Using the bleaching data of these workers it is, in fact, possible to obtain oscillator strength values which are sustantially different from their tabulated values. In particular there appears to be a discrepancy between the values obtained from their optical and thermal conversion experiments. Fairly consistent values of 0.08 for f_M

and 0.34 for f_R are obtained from the optical bleaching data of Reference (1), whereas values as high as 0.22 for f_M may be calculated from the thermal conversion data. These differences are almost certainly the result of the formation of colloidal centres during heating experiments above 100°C, and the lack of N band data. It is also possible that M centre reorientation occurred during optical bleaching. For the geometry of the experiments used to obtain Fig. 4.5, any reorientation effects leading to a non random distribution of M centres over the six [110] directions would give a correction much smaller than the factor of 3 required to fit the experiments with theory, There is clearly a need for further measurements of the oscillator strengths of aggregate centres in KBr.

The data of Fig. 4.5 give a value for the aggregation volume of $v = 5.3 \times 10^{-19}$ cm^3. This corresponds to a cube with sides some 12 lattice parameters long.

A graph of aggregate concentrations against the number of aggregation events tends to hide the fact that a much larger amount of F - light needs to be absorbed to produce one aggregation event in the later stages of aggregation. This is readily explained by the statistical model, since early aggregation events involve F centres in close proximity to each other, whereas later events involve ionic motion over larger distances.

4.5 Spectroscopic studies of crystals coloured at liquid nitrogen temperature

Similar experiments to those described in section 4.3, using the Perkin Elmer 450 spectrophotometer, were carried out on single crystal Harshaw KBr specimens that had been electron irradiated at liquid nitrogen temperature (90°K) and warmed slowly in the dark to room temperature, for bleaching with the 30 mW He/Ne laser. The results of the first experiment are illustrated in Fig. 4.6. Curve (a) shows the spectrum of the crystal prior to coloration, curve (b) the spectrum after

Fig. 4.6.

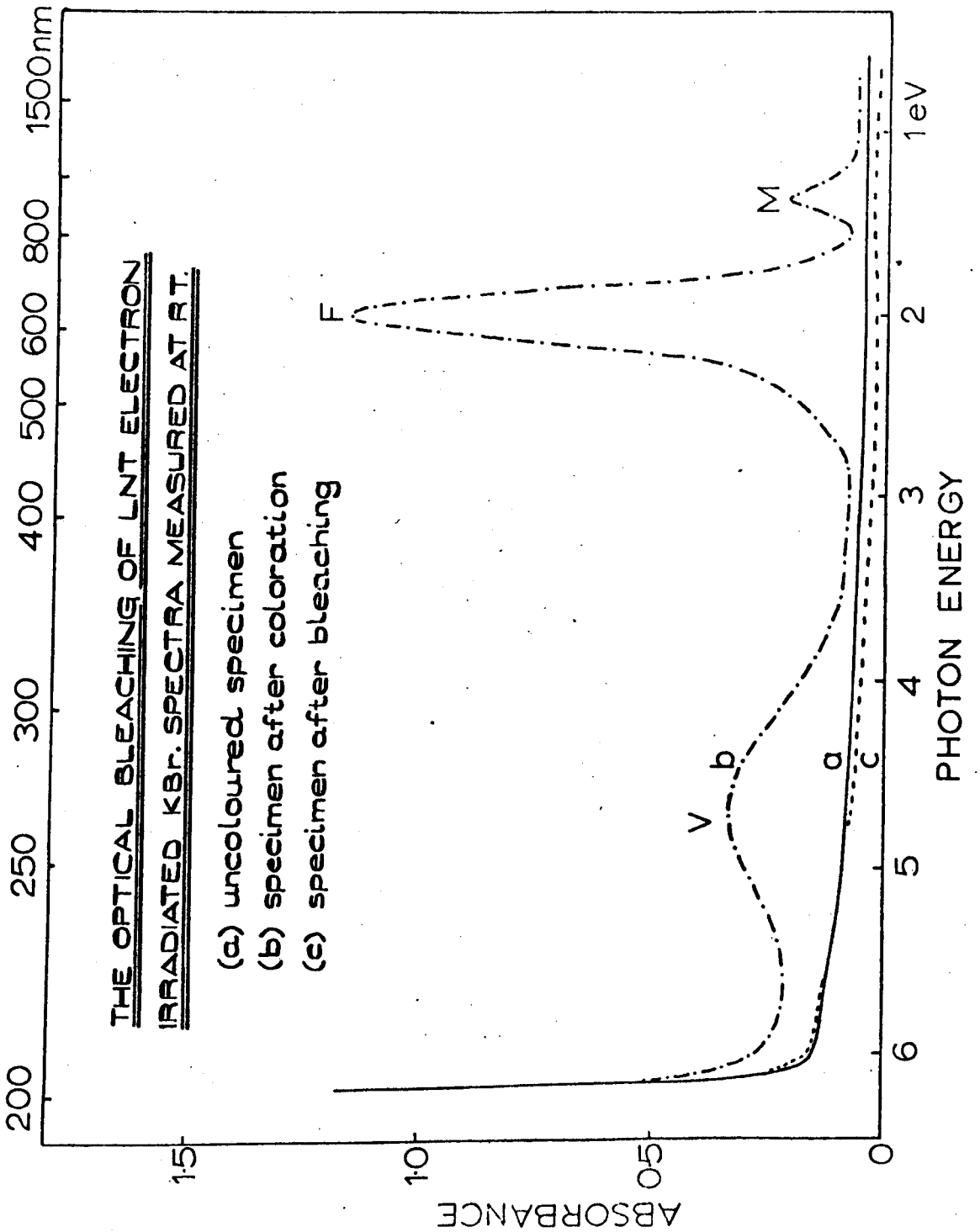
THE OPTICAL BLEACHING OF LNT ELECTRON
IRRADIATED KBr. SPECTRA MEASURED AT RT.
(a) uncoloured specimen
(b) specimen after coloration
(c) specimen after bleaching
200
250
300
400
500
600
800
1500nm
1·5
1·0
0·5
0
ABSORBANCE
F
M
V
b
a
c
6
5
4
3
2
1eV
PHOTON ENERGY

irradiation at 90°K and curve (c) the spectrum after prolonged bleaching at room temperature by the laser. All spectra were measured at room temperature. There is clearly a marked difference between this data and that of Fig. 4.3, obtained for the specimen irradiated at room temperature. Low temperature irradiation has produced the anticipated large F and small M bands, and a broad yet well defined absorption band in the ultra violet region near 265 nm. that can probably be identified with the V_2/V_4 band [25]. The most striking thing is that optical bleaching appears to have returned the specimen to its condition prior to irradiation. Both the interstitial (V) and vacancy (F,M) centre have been completely removed by bleaching (curve c), which strongly suggests that a vacancy/interstitial annihilation mechanism has occurred. During the transition from curve (b) to curve (c) in Fig. 4.6 the M band increased slightly, and a small R band appeared. These then decreased quite rapidly as the F and V bands bleached, and finally disappeared before all of the F centre coloration had gone.

This phenomenon was investigated more thoroughly by making a series of measurements of the intensity of the F, F aggregate and V bands during the optical bleaching of a LNT coloured specimen. The result is illustrated (for two specimens) in Fig. 4.7, which shows the optical density of the V band plotted against the corresponding total vacancy concentration, obtained from the F, M and R band absorbancies. Since the M and R bands never become as pronounced during bleaching as they did in the case of the RT coloured specimens, errors in vacancy concentration, due to incorrect M and R band oscillator strengths, are not likely to be too serious. (15% of total too high in the worst case i.e. when M centre concentration is at its highest and assuming that the true value of f_M is ~ 0.3. The R band did not grow sufficiently large to introduce any significant errors through the use of incorrect f_R values.) There is an approximately linear relationship between the

FIG. 4.7.

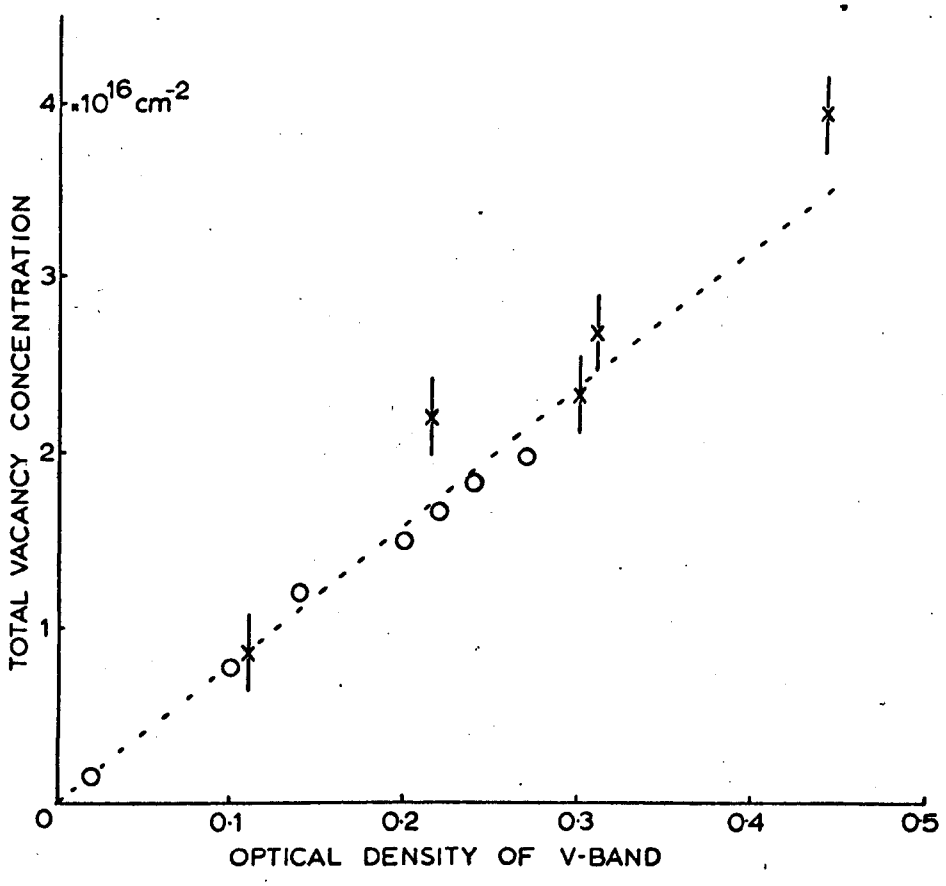

DEPENDENCE OF THE TOTAL VACANCY CONCENTRATION ON V BAND O.D. DURING THE OPTICAL BLEACHING OF A LNT IRRADIATED KBr CRYSTAL.

V band optical density and the total vacancy concentration, which is strong evidence in favour of a vacancy/interstitial annihilation mechanism for the bleaching. Moreover, it also suggests that the only interstitials important in this recombination are those responsible for the broad absorption band near 265 nm. This observation allows an explanation to be given for the complete disappearance in Fig. 3.4 of the F band in the LNT coloured specimen; there are no aggregate centres present to provide the residual optical density at 625 nm. found in the RT coloured samples.

The configuration of the centre responsible for the V band observed in Fig. 4.6 is unknown, as indeed are the configurations of most of the V centres seen in KBr [26,27]. From the data obtained in these experiments, however, the V band in Fig. 4.6 is fairly certain to be due to small atomically dispersed clusters of interstitials, which are able to annihilate anion vacancies during illumination. This is in marked contrast to the V band seen in Fig. 4.3 which takes no part in bleaching, and is therefore likely to be caused by larger more stable interstitial clusters, dislocation loops or small precipitates. It is reasonable to suppose that the interstitial ions formed in the F centre creation process are sufficiently mobile during electron irradiation at RT to diffuse together to form stable aggregates, whereas during LNT irradiation they do not undergo appreciable diffusion, and remain atomically dispersed as small clusters. They are clearly not able to coalesce when the specimen is warmed to RT, since the V band retains its separate identity from that seen in the RT coloured specimens, and in fact this V band does not change in character if crystals are kept in the dark at RT for 24 hours before bleaching.

By recording a series of spectra during the slow warming to room temperature of a specimen that had been electron irradiated at 90°K, evidence was found to suggest that the broad absorption band seen in Fig. 4.6 was due to two species of V centre. The specimen was kept in the

dark between spectral measurements, which were made on the Perkin Elmer 450 spectrophotometer. This evidence is presented in Fig. 4.8 curve (i) is the u-v spectrum at LNT directly after irradiation, and curves (ii), (iii) and (iv) during the warm up. Curve (v) shows the spectrum at RT, with a fairly weak V band at 265 nm. Spectra (ii) and (iii), recorded at temperatures between 90°K and RT show the presence of two well resolved absorption bands, at 255 nm. and 280 nm. Further experiments would be necessary to positively identify the structure in this spectrum; direct comparison between Fig. 4.8 and an earlier work on the V bands in KBr [26] is not possible, since the temperature at which spectra (ii), (iii) and (iv) were measured is not known, and the experimental conditions were considerably different.

The evidence does, however, suggest that the broad V band can be identified with the composite V_2/V_4 band observed in crystals which have been X irradiated at LNT. Faraday and Compton [26] found that the height of the V_4 band during X irradiation is proportional to the height of the F band, and that at LNT its peak is at 275 nm., with a V_2 band at 254 nm. There clearly is a correspondence between this data and the spectra of Fig. 4.8 and the bleaching kinetics of Fig. 4.7.

4.6 Summary of Chapter 4

A series of absorption spectra were taken, during optical bleaching at RT, of KBr specimens that had been coloured at RT by fast electron irradiation. A linear relationship was found between the number of F centres removed by optical bleaching at RT and the number of vacancies present in F aggregate centres. No change was observed during bleaching in the intensity of the broad V band (lying between 200 and 300 nm.) found in these specimens. It was therefore concluded that the optical bleaching (at RT) of RT irradiated specimens occurs solely by vacancy aggregation, and that most of the residual optical density of the RT specimen of Fig. 3.4 was due not to F centres, but to excited states of the M and R centres. The V band plays no part in

FIG. 4.8.

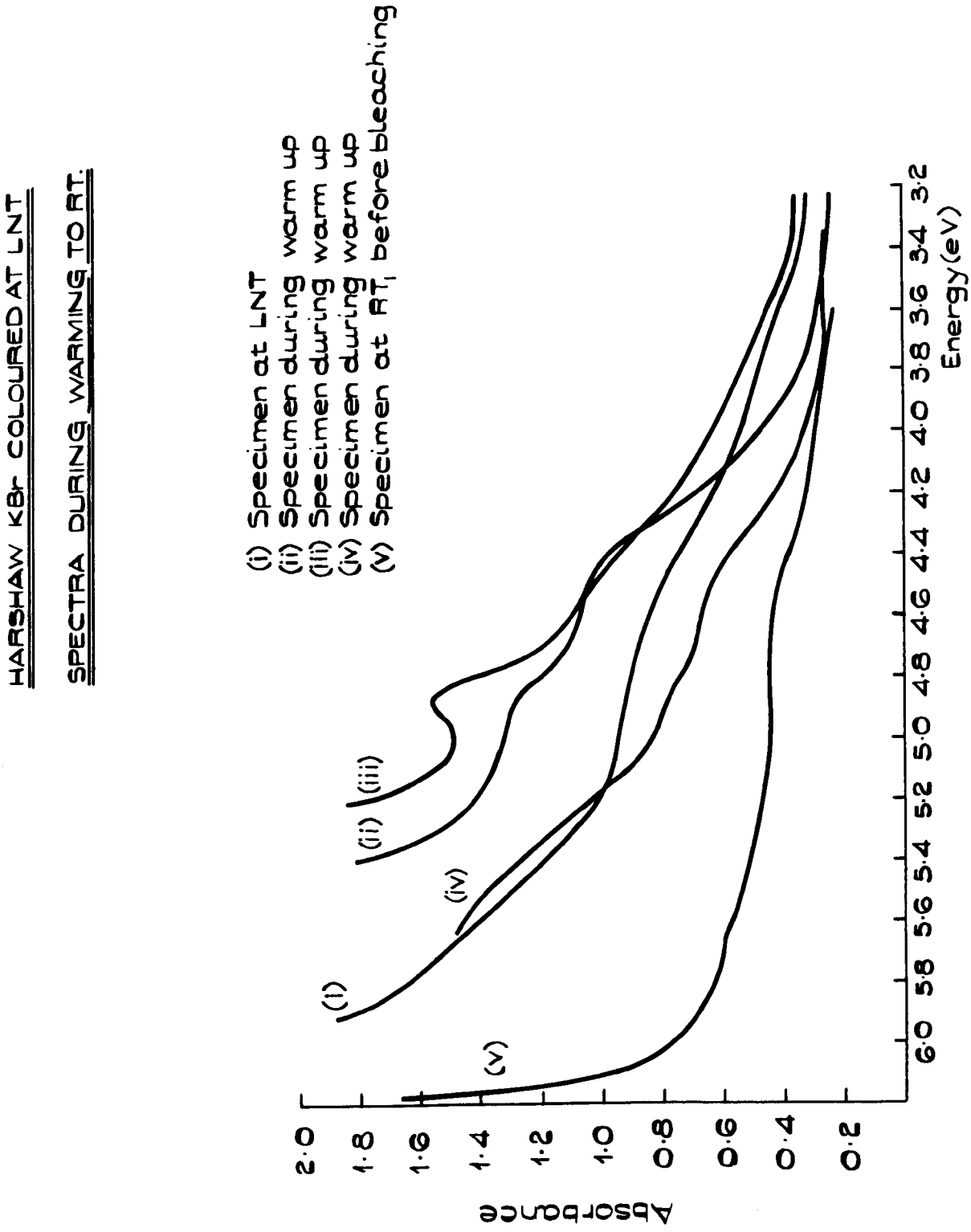
HARSHAW KBr COLOURED AT LNT
SPECTRA DURING WARMING TO RT.
(i) Specimen at LNT
(ii) Specimen during warm up
(iii) Specimen during warm up
(iv) Specimen during warm up
(v) Specimen at RT, before bleaching
Absorbance
Energy(eV)
2·0
1·8
1·6
1·4
1·2
1·0
0·8
0·6
0·4
0·2
6·0 5·8 5·6 5·4 5·2 5·0 4·8 4·6 4·4 4·2 4·0 3·8 3·6 3·4 3·2
(i)
(ii)
(iii)
(iv)
(v)

bleaching, and is probably caused by stable interstitial clusters, dislocation loops or small precipitates, which are formed during the electron irradiation. The aggregation process can be described by a random (Poisson) distribution of aggregation events among volumes some 5×10^{-19} cm^3 in size. The theory predicts that first the concentration of M centres, and then the concentration of R centres should pass through maxima as aggregation proceeds. This may be observed experimentally. This theory, and the bleaching data of Fig. 4.4 casts doubt on the reliability of the currently accepted oscillator strengths for the F aggregate centres in KBr.

Spectral measurements on KBr that had been coloured by electron irradiation at LNT reveal that it shows a different V band to that seen in RT coloured material, and that this V centre takes part in the bleaching process. An approximately linear relationship was found between the total vacancy concentration present in F, M and R centres and the V band throughout bleaching. This, coupled with the disappearance of the α band during bleaching, strongly indicates a vacancy/interstitial annihilation process. This explains the marked contrast seen in Fig. 3.4 between the LNT and RT coloured specimens after prolonged bleaching. The coloration at 625 nm. disappears completely in the LNT irradiated specimen, because no permanent vacancy aggregation occurs during bleaching, and there is consequently no residual coloration in the F band region due to excited states of M and R centres.

References

(1) Jain, S.C. and Jain, V.K., J. Phys. C. 1, 895 (1968)

(2) Fröhlich, D. and Mahr, H., Phys. Rev. 141, 692 (1966)

(3) Delbecq, C., Pringsheim, P. and Yuster, P., J. Chem. Phys. 19, 574 (1951)

(4) Brothers, A.D. and Lynch, D.W., Phys. Rev. 174, 958, (1968)

(5) Jacobs, G., Vanderwiele, L.G. and Hamerlinck, A., J. Chem. Phys. 36, 2946 (1953)

(6) Rolfe, J., Can. J. Phys. 42, 2195 (1965)

(7) Van Dowrn, C.Z., Philips Res. Rept. Suppl. 4, 1 (1962)

(8) Lüty, F., Z. Phys. 165, 17 (1961)

(9) Delbecq, C.J., Z. Phys. 171, 560 (1963)

(10) Farge, Y., Lambert, M. and Smoluchowski, R., Phys. Rev. 159, 700 (1967)

(11) Asai, K. and Okuda, A., J. Phys. Soc. Japan 21, 2197 (1966)

(12) Farge, Y., Lambert, M. and Smoluchowski, R., Solid State Commun. 4, 333 (1966)

(13) Nahum, J. and Wiegand, D.A., Phys. Rev. 154, 817 (1967)

(14) Nahum, J., Phys. Rev. 158, 814 (1967)

(15) Compton, W.D. and Rabin, H., Solid State Phys. 16, 121 (1964)

(16) Redman, M.J. and Tubbs, M.R., Phil. Mag. (in press) (1971)

(17) Vaisburd, D.I. and Melik-Gaikazyan, I. Ya., Doklady Akad. Nauk SSSR, 165, 1029 (1965) (trans. Soviet Phys. Doklady, 10, 1171 (1966)

(18) Pick, H., Z. Phys. 159, 69 (1960)

(19) Schneider, I., and Kabler, M.N., J. Phys. Chem. Solids, 27, 805 (1966)

(20) Lehmann, G., Z. Naturforsch., 23a, 1407 (1968)

(21) Kleinschrod, F.G., Ann. f. Physik 27, 97 (1936)

(22) Silsbee, R.H., Phys. Rev. 103, 1675 (1956)

(23) Lord, N.W., Phys. Rev. 106, 1100 (1957)

(24) Kawamura, H and Ishiwatari, K., J. Phys. Soc. Japan, 13, 33 (1958)

(25) Dutton, D and Maurer, R., Phys. Rev. 90, 126 (1953)

(26) Ishii, T. and Rolfe, J., Phys. Rev. 141, 758 (1966)

(27) Faraday, B.J. and Compton, W.D., Phys. Rev. 138, A893 (1965)

CHAPTER FIVE

SOME DIAGNOSTIC EXPERIMENTS, AND CONCLUSIONS ON THE BLEACHING PROCESSES OCCURRING IN ELECTRON IRRADIATED KBr

5.1 The Optical Bleaching of Additively Coloured Crystals

The optical bleaching, by illumination with F light, of additively coloured alkali halide crystals is known to occur via a vacancy aggregation process,[1] and leads to the formation of M,R,N ..... absorption bands. The experiments described in Chapter 4 showed that KBr crystals which had been coloured at room temperature by fast electron irradiation also bleached by a vacancy aggregation mechanism, the interstitial (V) band formed during the irradiation apparently playing no part in bleaching. As a further investigation into the similarities between the bleaching mechanism occurring in the two types of specimen, the kinetics of bleaching of an additively coloured crystal were measured, using the microspectrophotometer described in Chapter 2.

KBr crystals obtained from Hilger and Watts were used for these experiments; when electron irradiated they showed comparable bleaching kinetics to the Harshaw material, but were found to be much easier to cleave into very thin slices ($\sim$ 125μ m. thick approximately) than the latter material. The microspectrophotometer could only be used on specimens where the depth of the coloration was less than the depth of focus of the 10X objective lenses. This condition was satisfied for electron irradiated crystals but additively coloured samples presented some problems. Additive coloration usually yields specimens that contain F centres throughout the bulk of a crystal some mm. thick, and such specimens would clearly be of no use in microspectrophotometer bleaching experiments. Moreover, the F centre concentration in such specimens would be considerably lower than in those which had been coloured by electron irradiation. Shortening the time for which the KBr crystals were exposed to potassium vapour, and raising the temperature of coloration, produced an inhomogeneous coloration, with

a higher F centre density near the surface, but the coloration still penetrated too far (200 - 300 μm) into the crystals, and they were therefore unsatisfactory. The alternative solution found was to very heavily colour a crystal with excess potassium, and then cleave off very thin sections from it. The as coloured crystals were opaque to the eye, but by carefully removing slices that were between 125 and 250 μm. thick, specimens with an optical density of between 0.7 and 1.0 could be obtained. Whilst these were marginally too thick for examination with the microspectrophotometer, and the F centre concentrations still somewhat lower ($< 10^{18}$ centres cm^{-3}) than those of their electron irradiated counterparts, these additively coloured crystals were as close to the required specification as it was possible to achieve.

Samples cleaved from the bulk crystal, using the method briefly described at the end of Chapter 2, were rather small (typically 5 mm. square) and very fragile, so to facilitate handling they were affixed by one corner to a microscope cover glass, using a spot of cyanoacrylate adhesive. Prior to mounting, however, they were placed on a hotplate at about 600°C for a few seconds, and then quenched by rapidly transferring them onto a polished copper block that was at room temperature. Quenching in this manner produced M and R centre concentrations that closely resembled those found in electron coloured specimens. The heat treatment and subsequent mounting and alignment operations were carried out in very subdued yellow lighting, as they would have been with electron coloured materials. The experimental results now to be reported were obtained using the thinnest attainable specimens ($\sim$125 μm. thick) and so, hopefully, the errors in microspectrophotometric measurements should not be too severe.

Fig. 5.1 shows the optical density of a number of additively coloured KBr specimens plotted against the energy absorbed during bleaching, together with the corresponding result for a RT electron

FIG. 5.1.

OPTICAL BLEACHING OF AN ADDITIVELY COLOURED SPECIMEN OF KBr.

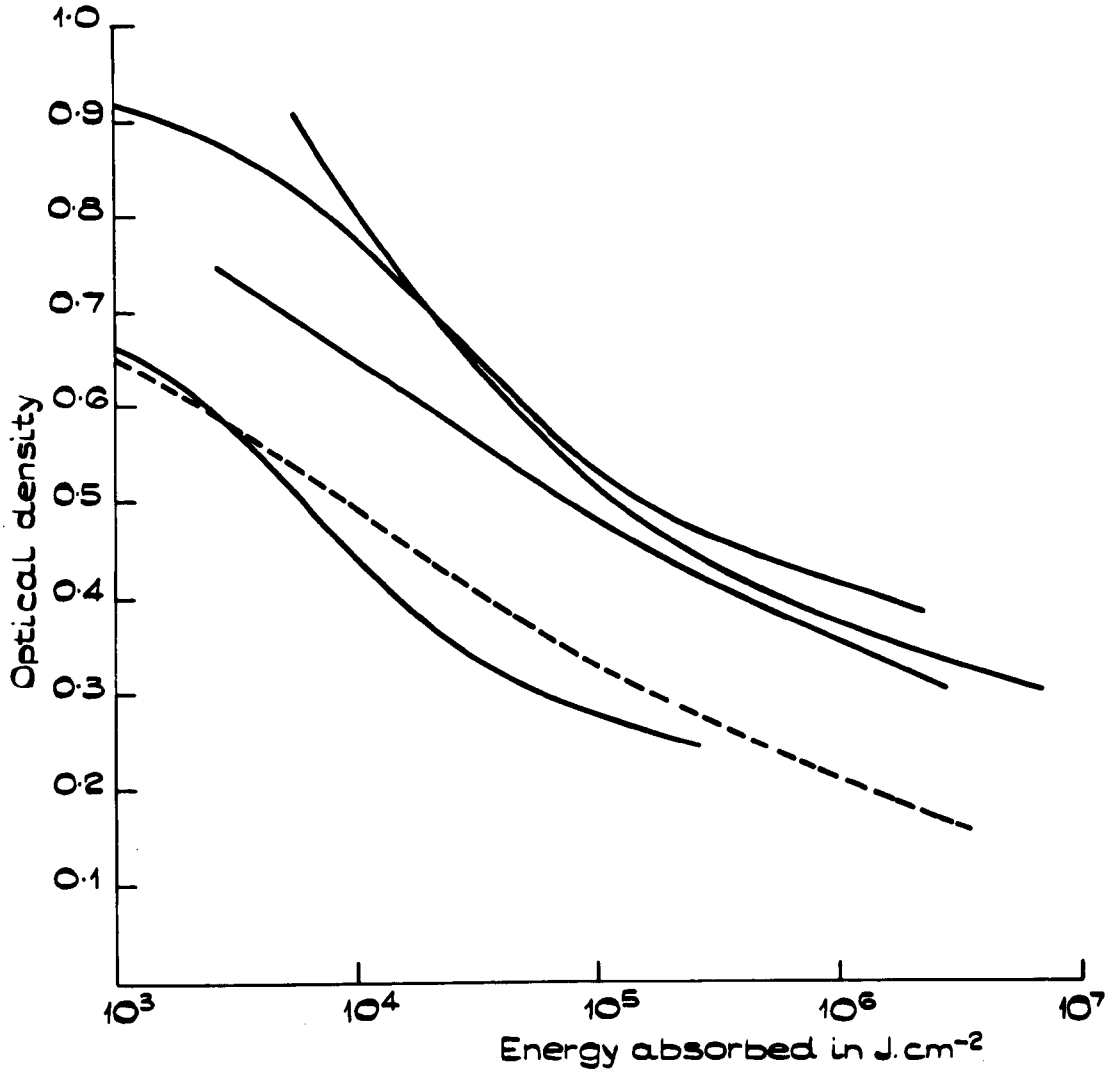

coloured crystal (broken line). There clearly is a close similarity between the bleaching curves for both types of specimen, which is to be expected if the mechanisms involved (aggregation) are indeed the same. The energy derivative of the optical density $\frac{dD}{dE}$ is plotted against the energy absorbed in Fig. 5.2; the dashed line represents the equation $\frac{dD}{dE} = \frac{5x10^{-2}}{E}$. It is evident from Fig. 5.2 and Fig.3 in Chapter 3, that the relationship $\frac{dD}{dE} = \frac{5x10^{-2}}{E}$ describes approximately the room temperature optical bleaching of KBr specimens that have been coloured either additively to high concentrations of excess alkali metal or by high energy electron irradiation at RT or below.

It can readily be seen from Fig. 5.3 that the bleaching of additively coloured KBr occurs by vacancy aggregation; this illustration shows the spectrum before and after prolonged illumination with F band light of a specimen which had been heat treated so that at the start of bleaching the concentration of F aggregate centres was zero. Prolonged bleaching leads to the disappearance of the F band, and the formation of a broad absorption band due to the presence of M,R and N centres. The dotted curve shows an intermediate spectrum, in which the M and R bands are individually resolved.

In both additively coloured crystals, and those coloured by ionising radiation, there is the possibility of forming colloidal metal particles, which give rise to absorption bands distinguishable from those due to normal trapped electron and trapped hole centres. The properties of colloids have been extensively studied, particularly by Scott [2,3] and his co workers. They found that if an additively coloured crystal is rapidly quenched from 500°C to yield a strong F band, and then heated in the dark to $\sim$300°C, the F band decreases in intensity and a new band appears on the long wavelength side of the F band. The precise position and shape of this absorption band depends on the size and shape of the metal particles, and thus on the heat

FIG. 5.2.

THE OPTICAL BLEACHING OF ADDITIVELY COLOURED KBr.

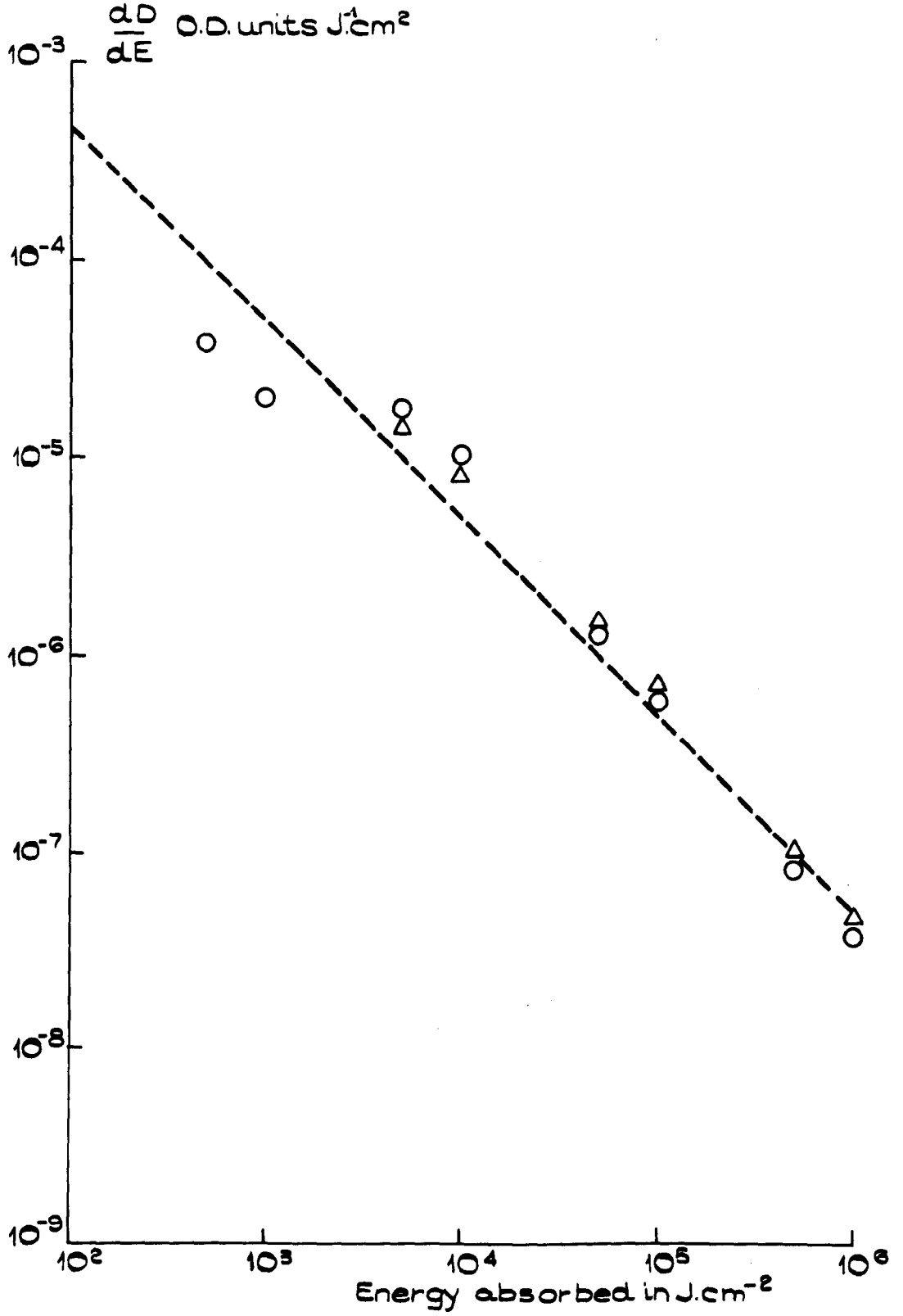

Fig. 5.3.

BLEACHING SPECTRA OF ADDITIVELY COLOURED KBr.

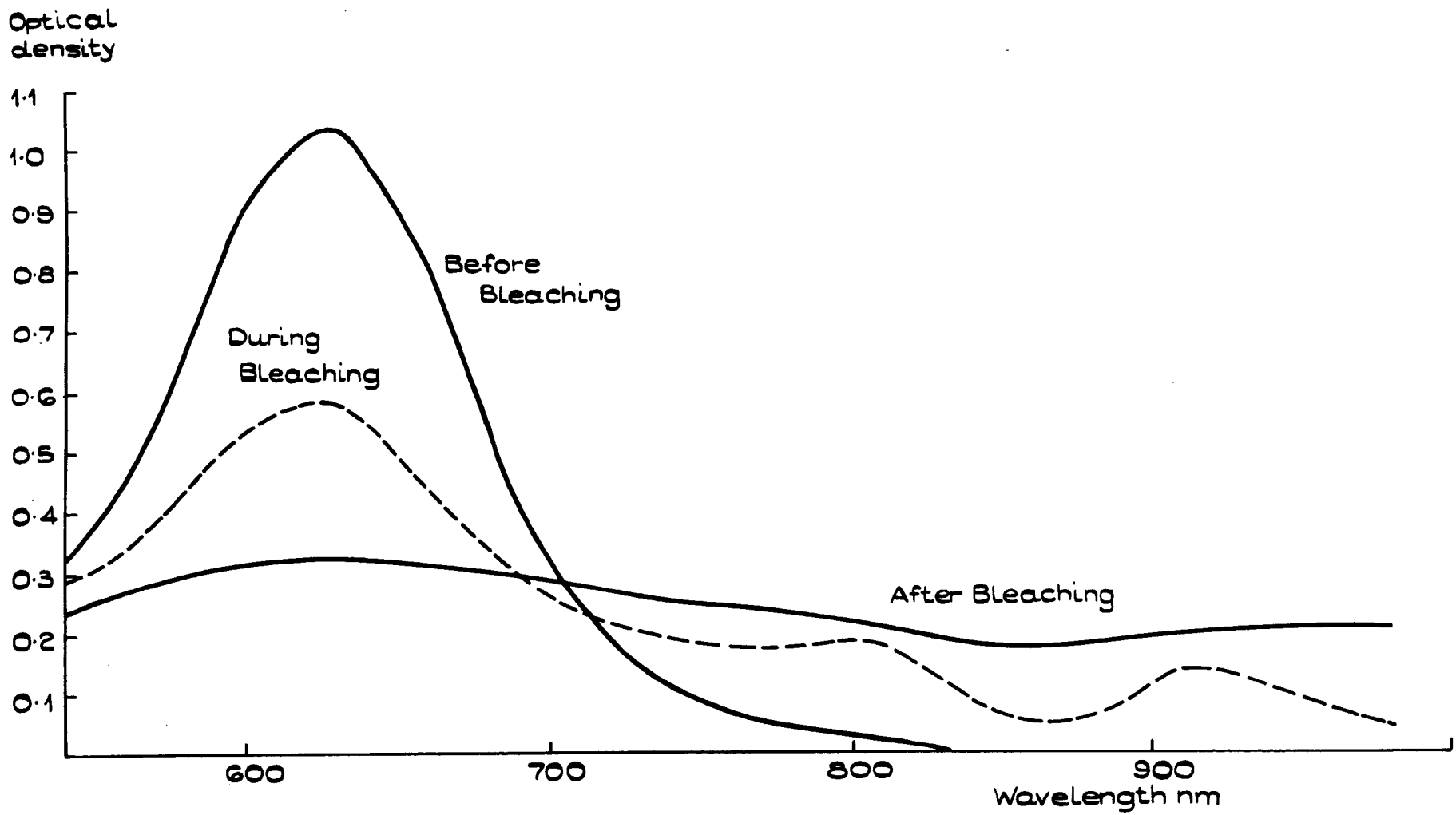

treatment (Fig. 5.4). The peak wavelength and shape of colloid absorption bands are essentially independent of temperature, unlike those due to true colour centres. Colloids, if sufficiently large ($> \sim 30 \mu m$.) also give rise to Tyndall scattering. It is thus relatively easy to distinguish between true colour centre absorption and that due to colloids.

It is unlikely, however, that any of the crystals used in the experiments described in this chapter contained a significant number of colloids, either initially or after bleaching. Before use they were quenched from sufficiently high a temperature to ensure that they only contained atomically dispersed defects, and optical bleaching at RT of additively coloured crystals does not usually lead to colloid formation. It was, unfortunately, impossible to check whether or not any of the residual coloration that remained after the prolonged optical bleaching of an additively coloured specimen was due to colloids, because the poor thermal contact between the crystal and specimen holder would not allow absorption measurements to be made at low temperature. No alternative methods of mounting the crystals were successful, because they were so small and fragile.

Spectra were recorded at intervals during the bleaching of one additively coloured specimen, and the total concentration of vacancies present at each time estimated from the heights of the F,M and R bands. It was not possible to extend the measurements far enough into the infra red to allow the N band to be seen, since the monochromator was not designed to be scanned beyond $1 \mu m$, nor could the Perkin Elmer 450 spectrophotometer be used with any success, since the specimens were too small. Even ignoring the contribution due to the N band, which would have been quite significant towards the end of bleaching, this data suggested that the total number of vacancies present is increasing as bleaching proceeds. This echoes one of the findings of the experiments

Fig. 5.4.

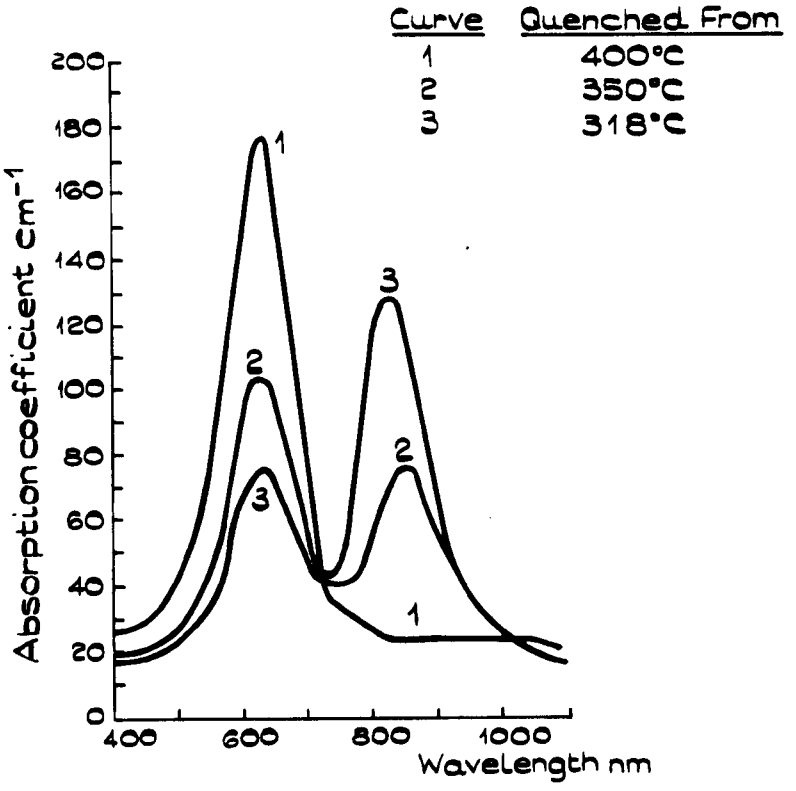

ABSORPTION BAND DUE TO COLLOIDS IN ADDITIVELY COLOURED KBr(3).

described earlier in Section 4 of Chapter 4, namely that there is a need for improved measurements to be made of the oscillator strengths of the F aggregate bands.

5.2 Modulation Spectroscopy of Transient Species

All of the spectral measurements so far described have yielded information on the defect concentrations present in the crystal after bleaching, and have given no insight into transient species that might be generated during illumination with intense laser light. For example, if the aggregation of F centres to M centres does proceed via the $F + \alpha \rightarrow M^+$ (4) reaction, one might expect to find some evidence for the existence of M^+ centres during illumination with F light. An experiment was therefore devised to study such transient phenomena during bleaching.

The bleaching microspectrophotometer was modified to allow it to be used for a new modulation technique, in which the bleaching laser beam was interrupted at a constant frequency and the microspectrophotometer used to look for synchronous variations in specimen transmittance in the spectral region extending from about 700 nm. into the infra red beyond the M band peak. The apparatus is shown diagramatically in Fig. 5.5, with a photograph of the pre sample holder optics in Fig. 5.6. It consists of the microspectrophotometer described in Chapter 2, with a chopper in the laser beam and a filter (F) in front of the monochromator entrance slit. The chopping frequency could be chosen to be 4 1/6 c/s, 66 2/3 c/s or 800 c/s (i.e. not simple multiples of 50 c/s) by a suitable combination of synchronous motor and chopper rotor. The Filter (F) was necessary to attenuate the laser beam before it entered the monochromator, for it was found that without it a significant level of laser light reached the photomultiplier tube by scattering within the instrument, regardless of the setting of the wavelength drum. This would have been very troublesome had it not been eliminated, because the signals being investigated were found to be exceedingly small. F was

Fig. 5.5

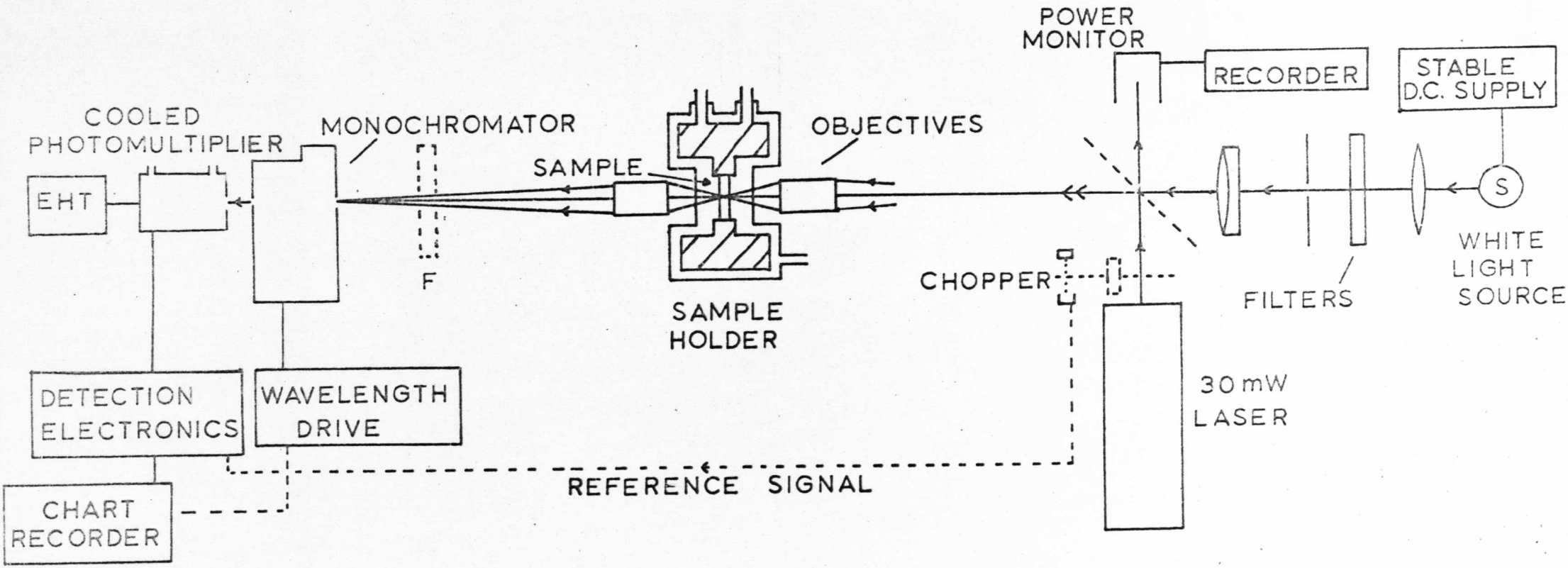

DIAGRAM OF THE APPARATUS USED FOR MODULATION SPECTROSCOPY.

Fig. 5.6.

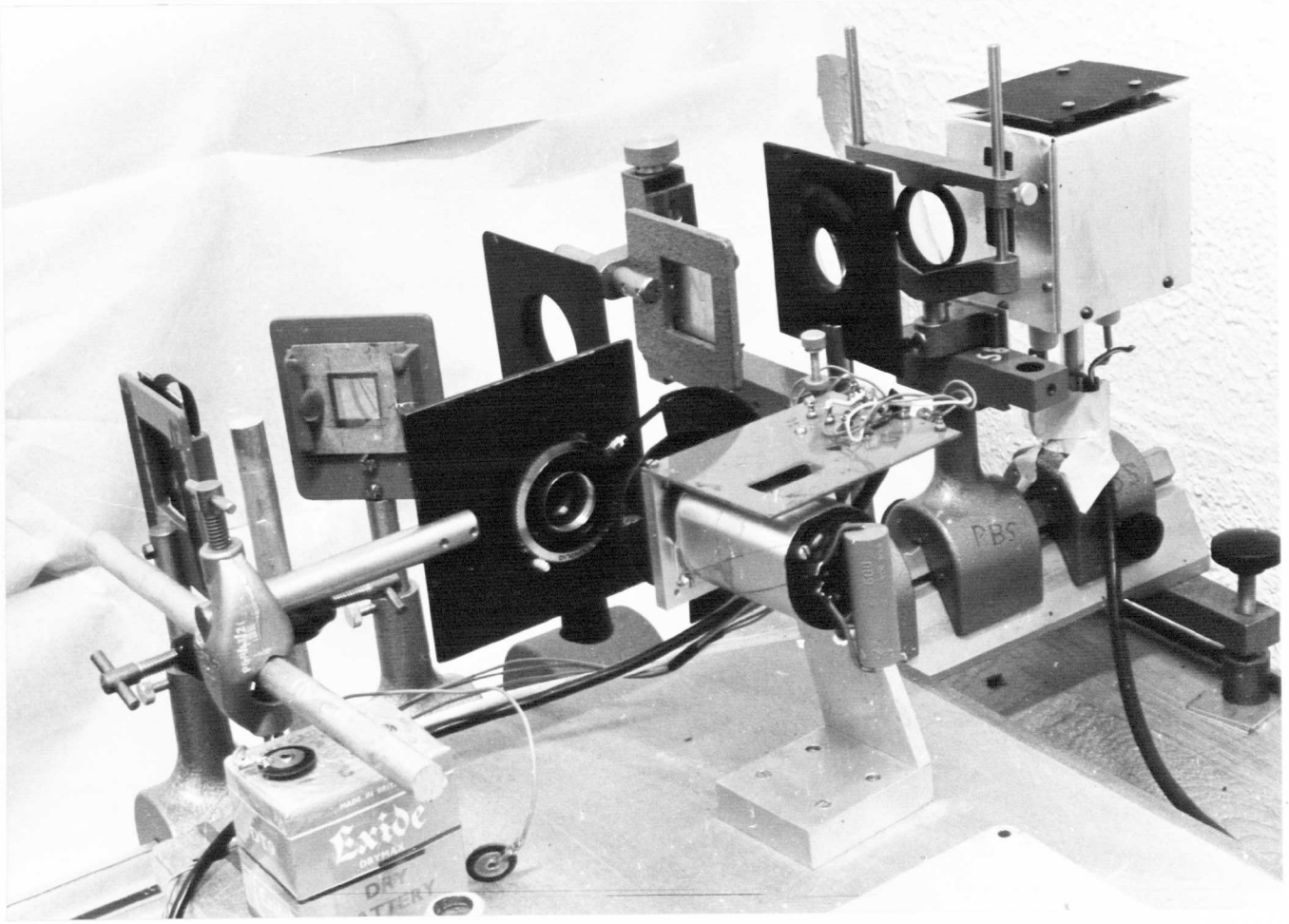

PHOTOGRAPH OF THE 'FRONT END' OF THE MODULATION SPECTROSCOPY APPARATUS.

in fact, a combination of filters, chosen so that it was virtually transparent in the region 700 nm. to 1 μm, with a sharp cut off at about 680 nm. giving an optical density of about 6.0 at 632.8 nm. The signal from the cooled 150 CVP photomultiplier tube was connected to a phase sensitive detector (P.S.D.) (manufactured by Automatic Systems Ltd.), so that the in phase component of the transmitted spectrophotometer beam could be measured at a wavelength of interest. The reference signal for the P.S.D. was provided by light from a pea lamp shining through the rotating chopper blades onto a phototransistor. The phase shift was adjusted so that a zero quadrature signal was obtained when the small amount of laser light transmitted by the filter (F) was allowed to reach the photomultiplier, by setting the monochromator to 633 nm. (It was possible to continuously check phasing during an experiment, since the A.S.L. P.S.D. has both in phase and quadrature signal meters.) The sense of the resulting in phase signal was deemed to be positive. Hence a positive signal at, for example, 750 nm. corresponds to an increase in transmittance at that wavelength during the half cycle when the laser beam is incident on the crystal. A chopping frequency equal to that of the mains supply was deliberately avoided, in order to eliminate the possibility of erroneous signals being derived from e.g. faulty screening of input leads. The P.S.D. was also provided with a powerful mains rejection filter, which could obviously only be used if the signal frequency was removed from 50 Hz.

The variation of the P.S.D. signal over the 700 nm. to 1μm. range, for a chopping frequency of 4 1/6 c/s, is shown in Figs. 5.7 and 5.8 for both additively coloured crystals and crystals coloured by electron irradiation at room temperature. The individual points on the curves of Fig. 5.7 and 5.8 were plotted using a noise averaging process rather similar to that performed electronically by a computer of average transients. The monochromator was set to the desired wavelength, and the somewhat noisy output from the P.S.D. recorded for half a minute.

FIG. 5.7.

MODULATION SPECTRUM OF ADDITIVELY COLOURED KBr

LASER CHOPPED AT 4 1/6 C/S.

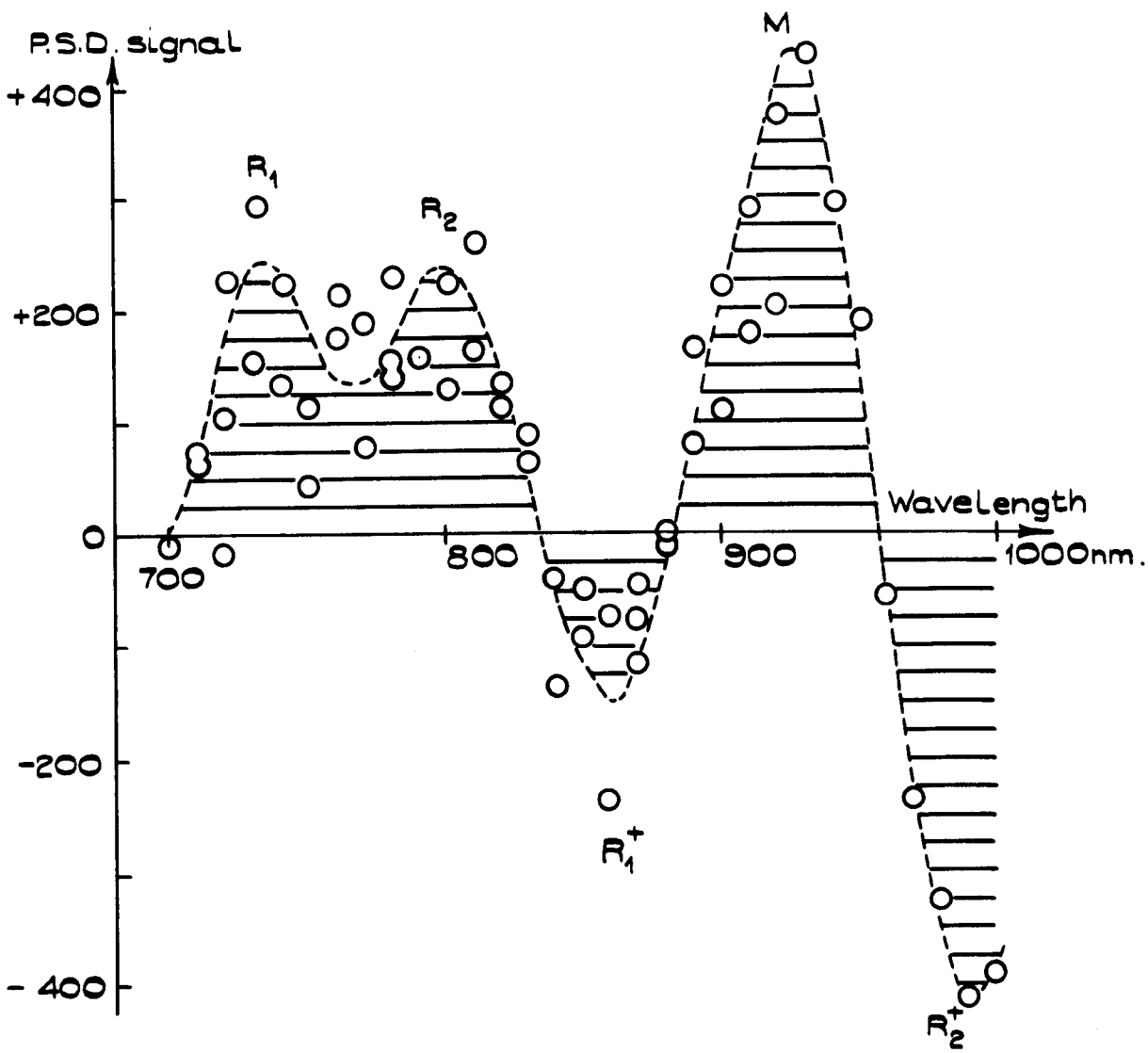

FIG. 5.8.

MODULATION SPECTRUM OF RT ELECTRON IRRADIATED KBr

LASER CHOPPED AT 4 1/6 C/S.

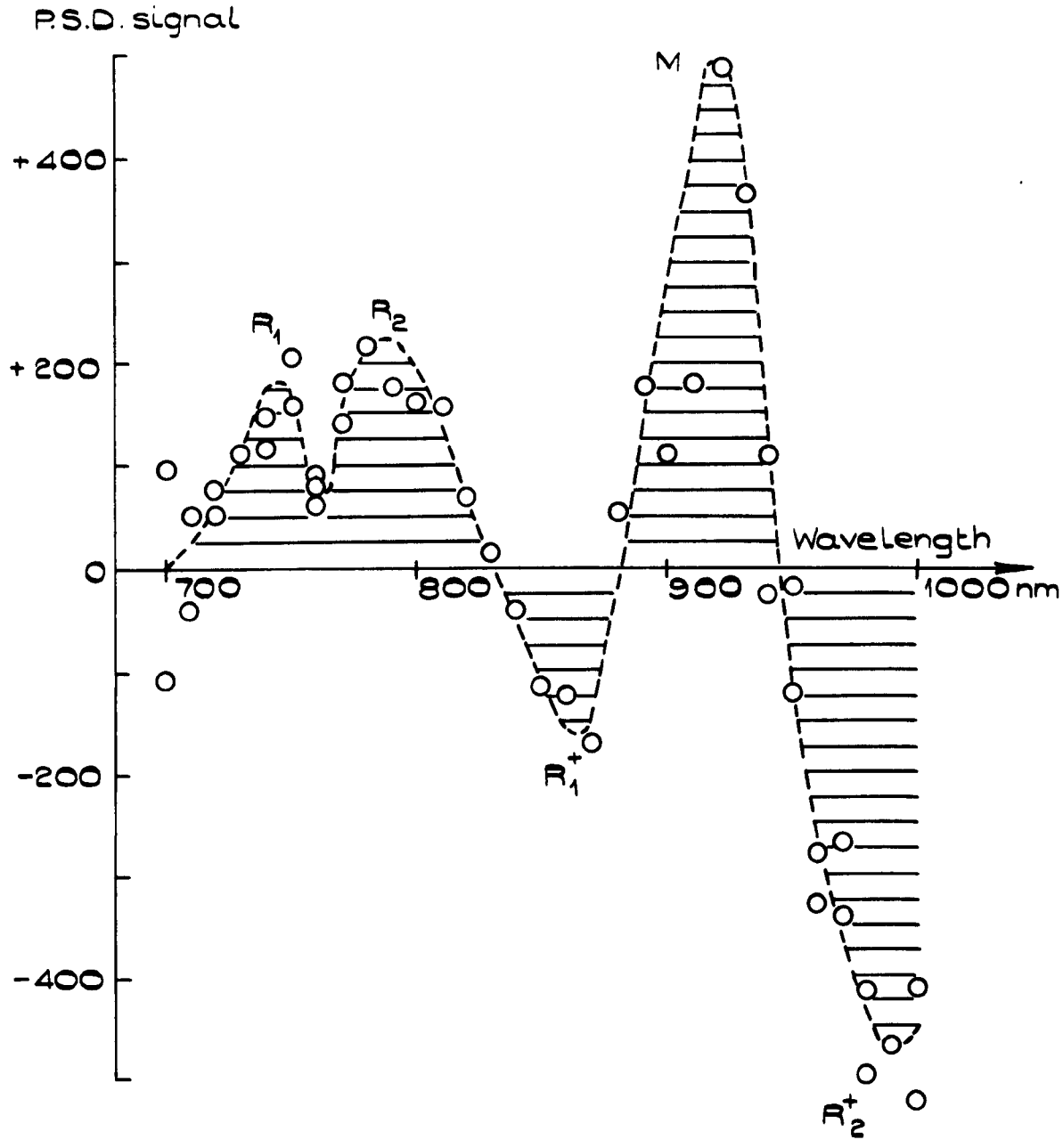

The recorder trace for this interval was intersected by ten equidistant vertical lines, and the amplitude of the trace measured at each of the points of intersection. These ten values were then added together, and plotted as one point on a spectrum. The signal at any particular wavelength gradually decreased with time, due to bleaching of the specimen. To try to minimise this effect the specimen was repositioned from time to time, to bring a fresh part of the crystal into the laser beam. This is why in Figs. 5.7 and 5.8 there is sometimes more than one point at a particular wavelength, each point corresponds to the signal from a different part of the same crystal, coloured to the same extent initially, and at approximately the same stage of bleaching.

Four main features can be distinguished in both spectra; a double positive peak near 760 nm, a single positive peak near 920 nm, and negative peaks at 860 nm. and 990 nm. The 5 letters on Figs. 5.7 and 5.8 indicate the expected positions of the R_1, R_2, M, R_1^+ and R_2^+ bands. The M band in KBr is normally observed at 918 nm. at RT [1], and the positive peak at 920 nm is therefore associated with M centres. The R_1 and R_2 bands are not normally resolved at RT; Fig. 4.1 shows a broad "R" absorption near 790 nm. The Ivey relations predict R_1 and R_2 bands at 732 nm. and 792 nm. respectively at RT [1], and the double positive peak in Fig. 5.8, with components at approximately 740 nm. and 790 nm, is identified with R_1 and R_2 centres. The R_1^+ and R_2^+ bands, corresponding to transitions of ionised R centres, are more difficult to place. They are observed at 1.01 μm. (R_1^+) and 0.89 μm (R_2^+) at LNT [5], but there appears to be no reported measurement of their positions at RT. The available data on the positions of the ionised M and R bands [5,6,7] is summarised in Table 1, and suggests that the peak positions of all the ionised aggregate bands move to shorter wavelengths with increasing temperature.

Table 1

Peak positions of the ionised aggregate bands in KBr and KCl (μm).

		Liquid Helium Temp.	Liquid Nitrogen Temp.	250°K
KCl	M^+	1.40	1.37	1.35
KBr	M^+	1.49	1.44	-
KBr	R_1^+	1.02	1.01	-
KBr	R_2^+	-	0.89	-
KCl	R_1^+	0.96	0.94	-

The R_1^+ and R_2^+ bands might thus be expected to lie at about 0.99 and 0.87 μm.at RT, and therefore the negative peaks at 0.99 and 0.86 μm.in Figs. 5.7 and 5.8 are identified with the R_1^+ and R_2^+ bands.

It is clear from Figs. 5.7 and 5.8 that comparable changes in the R_1, R_2, M, R_1^+ and R_2^+ bands are induced by F band laser irradiation in both additively and RT electron coloured samples. This is a further indication of the similarities between the bleaching mechanisms in additively coloured and RT electron coloured specimens, and supports the evidence of Chapter 4 that bleaching in the latter case involves only vacancy aggregation.

The spectra of Fig. 5.7 and 5.8 show that the transmission in the M, R_1 and R_2 bands increases (or the number of centres decreases) during the half cycle when laser power reaches the crystal, whereas the transmittance in the R_1^+ and R_2^+ bands decreases. The samples used to obtain this data had received a sufficient dose of F light during the final optical alignment of the apparatus to take them past the peak of the $(O.D.)_M$ vs. n curve of Fig. 4.35, so that further illumination was expected to lead to an increase in transmittance at the M band and a reduced transmission at the R bands. The increased M transmission is observed. The overall effective transmission for F_3 centres does decrease, but the decrease is made up of a small increase for the R_1 and R_2 bands (possibly related to N centre formation) and a large decrease for the

ionised R_1^+ and R_2^+ centres. There are two explanations for the presence of a large R^+ absorbance during illumination. The first is that reactions of the form $M + \alpha \rightarrow R^+$ occur under illumination with F light, while the second involves ionisation of R centres by the laser light, through the R_F excited transition lying under the F band. The latter explanation is less likely, since the R_F band lies on the high energy side of the F band peak in KBr [1], away from the 632.8 nm. laser line which lies on the low energy side. Further evidence to support the $M+\alpha\rightarrow R^+$ theory comes from the fact that the signal obtained in these modulation experiments was strongly frequency dependent. The spectrum at a chopping frequency of 66 2/3 c/s.$^{-1}$ became very difficult to discern from noise (Fig. 5.9) and at 800 c/s.$^{-1}$ it had disappeared altogether. This is consistent with R^+ centres being formed by a process involving slow ionic motion (such as $M+\alpha\rightarrow R^+$) rather than one involving electronic excitation, which would be expected to be largely frequency independent in this range.

As a simple test to check that the kinetics of bleaching in these modulation experiments were the same as those found for continuous illumination, a bleaching experiment (using the microspectrophotometer) was performed with a 66 2/3 c/s.$^{-1}$ chopper in the laser beam. The results of this experiment are illustrated in Fig. 5.10 with a curve for a continuously bleached specimen shown, as the broken line, for comparison. The kinetics clearly are the same, and therefore the deductions of the modulated bleaching experiments, namely that mechanisms of the type $M+\alpha\rightarrow R^+$ occur during optical bleaching, can be applied to bleaching in general.

The optical modulation spectroscopy technique was also tried on specimens coloured at LNT. Initially the chopper was left in the laser beam, and the V band at 260 nm. examined for synchronous variations in transmittance. To allow this to be done, the spectrophotometer had to

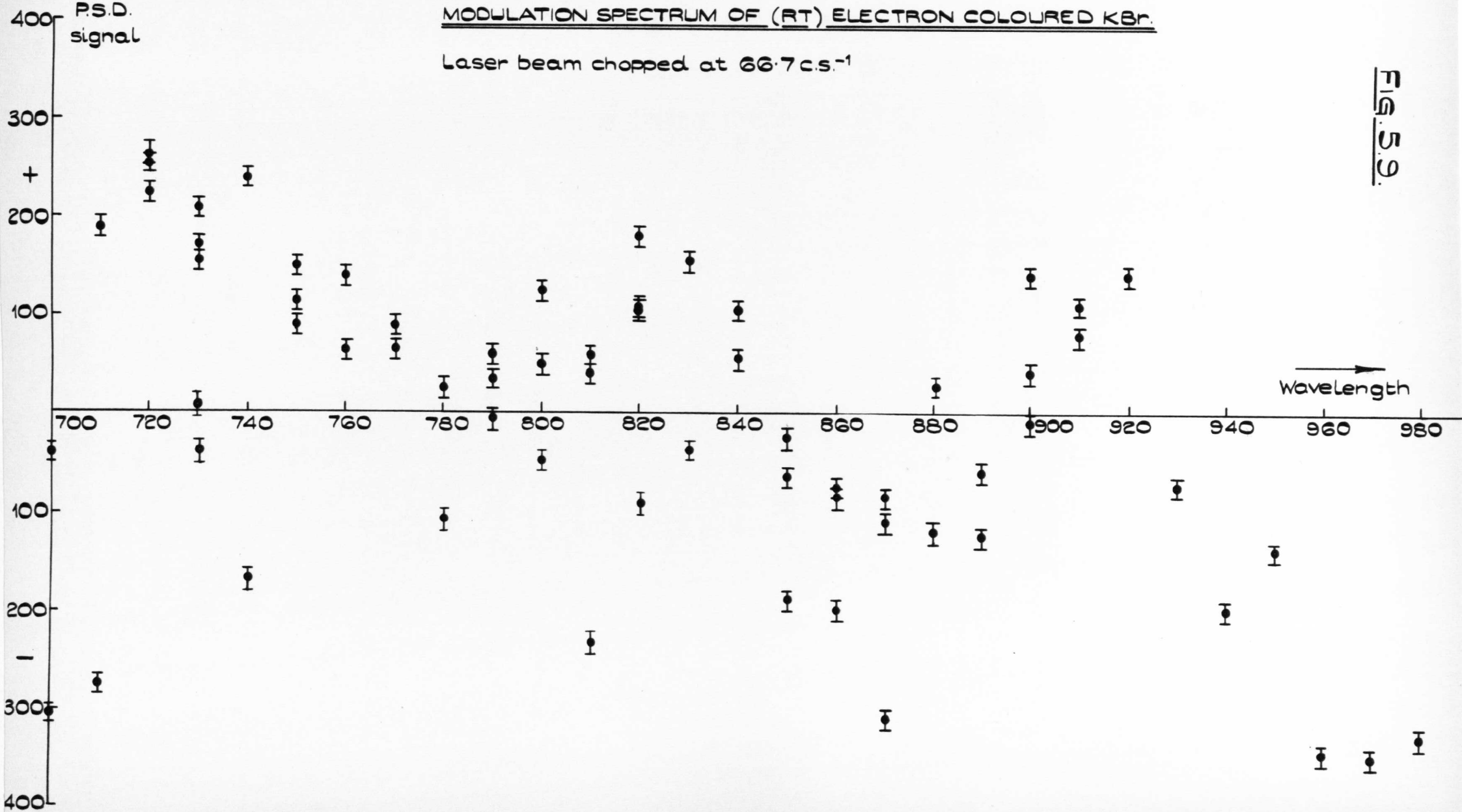
MODULATION SPECTRUM OF (RT) ELECTRON COLOURED KBr.
Laser beam chopped at 66·7 c.s.⁻¹
P.S.D. signal
400
300
+
200
100
700
720
740
760
780
800
820
840
860
880
900
920
940
960
980
Wavelength
100
200
−
300
400

FIG. 5.9.

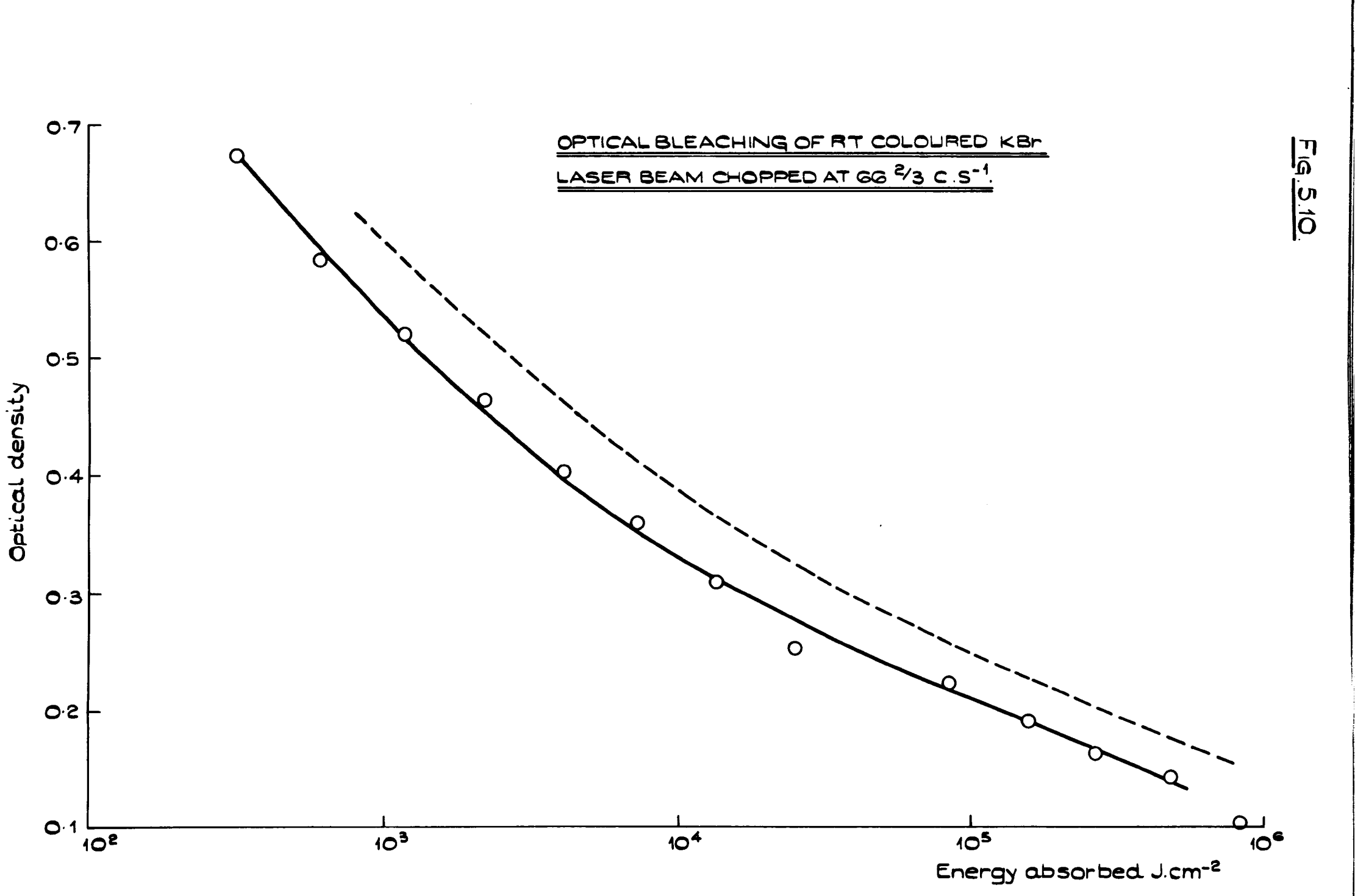
OPTICAL BLEACHING OF RT COLOURED KBr
LASER BEAM CHOPPED AT GG 2/3 C.S-1.
Optical density
0·7
0·6
0·5
0·4
0·3
0·2
0·1
10²
10³
10⁴
10⁵
10⁶
Energy absorbed J.cm-2

FIG. 5.10.

be modified to operate in the ultra violet. The tungsten source was replaced with a deuterium lamp, quartz lenses were substituted for the glass components, and a 6217 photomultiplier tube coupled to the monochromator. The signal obtained from this arrangement when it was used as a D.C. spectrophotometer was not very great, but it was sufficient to allow the 260 nm. absorption band in a LNT coloured KBr specimen to be plotted satisfactory. However, when the laser beam was chopped (at any of the frequencies available) no signal was detected on the P.S.D. with the monochromator tuned to 260 nm.

An alternative arrangement was tried, in which the V-band was illuminated with chopped light, and the F band examined for synchronous intensity variations. This was accomplished with much the same sort of experimental arrangement as that used to investigate the RT coloured specimens, with the exception that the laser was replaced with a high pressure mercury arc source and Woods glass filter, and the objective focusing the bleaching source onto the specimen was replaced with a quartz component. No modulation in the F band could be detected when the V band was illuminated with light chopped at 4 1/6 c/s or higher frequencies, nor was there any obvious decrease in the F band coloration.

One obvious explanation for the lack of response in these experiments is that the modulated signal in the F or V band was buried in noise. This, unfortunately cannot be entirely ruled out. The alignment, and more particularly the focusing of the spectrophotometer and bleaching beams could not be carried out with the precision of previous experiments, largely due to the chromatic aberration of the lens system. A reasonably satisfactory compromise focus of the red F-light and ultraviolet V band light could be found when the specimen was replaced by a piece of u-v fluorescent glass, but judging the position of focus using a real specimen, with only the violet emission from the mercury lamp visible, was considerably more difficult. The

defocusing of the modulated excitation beam at the specimen may have reduced the effective power density to a level below that required to give a satisfactory signal to noise ratio; it was certainly found that with the RT coloured specimens setting up was quite critical, the signal could very easily be lost by small misalignments or a reduction in laser power. It does, however, seem unlikely that this type of experimental error would be the reason for the failure to detect any coherent signal in all of the attempts that were made to do so.

The lack of modulation in the F band when the V band light is chopped suggests that the V centres in LNT coloured KBr are more stable than the data of Chapter 4 suggests. It is possible that they are clusters of interstitials that are not readily ionised or broken up by light. This does not, however, completely explain the lack of V band signal when the F light was modulated. The bleaching kinetics clearly show that when the crystal is illuminated with F light the F and V bands annihilate each other, presumably by a vacancy interstitial recombination mechanism. One can therefore reasonably expect a positive result in the case of the chopped F-light experiment. It is quite possible, however, that the time constant of the F-V centre annihilation mechanism is too long for a modulation frequency of 4 1/6 $c/s.^{-1}$ i.e. it is > 0.25 sec. This may be because the mechanism involves several stages, for example

$$F + h\nu \rightarrow \alpha + e^-$$

$$V + e^- \rightarrow V'$$

$$V' + \alpha \rightarrow \text{normal occupied lattice site.}$$

The time constant could also be rather long if the driving force for processes involving V centres is weaker than the coulomb-dipolar one for $F \rightarrow M$ conversion.

Therefore the most likely conclusions to be drawn from the negative results of these pulsed bleaching experiments is that the V centres in LNT coloured KBr are fairly stable clusters of interstitials,

not easily ionised or broken up by direct optical excitation, but which are readily annihilated by mobile vacancies generated by F band excitation. It is also probable that the F-V interaction involves a fairly long time constant (>0.25 sec.).

5.3 Discussion of Optical Bleaching in Electron Irradiated KBr

The experiments described in this and the two preceding Chapters of this thesis form a fairly extensive investigation into the bleaching at room temperature of KBr single crystals that had been coloured by high energy electron irradiation. Since the penetration depth of the electron beam was small ($\sim 25\mu$m.), the initial F centre densities were high, between 10^{18} and 10^{19} per cm^3. The bleaching was carried out using a focused He-Ne laser, which enabled power densities at the specimen of up to 10 KW. cm^{-3} to be obtained. At such high illumination intensities it was possible to make measurements over a range of absorbed energy densities from 1 to 2×10^{9} $J.cm^{-3}$.

There was found to be a marked difference between the optical bleaching (at room temperature) of crystals which had been irradiated at RT and those which had been irradiated at LNT ($\sim 90^{\circ}K$) and warmed in the dark to RT. The F band in specimens coloured at LNT can be completely bleached, whereas crystals coloured at RT behaved very similarly to ones that have been additively coloured, prolonged bleaching leading to a residual colouration at 625 nm that is extremely difficult to bleach any further. Subsequent spectroscopic investigation showed the reason for the different behaviour of the two types of specimen under F band illumination; a vacancy-interstitial annihilation mechanism occurs in specimens that have been irradiated at $90^{\circ}K$, whilst vacancy aggregation takes place in those coloured at RT.

5.3(a) KBr electron irradiated at room temperature

The presence of a large V band between 200 and 300 nm.signifies that interstitial clusters are formed during the electron irradiation of KBr at room temperature, but they apparently play no part in the

bleaching mechanism, since the magnitude of the V band absorption does not change and the total vacancy concentration remains constant during bleaching. This V band can be identified with a broad, stable V band that forms when KBr is subjected to prolonged X-irradiation, or is additively coloured with excess bromine; it has been designated the V_2/V_3 absorption, or more recently the W band [8]. Its presence can reasonably be attributed to stable interstitial clusters, dislocation loops or small precipitates of bromine molecules. In the case of electron irradiation the interstitials only gain sufficient mobility to diffuse into stable clusters during irradiation at RT, since after irradiation at LNT they appear to remain either atomically dispersed, or as smaller, less stable clusters when the crystal is warmed to RT.

The evidence strongly suggests that the optical bleaching of KBr which has been coloured by electron irradiation at RT occurs solely by the aggregation of vacancies into F_2, F_3, F_4 ..... centres, indicated by the formation of M,R, ... bands. The residual coloration at 625 nm. found in crystals that have received in excess of 10^6 J. $cm.^{-2}$ of F light is therefore thought to be due to allowed optical transitions of the M and R centre (the M_F and R_F bands) which fall slightly to the short wavelength side of the F band peak. There are two possible mechanisms for the vacancy aggregation in these RT irradiated specimens. The first involves the long range coulomb attraction between F' and α centres [9], operating at distances of up to about 20 lattice spacings, and the second is a relatively short range ($\sim$5 lattice spacings) monopole-dipole (or covalent) attraction between F and α (or M and α) centres [10,11]. Illumination of the crystal with F light creates α centres either by excitation and thermal ionisation or at high F centre concentrations by an electron tunneling from the excited state of an F centre to a neighbouring F centre, to form an α centre and a metastable F' centre. Bleaching at its onset is

found to be quite rapid; presumably at this stage aggregation is occurring by both the $F' - \alpha$ and $F - \alpha$ mechanisms. As bleaching proceeds, however, and the F centre concentration falls, it is likely that there is a condensation of F centres in which the long range $F' - \alpha$ attraction causes the nearest neighbour pair distribution to shift to shorter separations. When two F centres are sufficiently close (~ 5 lattice spacings) the covalent $F - \alpha$ attraction becomes effective. The $F - \alpha$ mechanism will lead initially to the formation of ionised M centres, (M^+ centres), which subsequently capture electrons to yield ground state M centres. Presumably the aggregation process can then proceed one stage further, through an $\alpha + M \rightarrow R^+$ type reaction to produce R centres, and so onto still larger aggregate centres. Evidence which suggests that the covalent reaction does occur was obtained from the modulated bleaching experiments described in this Chapter; two peaks in the modulation response curve were obtained which can reasonably be identified with the R_1^+ and R_2^+ bands. Further evidence, in the form of an M^+ absorption could not be obtained, as this band would be expected to fall outside the wavelength range of the present apparatus[5], beyond $1\mu m$.

The aggregation process can be approximately described by considering a random distribution of aggregation events among volumes some $5 \times 10^{-19} cm^3$ in size. The experimental observation that the concentration of M centres, and then the concentration of R centres passes through a maximum as aggregation proceeds is consistent with this model. It is found experimentally that as bleaching proceeds the rate of bleaching gradually decreases; this can be attributed to the fact that the $F' - \alpha$ mechanism must operate over progressively larger distances between the more widely spaced centres, and consequently each aggregation event will involve an increasing number of optical excitations. Thus with a constant incident light flux the rate of bleaching will decrease. The optical bleaching "rate" or "efficiency" of room

temperature coloured KBr, expressed in terms of the optical energy absorbed by the crystal during an incremental reduction in F band amplitude, is independent of the intensity of illumination. For example, bleaching curves for crystals coloured at room temperature were essentially identical over a range of illuminating intensities from 20 to 5×10^3 $W.cm^{-2}$. Moreover the energy derivative of the optical density in the F band $\left(\frac{dD}{dE}\right)$ is approximately proportional to the reciprocal of the absorbed energy in the F band (E) over more than six decades of E. This relationship appears to apply to the room temperature optical bleaching of all specimens, regardless of their temperature of coloration.

5.3(b) KBr electron irradiated at 90°K

The room temperature optical bleaching of KBr that has been electron irradiated at liquid nitrogen temperature is particularly interesting, in that prolonged exposure to F light results in the complete disappearance of all of the optical absorption bands, and the crystal returns to its state prior to coloration. A vacancy-interstitial recombination process occurs, there being a direct correspondence throughout bleaching between the total number of vacancies in the F, M and R bands and the height of the V band centred at 260 nm.

The precise configuration of these V centres is not known, although they must presumably be fairly small clusters of bromine interstitials. The possibility of them being single interstitials can be eliminated, since these have been identified with an absorption band seen in KBr which has been X irradiated at 5°K. This is designated the H band [12] and peaks at 380 nm; warming the crystal to 30°K causes its disappearance. The V band seen in the specimens electron irradiated at LNT is stable at room temperature, and appears to be a combination of the V_2 and V_4 bands previously found in KBr which has been X irradiated at 80°K; these bands have absorption peaks (at 80°K) at 254 nm. and 275 nm. respectively. The broad V band in the electron

coloured specimens is, in fact, resolved into two components at 255 nm. and 275 nm. during warming to room temperature. The linear relationship between the vacancy concentration and V band amplitude observed during bleaching further suggests that identifying the latter with the V_2/V_4 bands is correct, since the growth of these bands during X irradiation is proportional to the growth of the F band [13]. It is evident from the results of the modulated bleaching experiments that the interstitial clusters responsible for the V_2/V_4 band are sufficiently stable at room temperature not to be broken up by direct optical excitation, but they clearly cannot be as stable as those found in RT coloured crystals since they are able to take part in bleaching. Any explanation of this difference must involve the increased mobility of the interstitials during electron irradiation at room temperature. The aggregation of atomically dispersed interstitials must take place during irradiation, otherwise the warm up period of LNT coloured specimens ought to be quite long enough for further aggregation to occur, and for the small clusters to lose their separate identity from the stable V centres found in RT coloured crystals. It was, in fact, found that crystals which had been coloured at 90°K and then stored in the dark at room temperature for 24 hours still showed no sign of the broad V_2/V_3 absorption, and bleached by vacancy interstitial recombination. It is apparent, therefore, that bleaching occurs by the annihilation of these small interstitial clusters by mobile vacancy centres, which are the result of F band optical excitation.

In marked contrast to the behaviour of crystals coloured at room temperature, the coloration in LNT irradiated KBr disappears completely after prolonged F light illumination. This is quite simply because no F-aggregate centres remain to give a residual coloration; in point of fact the vacancy (α band) concentration appears to fall to its value prior to the crystal being irradiated. This would seem to indicate that electron irradiation at 90°K, followed by room tempera-

ture F-light bleaching is a cycle which could, in theory at least, be repeated a great number of times without leading to the build up of a persistent coloration, or fatigue, of the crystal. There is, of course, the possibility that there may be "debris" left after bleaching which does not lead to any optical absorption but which hinders further coloration-bleach cycles.

Another interesting point about the bleaching of specimens coloured at LNT is that the energy derivative of the optical density in the F band $\left(\frac{dD}{dE}\right)$ is found to be inversely proportional to the absorbed F band energy (E), which is precisely the relationship found for the RT coloured material. Moreover, the constant of proportionality is found to be the same for both classes of specimen. This would suggest that the mechanism of bleaching of LNT irradiated KBr must be somewhat similar to the RT case. The atomic mechanism must presumably involve interactions between vacancies and V centres of the type $V_{-\alpha}$ and $V'_{-\alpha}$. Until more is known about the structure and properties of those V centres stable at room temperature, it is impossible to be more precise about the mechanism of bleaching.

References

(1) Compton, W.D. and Rabin, H., Solid State Phys. 16, 121, (1964)

(2) Scott, A.B. and Smith, W.A., Phys. Rev. 83, 982 (1951)

(3) Scott, A.B., Smith, W.A., and Thompson, M.S., J Phys. Chem. 57, 757 (1953)

(4) Farge, Y., Lambert, M.and Smoluchowski, R., Phys. Rev. 159, 700, (1967)

(5) Nosenzo, L., Ruguzzoni, E., Samoggia, G. and Udod, V., Phys. Lett. 32A, 415 (1970)

(6) Schneider, I. and Rabin, H., Phys. Rev. 140A, 1983, (1965)

(7) Matsuyama, T. and Hirai, M., J. Phys, Soc. Japan 27, 1926 (1969)

(8) Ishii, T. and Rolfe, J., Phys. Rev. 141, 758 (1966)

(9) Luty, F., Z. Phys. 165, 17 (1961)

(10) Delbecq, C.J., Z. Phys. 171, 560 (1963)

(11) Brothers, A.D. and Lynch, D.W., Phys. Rev. 164, 1124 (1967)

(12) Schulman, J.H. and Compton, W.D., Colour Centres in Solids, 154. Pergamon Press (1963)

(13) Faraday, B.J. and Compton, W.D., Phys. Rev. 138, A893 (1965)

CHAPTER SIX

THE SODALITES

6.1 Introduction

In section 1.3 of Chapter One it was pointed out that colour centre phenomena are not unique to the alkali halides, but can be observed in a number of different materials. However, the study of these other materials has by no means been as extensive as the investigations into the properties of the alkali halides. Similarly, from the technological angle, for the construction of devices for the reversible storage and display of information, the alkali halides were an obvious choice, although in this field there has not been a great deal of success. The "skiatron" [1] dark trace long persistence cathode ray tube is an example of a device that had only limited success under the special conditions of the second World war. This device suffered from fatigue effects associated with the aggregation of F centres to M and R centres, and colloid formation, in its evaporated KCl screen; after a relatively short period of operation the sensitivity fell and a persistent coloration built up which could not be optically bleached. With ever increasing demands being placed on the speed and storage capacity of modern computer memories, and the need arising for reliable dark trace storage c.r.t.'s for radar and similar data display applications, more attention is now being given to some of the materials which exhibit photochromic and cathodochromic properties similar to those of the alkali halides, but which, hopefully, may not show any fatigue effects. (The term "photochromic" is usually applied to materials which change colour when illuminated with light or X rays, and "cathodochromic" to materials which colour when they are irradiated with electrons.) These materials are large in number, but interest has mainly been centred around rare earth doped calcium fluoride, transition metal doped strontium and calcium titanate and the sodalites; [2] this chapter deals with the last of these materials.

Sodalite is the name that has been given to a specific mineral having chemical composition $6NaAlSiO_4 . 2NaCl$, although it is now more usually used as a generic term for the group of minerals which include, for example, sodalite, noselite, hauynite and lazurite, and various synthetic forms of these materials. The general formula of the sodalites may be written $6RR'R''O_4 . 2RX$

where R is (e.g.) Na, K, Cs, Rb, Li, Ag and Ca;

R' is (e.g.) Al, Be, Cr, Mn and Fe;

R'' is (e.g.) Si, B, Ge and TL

and X is (e.g.) Cl, Br, I, F, S, Se, SO_4 and WO_4.

The photochromic properties of one of these materials, namely hackmanite, were first reported in Allan's "Manual of Mineralogy" published in 1834, thus preceding Goldstein's report of the similar phenomenon in the alkali halides by some 62 years. Natural hackmanite, which is very similar to the synthetic materials used for the experiments to be described in this chapter, exhibits a brilliant magenta colour when first removed from the ground, presumably due to exposure to natural radioactivity in the surrounding rocks. If the coloured hackmanite is then left for a short time in sunlight, it fades to a dull greyish hue. Fig. 6.1 shows the absorption spectrum of natural hackmanite.

After this very early reference to the sodalites, interest in them appears to have waned until fairly recent times, when it was discovered that they could be synthetically produced [3]. The synthetically produced sodalites usually have the basic formula $6NaAlSiO_4.2NaCl$, and variations generally involve replacement, without significant change in crystal structure, of sodium by another alkali metal, chlorine by another halogen, or NaCl by a wide variety of other salts, which usually contain sulphur e.g. Na_2SO_4. At one time the presence of sulphur (not necessarily as Na_2SO_4) appeared to be a prerequisite for the material to be photochromic, although various workers have since cast doubts on this hypothesis.

FIG. 6.1.

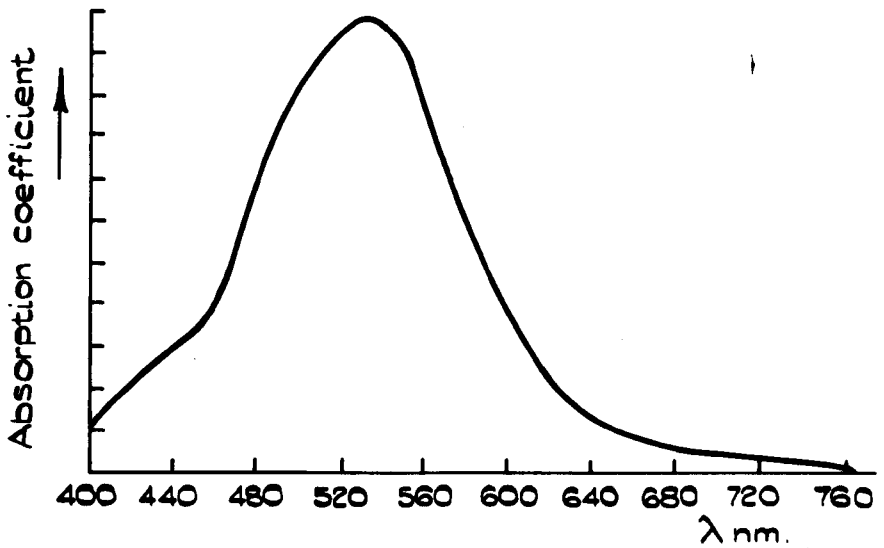

THE ABSORPTION SPECTRUM OF NATURAL HACKMANITE [3].

6.2 The Growth and Sensitisation of Sodalite

Sodalite crystals are usually synthesised hydrothermally, although they have also been prepared from solid state reaction [3] i.e. sintering at high temperature (700° to 1050°C) or by the interaction of H_2S with a molecular sieve derived from Zeolite X (SiO_4:AlO_4 in approx 1:1 ratio) at more moderate temperatures [4]. Hydrothermal growth is to be preferred, since being a closed system method it is more flexible and gives more control over the presence of dopants and contaminants. Both the powder screen of the Ferranti c.r.t. and the single crystals from the Royal Radar Establishment used in the experiments described in this chapter were prepared hydrothermally.

The basic procedure is to compound the constituent materials (e.g. Al_2O_3, SiO_2 and NaCl) adding sulphur as a sulphate, sulphide or thiosulphate, in water, and to adjust the water content to fall between 30 and 70% by evaporation. The mixture is then sealed in a platinum container and placed in an autoclave for between one half and six days, at a temperature between 250°C and 400°C and a pressure of between 2000 and 4000 p.s.i. The crystals found when the container is opened at the end of the growth process are carefully washed and oven dried.

The as grown crystals are generally neither photochromic nor cathodochromic, and have to be sensitised before use. Sensitization usually involves heating the crystals at around 900°C for about 30 minutes in an argon or hydrogen reducing atmosphere; it is unfortunate that thermal stresses cause larger crystals to become cloudy and fracture into small crystallites during this treatment. Recently, however, it has been suggested that small areas of large crystals may be satisfactorily sensitised, without risk of shattering, by electron irradiating them in a scanning electron microscope [5]. Presumably the very high electron current density obtainable in the s.e.m. is sufficient to locally heat the crystal surface to the necessary high temperature. The obvious disadvantages of this method are that only a very small

area of the crystal surface may be sensitised at a time, and that crystals sensitised in this way have a much lower photochromic efficiency than powders.

In view of the difficulty of sensitising large single crystals of sodalite, commercial producers usually pulverise the as grown crystals before sensitisation; this yields a fine powder, suitable for deposition as a dark trace cathode ray tube screen by the normal technique of settling from suspension.

6.3 The crystal Structure and Nature of the Colour Centres in the Sodalites

The crystal structure of sodalite ($6NaAlSiO_4 . 2NaCL$) is considerably more complex than that of the alkali halides, although it does show the overall cubic symmetry of the latter materials. The sodalite unit cell is an open cubo-octahedral cage built up of $Al\ O_4$ and $Si\ O_4$ tetrahedra, with aluminium and silicon atoms alternately situated at the corners, linked to each other by shared oxygen atoms (Fig. 6.2). At the centre of each cage, joined to it through 3 oxygen atoms, there is an $(Na_4Cl)^{3+}$ tetrahedron, which balances the negative charge of the framework.

It is relatively simple to grow sodalites having chemical compositions differing from the basic $6NaAlSiO_4 . 2NaCl$, for example Ge may replace Si and Ga Al in the cage framework, and the Cl at the corners of the cages may be substitutionally replaced by OH, Br, I or S. As an example, the replacement of the 2NaCl in the sodalite lattice by Na_2SO_4 yields a synthetic form of the mineral noselite.

The atomic entity responsible for the coloration in photochromic and cathodochromic sodalite has been identified as an F centre, formed by an electron trapped at a Cl^- vacancy, with four sodium atoms as nearest neighbours. The coloured material gives a 13 line e.s.r. spectrum, whose intensity is proportional to the degree of coloration and which can be assigned to an unpaired electron interacting with

FIG. 6.2.

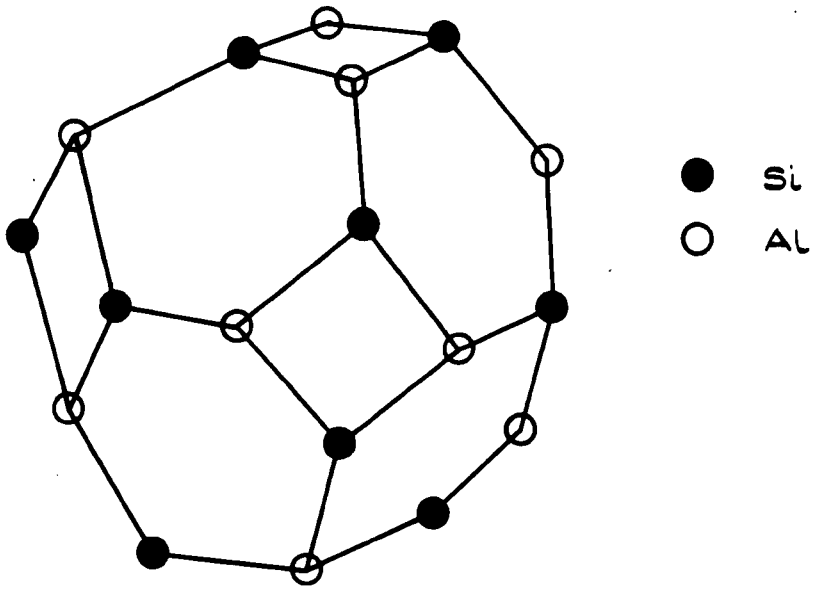

THE OPEN CUBO-OCTAHEDRAL CAGE STRUCTURE FORMED BY THE Si AND Al LATTICE POINTS IN SODALITE.

4 equivalent Na^{23} atoms [4]. This model has not, so far, been verified by replacing the sodium by nuclei having a different spin.

Although the nature of the coloration in the sodalites is now reasonably well understood, the precise mechanism for the formation of F centres is still uncertain. When F centres are produced in sodalite, the coloration apparently goes through two stages, rather like it does in the alkali halides [6]. There is an early (photochromic) stage, in which F centre concentrations up to about $5x10^{17}$ cm^{-3} may be produced, either by u-v light or electron irradiation. The coloration in this early stage may be bleached by light alone, and appears to be completely reversible. Using electron irradiation it is possible to achieve F centre concentrations higher than $\sim 5x10^{17}$ cm^{-3}, although the production efficiency in this second (intrinsic) coloration region is lower, and the F centres do not optically bleach. Finally, a stable coloration may be produced additively, with F centre concentrations higher than 10^{19} F centres cm^{-3}. The early, photochromic, stage of coloration seems to involve the formation of F centres by populating existing Cl^- vacancies with electrons, whereas the second stage may involve the generation, by electron irradiation, of further F centre vacancies, and possibly even the formation of aggregate centres. (There is certainly a change in e.s.r. spectra when a sodalite is coloured into Stage II, the characteristic 13 line F centre spectrum is greatly modified, and becomes dominated by a single isotropic line [6])

Many workers have reached the conclusion that the photochromic properties of the stage 1 coloration are due to sulphur, in one form or another, donating electrons to Cl^- vacancies.[7,8,9] Emission spectroscopy has given evidence for the presence of sulphur as S_2^- (7) and possibly S^{--} in photochromic sodalite, and e.s.r. has indicated, some what inconclusively, that S_3^-, SSO^- and SO_3^- or $S_2O_2^-$ radicals are present.[9] Closely associated with the formation of F centres in

sodalite is an absorption band centred at 4.7 eV which appears when the material is sensitized (Fig. 6.3); illumination into this band produces the photochromic response. The height of the u-v band decreases as the F band increases, and grows again when the F band is bleached; the change in the u-v band amplitude is, however, not as great as the change in the F band, although this probably only represents differences in oscillator strength values. This ultraviolet band is generally thought to be due to the presence of sulphur, although it has recently been reported that if a sulphur free sodalite is doped with Se or Te the position of the absorption remains unchanged, and the photochromic behaviour of the material is unaltered. (5) This might indicate that perturbations of the fundamental absorption are not necessarily very sensitive to ion size in the sodalite structure. However, Ballentyne and Bye conclude that the u-v absorption in the photochromic material is not due to sulphur, and propose instead that O^{2-} ions are responsible for it. Coloration by u-v light will therefore involve the transfer of an electron from an O^{2-} ion to a Cl^{-} vacancy. However, the confirmation of this mechanism, by the detection of an e.s.r. signal due to the O^{2-} ions whose intensity should be inversely proportional to the F band amplitude, is still awaited.

Hence, although the precise mechanism for the photochromic response of the sodalites is still uncertain, F centre formation appears to involve the transfer of an electron from the entity responsible for the u-v absorption to a chlorine ion vacancy. Whilst sulphur may not be directly responsible for the u-v absorption band, photochromic coloration appears to be greatly enchanced by the presence of this element. Optical bleaching of a coloured sodalite will simply involve the transfer of the F centre electron back to the donor ion i.e. it is a purely electronic process. The mechanism for the formation of F centres in the Stage II, cathodochromic coloration region is still largely speculative, although it now appears that ionic displacement

FIG. 6.3.

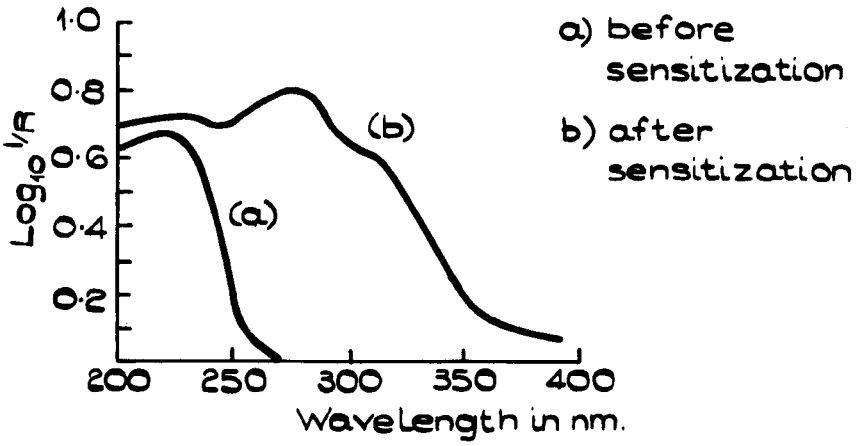

THE REFLECTANCE SPECTRA OF CHLORO-SODALITE POWDER CONTAINING SULPHUR [9].

may be involved.[6] It is reported that cathodochromic coloration can be induced in sodalite which contains less than 10 pp.m. of sulphur [5], although it does not colour as rapidly as material known to contain sulphur.

In conclusion, it ought to be pointed out that no absorption bands have ever been reported on the long wavelength side of the F band in the sodalites, i.e. there is no evidence to suggest the formation of F aggregate centres. This is not very surprising, in view of the large aluminosilicate "cage" surrounding each Cl^- vacancy and the consequent large spacing (~ 7.7Å) between adjacent vacancies. This apparent freedom from M and R centre formation makes the sodalites particularly interesting from the applications standpoint, for most of the difficulties in alkali halide optical display and storage devices have been associated with vacancy aggregation in the storage medium. However, a completely fatigue free sodalite has yet to be found, since although vacancy aggregation has never been observed, c.r.t. screens of sodalite powder gradually lose their writing speed and show a persistent stain after a number of coloration-bleach cycles. The only commercially available sodalite screen c.r.t.s (manufactured by the Optel Corporation) use thermal and not optical erasure, since it is not yet possible to achieve an adequate fatigue life with the latter method. The causes of the fatigue are, as yet, not understood, although it is possibly due to some change occurring in the electron donor centres, or to the slow loss of an active ingredient from the individual grains of the screen during electron irradiation. Also, the possibility of aggregate formation cannot be entirely ruled out. The majority of the measurements described in the following sections were made on a sodalite powder screened c.r.t., and after these experiments it had obviously fatigued, although the deterioration was not very marked.

6.4 The Coloration and Bleaching Characteristics of a Sodalite Powder Screened Cathode Ray Tube

The experiments described in this section represent an attempt to gain quantitative data on the electron beam coloration and, more specifically, optical bleaching characteristics of a chloro sodalite powder, using a special purpose cathode ray tube manufactured by Ferranti Ltd., of Oldham, with a screen deposited from chlorosodalite powder supplied by the American Cyanamid Co., of Stamford U.S.A.

The c.r.t. electron gun assembly was a Ferranti Type 21 built into a Type 5G glass envelope; the screen was deposited in precisely the same way as a conventional phosphor, by settling from aqueous suspension, and was aluminised. The tube was connected into a Ferranti c.r.t. test assembly, which allowed variation of the e.h.t. volts and beam current, and optimisation of the focus; vertical and horizontal time base generators fed a scanning yoke, to enable a raster approximately 4" square to be displayed on the screen.

The experimental configuration used in these experiments is illustrated in Fig. 6.4; it is essentially a single beam reflection spectrophotometer that allows monitoring of the screen coloration simultaneously with electron irradiation or optical bleaching. The microscope illuminator (a) evenly illuminates the tube faceplate, and an image of the coloured region is focused by the lenses (c) onto the end of a fibre optic probe (d). The other end of (d) is connected to the entrance slit of a Bausch and Lomb monochromator (e). An R.C.A. 4463 photomultiplier tube, connected to a Gamma Scientific Model 2020 photometer (f) measures the intensity of the light at the monochromator exit slit, and a T.I. Servoriter II pen recorder (g) supplies a "hard copy" of the photometer output. In order to eliminate any long term drift in the light output of the microscope illuminator, it is fed at reduced voltage from a Variac and constant voltage transformer, transients were filtered by the 2020 photometer time constant.

Fig. 6.4.

SCHEMATIC DIAGRAM OF APPARATUS FOR COLORATION MEASUREMENT.

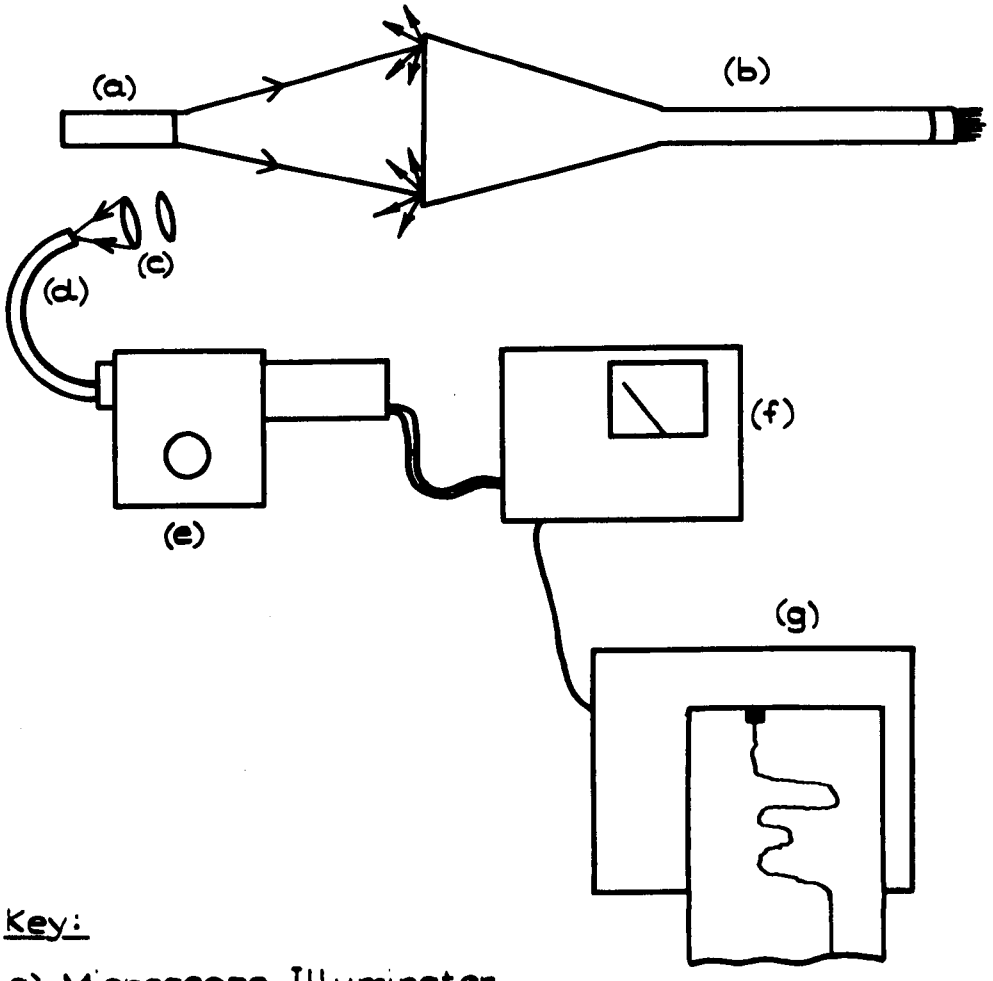

Key:

a) Microscope Illuminator

b) Cathode Ray Tube

c) Lenses, to focus image of screen onto end of (d)

d) Fibre Optic Probe

e) Bausch & Lomb Monochromator, with R.C.A. 4463 Photomultiplier

f) Gamma Scientific Model 2020 Photometer

g) Texas Instruments Servo/riter II Pen recorder.

Throughout the measurements it was assumed that the screen was a perfectly diffuse reflector obeying Lambert's law, with the incident light being redistributed in all directions independently of the direction of illumination, so that the screen ought to have looked equally bright when viewed from any angle. It was not possible to verify this experimentally, but it is a reasonable assumption to make for a screen composed of very small, approximately spherical particles.

The coloration at a particular wavelength has been expressed as the quantity $\log_{10} {}^{1}/R$, where R is the percentage reflectivity relative to the uncoloured screen; this expression was used because of it's analogy with the optical density measurements made on transparent specimens. (Its use is based on the reasonable assumption that the reflection is mostly back reflection from the aluminisation; Fig. 6.5)

The reflectivity spectrum of the coloured screen was measured at a number of incident electron energies, up to a maximum of 25 KeV; the spectra are illustrated in Fig. 6.6 The tube was operated at constant beam current during these measurements, and a correction was made for the cathodoluminescence of the sodalite (by making measurements in the dark with the spectrophotometer light off), about which more will be said later. The material shows a pronounced F band centred at 530 nm., which is the same as that reported by previous workers [8], and there are indications that the absorption again increases at wavelengths below 380 nm. This will be the "sulphur" band of Fig. 6.3. It was impossible to extend these measurements below 380 nm. owing to the optical absorption of the c.r.t. faceplace in this region.

Having located the wavelength of the peak of the F band absorption, the coloration was measured as a function of dose, with the irradiating electron beam energy and current as parameters. During these experiments, in order to prevent optical bleaching, the light reaching the screen was limited to a fairly narrow waveband of low intensity, falling within the sodalite F band. This was done by

FIG. 6.5.

SECTION THROUGH C.R.T. SCREEN.

(not to scale)

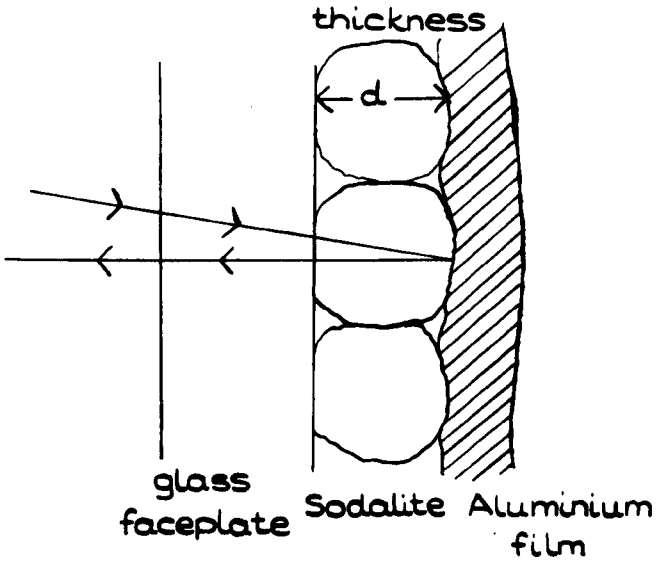

Light is attenuated by a factor $\sim e^{-2\alpha d}$ when making a double pass through the particles of the screen. Thus the measured reflectivity $R \simeq$ (the transmittance)^2, and $\log(1/R) \simeq 2\log(1/T) \equiv$ the optical density.

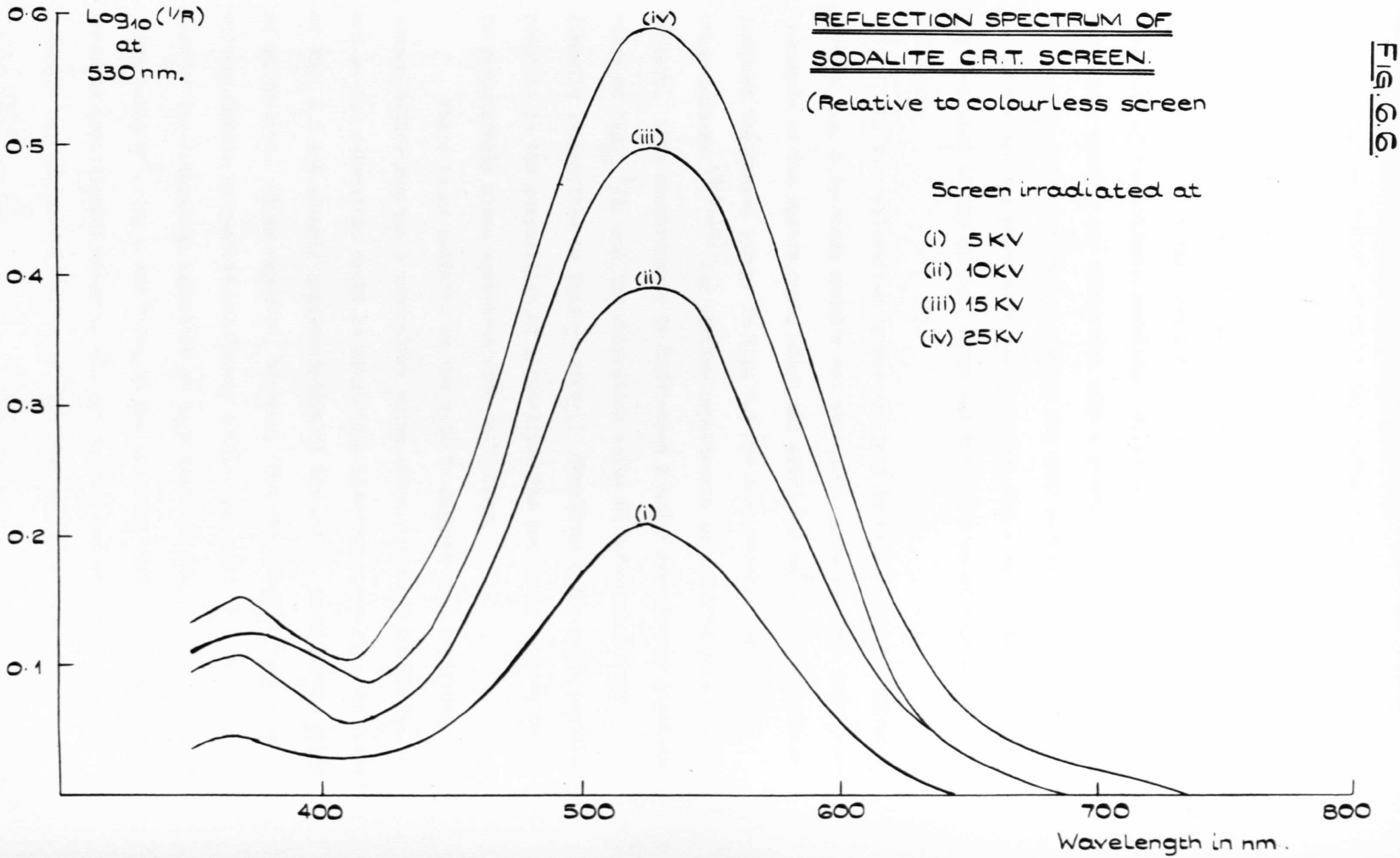
REFLECTION SPECTRUM OF
SODALITE C.R.T. SCREEN.
(Relative to colourless screen
Screen irradiated at
(i) 5 KV
(ii) 10KV
(iii) 15 KV
(iv) 25KV
Log10 (1/R)
at
530 nm.
0·6
0·5
0·4
0·3
0·2
0·1
(iv)
(iii)
(ii)
(i)
400
500
600
700
800
Wavelength in nm.

Fig. 6.6.

placing a Balzers "Calflex" B1/K1 heat reflecting interference filter and an Ilford 624 green colour filter in front of the microscope illuminator. The supply voltage to the light source was also reduced to about 50% of its nominal value. The precautions thus taken resulted in a photometer beam that would not induce any significant optical bleaching of the coloured sodalite. Measurements were made by first completely erasing any coloration with a quartz iodine lamp placed close to the tube face, and then recording the 100% reflectance value. Having started the photometer pen recorder, the electron beam current was increased to the desired value and the build up of coloration monitored.

The dose-coloration curves obtained in this manner are illustrated in Fig. 6.7; these results are obviously average values taken over the whole of the raster area, which was about 6.0 cm^2. For comparison purposes the dashed curves in Fig. 6.7 are some results obtained by other workers [2,9,10] for similar experiments on sodalite powder c.r.t. screens. (The measurements in References 2 and 9 are already given in terms of $\log_{10} 1/R$, and the coloration units in Reference 10 are directly convertible to this quantity.) Considering the great variations possible in the composition of a sodalite, the four sets of data are in surprisingly close agreement with each other.

There is no evidence in the data to suggest that the F centre concentration reaches a saturation value after prolonged irradiation, and as the coloration could be completely bleached optically, the curves of Fig. 6.7 are clearly representative of the early, photochromic stage of coloration. It is reported, however, that the stage II region in chlorosodalite is reached relatively easily, and that then the reversible part of the coloration saturates at high electron dose. [2,9] To avoid permanently damaging a new tube, it was intended that saturation effects would be investigated using an old c.r.t. that had one or two minor burns on the screen. (Sodalite powder screens, in common with their

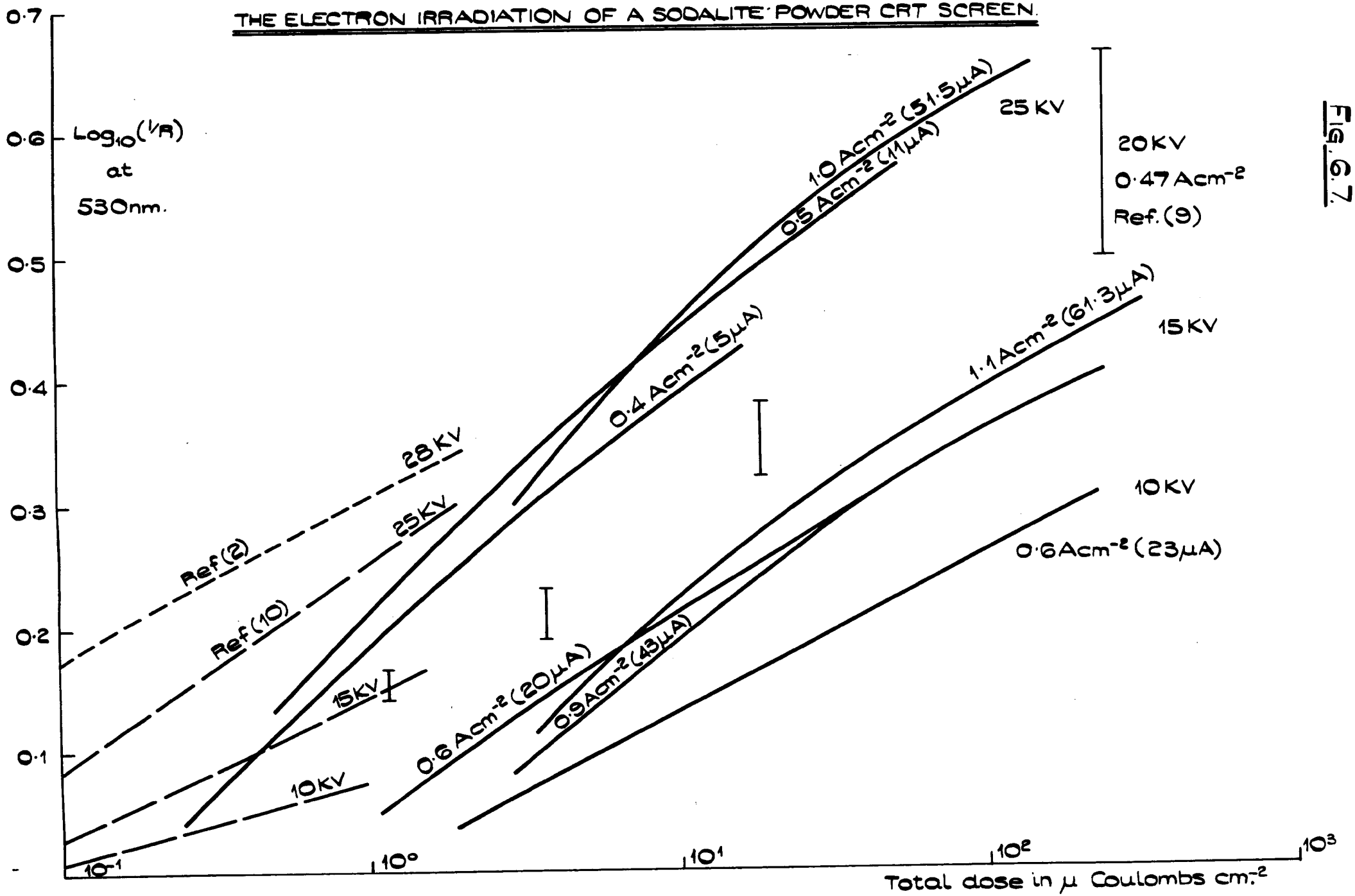
THE ELECTRON IRRADIATION OF A SODALITE POWDER CRT SCREEN.
0·7
0·6
0·5
0·4
0·3
0·2
0·1
-
Log10(1/R) at 530nm.
25 KV
1·0 Acm-2 (51·5μA)
0·5 Acm-2 (11μA)
20KV
0·47 Acm-2
Ref. (9)
15 KV
1·1 Acm-2 (61·3μA)
0·4 Acm-2 (5μA)
10 KV
0·6 Acm-2 (23μA)
28 KV
Ref (2)
25KV
Ref (10)
15KV
10KV
0·6 Acm-2 (20μA)
0·9 Acm-2 (43μA)
10-1
10°
10¹
10²
10³
Total dose in μ Coulombs cm-2

Fig. 6.7.

conventional phosphor counterparts, burn quite rapidly if the beam current is increased too far in the absence of beam deflection,) It was unfortunate that the electron gun of this tube failed before anything more than preliminary setting up experiments could be performed, so these investigations had to be abandoned. One or two curves (Fig. 6.8) were obtained which certainly flatten off at high dose, but these results by no means confirm saturation. The coloration was still completely reversible.

It was proposed that the optical bleaching characteristics of the sodalite c.r.t. screen would be investigated quantitatively over as wide as possible range of lighting conditions. With this in mind three separate types of experiment evolved, which were as follows:

(i) Bleaching under low intensity illumination, such as ordinary room lighting.

(ii) High intensity bleaching by, for example, a quartz halogen lamp.

(iii) Flash bleaching, by a short duration high intensity pulse of light from a photoflash tube.

(i) Low Intensity Bleaching

The apparatus illustrated in Fig. 6.4 was used for these measurements, with the microscope illuminator acting as the light source both for the reflectivity measurement and bleaching. The light incident on the c.r.t. screen was limited by an Ilford 624 (green) filter to a fairly narrow band of wavelengths falling within the sodalite F band, and two Balzers heat reflecting filters removed the major part of the i.r. beyond 750 nm. that would have been transmitted by the colour filter. Power onto the screen, which was about 1.6×10^{-5} W.cm^{-2}, was measured by a Scientifica and Cook Electronics laser power monitor; this conveniently gave the power in mW. cm.$^{-2}$ at 530 nm. after applying the appropriate correction factors. In a similar manner to that described for the electron dose-coloration measurements, continuous records of the decrease in coloration (i.e. $\log_{10} 1/R$) with time of illumination

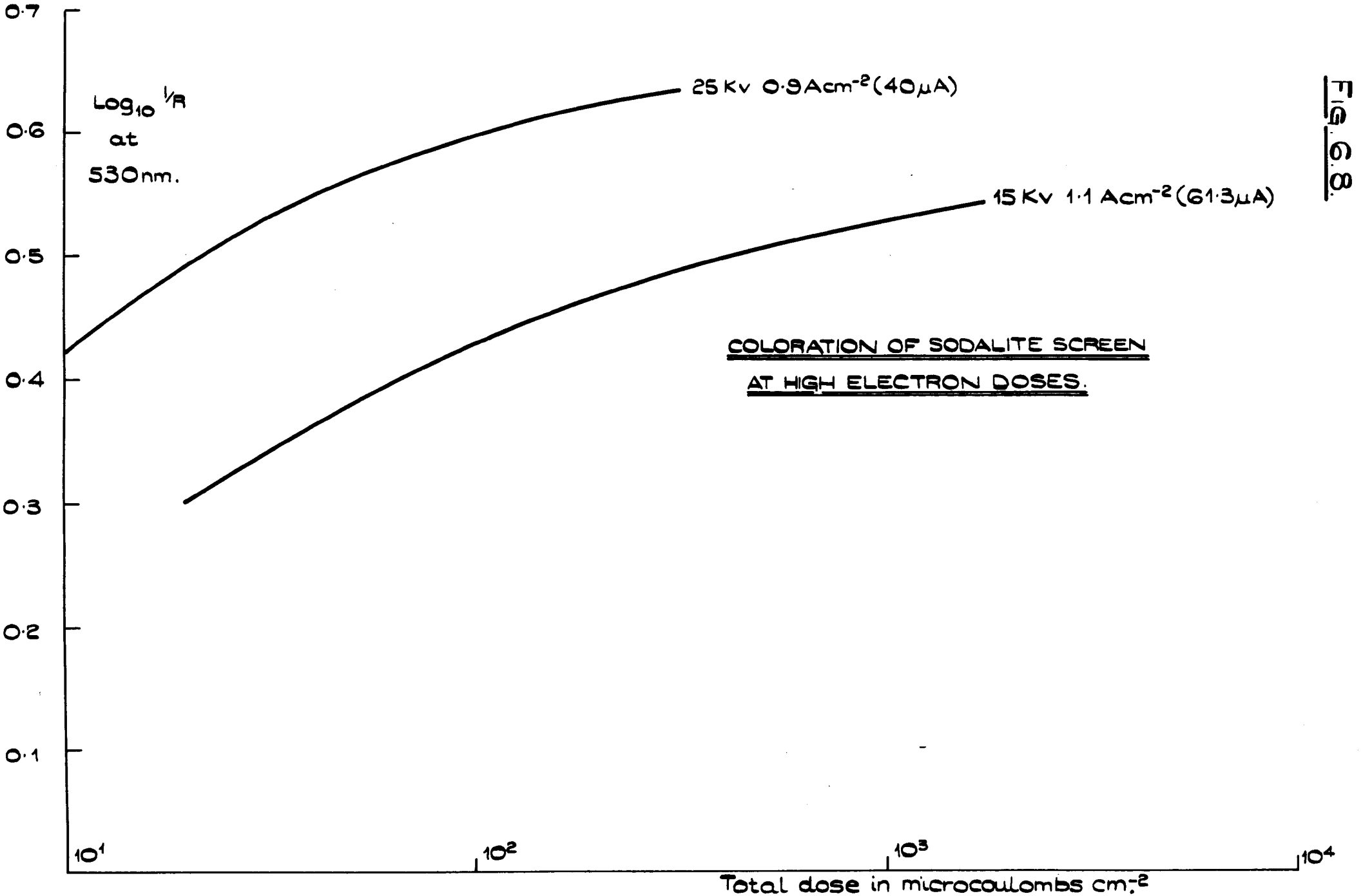
0·7
0·6
0·5
0·4
0·3
0·2
0·1
Log10 1/R at 530nm.
25 Kv 0·9 Acm-2 (40 μA)
15 Kv 1·1 Acm-2 (61·3 μA)
COLORATION OF SODALITE SCREEN
AT HIGH ELECTRON DOSES.
10¹
10²
10³
10⁴
Total dose in microcoulombs cm-2

were obtained. Graphs of F band coloration vs. illumination time of a sodalite powder coloured by irradiation with 10, 15 and 25 KeV electrons are illustrated in Fig. 6.9. Estimates of the energy absorbed by the sodalite during bleaching were made using a method similar to that described in Chapter 3, for calculating laser energy absorbed by the F band in KBr. Graphs showing the decrease in coloration with energy absorbed in the F band, corresponding to the coloration vs. time curves of Fig. 6.9, are illustrated in Fig. 6.10.

(ii) High Intensity Bleaching

The c.r.t. screen was illuminated for bleaching and for reflectivity measurements by a single 24 volt 150 Watt quartz iodine projector lamp, situated at the focus of a 7" focal length, f 2.8 achromatic lens. This system replaced the microscope illuminator of Fig. 6.4, and gave a bright, evenly lit c.r.t. faceplate, The quartz iodine lamp was driven from a 20 volt D.C. regulated power supply, to ensure that its light output would be sufficiently stable for photometry. An Ilford 624 and two Balzers B1/K1 filters in the collimator limited the light falling on the screen to a narrow band of wavelengths within the sodalite F band, with a measured intensity of 2.1×10^{-4} W.cm^{-2}. Figs. 6.11 and 6.12 illustrate typical results of high intensity F light bleaching of chlorosodalite, showing the decrease of coloration with time and absorbed energy respectively.

In all of the chlorosodalite bleaching measurements described in this chapter the F band coloration was completely erased between recording each set of data, by 5 minutes illumination with an unfiltered quartz-iodine lamp. However, no difference is found in either the coloration or the bleaching characteristics of the sodalite if it is subjected to a series of partial bleaching-recoloration cycles; Fig. 6.13 shows the bleaching of the chlorosodalite over four successive cycles.

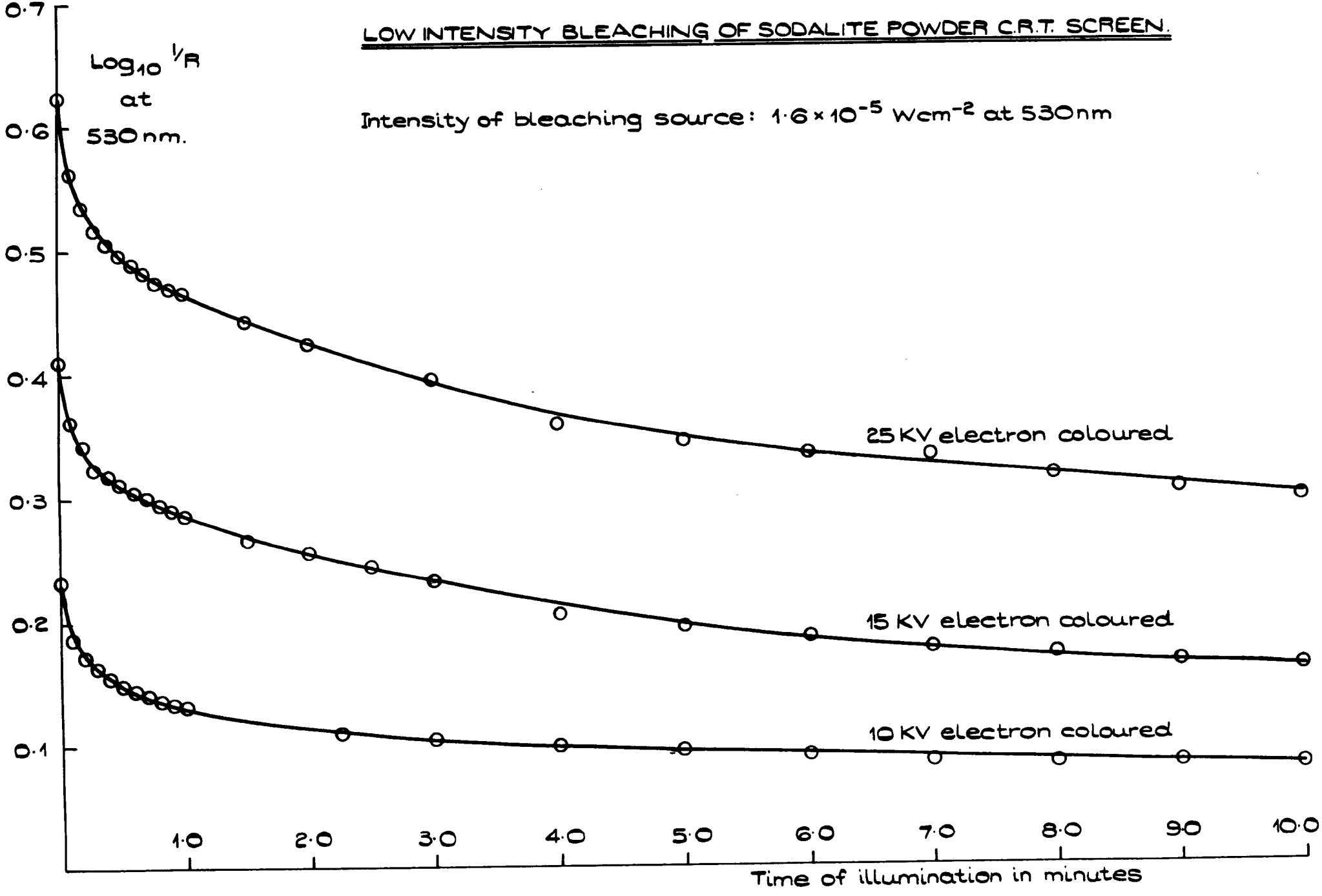
LOW INTENSITY BLEACHING OF SODALITE POWDER C.R.T. SCREEN.
Intensity of bleaching source: 1·6 × 10⁻⁵ Wcm⁻² at 530nm
Log10 1/R at 530nm.
0·7
0·6
0·5
0·4
0·3
0·2
0·1
25 KV electron coloured
15 KV electron coloured
10 KV electron coloured
1·0
2·0
3·0
4·0
5·0
6·0
7·0
8·0
9·0
10·0
Time of illumination in minutes

Fig. 6.6

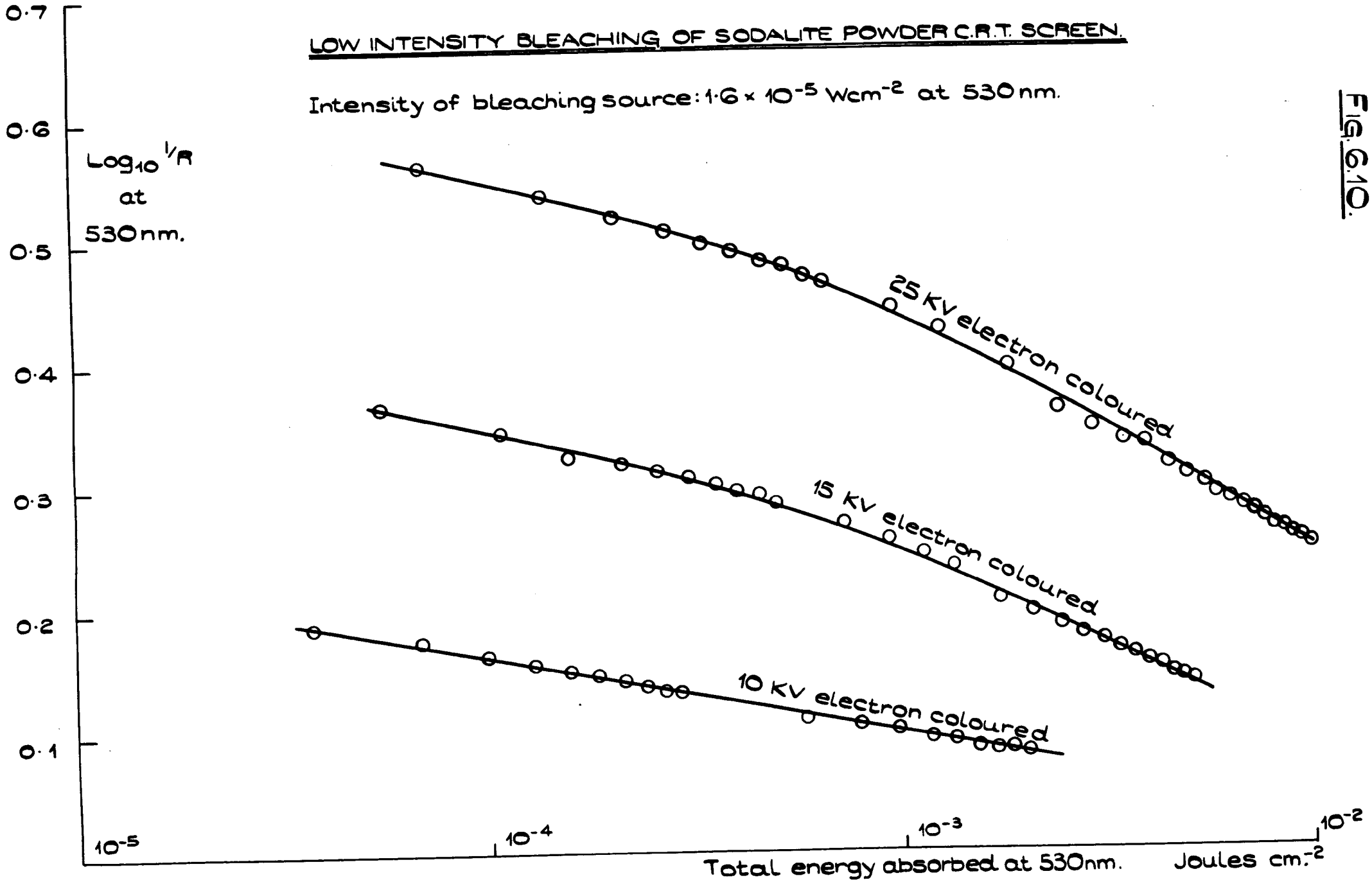
LOW INTENSITY BLEACHING OF SODALITE POWDER C.R.T. SCREEN.
Intensity of bleaching source: 1·6 × 10⁻⁵ Wcm⁻² at 530nm.
Log10 1/R at 530nm.
0·7
0·6
0·5
0·4
0·3
0·2
0·1
25 KV electron coloured
15 KV electron coloured
10 KV electron coloured
10⁻⁵
10⁻⁴
10⁻³
10⁻²
Total energy absorbed at 530nm. Joules cm⁻²

Fig. 6.10.

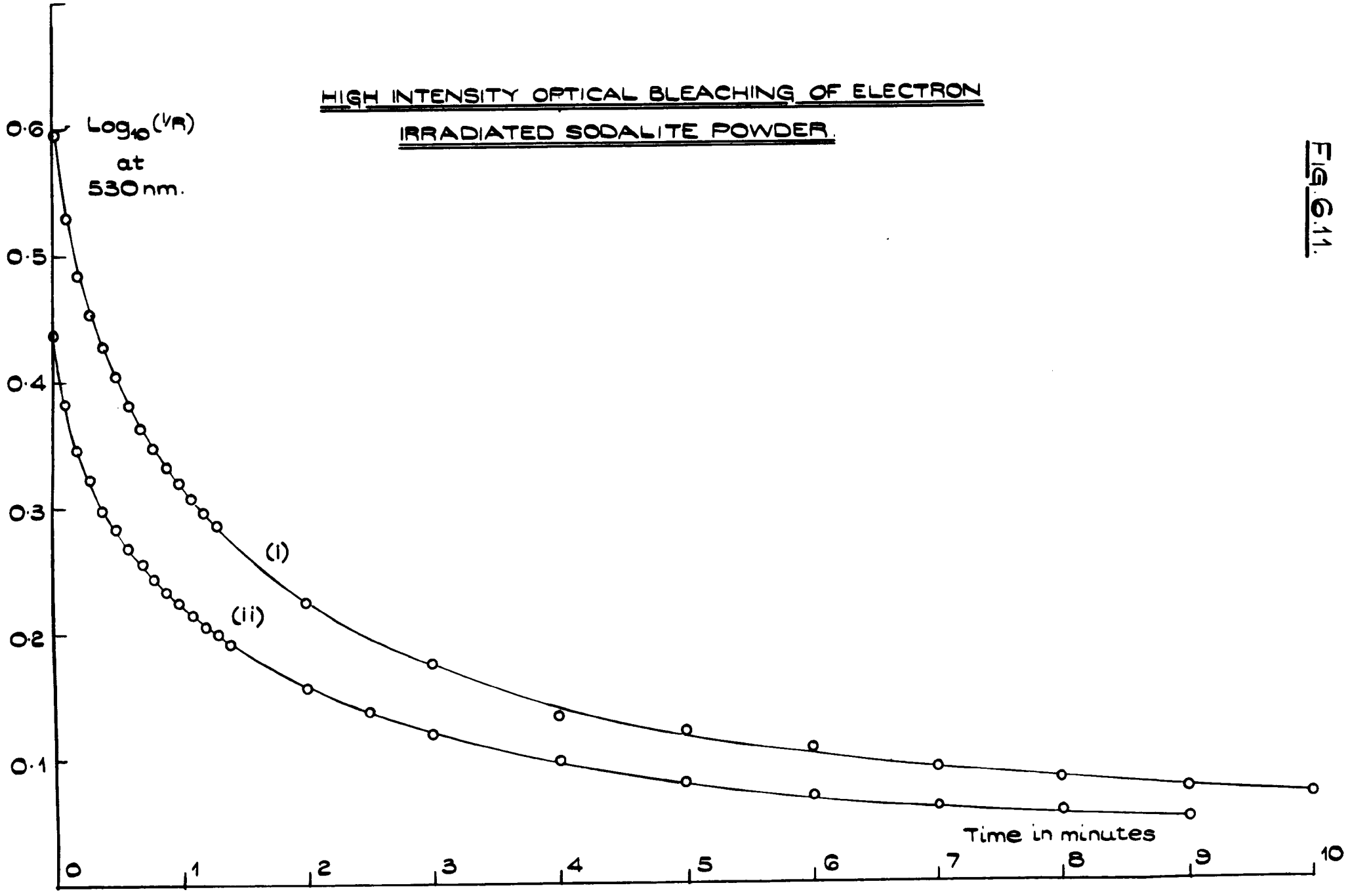
HIGH INTENSITY OPTICAL BLEACHING OF ELECTRON IRRADIATED SODALITE POWDER.
Log10 (I/R) at 530nm.
0·6
0·5
0·4
0·3
0·2
0·1
(i)
(ii)
Time in minutes
0
1
2
3
4
5
6
7
8
9
10

Fig. 6.11.

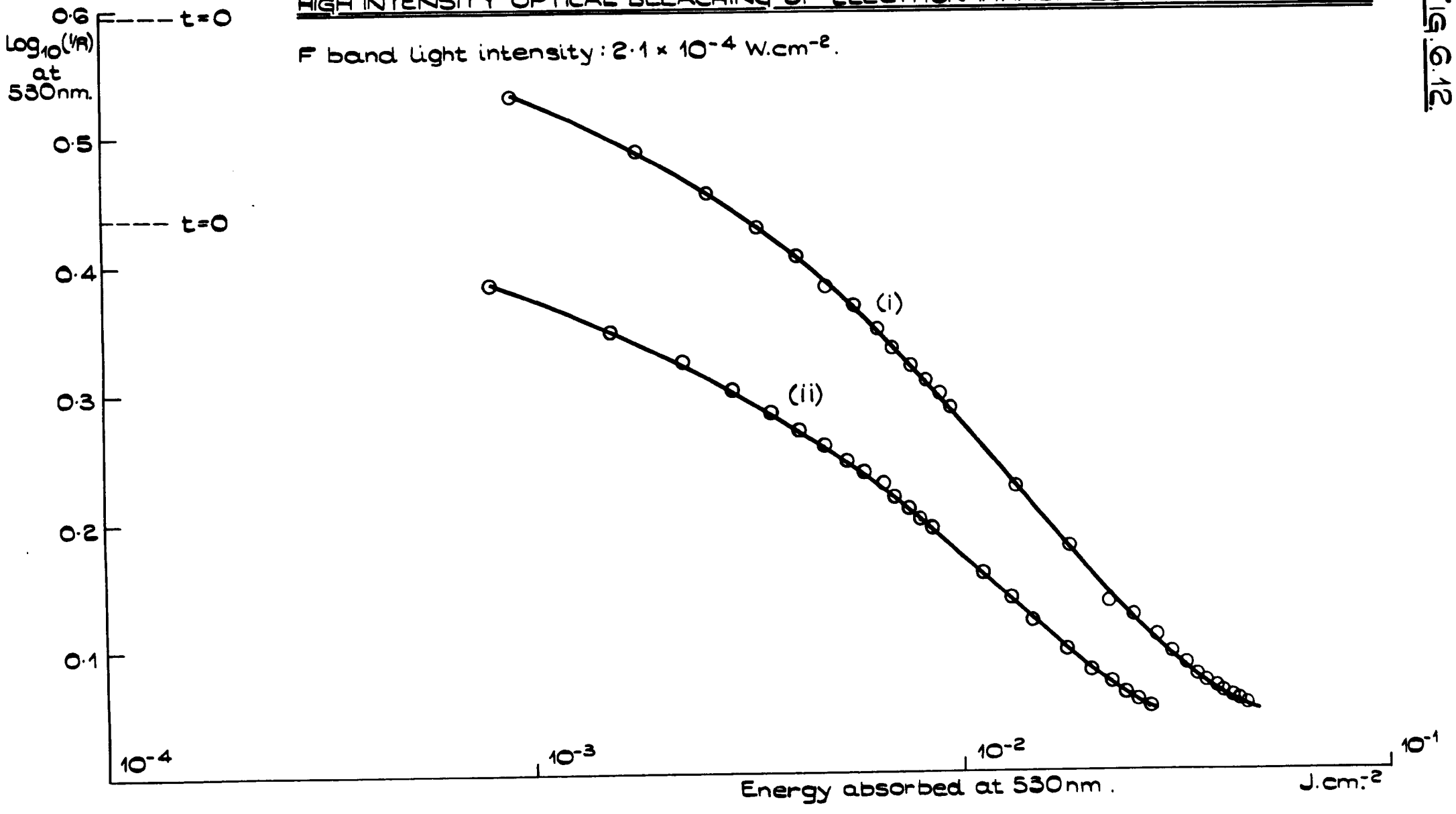
HIGH INTENSITY OPTICAL BLEACHING OF ELECTRON IRRADIATED SODALITE POWDER.
F band light intensity : 2·1 × 10⁻⁴ W.cm⁻².
0·6
t=0
Log10(1/R) at 530nm.
0·5
t=0
0·4
0·3
0·2
0·1
(i)
(ii)
10⁻⁴
10⁻³
10⁻²
10⁻¹
Energy absorbed at 530nm.
J.cm⁻²

FIG. 6.12.

Fig. 6.13.

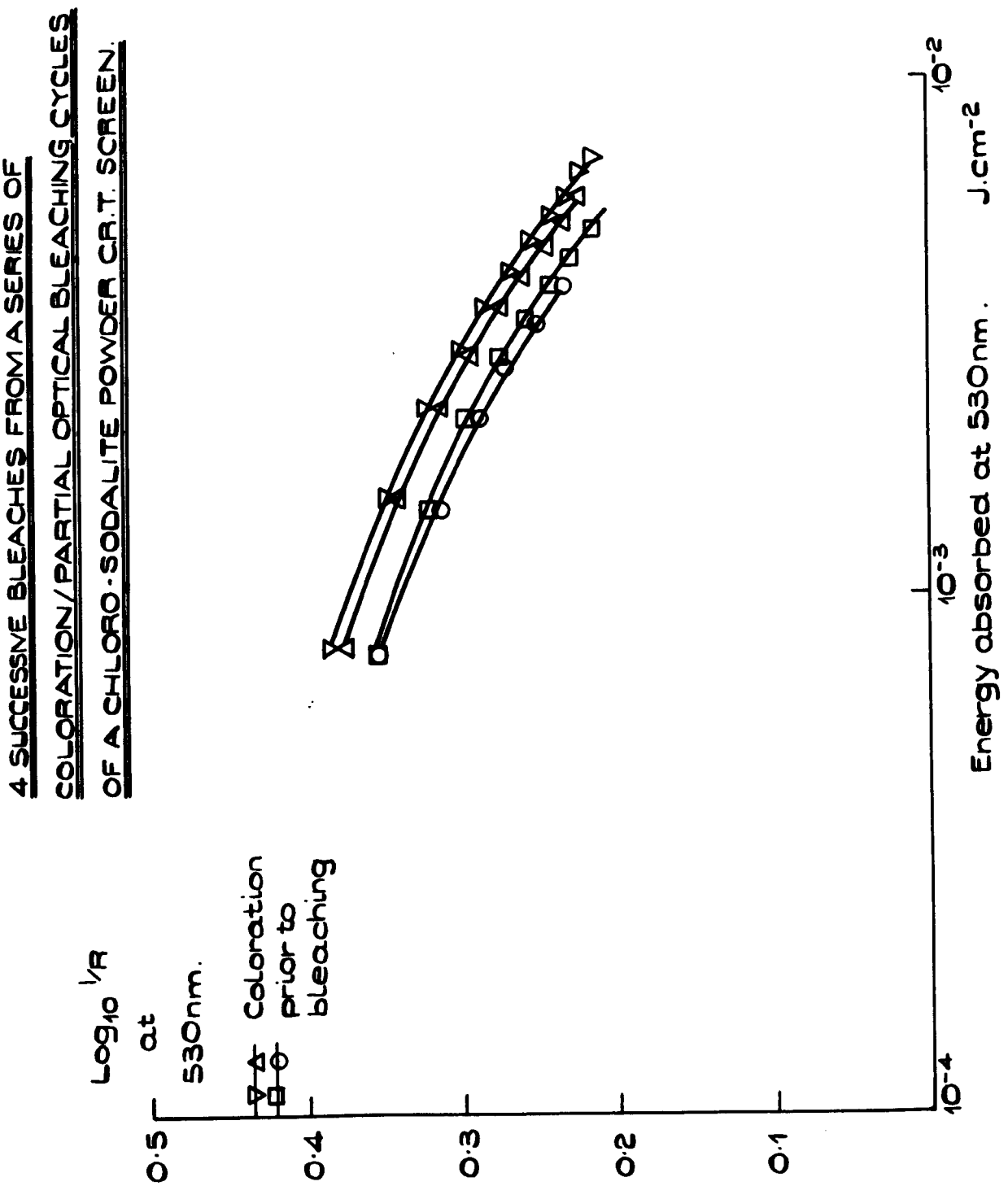
4 SUCCESSIVE BLEACHES FROM A SERIES OF
COLORATION/PARTIAL OPTICAL BLEACHING CYCLES
OF A CHLORO-SODALITE POWDER CR.T. SCREEN.
Log10 1/R at 530nm.
Coloration prior to bleaching
0·5
0·4
0·3
0·2
0·1
10-4
10-3
10-2
Energy absorbed at 530nm. J.cm-2

(iii) Photoflash Bleaching

These experiments demonstrated that it is possible to completely erase a chlorosodalite powder c.r.t. screen with a single high intensity short duration pulse of light, from a xenon photoflash tube. A photoflash tube placed close to the coloured c.r.t. screen was used for bleaching, and was subsequently removed to allow the reflectivity to be measured using the simple spectrophotometer illustrated in Fig. 6.4. Firstly a small Toshiba stroboscopic flash unit was used for bleaching; this has a reflector mounted Ferranti EN57 xenon filled tube with an input of 1.2 Joules. No significant bleaching occurred with one flash, even with the edge of the reflector touching the screen, so the unit was operated in its repetitive mode at 1 flash per second. Typical bleaching curves for this light source are illustrated in Fig. 6.14; they show quite clearly that a flash tube with an input of $\sim$ 1 Joule is not very useful for the erasure of sodalite dark trace c.r.t. screens, since in excess of 500 flashes are necessary for complete bleaching.

It was found that if the EN57 unit is replaced by a Ferranti CD50 xenon flash tube, one flash at a distance of 5 cm. from the screen will almost completely bleach an F band coloration ($\log_{10} {}^{1}/R$) of about 0.5. However, the CD50 is a large tube with an input of approximately 1000 Joules, requiring a 2000 volt high current power supply to charge a bank of paper dielectric capacitors. Its use clearly demands stringent safety precautions, to protect the operator from electric shock and the risk of the envelope exploding. This, coupled with the relatively short life of the device and its need for a bulky power supply, probably make it just as unsuitable for bleaching sodalite storage displays as the 1 Joule flash tube. It is possible, however, that a satisfactory compromise could be found between these two extremes of bleaching source.

It is difficult to make anything more than an order of magnitude estimate of the energy absorbed by the sodalite during flash bleaching, since the extremely short duration of the flash makes it hard to

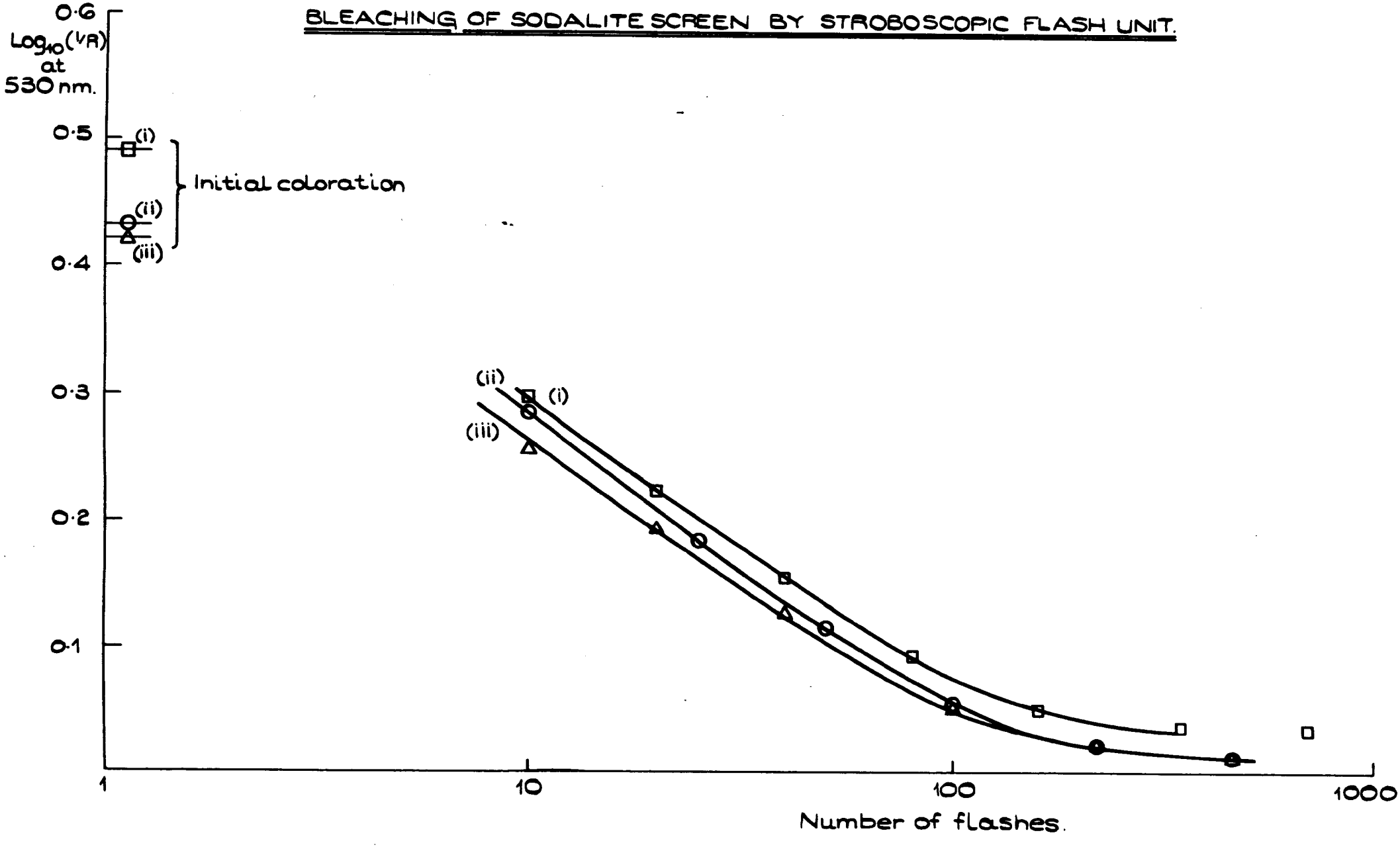
BLEACHING OF SODALITE SCREEN BY STROBOSCOPIC FLASH UNIT.
0·6
Log10(1/R) at 530 nm.
0·5
0·4
0·3
0·2
0·1
(i)
(ii)
(iii)
Initial coloration
1
10
100
1000
Number of flashes.

FIG. 6.14.

measure the spectral distribution with any degree of precision. However, the manufacturers of the EN57 photoflash state in their literature that it gives essentially a "flat" output in the visible spectrum, which simplifies the problem to one of setting an absolute value to the light intensity at a chosen wavelength or narrow band of wavelengths, and measuring its variation with time. This was done using an International Light Photometric Photocell, Type FT100, with a 624 green filter over the window. Its output was displayed on an oscilloscope, fitted with a camera. Using the oscilloscope trace, which showed the variation in intensity of the flash with time for a specific band of wavelengths, it was possible to estimate the energy absorbed in the sodalite F band. (An allowance was made for the absorption of the filter, and the F band envelope of the sodalite was similarly taken into account; as a further calibration check the FT100 was compared against the Scientifica Power Monitor, with an identical 624 filter in front of each cell, using a quartz-halogen lamp as the light source.) In the absence of any information on the Ferranti CD50 flash tube (which is now obsolete), the energy absorbed by the sodalite during bleaching was estimated in a similar way to that used for the EN57. The results of these absorbed energy estimates, for both flash tubes, are illustrated in Fig. 6.15. The energies involved are in agreement with what might be expected from the high intensity bleaching curves, Fig. 6.12.

The low and high intensity bleaching curves (Figs. 6.10 and 6.12 respectively) are not in very close agreement with each other, apparently more so at the lower end of the absorbed energy scale. Taking specific examples, $\log_{10} {}^{1}/R$ falls from a value of 0.625 to 0.437 with the absorption of 10^{-3} J. cm^{-2} under low intensity illumination, whereas high intensity bleaching results in a decrease from 0.595 to 0.525 for a similar energy absorption. The dissimilarity between the two sets of data is more clearly illustrated in Fig. 6.16, which shows plots of the energy derivative of the coloration vs. energy absorbed. Fig. 6.16

FIG. 6.15.

ESTIMATE OF THE ENERGY ABSORBED BY SODALITE POWDER DURING FLASH BLEACHING.

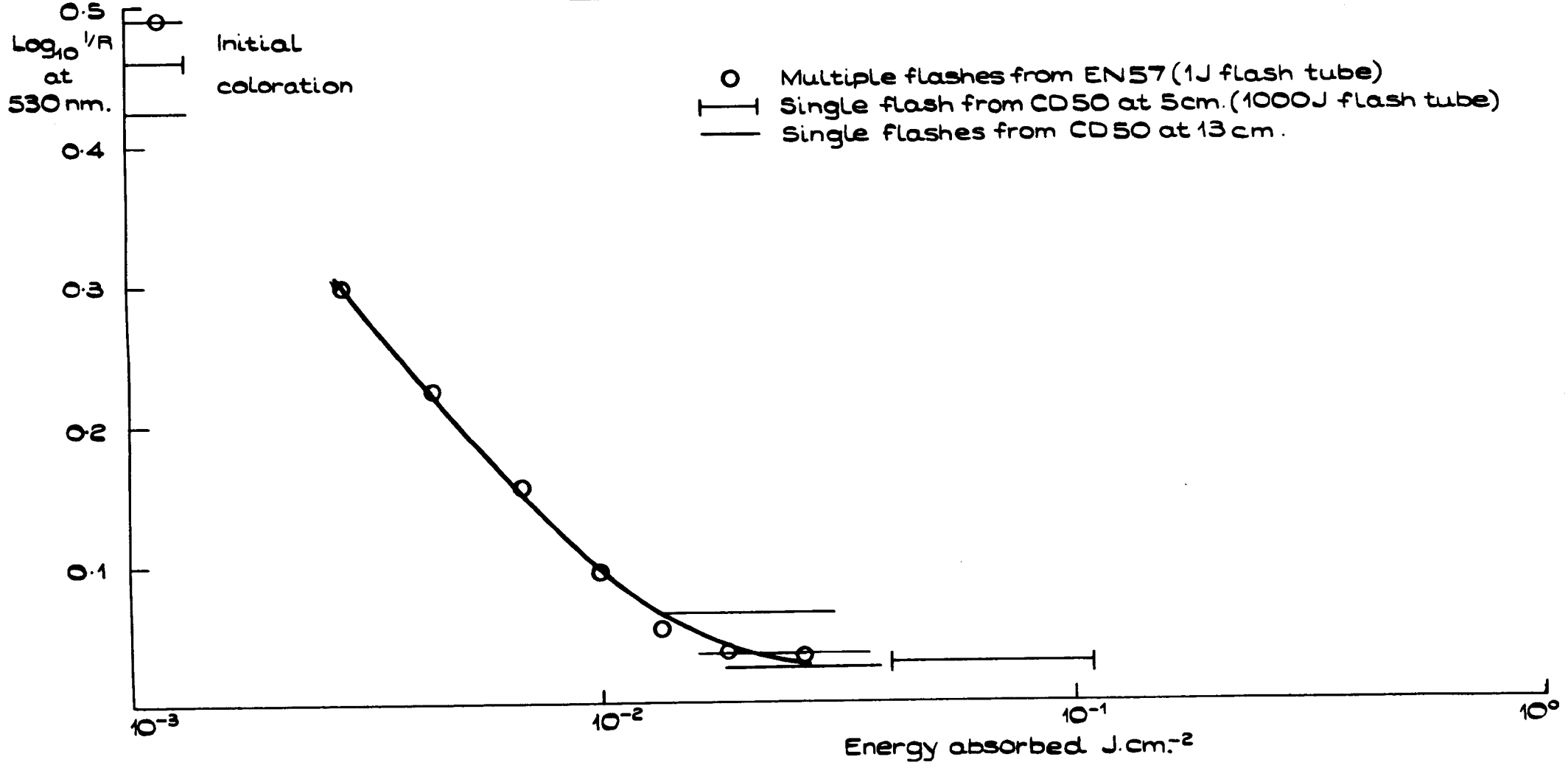

FIG. 6.16.

'RATE' OF BLEACHING OF COLOURED SODALITE.

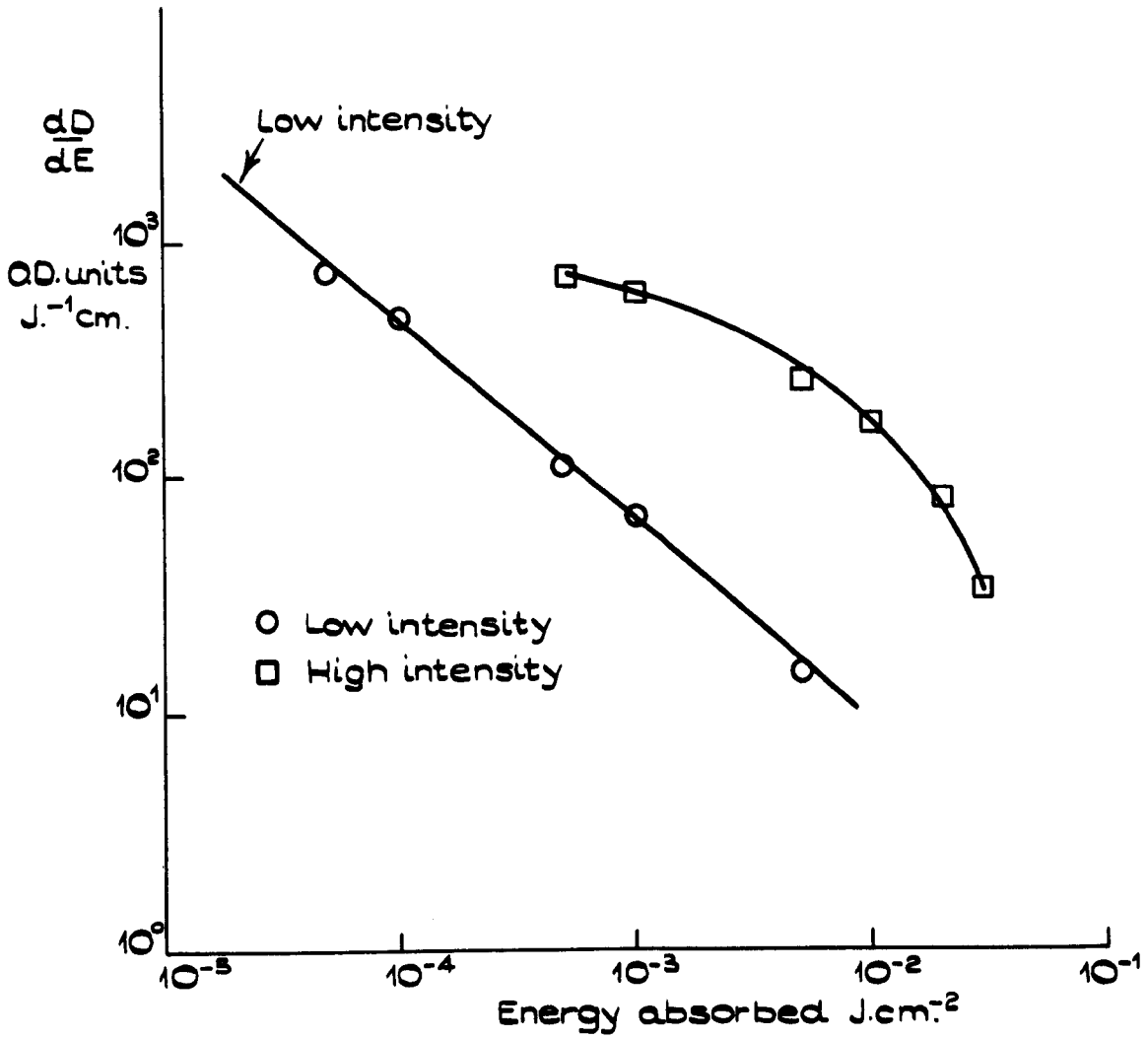

appears to suggest that different bleaching mechanisms are occurring in the two cases. However, returning to the examples quoted above, in the first case the time taken for the specimen to absorb 10^{-3} J. cm.$^{-2}$ is about 100 seconds, whereas in the high intensity case it is only 6 seconds. Therefore the most likely explanation for the apparent discrepancy is that room temperature thermal bleaching occurs in the sodalites to a much greater extent than it does in the alkali halides, and so makes a significant contribution to the bleaching observed over comparatively brief time intervals. Thermal bleaching has, in fact, been recently reported in bromo-and iodosodalite. (2)

In order to determine the extent to which thermally activated bleaching occurs in a chlorosodalite powder, the c.r.t. screen was irradiated to a fairly dense coloration and then kept in the dark for 42 minutes, except for intervals of 2 seconds duration when it was exposed to the spectrophotometer light for reflectivity measurement. At the end of 42 minutes, continuous illumination was started. Fig. 6.17 shows the log. reciprocal reflectance plotted against time; the point at which continuous optical bleaching starts is sharply defined by an increase in slope, although up to that point the bleaching has still been considerable. Clearly some of the bleaching in the first 42 minutes may be attributed to the 2 second exposures to light necessary for the reflectivity measurements. The energy absorbed from this source was calculated and plotted against the coloration in Fig. 6.18, which also shows the continuous bleaching session at the conclusion of the experiment. Again, the transition from intermittent to continuous illumination is clearly defined, this time by an apparent decrease in the rate of optical bleaching. The anomaly between Figs. 6.17 and 6.18 can best be resolved in terms of a substantial thermally activated contribution to the reduction in coloration observed during the first part of the experiment, which would make the slope of a coloration vs. absorbed optical energy plot appear high. When continuous illumination

Fig. 6.17.

SODALITE SCREEN BLEACHING, LOW INTENSITY ILLUMINATION.

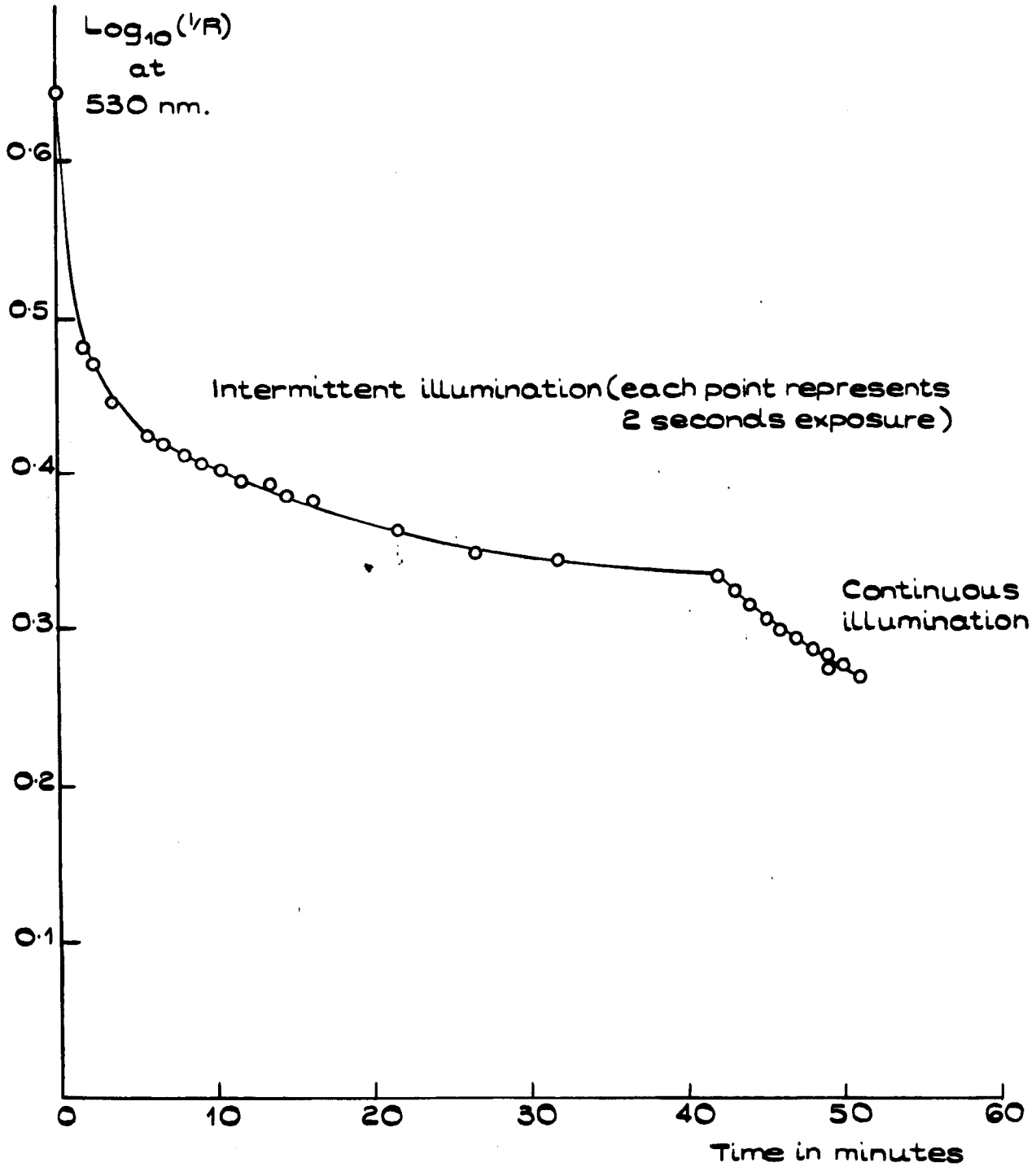

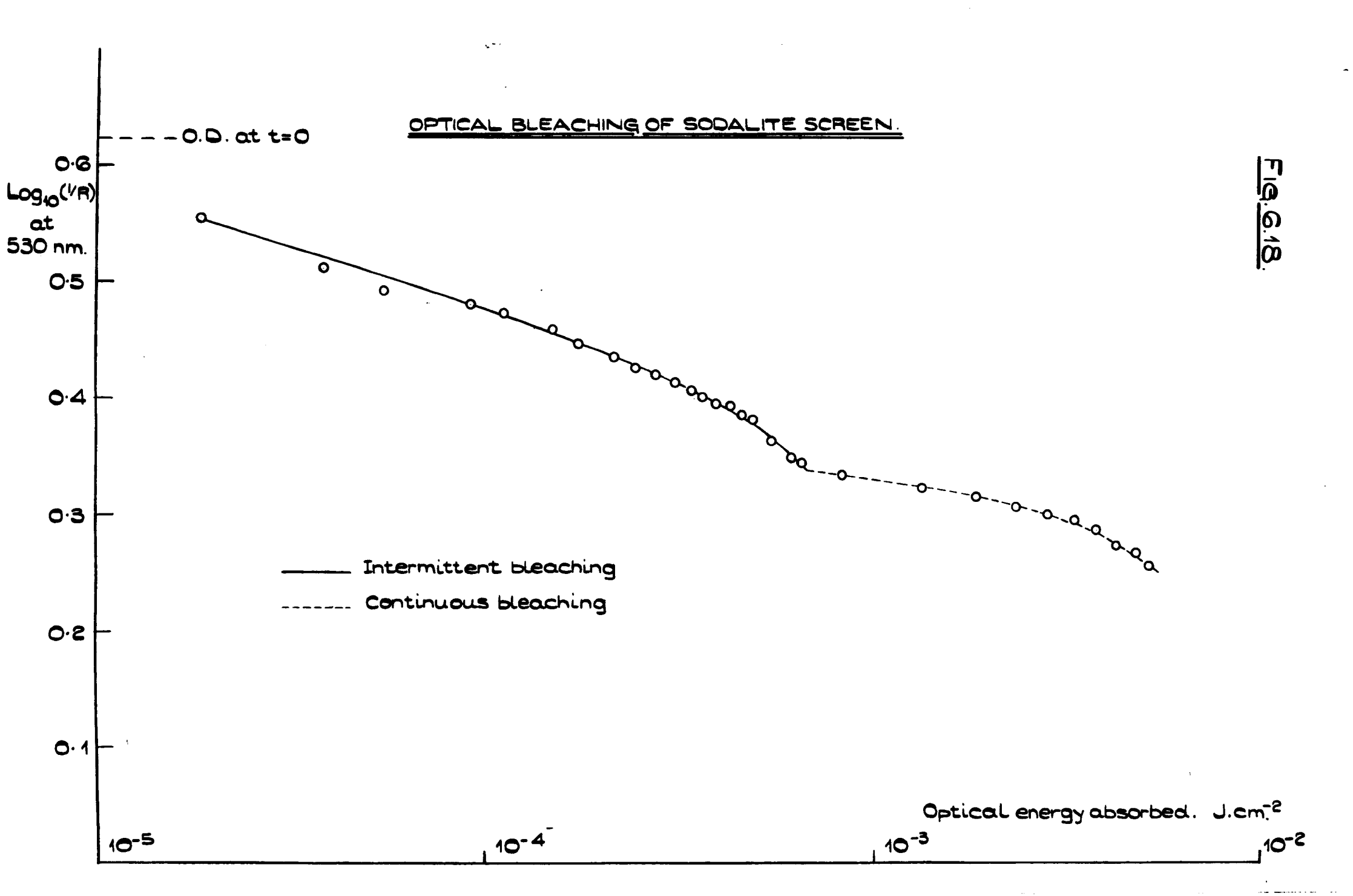
OPTICAL BLEACHING OF SODALITE SCREEN.
O.D. at t=0
0·6
Log10(1/R) at 530 nm.
0·5
0·4
0·3
0·2
0·1
Intermittent bleaching
Continuous bleaching
Optical energy absorbed. J.cm-2
10-5
10-4
10-3
10-2

Fig. 6.18.

is started bleaching becomes more characteristically optical in nature, with the thermal component becoming a less significant part of the total. Obviously the higher the intensity of the optical bleaching source the less significant will be the thermal contribution to the observed bleaching. An estimate of the optical contribution to the bleaching during the first 42 mins. of Fig. 6.17 can be made with reference to the high intensity bleaching data since in the latter case the thermal component at low absorbed energies can probably be neglected with reasonable accuracy. Adding back the optically removed coloration to Fig. 6.17 yields what ought to be a fairly accurate thermal bleaching curve for chlorosodalite (Fig. 6.19). Fig. 6.19 shows that thermal bleaching appears to follow a relationship of the form $(D_o - D)\alpha = \log_e t + \beta$, where D_o is the coloration ($\log_{10} {}^1/R$) at time t = 0, D its value at time t = t minutes, and α and β are constants, equal to 20.6 and 2.33 respectively for this data.

It is evident, from Fig. 6.19, that the thermally activated contribution to bleaching at room temperature is appreciable. Raising the temperature of the sodalite will obviously increase the thermally bleached coloration still further.(9) Replotting the low and high intensity bleaching data (Figs. 6.10 and 6.12) after making allowance for thermal bleaching, yields Fig. 6.20, in which the apparent discrepancy between the two sets of results has been removed.

Illumination with F band light and near infra red radiation does not, however, appear to have any noticeable affect on the bleaching rate. Repeating the high intensity bleaching experiment with the two Balzers n.i.r. reflecting filters removed from the optical system gave results (Fig. 6.21) that are indistinguishable from those obtained with them present, despite the fact that the total infra-red radiation reaching the screen is now considerably greater than the F band light.

In many envisaged applications for dark trace photochromic cathode ray tubes the screen will be flooded with white light, rather

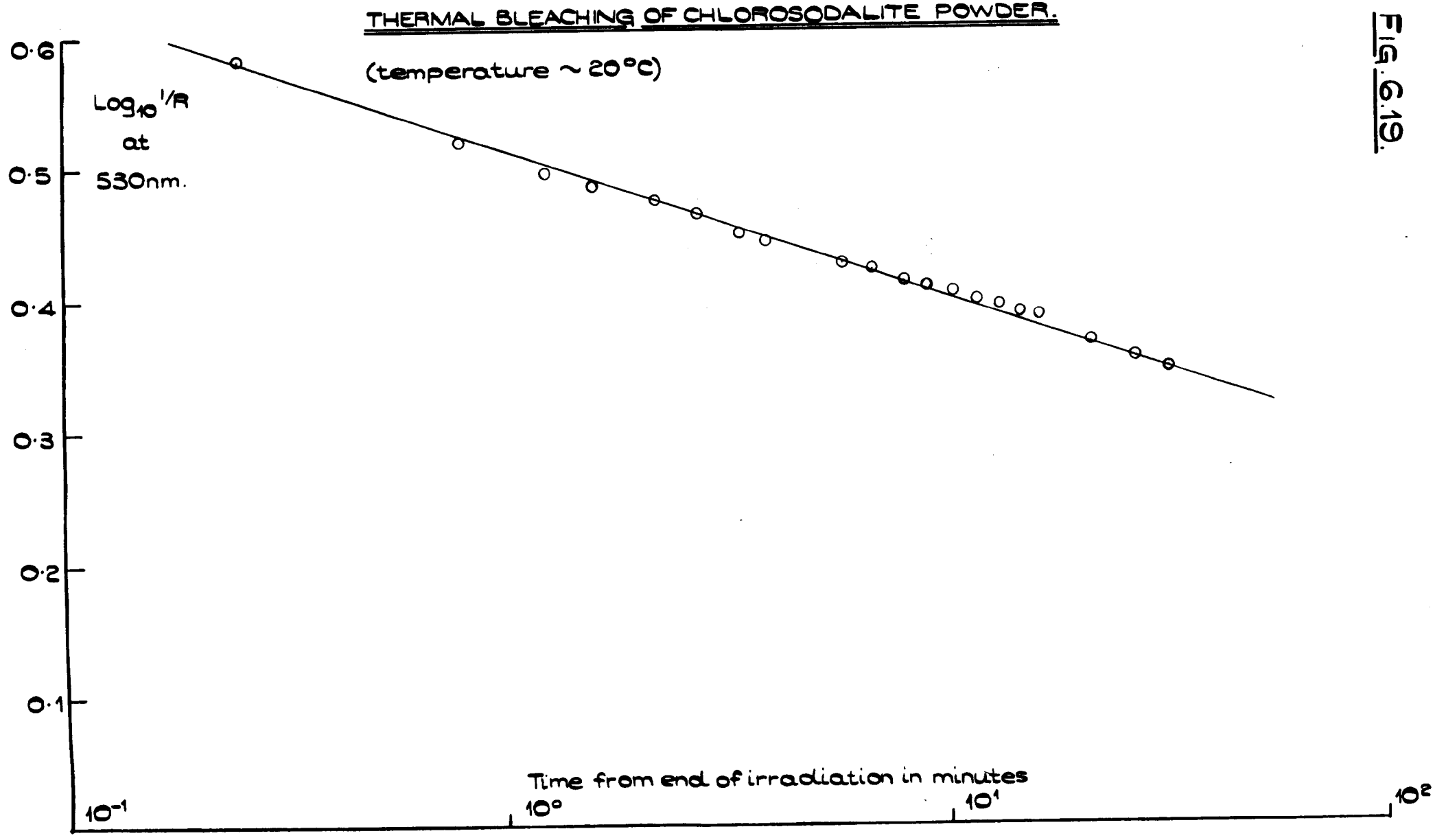
THERMAL BLEACHING OF CHLOROSODALITE POWDER.
(temperature ~ 20°C)
$Log_{10}{}^{1}/_{R}$ at 530nm.
0·6
0·5
0·4
0·3
0·2
0·1
Time from end of irradiation in minutes
10^{-1}
10^{0}
10^{1}
10^{2}

Fig. 6.19.

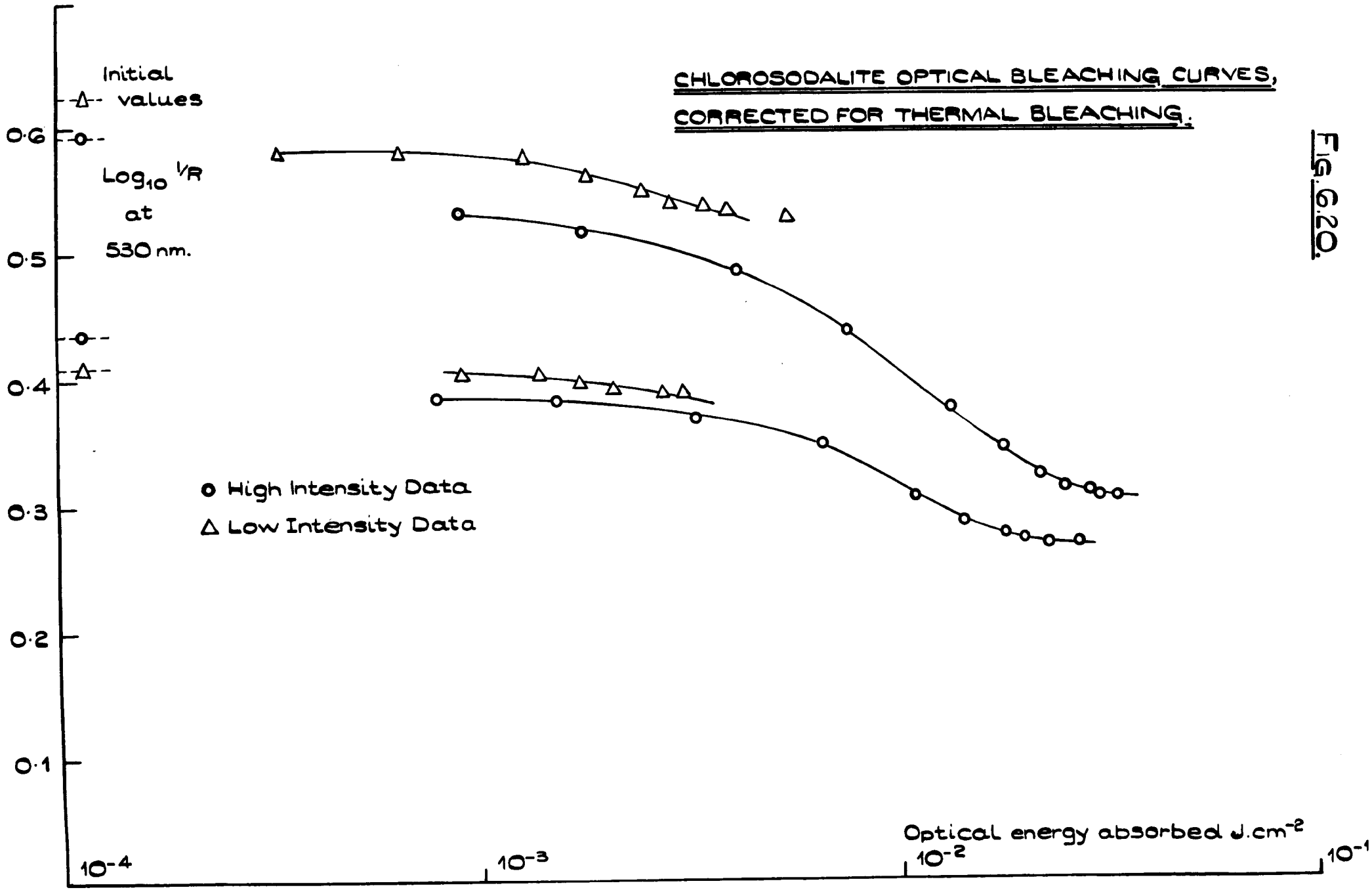
CHLOROSODALITE OPTICAL BLEACHING CURVES,
CORRECTED FOR THERMAL BLEACHING.
Fig. 6.20.
Initial values
0·6
Log10 1/R at 530 nm.
0·5
0·4
0·3
0·2
0·1
o High Intensity Data
Δ Low Intensity Data
Optical energy absorbed J.cm-2
10-4
10-3
10-2
10-1

SODALITE SCREEN HIGH INTENSITY BLEACHING

BY Q.I. LAMP, 624 FILTER IN BEAM.

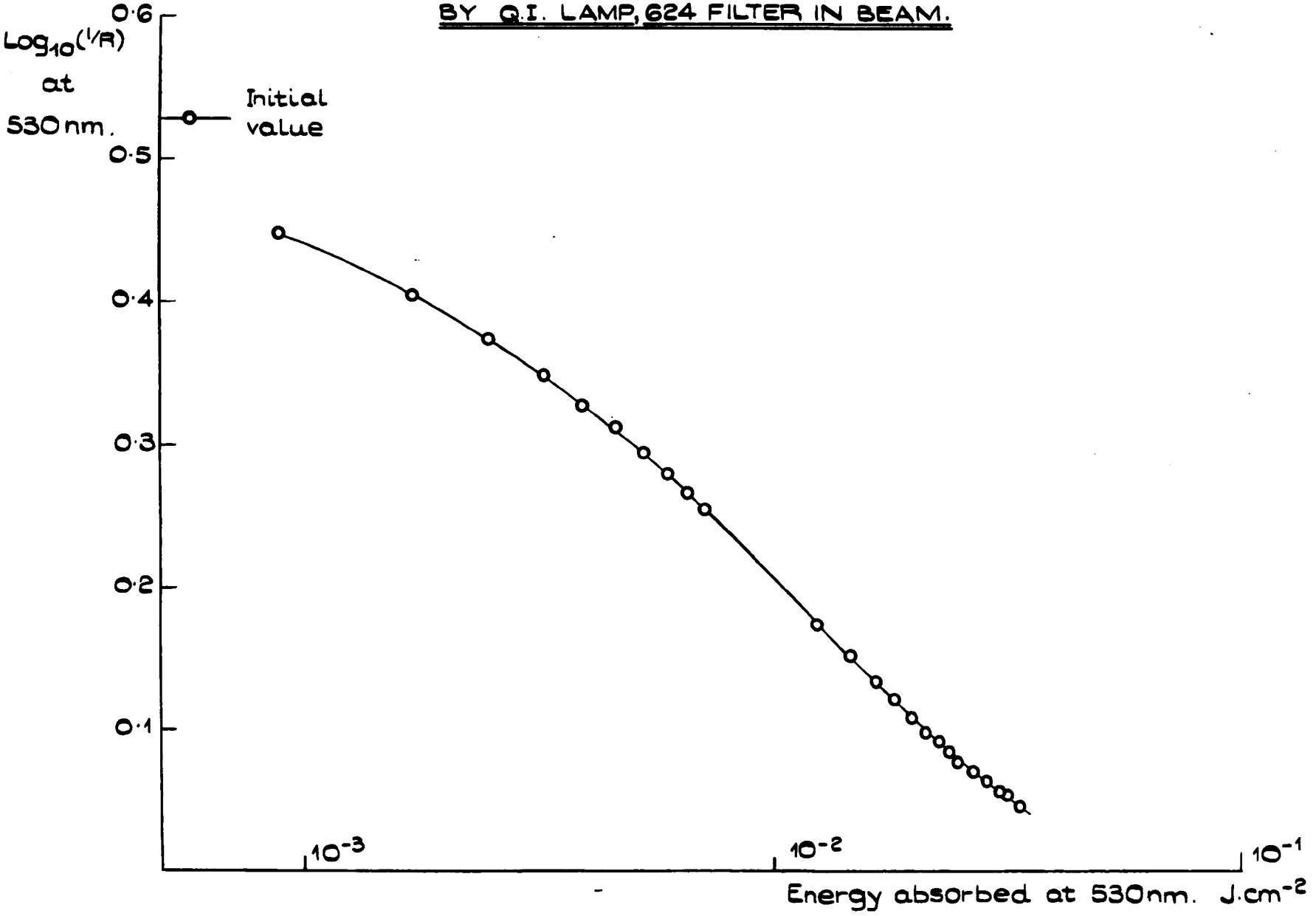

FIG. 6.21.

than with the wide band monochromatic light used in these measurements. Therefore, in conclusion, a number of bleaching curves were obtained with the filters removed from the Q.I. illuminator system. Two typical results are illustrated, as coloration vs. time curves, in Fig. 6.22. The intensity of the illumination during these experiments was measured at approximately 6 $mW.cm^{-2}$ in the visible spectrum, out to 700 nm. If the approximation is made that the output of the lamp varies linearly with wavelength over the range 400 to 600 nm, and knowing the shape of the sodalite F band in this region, it is possible to estimate the energy absorbed by the screen during white light bleaching, using a crude numerical integration technique. Fig. 6.22 replotted, using this method, as graphs of coloration vs. absorbed energy is illustrated in Fig. 6.23; the data shows good agreement with the previous results for high intensity monochromatic bleaching. However, if the data is corrected for thermal bleaching (broken lines) it differs from the similarly obtained data of Fig. 6.20. This rather suggests that there is a non linear intensity dependence at higher illumination intensities, which is masked by the thermal bleaching effect. Alternatively it may be due to the innaccuracies in estimating the energy absorbed by the sodalite F band during white light bleaching. It is evident that further, more controlled experiments would be necessary to investigate whether there really [15] was a non linear intensity dependence of bleaching.

During the course of these final experiments on the bleaching of chlorosodalite powder it was observed that a brightly lit screen attains a lower coloration than one operated in the dark at the same electron beam current and energy. Bleaching obviously occurs simultaneously with F centre production, and the two processes reach an equilibrium whereby the coloration is lower than it would be if the tube were in low ambient lighting. The extent of this effect can be seen in Fig. 6.24, which was obtained by interrupting the screen illumination for a short interval whilst the tube was operating at constant voltage and current;

FIG. 6.22.

SODALITE C.R.T. SCREEN
WHITE LIGHT BLEACHING.

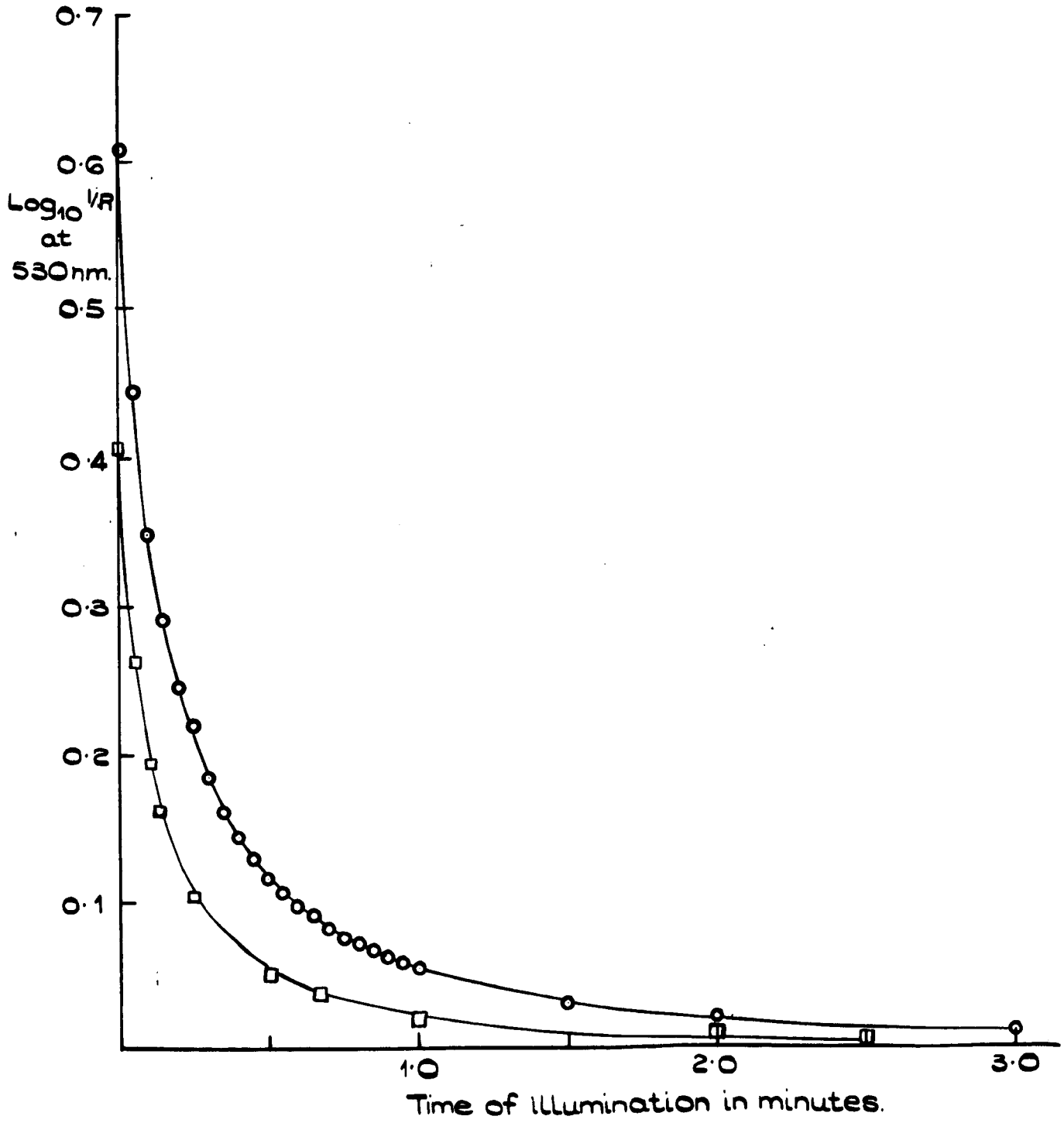

FIG. 6.23.

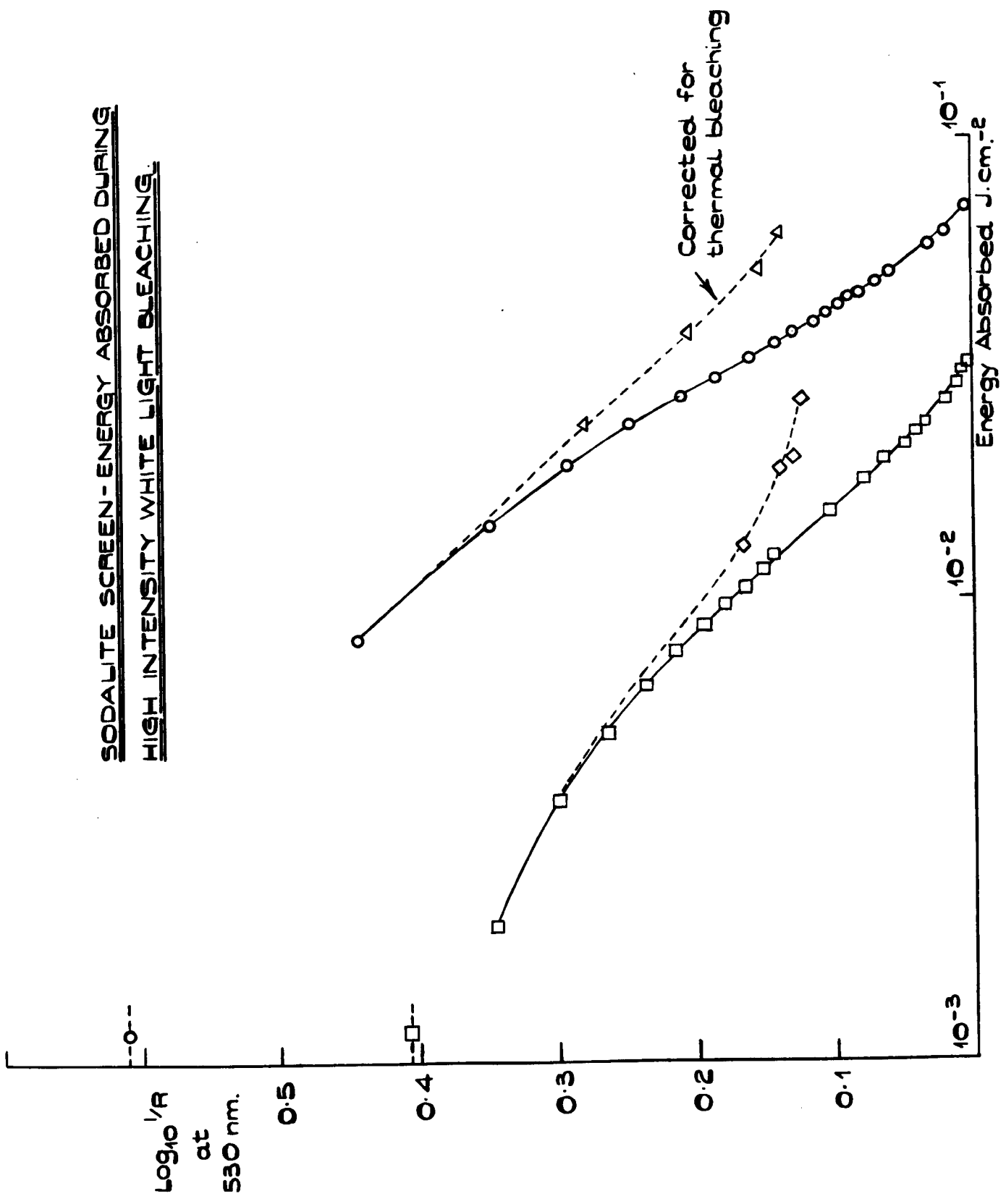
SODALITE SCREEN - ENERGY ABSORBED DURING
HIGH INTENSITY WHITE LIGHT BLEACHING.
Corrected for thermal bleaching
$\log_{10} 1/R$ at 530 nm.
0
0·5
0·4
0·3
0·2
0·1
10^{-3}
10^{-2}
10^{-1}
Energy Absorbed J.cm.$^{-2}$

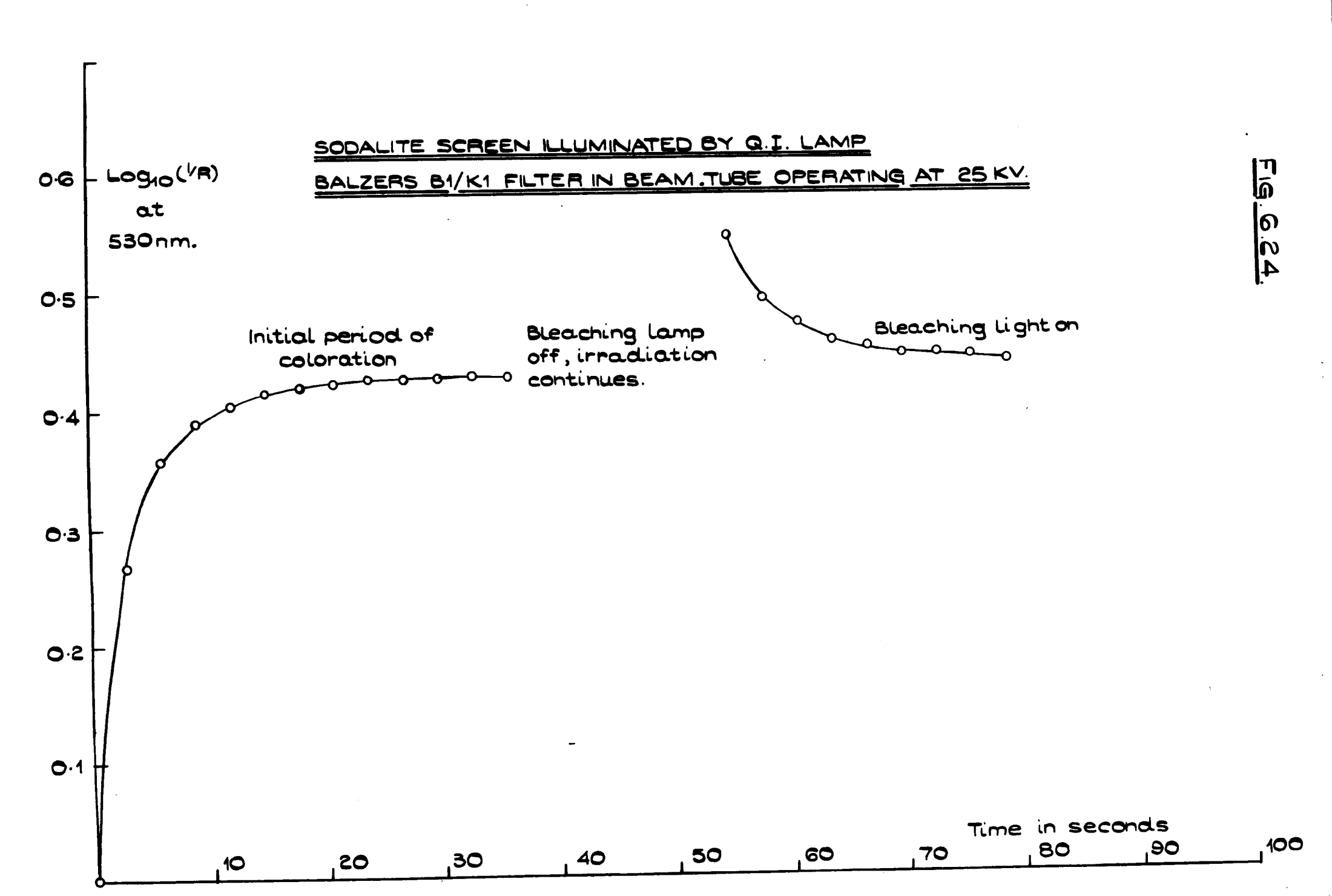
SODALITE SCREEN ILLUMINATED BY Q.I. LAMP
BALZERS B1/K1 FILTER IN BEAM. TUBE OPERATING AT 25 KV.
Log10(1/R) at 530nm.
0·6
0·5
0·4
0·3
0·2
0·1
Initial period of coloration
Bleaching lamp off, irradiation continues.
Bleaching light on
10
20
30
40
50
60
70
80
90
100
Time in seconds

Fig. 6.24.

it is evident that the coloration increases during the dark period and decreases again when illumination is resumed. The practical consequence of this phenomenon is that in an application where a sodalite screen c.r.t. is used under high ambient lighting conditions the contrast of the display is effectively lowered, by a not inconsiderable amount.

6.5 Fatigue and Luminescence of a Chlorosodalite Powder

The sodalites appear to be ideally suited for use in optical display devices (e.g. dark trace c.r.t.s) for they colour easily (after activation) when electron irradiated, are much more sensitive to optical bleaching than the alkali halides and, unlike the latter materials, do not appear to form complex vacancy aggregate centres under illumination. In practice, however, the sodalites fatigue after comparatively few coloration-bleach cycles; they become more difficult to colour and erase, and retain a slight yellowish stain which cannot be bleached optically, however intense the illumination. The c.r.t. used in the measurements described in section 6.4 had begun to show a certain amount of fatigue by the end of the experiments, particularly in respect of a persistent stain and a lowering of coloration sensitivity. The latter effect can quite clearly be seen in Fig. 6.25. This photograph was obtained by completely bleaching the screen (except for the slight discoloration) and then recolouring it with the raster scan amplitude increased so that a larger area of sodalite was coloured than had been previously. The freshly coloured area of the screen shows up darker than the central area, which had undergone a fairly large number of bleaching/coloration cycles. The effect on bleaching performance was not so marked, there was no significant difference between bleaching data obtained when the sodalite had been cycled relatively few times and after it had been erased a large number of times.

It is observed that there is a significant change in the luminescence spectrum of the sodalite (under electron irradiation) associated with the fatigue effect. As the number of coloration-bleaching cycles

FIG. 6.25.

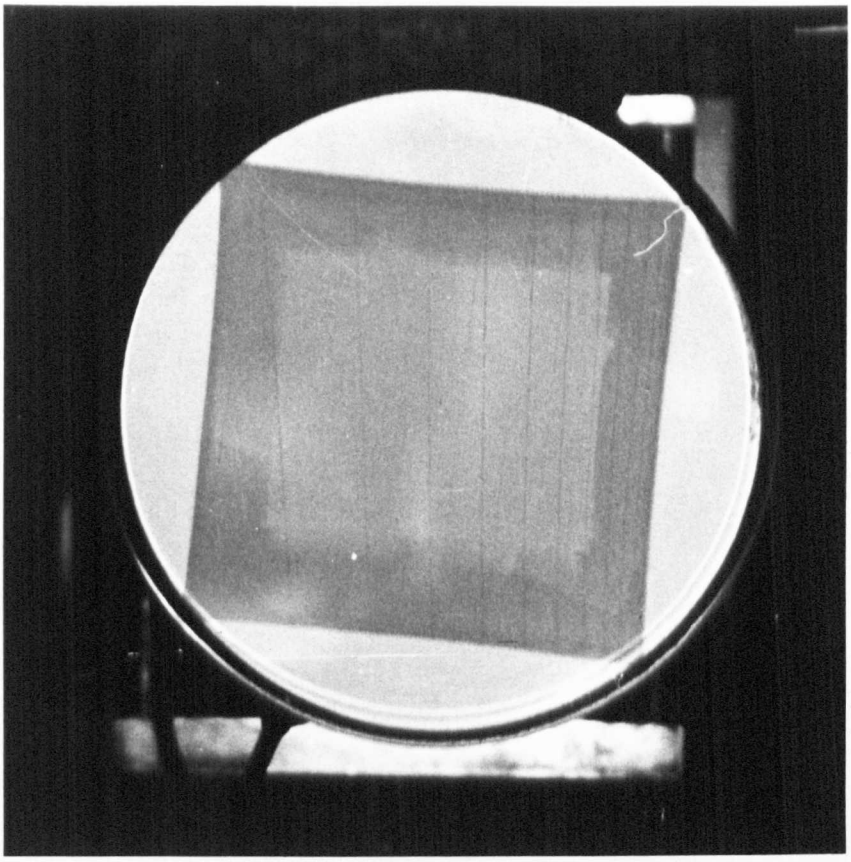

PHOTOGRAPH OF THE FATIGUED AREA

OF THE CHLOROSODALITE C.R.T. SCREEN.

to which the material has been subjected increases, the luminescence of the screen during irradiation appears, to the eye, to change gradually from blue to an orange-pink colour. Fig. 6.26 (a) and (b) show this change in luminescence spectrum quite clearly. From the point of view of understanding the fatigue mechanism it would be desirable to investigate this change in luminescence spectrum at low temperature. This is clearly impracticable with the present apparatus, complete redesign of the c.r.t. would be necessary before the sodalite could be cooled to LNT. However, the strong luminescence between 600 and 700 nm. observed in the fatigued material appears to be similar to that observed by Kirk [7] and others in samples of hackmanite and sodalite under u-v excitation. If the specimen is cooled to $\sim 100^{\circ}K$, this luminescence spectrum shows a banded structure superimposed on a structureless band. [9] The banded structure is characteristic of a vibrating diatomic molecule, and has been associated with the presence of S_2^-. The structureless emission is thought to be due to another radical, possibly S^{2-}. It has also been suggested that the fatigue is connected with the formation of di-and tri-atomic molecules. [9]

It is probable that the decrease in coloration sensitivity arises because the nature of the electron donor centres (sulphur ions, O^{2-}, etc.) changes during repeated coloration bleach cycles, so that the number of centres which are able to donate electrons to halogen vacancies decreases, Another possibility is that the impurity centres in the fatigued material are efficient electron traps, and inhibit the formation of F centres by preventing electrons from reaching halogen vacancies. It may also be that repeated electron irradiation results in the loss of an active constituent from the sodalite powder. Whatever the fatigue mechanism is, it is clear that it is the main problem to be overcome before the sodalites can usefully be employed in optical display systems. The sodalites do not, however, appear to be very suitable for data storage applications, owing to the problem of obtaining non destructive

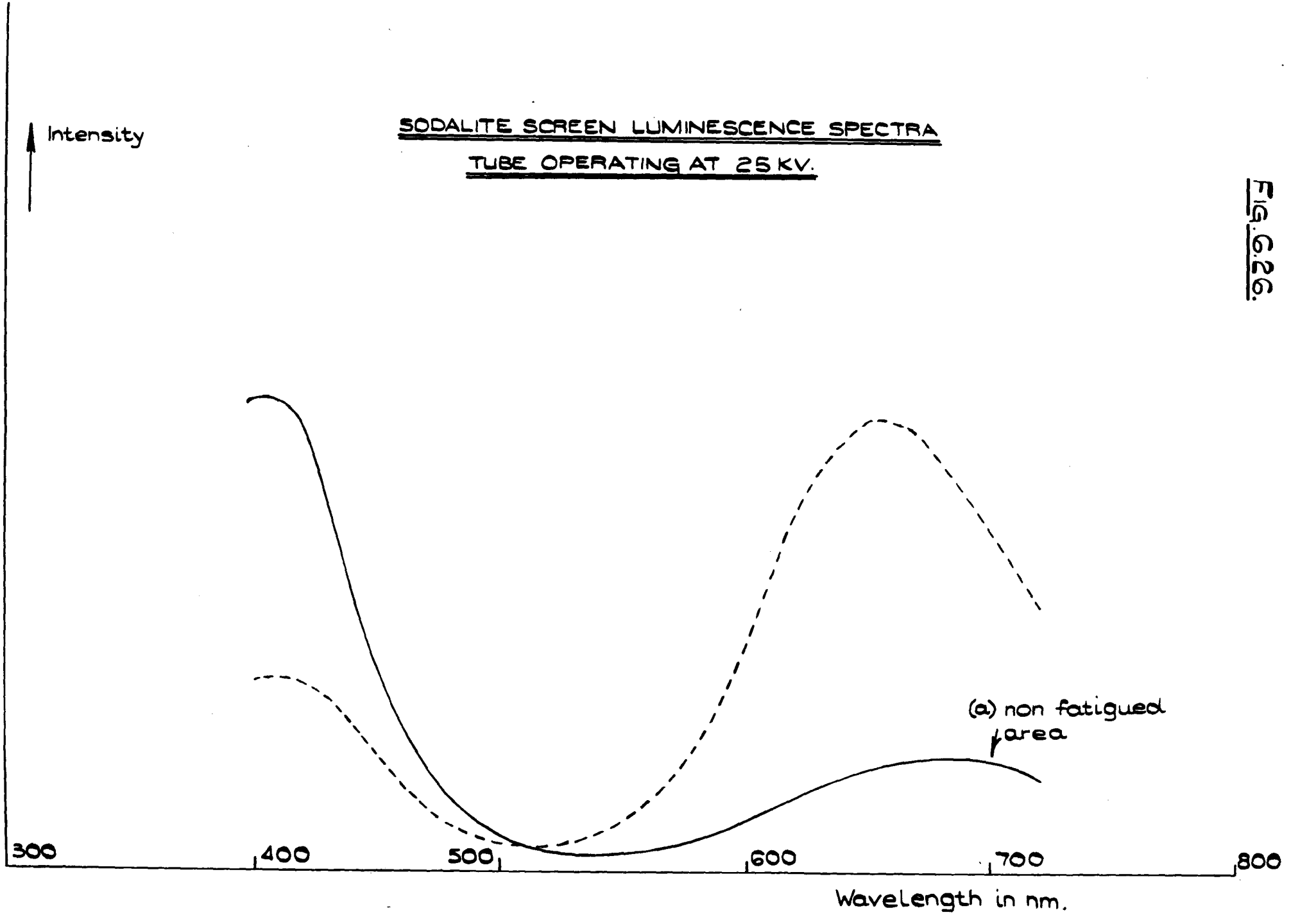
Intensity
SODALITE SCREEN LUMINESCENCE SPECTRA
TUBE OPERATING AT 25 KV.
FIG. 6.26.
(a) non fatigued area
300
400
500
600
700
800
Wavelength in nm.

read out. Clearly the sodalite used in these experiments would be completely bleached after relatively few optical read outs (by illumination with low intensity F light), even in the absence of the significant thermal bleaching seen in this material.

6.6 Measurements on a Single Crystal of iodosodalite

The sodalite powder used on the Ferranti c.r.t. screen has a tentative chemical composition of $6NaAlSiO_4$ 2NaCl, with sulphur and possibly other impurities present. Of the many variations of this composition possible, one of the simplest is the substitution of the chlorine by another halogen, such as iodine. Fig. 6.27 shows the absorption spectrum of a small hydrothermally grown sodalite crystal, coloured by irradiation with 25 KeV electrons. The substitution of iodine for chlorine in the sodalite structure clearly produces a shift of the F band peak to longer wavelengths, as has been observed by other workers. (9) The spectrum was obtained using the microspectrophotometer described in detail in Chapter Two. Since the crystal was only a few hundreds of microns across, and the transparent area of the top face much smaller than this, it was attached to an electron microscope diffraction aperture, with the clear region over a 50 μm. diameter hole. This greatly facilitated handling the specimen, and positioning it in the microspectrophotometer beam, since the transparent region completely covered the diffraction aperture. The small size of the crystal necessitated a two stage procedure for absorbance measurement; a 100% transmittance measurement was made on the uncoloured specimen, which was then removed from the microspectrophotometer, irradiated and subsequently remeasured in the apparatus. This practice was clearly not entirely satisfactory, but it was the best method possible in the circumstances.

The presence of a "tail" on the long wavelength side of the F band may not be indicative of the presence of F aggregate centres, for

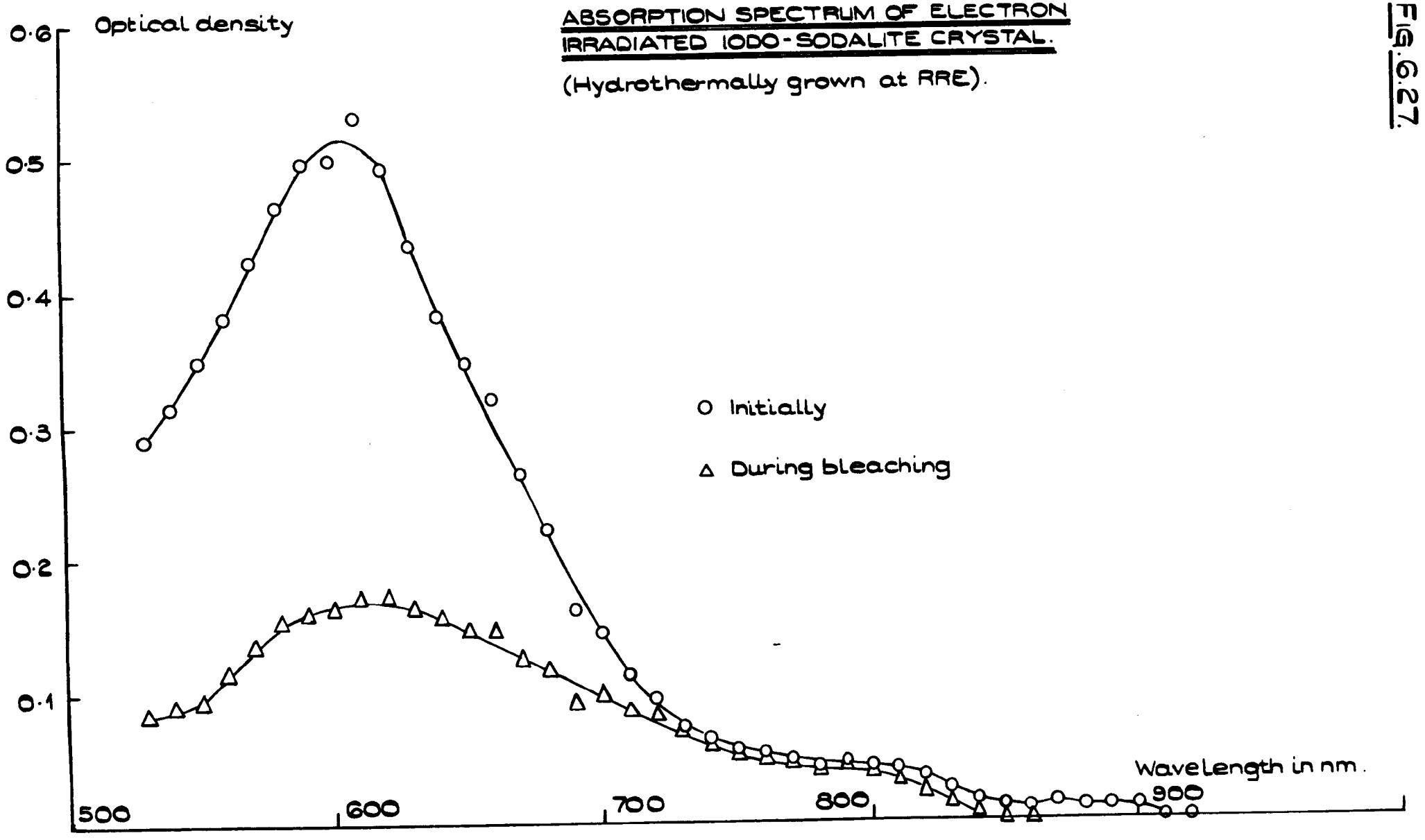
ABSORPTION SPECTRUM OF ELECTRON IRRADIATED IODO-SODALITE CRYSTAL.
(Hydrothermally grown at RRE).
Optical density
0·6
0·5
0·4
0·3
0·2
0·1
O Initially
Δ During bleaching
Wavelength in nm.
500
600
700
800
900

Fig. 6.27.

it disappears on optical bleaching with F band light. The iodosodalite single crystal bleached as easily as the chlorosodalite powder, the spectrophotometer beam was sufficiently bright to completely erase the coloration after a short exposure. A bleaching curve obtained by this method appears in Fig. 6.28. The striking thing about this result is the high absorbance ($\sim$1.7) of the sodalite at the start of measurement, this was by no means untypical; the production of optical densities in excess of unity by electron irradiation was relatively easy with this particular crystal, even though coloration had not been taken beyond the early, reversible photochromic stage. It is unfortunate that further, more detailed, measurement on this crystal was not possible, owing to its loss after coming unstuck from the electron microscope aperture. Subsequent attempts at mounting, in a similar fashion, the one or two smaller crystals that were available met with failure.

6.7 Summary

Data on the electron coloration and optical bleaching characteristics of chlorosodalite has been obtained, using a specially manufactured cathode ray tube with sodalite powder deposited on the screen instead of the conventional phosphor. The coloration curves (Fig. 6.7) show that chloro-sodalite is fairly sensitive to coloration by electron irradiation, and that it is possible to achieve adequate contrast for dark trace display systems using standard cathode ray tube assemblies. The optical bleaching experiments (Figs. 6.9 - 6.10) demonstrate that illumination with relatively low intensity tungsten light sources is quite satisfactory for erasing the sodalite F band. Thermally activated bleaching makes a substantial contribution to the observed fall in coloration at low ("ambient") illumination levels, when the material is at RT (Fig. 6.19). Experiments also showed that the coloured sodalite powder can be bleached virtually instantaneously ($< 2\text{x}10^{-3}$ second) by a single flash from a 1000 Joule photoflash tube. However, the need for bulky power supplies and trigger units for large flash tubes, and

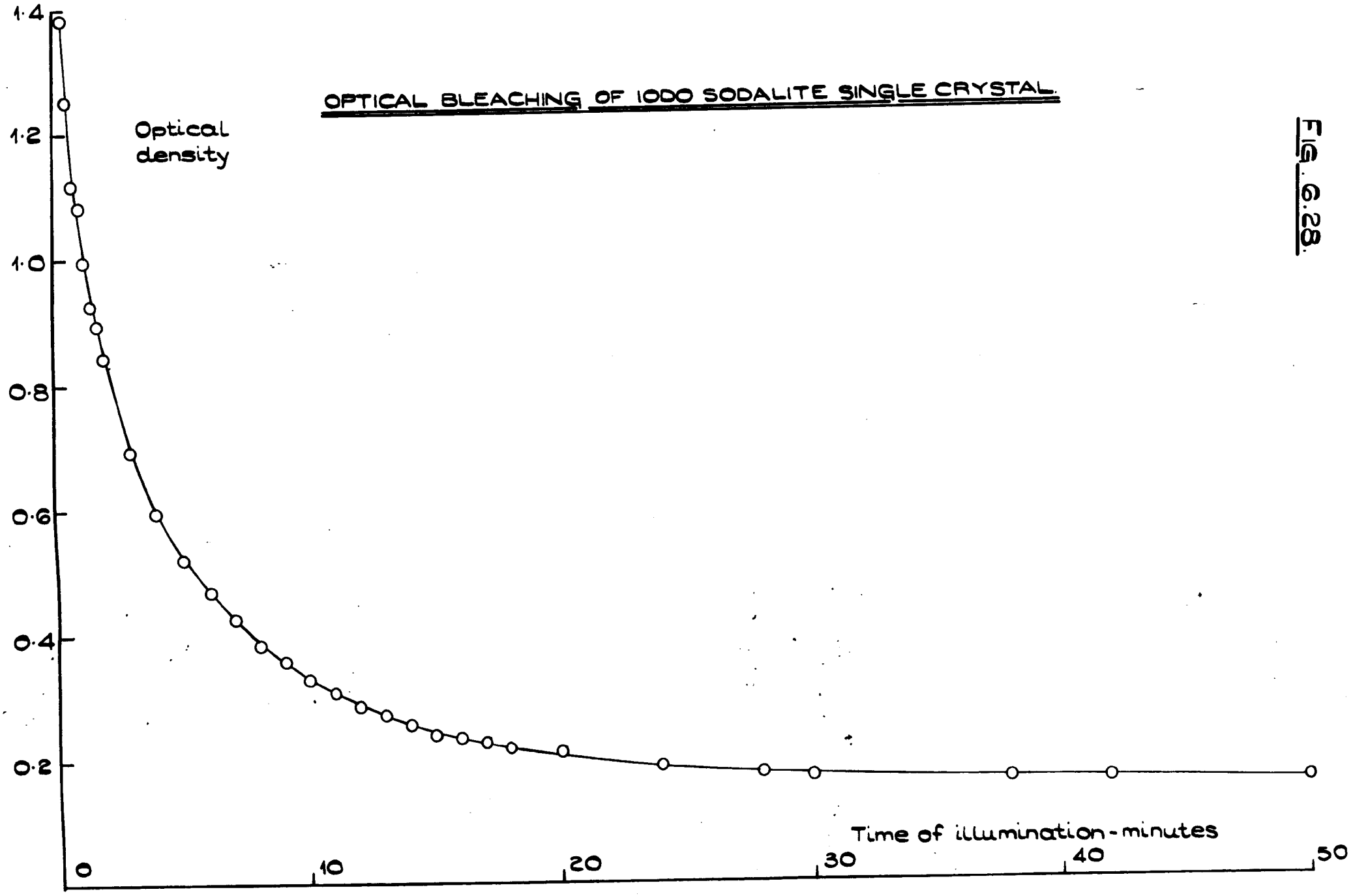
OPTICAL BLEACHING OF 1000 SODALITE SINGLE CRYSTAL.
Optical density
1·4
1·2
1·0
0·8
0·6
0·4
0·2
0
10
20
30
40
50
Time of illumination - minutes

FIG. 6.28.

the short life of such devices, would seem to far outweigh the advantage that they offer of rapid'one shot' bleaching. It ought to be possible to use a smaller tube, of say 100 joules input, which would mean that a number of flashes would be required for bleaching. The drawback to a bleaching system such as this would be the time taken to recharge the reservoir capacitors between successive flashes.

Some measurements were also made on the bleaching of an iodosodalite single crystal. This showed similar characteristics to the chlorosodalite, except that it did not appear to thermally bleach as effectively as the latter. It was apparently possible to colour this specimen to a much higher F band O.D. than the chlorosodalite, although it is not strictly correct to make direct comparisons between the chlorosodalite reflectivity data and the iodosodalite transmittance measurements. The position of the F band peak ($\sim$ 615 nm.) in iodosodalite, and its high bleaching sensitivity, would clearly make it suitable for temporarily recording holograms, using a helium-neon laser, if sufficiently large crystals were available.

All measurements were made on sodalite that had not been coloured beyond the early, reversible photochromic stage, since the F band could be completely bleached by illumination at room temperature. Coloration and bleaching in this region is thought to be an entirely electronic process, involving only the trapping of electrons at existing halide ion vacancies. The electrons may be donated by impurity ions e.g. S_2^-, or, in the case of electron coloured material, come from the irradiating electron beam. Bleaching will involve the liberation of the F centre electrons by optical excitation, and their subsequent trapping by impurities. At the present time there is no evidence to suggest that vacancy aggregates are formed during bleaching.

In view of the proposal that bleaching occurs by a simple electronic mechanism, it ought to be possible to fit the data to a simple model. Attempts were made at fitting the data to relationships

such as $\frac{dn_F}{dt} = bn_F + a$, but were unsuccessful. This may be because the basic assumption that log ($^1/R$) is proportional to n_F, the number of F centres, is incorrect. It is also unfortunate that more data is not available on the thermal bleaching of the chlorosodalite powder, to check the reproducibility of Fig. 6.19. It is interesting to note that the results obtained by Duncan et al [2] for the thermal bleaching of bromosodalite do fit a relationship of the form O.D. $\propto$ log t , but that their results for iodosodalite do not. It is clear that further investigations into thermal bleaching would be desirable.

The results reported in this chapter, and elsewhere, show that sodalites are highly suited to information display applications, and particularly for use in dark trace cathode ray tubes. (They are not likely to be suitable for data storage, unless a non destructive "read" process can be found.) Their sensitivity to electron coloration and optical bleaching is perfectly adequate, and the resolution of even powder screens is limited not by the material itself but by the electron beam diameter. They do, however, fatigue after a fairly modest number of coloration/erasure cycles, becoming progressively more difficult to colour and bleach, and in extreme cases they exhibit a permanent stain. The fatigue problem is by far the greatest obstacle to the widespread use of sodalite in display systems, for the generally acceptable minimum active device life of 1000 hours cannot be attained without appreciable fatigue occurring. The precise nature of the fatigue is, as yet, unidentified, although it seems to be accompanied by a marked increase (in chlorosodalite) in luminescence beyond 600 nm. It is evident, however, that until more is known about the fatigue mechanism occurring in the sodalites, their potential as reversible optical display media cannot be fully realised.

References

(1) King, P.G.R. and Gittins, J.F., I.E.E. Journal 93, 822 (1946)

(2) Duncan, R.C., Faughnan, B.W. and Phillips, W., Appl. Optics 9, 2236 (1970)

(3) Medved, D.B., Am. Mineral. 39, 615 (1954)

(4) Hodgson, W.G., Brinen, J.S., Williams, E.F., J. Chem. Phys. 47, 3719 (1967)

(5) Ballentyne, D.W.G and Bye, K.L., J. Phys. D., 3, 1438 (1970)

(6) Faughnan, B.W. and Shidlovsky, I. Abstract G138, International Conference on Colour Centres in Ionic Crystals, Reading (1971)

(7) Kirk, R.D., Am. Mineral. 40, 22 (1955)

(8) Williams, E.F., Hodgson, W.G. and Brinen, J.S., J. Am. Ceram. Soc. 52, 139 (1969)

(9) Forrester, P.A., Marshall, D.J., McLaughlan, S.D. and Taylor, M.J., XVII th AGARD-NATO Technical Symposium on Opto Electronics Signal Processing Techniques. Norway (1969).

(10) Phillips, W. and Kiss, Z.J., Proc. I.E.E.E. 56, 2072 (1968)

CHAPTER SEVEN

THE OPTICAL BLEACHING OF F CENTRES IN KBr AND SODALITE, AND ITS APPLICATIONS

7.1 Summary

The experiments described in Chapters 3 to 5 of this thesis together constitute a fairly detailed study of the optical bleaching of F centres, at room temperature, in electron irradiated KBr. The kinetics of bleaching were investigated for specimens having high initial F centre concentrations ($> 10^{18}$ cm.$^{-3}$) under high intensity ($\sim 5 \times 10^{3}$ W. cm.$^{-2}$) F light illumination, using a 30 mW. He/Ne laser in a specially constructed bleaching apparatus. Data were obtained showing how the F centre concentration decreased with time of illumination (Fig. 3.3) or optical energy absorbed /cm.^{2} (Fig. 3.4). Experiments on intensity dependence showed that the bleaching rate $\left|\frac{dD}{dt}\right|$ is linearly dependent on energy, or very nearly so, over the range 1 W. cm^{-2} to 5×10^{3} W. cm^{-2}. It was found that KBr crystals which have been electron irradiated at room temperature bleach by vacancy aggregation, leading to the formation of M, R, N ..... centres. The broad V band observed in these specimens appears to be quite stable at RT, and takes no part in bleaching. (It has been reported to be due to small aggregates of interstitials at F centre concentrations up to 5×10^{17} cm.$^{-3}$ (1,8). Aggregation initially proceeds via both the F' - α (2,3) and F - α (4,5) mechanisms, with the concentration of F centres progressively falling and the concentrations of M and higher order aggregate centres rising. A condensation of F centres is also occurring, by the long range F' - α interaction. The nearest neighbour pair distribution gradually shifts to shorter separations, so that aggregation proceeds further as pairs of F centres become sufficiently close for the shorter range F - α mechanism to operate. This leads to an increase in the number of M centres present, which will in turn aggregate to R and N centres, presumably through similar reactions. The modulated bleaching experiments described in Chapter 5 showed the presence of R_1^+ and R_2^+ bands

during illumination, which strongly suggests that aggregation reactions of the type $\alpha + M \rightarrow R^+$ are operating. The bleaching of room temperature coloured specimens can be approximately described by considering a random distribution of aggregation events occurring among volumes some 5×10^{-19} $cm.^3$ in size. This model correctly shows that first the M and then the R centre concentrations pass through maxima as bleaching proceeds, and predicts with fair accuracy the positions of the peaks relative to the total number of aggregation events that have occurred since the onset of bleaching. The efficiency of F centre aggregation decreases quite markedly during bleaching (Fig. 3.6); this may be understood since the $F' - \alpha$ interaction has to operate over progressively larger distances, so that the number of optical excitations per aggregation event will gradually increase. It must be stressed, however, that the precise atomic mechanism of F centre aggregation is by no means definitely settled.

The optical bleaching of KBr specimens which have been irradiated at room temperature is clearly not a reversible process, since the crystal is not returned to its state prior to irradiation, even after the absorption of 10^7 $J.cm.^{-2}$ of optical energy. The residual coloration observed in the F band region (Fig. 3.4) of such crystals is most probably due not to F centres but to excited states of M and R centres. This residual coloration may be removed by a subsequent electron irradiation, which breaks up the aggregates and allows 10^4 to 10^5 reversals, although the crystal is certainly not completely returned to its original state [7]. However, if KBr is coloured by fast electron irradiation at liquid nitrogen temperature ($\sim 90^\circ$ K), and warmed to room temperature in the dark, bleaching is apparently complete and reversible, in that all of the centres giving rise to optical absorption are removed. (There may, of course, be debris remaining after bleaching which does not give rise to any optical absorption but which may hinder further coloration-bleach cycles, and so lead to fatigue.) Bleaching occurs by

what appears to be a vacancy-interstitial annihilation mechanism; there is a direct proportionality between the total number of vacancies calculated to be present in the F, M, R and N bands and the strength of the V band which peaks at about 265 nm. in these specimens. Prolonged illumination leads to the disappearance of this V band and the F and F aggregate bands, and the optical absorption spectrum of the crystal becomes similar to the spectrum seen prior to irradiation. It is surprising that the energy derivative of the optical density in the F band $\left|\frac{dD}{dE}\right|$ for specimens coloured at both RT and LNT obeys the relationship $\frac{dD}{dE} = \frac{5 \times 10^{-2}}{E}$, over 6 or more decades of absorbed energy (E). This suggests that there is some similarity between the bleaching mechanisms in the two cases. It may be, therefore, that the bleaching of crystals coloured at LNT proceeds via reactions of the type $V' - \alpha$ and $V - \alpha$, similar to the $F' - \alpha$ and $F - \alpha$ mechanisms that occur in RT irradiated material. However, a modulated bleaching experiment, in which the F band (laser) illumination was chopped and the V band examined for synchronous intensity variations, failed to establish any direct connection between the F and V bands in the low temperature coloured material. It is impossible to be more precise about this mechanism, since the configurations of those V centres in KBr stable at room temperature are by no means certain, although recent work [8] shows that they are interstitial clusters $\sim$ 100 to 1000Å in diameter, the smaller clusters being formed by low temperature irradiation. It is likely that the clusters formed during irradiation at 90°K have sufficient stability at room temperature not to be affected by direct optical excitation, but are still able to recombine with mobile vacancies (α centres and F centres in the relaxed excited state) when the crystal is illuminated with F light.

Whilst the F absorption band in KBr coloured at 90°K can be completely bleached at room temperature by illumination with F light, as a means of recording optical images it is rather inefficient when

compared, for example, with the conventional photographic process. Although only about 150 photons (from Fig. 3.14) are absorbed for the removal of one F centre at the onset of bleaching, directly after warming to room temperature, the bleaching efficiency decreases rapidly with time of illumination, until in the later stages in excess of 10^8 photons are absorbed per removed F centre. (from Fig. 3.4)

The sodalites, in comparison, bleach considerably more easily, provided coloration has not been extended beyond the early, photochromic stage. The experiments described in Chapter 6 show that relatively low intensity light sources and short exposures can be used to completely erase the F band in chloro and iodosodalite. It is difficult to make precise measurements of the bleaching efficiency of these materials in terms of photons absorbed per F centre bleached, since insufficient information is available to allow the F centre concentration to be calculated from the reflectivity data. However, the energy derivative of the coloration in the F band $\left|\frac{dD}{dE}\right|$ is a useful factor for comparing the bleaching efficiencies of sodalite and KBr. F or chlorosodalite $\left|\frac{dD}{dE}\right|$ can be as high as 60 coloration units $(\log_{10} {}^{1}/R) J.^{-1}$ cm.^{2} at the onset of bleaching, falling to approximately 4 coloration units $J.^{-1}$ cm^2 when nearly all of the F centres have been removed(from Fig. 6.1[2]). Similar figures measured for KBr coloured at room temperature are 8×10^{-1} O.D. units $J.^{-1}$ cm.^{2} and about 10^{-8} O.D. units $J.^{-1}$ cm.^{2} respectively (from Figs. 3.4 and 3.14). These two sets of figures clearly reflect the differences between the bleaching mechanisms in the two cases. The optical bleaching of sodalites which have only been irradiated into the early, photochromic, stage of coloration is thought to involve the transfer of an F centre electron to a neighbouring O^- ion or similar entity [6], without any ionic motion. This is in marked contrast to the bleaching at RT of electron irradiated KBr, in which ionic diffusion clearly does occur. Therefore it is not strictly correct to make direct comparisons between the sodalite and KBr bleaching data. It would seem more appropriate to compare the sodalite results with the

reversible $F \rightarrow F'$ process in KBr, which is purely electronic in nature, and has a quantum efficiency of 2 at a suitable temperature [18]. This bleaching efficiency figure corresponds to a $\left|\frac{dD}{dE}\right|$ of over 500 O.D. units $J.^{-1}$ cm^2, which is an order of magnitude higher than the similar figure for sodalite. The $F \rightarrow F'$ process does not, moreover, show any fatigue, unlike sodalite, in which there is a gradual build up of persistent coloration that does not optically bleach. Although the fatigue that occurs when a sodalite has been repeatedly coloured and bleached is not well understood, it may be due to F aggregate formation. There is also the problem that colouring sodalites into the stage II region (to F centre densities $> \sim 5 \times 10^{17}$ centres cm^{-3}) appears to produce F centres which cannot be bleached optically. Therefore although the sodalites may appear to be more suitable for reversible cathodochromic applications at RT (e.g. dark trace c.r.t.s.) than the alkali halides, they do not compare so favourably with the latter material when considered in terms of reversible photochromic performance.

7.2 Extensions to the experimental work described in this thesis

Whilst efforts were made to ensure that the data presented in this thesis are reasonably complete there are, inevitably, some areas which merit further experimental work.

(i) Measurement of the oscillator strengths of the F aggregate bands in electron coloured KBr

The results of the experiments described in Chapter 4 indicate that there is a need for more precise measurement of the oscillator strengths of the F aggregate centres in electron coloured KBr. It ought to be quite possible to measure these values using a bleaching method similar to that employed by other workers [9], based on the assumption that the total number of vacancies remain constant throughout bleaching. By making a series of observations of the amplitude of the F- and F-aggregate bands during bleaching it is possible to obtain a set of simultaneous equations which may be solved to obtain values f_M, f_R etc. There are, however, difficulties associated with

this method. Neither is it easy to make precise measurements of the half widths of some of the aggregate bands, since they do not occur in isolation, nor are the configurations of some of the higher order aggregate centres certain, the N centre being a specific example. Care is also needed to ensure that colloidal metal particles are not formed during bleaching; cooling the specimen prior to each measurement would ensure that colloids did not go undetected (absorptions due to colloids will not narrow or shift in wavelength when cooled to LNT). This method, by its very nature, demands that the F and all of the F aggregate centres are measured, to ensure that no vacancies are "lost" by being unobserved in bands outside the spectral range of the spectrometer. It would thus be important to monitor accurately the specimen absorbance over the wavelength region extending from about 550 nm to 1.2 or 1.3 μm.

Since bleaching occurs by vacancy aggregation in crystals which have been electron irradiated at RT, and the V bands do not change during bleaching, such crystals may prove to have advantages over the additively coloured specimens used in previous oscillator strength determinations. (e.g. no heat treatment would be necessary.)

(ii) The modulated bleaching experiments

The results of the modulation spectroscopy experiments described in Chapter 5 could be improved in accuracy and extended with suitable modifications to the microspectrophotometer. So far only the R_1^+ and R_2^+ bands have been seen during bleaching; it would be particularly useful if the existence of the M^+ band could be similarly observed, to demonstrate with some certainty that the $F + \alpha \rightarrow M^+$ reaction occurred during optical bleaching. This band cannot be seen with the apparatus in its current form, since neither monochromator nor detector will function satisfactorily in the wavelength region 1 to 2μm. (At R.T. the M^+ band in KBr is expected to lie somewhere near 1.4 μm.) Whilst there is no problem in finding a suitable monochromator, low

noise detectors to work in this spectral region, with sensitivities as high as photomultiplier tubes, do not, unfortunately, appear to be readily available. It is likely, therefore, that some considerable improvement in signal to noise ratio will be necessary before any useful measurements can be made at wavelengths beyond 1 μ m.

Whilst it is unlikely that any great increase could be made in the light reaching the p.m.t., the signal/noise ratio and resolution may effectively be increased by connecting a computer of average transients (CAT) between the p.s.d. and output chart recorder. The CAT could then carry out automatically the noise averaging process described in Chapter 5, with greater speed and accuracy. A continuous monochromator drive might then be used, to enable a greater number of scans to be made in a shorter time. This would hopefully eliminate another source of signal variation, the appreciable bleaching of the specimen with time. If, however, this still proved to be a problem, it may be possible to overcome it by slowly moving the crystal through the microspectrophotometer beam during the experiment. Having thus improved the signal to noise ratio a suitable detector may then not be so difficult to find, a possibility being a new microwave biased germanium photoconductor, under development by the Plessey Company.

(iii) The triboluminescence of KBr

During the course of the experiments discussed in this thesis it was discovered that KBr "triboluminesces". If a sharp point is drawn across the surface of an electron coloured KBr crystal in a darkened room, a faint bluish green glow can be seen, emitted from the region of the crystal directly under the point. This phenomenon was not pursued any further, but it is sufficiently interesting to merit closer investigation, particularly as it has not been reported elsewhere. It is likely that the luminescence is the result of an electron hole recombination process, with F centre electrons annihilating the holes trapped at the optically stable V centres which are responsible for the

broad absorption between 200 and 300 nm.

It is possible that the phenomenon of "aquoluminescence" is related [10,11]. This occurs when a γ or electron irradiated alkali halide is dissolved in distilled water; a bluish green light is emitted, peaking around 500 nm., which decays over a period of 2 to 3 seconds. The wavelength of the emission is not dependent on which of the alkali halides is being dissolved, or at least NaCl, NaBr and KCl are reported to give the same effect, and it has been identified with a triplet to ground state transition of the water molecule [11]. Precisely how the triplet state is populated is, however, not clear.

The presence of trapped hole centres in a crystal seems to be a prerequisite for tribo-and aquoluminescence, since neither phenomena can be observed in additively coloured KBr. It is apparent that more data is required before any definite conclusions can be drawn about the nature of the luminescence, and it seems likely that measurement of the emission spectra would be useful. A precise measurement of the spectra, using a conventional spectrograph, might be rather difficult, since both emissions are very weak and decay quite rapidly. In the case of triboluminescence there is the additional problem of continuously scratching the crystal during measurement, although this could doubtless be accomplished by moving it slowly over a point with a lead screw. It might be possible to make an approximate spectral distribution measurement using a crude spectrometer consisting essentially of a photomultiplier tube with a rotating wedge interference filter in front of its window. The filter would rotate with a shorter period than the decay time of the luminescence, and during one revolution would scan the whole of the visible spectrum. A contact on the drive shaft could provide a time base trigger for the c.r.o. to which the photomultiplier would be connected. The c.r.o. would thus display a series of superimposed traces, which after correcting for p.m.t. response etc. would provide a record of the spectral distribution of intensity of the tribo

and aquoluminescence. By making measurements of tribo and aquoluminescence spectra for two or three different alkali halides one might thus obtain a little more basic information about these two interesting phenomena, and certainly establish whether or not they are connected.

(iv) Fatigue of the sodalites

There is a very obvious need for more knowledge about the fatigue that occurs in the sodalites. The experiments described in Chapter 6 shed very little light on this problem, apart from indicating that there appears to be a connection between the degree of fatigue and the luminescence spectrum during electron irradiation. The gradual change in luminescence from a blue to a pinkish red emission as the material fatigues does not, however, seem to be universal. It has been reported that sodalites which have been sensitized by firing in argon exhibit the pink luminescence the first time they are irradiated [13], although in hydrogen fired sodalites the strength of the pink luminescence seems to be directly related to the degree of fatigue. A thorough investigation of the whole fatigue phenomena in the sodalites appears to be necessary, to correlate the luminescence spectrum and chemical composition of a particular sodalite with the extent to which it fatigues. (Before this is possible some suitable measure of the degree of fatigue needs to be found, it might conveniently be obtained from the efficiency of coloration or bleaching at a particular optical density after a certain number of coloration-erase cycles) A study of this nature is clearly beyond the scope of the simple apparatus described in Chapter 6, for one thing there is no facility for cooling down the sodalite in order to reveal the fine structure of the luminescence spectrum. This could best be achieved by constructing a demountable c.r.t., with the screen mounted on a holder thermally insulated from its surroundings which could be refrigerated by passing cold gas or liquid nitrogen through it. It would also be desirable to

be able to grow sodalite specimens having selected chemical compositions.* It is therefore thought unlikely that the data presented in Chapter 6 could be added to without a drastic redesign of the apparatus, and the acquisition of crystal growing facilities.

7.3 Applications

Reference has been made in this thesis to the use of the alkali halides, the sodalites and similar cathodo-and photochromic materials for optical memories and data display devices. In conclusion, therefore, some of these applications will be described in a little more detail.

(i) Dark Trace Cathode Ray Tubes

The first practical device to utilise the coloration and bleaching of F centres in an alkali halide was the 'skiatron' [12], a projection cathode ray tube system for the display of radar information. The heart of the equipment was a dark trace cathode ray tube with a screen that consisted of a translucent, polycrystalline film of evaporated KCl, which was illuminated by powerful lamps and imaged onto a large screen (Fig. 7.1). Although a number of operational skiatrons were made and used during the last war, the device was not altogether successful, for reasons which are now obvious. The bleaching of an alkali halide coloured by electron irradiation at room temperature occurs by vacancy aggregation, and is not strictly a reversible process. In the skiatron, repeated coloration-bleach cycles, particularly when displaying a stationary pattern, brought about the formation of complex colour centres or colloidal metal particles, which were difficult to disperse optically. This led to the build up of a persistent coloration of the screen, i.e. fatigue. Various attempts were made at overcoming this problem, such as heating the screen or doping the KCl with aluminium

*Being attempted at Imperial College of Science & Technology

Fig. 7.1.

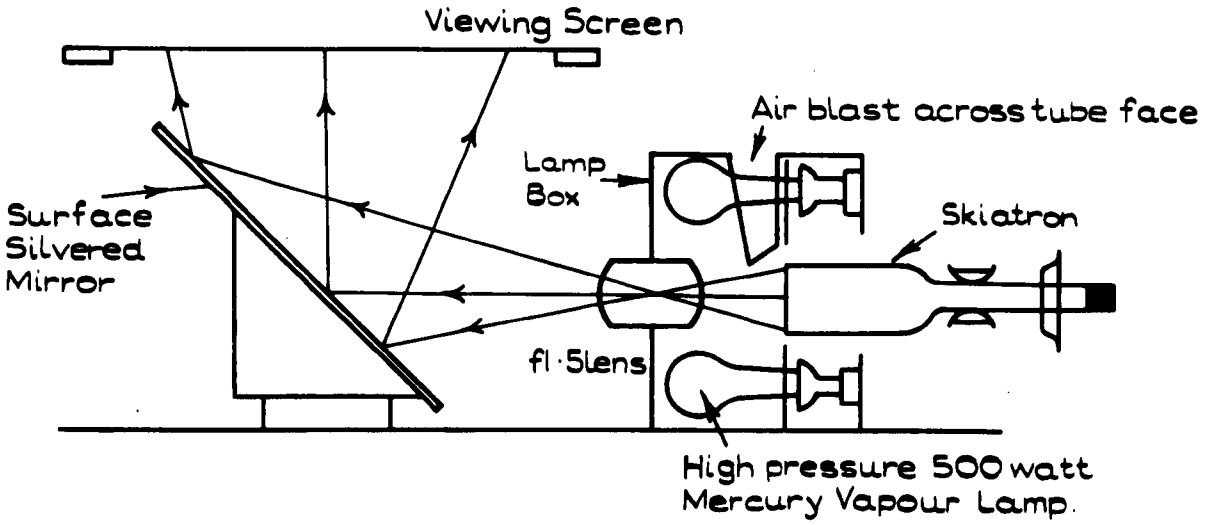

DIAGRAM OF THE "SKIATRON" APPARATUS.

or thorium, but at best they only succeeded in delaying the onset of fatigue. For this reason the development of the skiatron was abandoned at the end of the war, as had been the idea of using transparent single crystals of an alkali halide in large screen projection television systems [14].

However, the requirement for a reliable dark trace cathode ray tube with a medium to long persistence (fractions of a second up to several seconds) has become more pressing over the last few years, particularly for use in air traffic control radars and computer graphics displays. Admittedly there are now various types of storage c.r.t. generally available, but they all make use of light emitting phosphors, which generally have to be viewed in highly subdued lighting. As a consequence there has been considerable interest shown recently in the use of sodalite powder as a screen material for devices similar to the skiatron.

Ferranti Ltd. have manufactured a number of c.r.t.'s with aluminized chlorosodalite powder screens; one of these was used for the experiments described in Chapter 6, and they have been evaluated elsewhere in such applications as P.P.I. radar presentation [13]. Despite the considerable improvement of the sodalite powder over evaporated KCl, the useful life of these tubes is still considerably less than the generally acceptable figure of 1000 hours. However, the fatigue that occurs in the sodalites is far from understood, it is likely that it is an effect which is not intrinsic to bleaching and can be eliminated without impairing the performance of the material as a photochromic. If a fatigueless sodalite can be produced, there is no doubt that it will be first made use of in a dark trace cathode ray tube. (A successful <u>thermally</u> erased sodalite screen c.r.t. has already been made by the Optel Corporation, Princeton, U.S.A., but this has a maximum frame repetition time of $\sim$ 6 seconds.)

(ii) Holography

The recording of optical holograms requires high resolution photographic emulsions, which have to be chemically processed before the reconstructed wavefront can be viewed. Polished single crystals of KBr, coloured by electron irradiation, would appear to offer an alternative recording medium for holography using a He-Ne laser. Whilst not as sensitive as even the slowest photographic emulsions, the resolution capability of a coloured KBr crystal is inherently very much greater than the finest grain photographic emulsions. The hologram may, moreover, be viewed directly after it has been made, without the need for intermediate processing. Holograms recorded by bleaching electron irradiated KBr will not, of course, be as permanent as a developed and fixed photographic plate, since the laser beam (normally of low intensity) used for reconstructing the image will slowly bleach the crystal. For many applications this will not be too much of a disadvantage. KBr might also be used for recording volume holograms, which are particularly suitable for the storage of information, since the bulk of the crystal can be used. (X rays or extremely energetic electrons will colour a crystal throughout its volume, apart from the additive coloration process.)

The recording of holograms on an electron irradiated alkali halide single crystal has been demonstrated with both KBr and NaCl, using, in the latter case, a krypton ion laser for bleaching [15]. It was reported that the NaCl crystals could be re-used when the hologram was no longer required, simply by recolouring the crystal by electron irradiation. This, it was said, disperses the F aggregate centres formed during the bleaching, although the life of the crystal is still not very great, owing to the gradual 'crazing' of the polished surface by the electron irradiation.

(iii) Coherent Optical Processing in Real Time

A combination of the techniques discussed under headings (i)

and (ii) of this section form the basis of a real time optical processing system. If an object is illuminated with long wavelength coherent radiation (e.g. microwaves or ultrasonic radiation) and the reflected energy allowed to interfere with a reference signal, a hologram may be constructed by scanning the interference pattern with a detector. This is completely analoguous to the production of holograms at optical wavelengths. If the output of the detector is then used to modulate an electron beam scanning in synchronism with it, the hologram may be recorded by allowing the electron beam to scan over the surface of a single crystal of cathodochromic material e.g. KBr. The resultant hologram can then be reconstructed, to give a visible three dimensional image corresponding to the original objects, by shining a laser beam, of suitable wavelength, through the crystal. Such a system has already been demonstrated by E.M.I. Electronics Ltd. [16], using a KBr crystal and a He-Ne laser for hologram reconstruction. The speed of recording and the life of the crystal are the limiting factors of this system; a sodalite may be the solution to the problem, although at present it is impossible to grow single crystals of suitable size and performance. A typical application for a real time optical processor might be the display of coherent radar holograms, where at present a conventional photograph is taken of the c.r.t. display which has to be developed before it can be reconstructed [17].

(iv) Optical Information Stores

There is the possibility of using the production of F centres in an alkali halide crystal as on information store, or 'memory', for a computer. If a binary 'bit' is represented by an area of crystal approximately 1 μm. in size, so that when coloured it represents a '1' state and remains uncoloured or is bleached for the '0' state, it is possible, in principle at least, to achieve storage densities of $10^6 - 10^7$ bits cm^{-2} of crystal.

Two modes of operation of such an information store have been

suggested [7]. The first is a cathodochromic system, which operates at room temperature. F centres are generated by an electron beam, bleached with a laser, and monitored using optical absorption or cathodoluminescence (it is found that if a crystal is electron irradiated at very low beam current, so as not to produce further F centres in any number, those areas which contain F centres have a smaller secondary electron emission coefficient, and emit less cathodoluminescence). Although currently available electron beam technology could be used to construct a memory of this type, it is likely that it would show serious fatigue after 10^4 to 10^5 write-erase cycles, due to the formation of stable defect clusters and metal precipitates.

The alternative system proposed operates at low temperature ($\sim 80^{\circ}K$) using an additively coloured crystal and the $F' \rightarrow 2F$ and $2F \rightarrow F'$ conversions. The former reaction proceeds with a quantum efficiency of 2 at $80^{\circ}K$, whilst the latter is very inefficient. If, however, the crystal is illuminated with F light whilst it is in a strong electric field ($\sim 2 \times 10^5$ V cm^{-1}), field assisted bleaching occurs, and the $2F \rightarrow F'$ conversion becomes efficient. It was suggested, therefore, that the memory would be "written" into by applying a strong electric field across the crystal and illuminating it with a laser whose output wavelength was in the F band. Non destructive reading would be accomplished using the same laser without the field, and erasing by illuminating the crystal with another laser, whose emission line falls within the F' absorption band. Using this system it is stated that the crystal had not shown any signs of fatigue after 10^5 write-erase cycles.

It is unlikely that optical stores of this type will supercede the ferrite core and integrated circuit systems in use as fast access memories in present day computer systems, since they are unlikely to be any cheaper, faster or more reliable. However, as a peripheral

device to replace magnetic tape and disc units, optical memories could offer very real advantages, particularly with respect to random access time and reliability, since they could be constructed without any moving parts.

References

(1) Clarke, C.D. and Newman, D.H. J. Phys. C. 4, 1130 (1971)

(2) van Doorn, C.Z., Philips Res. Rept. Suppl. 4, 1 (1962)

(3) Lüty, F. Z. Phys. 165, 17 (1961)

(4) Delbecq, C.J., Z. Phys. 171, 560 (1963)

(5) Farge, Y, Lambert, M.and Smoluchowski, R., Phys. Rev. 159, 700 (1967)

(6) Ballentyne, D.W.G. and Bye, K.L., J. Phys. D., 3, 1438 (1970)

(7) Tubbs, M.R. and Wright, D.K. to be published.

(8) Hobbs, L.W. and Goringe, M.J. G 139 International Conference on Color Centres in Ionic Crystals. Reading (1971)

(9) Jain, S.C. and Jain, V.K., J. Phys. C. 1, 895 (1965)

(10) Arnikar, H.J., Damle, P.S., Chaure, B.D. and Madar Rao, B.S., Nature, 228, 357 (1970)

(11) Mittal, J.P., Nature Phys. Sci. 230, 160 (1971)

(12) King, P.G.R. and Gittins, J.F., I.E.E. Journal 93, 822 (1946)

(13) Forrester, P.A., Marshall, D.J., McLaughlan, S.D. and Taylor, M.J., XVIIth AGARD-NATO Technical Symposium on "Opto Electronics Signal Processing Techniques". Norway (1969)

(14) Rosenthal, A.H., Proc. I.R.E. 28, 203 (1940)

(15) Mackin, A.S. Appl. Optics, 9, 1658 (1970)

(16) E.M.I. Ltd. T.L. No. 1839 Issue 1

(17) Kock, W.E., Electronics 43, 80 (1970)

(18) Pick, H. Nuovo Cimento VII (Ser X), 498 (1958)

COLOUR CENTRE MODULATION SPECTROSCOPY IN KBr SINGLE CRYSTALS

M. J. REDMAN * and M. R. TUBBS
School of Physics, University of Warwick, Coventry CV4 7AL

Received 11 March 1971

Colour centre modulation spectra are reported for coloured KBr single crystals illuminated with a chopped laser beam. This new technique allows the R_1, R_2 and R_1^+, R_2^+ bands to be resolved at room temperature so their behaviour can be followed during bleaching.

We have made a detailed study of laser bleaching of F-centres in electron irradiated Harshaw KBr single crystals coloured to 10^{18} - 10^{19} centres/cm^3 and illuminated with a focussed helium/neon laser giving bleaching intensities in the F-band up to 10kW/cm^2. A micro-absorption spectrophotometer has been developed to enable optical absorption spectra to be measured between 400 and 1000 nm on the 15 μm diameter area of a crystal that is illuminated by the focussed laser beam. Information has also obtained on the transient defect species that are produced during optical bleaching. To do this the laser beam in chopped at a frequency between 3 and 800 c/s and laser light is excluded from the photomultiplier detector by a filter that absorbs strongly at 632.8 nm but transmits at longer wavelengths. An A. S. L. phase sensitive detector (PSD) is used to monitor the in phase component of the transmitted spectrophotometer beam at any wavelength between 700 and 100 nm. The reference signal for the PSD is provided by a pea lamp placed next to the chopper and the phase shift is adjusted so that a zero quadrature signal is obtained from the residual laser light at 633 nm. The sense of the resulting in phase signal deemed to be positive so that a positive PSD signal at any other wavelength corresponds to increased transmittance during the half cycle when the laser beam reaches the crystal.

The variation of PSD signal with wavelength between 700 and 1000 nm is shown in fig. 1 for a chopping frequency of $4\frac{1}{6}$ c/s and a KBr crystal coloured by electron irradiation at room temperature. The individual points on this curve were

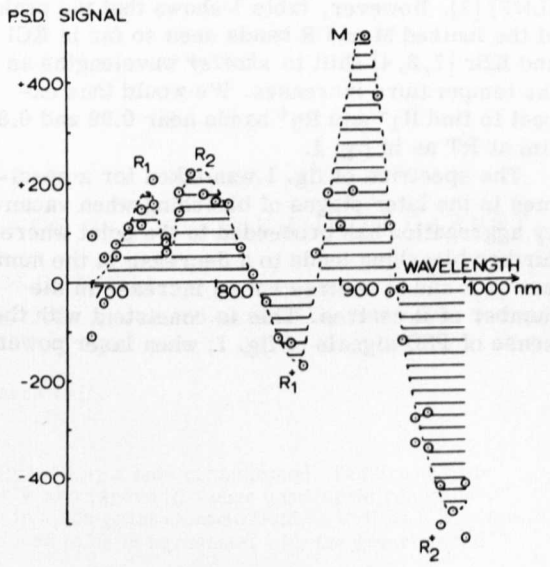

Fig. 1. Laser modulation spectrum for electron irradiated KBr at room temperature.

obtained by a noise averaging process. As the sample bleached the signal at any wavelength changed with time so a fresh part of the crystal was moved into the beam at intervals to ensure that each point represents a signal characteristic of the same stage of bleaching. Five main features can be distinguished in fig. 1; a double positive peak near 760 nm, a positive peak near 920 nm and negative peaks at 860 and 990 nm. The M band in KBr is usually seen at 918 nm at RT (1) and we thus associate the single positive peak at 920 nm with M centres. The R_1 and R_2 bands are not normally resolved in KBr at room temperature and occur as a single R band near

* Now at Government Communications Headquarters, Cheltenham.

Table 1

Material	Absorption band	LHeT	LNT	250°K
KCl	M^+	1.40 μm	1.37 μm	1.35 μm
KBr	M^+	1.49	1.44	-
KCl	R_1^+	0.96	0.94	-
KBr	R_1^+	1.02	1.01	-
KBr	R_2^+	-	0.89	-

800 nm. However, the Ivey relations predict R_1 and R_2 bands at 732 and 792 nm at RT and we identify the double positive peak with components at 740 and 790 nm with the R_1 and R_2 bands. The bands at 860 and 990 nm are associated with the R_1^+ and R_2^+ bands although these occur at 1.01 μm and 0.89 μm at liquid nitrogen temperature (LNT) [2]. However, table 1 shows that the peaks of the ionized M and R bands seen so far in KCl and KBr [2, 3, 4] shift to *shorter* wavelengths as the temperature increases. We would thus expect to find R_1^+ and R_2^+ bands near 0.99 and 0.87 μm at RT as in fig. 1.

The spectrum of fig. 1 was taken for a specimen in the later stages of bleaching when vacancy aggregation has proceeded to the point where further bleaching leads to a decrease in the number of F and M centres but an increase in the number of R centres. This is consistent with the sense of PSD signals of fig. 1; when laser power is incident on the sample the M band transmission increases while the total R band transmission ($R_1 + R_2 + R_1^+ + R_2^+$) decreases. The modulation spectrum demonstrates the direct connection between the decrease in the numbers of F and M centres dureing bleaching as M centres are converted to R centres. The observation of strong R_1^+ and R_2^+ bands during bleaching strongly suggests that a dipolar or covalent M - α attraction is responsible for this conversion. The M - α process would involve slow ionic motion and this explains why the amplitude of the modulation spectrum rapidly decreases as the chopping frequency is increased.

We should like to thank the Science Research Council for a generous research grant in support of this work. One of us (MJR) wishes to thank the S.R.C. for a maintenance award.

References

[1] W. D. Compton and H. Rabin, Sol. St. Phys. 16 (1964) 121.
[2] L. Nosenzo, E. Reguzzoni, G. Samoggia and V. Udod, Phys. Letters 32A (1970) 415.
[3] I. Schneider and H. Rabin, Phys. Rev. 140 (1965) 1983.
[4] T. Matsuyama and M. Hirai, J. Phys. Soc. Japan 27 (1969) 1526.

*****